RECONSTRUCTING MODERN AND PLIOCENE (C. 5.4-2.4 MA) DECADAL CLIMATE VARIATIONS IN THE PALEOENVIRONMENTS OF THE MIDDLE ATLANTIC BIGHT USING ISOTOPE AND INCREMENT SCLEROCHRONOLOGY

Joel Wayne Hudley

A dissertation submitted to the faculty of the University of North Carolina at Chapel Hill in partial fulfillment of the requirements for the degree of Doctor of Philosophy in the Department of Geological Sciences

Chapel Hill
2012

Approved by:

Dr. Donna M. Surge

Dr. John M. Bane.

Dr. Larry Benninger

Dr. Joseph G. Carter

Dr. Jonathan M. Lees

© 2012
Joel Wayne Hudley
ALL RIGHTS RESERVED

ABSTRACT

JOEL W. HUDLEY: Reconstructing modern and Pliocene (c. 5.4-2.4 Ma) decadal climate variations in the paleoenvironments of the Middle Atlantic Bight using isotope and increment sclerochronology (Under the direction of Donna Surge)

Ocean characteristics on geologic timescales are poorly understood, have varied in the past, and are critical to understanding how the ocean may respond to future human-induced climate change. Recent climate studies have identified that environmental variations in the Mid-Atlantic Bight (MAB) are related to larger global climate variations throughout the Late Cenozoic such as the Atlantic meridional overturning circulation pattern and ocean-atmospheric teleconnections. Modern physical oceanographic studies in the MAB using the modern instrument records show high interannual variability with longer, multi-decadal warming trends. The goal of this investigation is to reveal annual to multi-decadal variations in sea surface temperatures of the MAB during the Pliocene (5.4-1.8 Million years ago (Ma). This investigation employs isotope and increment records from marine bivalves as proxies for ocean bottom temperature in conjunction with a basic understanding of the modern physical oceanographic flow model along the Atlantic continental shelf.

In the present study, live-collected bivalves from the MAB and fossil bivalve shells from Pliocene deposits along the US Mid-Atlantic Coastal Plain (MACP) were used to estimate oceanic conditions (seawater temperature, salinity, etc.) and ocean/atmosphere internal oscillations that currently dominate the basin. Sclerochronologic and stable isotope analyses were used to study this problem. Using the growth increments and isotope records of the modern *Hemimactra* as a comparison, Pliocene surf clams were employed to estimate paleoecologic and paleoclimatologic conditions along with the MACP. Pliocene surf clams documented annual increment marks and oxygen isotope ratios indicating greatly reduced seasonality, similar to the modern *S. s. similis*, but with similar average temperatures relative to modern SST at the same latitude. Since the surf clams present within the Pliocene MACP represent the short-lived species (~ 5 years old), in order to investigate multi-decadal variations during the Pliocene new bivalve proxies were explored. Large and abundant MACP bivalves, *Glycymeris americana* and *Panopea reflexa* were identified as having annual growth increments and significant longevity. Ages of fossil shells were comparable to extant species *G. glycymeris* (~100 years) and were used to reconstruct regional SST and a spectral analysis of past NAO. Oxygen isotope values were consistent with previous bivalve studies.

ACKNOWLEDGEMENTS

I would most like to thank Dr. Donna Surge for allowing me to create this project. Without her, I would not have gained so many valuable experiences. I am truly grateful to Dr. Jay Burnett of NOAA Northeast Fisheries Science Center, who generously donated me the Jeep Cherokee full of live collected *Spisula* and *Arctica* and answered all my questions on shell aging. I would like to extend my great thanks to my committee members, Dr. John M. Bane, Jr., Dr. Larry Benninger, Dr. Joseph G. Carter, and Dr. Jonathan Lees for their advice. Thank you Surge Lab: Ann Goewert, Jose Rafa Garcia March, Ting Wang and Ian Winklestern. Lastly, I must thank my family for their endless love and encouragement. This is especially true for my sweet and beautiful wife Melissa and my mother Janice Edgerson who proofread early drafts even though she claims to know nothing about geology.

TABLE OF CONTENTS

LIST OF TABLES

LIST OF FIGURES

LIST OF ABBREVIATIONS AND SYMBOLS

1. ±	plus or minus
2. ‰	per mil or parts per thousand
3. ^{13}C	carbon isotope 13
4. ^{14}C	radiocarbon isotope 14
5. ^{18}O	oxygen isotope 18
6. *A. islandica*	*Arctica islandica*
7. AMS	accelerator mass spectrometry
8. cm	centimeter
9. DIC	dissolved inorganic carbon
10. et al.	and others
11. GBS	Georges Bank-Scotian Shelf
12. GI	Growth index
13. *G. americana*	*Glycymeris americana*
14. *G. glycymeris*	*Glycymeris glycymeris*
15. HCO_3^-	bicarbonate
16. i.e.,	that is
17. MAB	Middle Atlantic Bight
18. MACP	Middle Atlantic Coastal Plain
19. MPWP	Mid Pliocene Warm Period
20. mm	millimeter
21. NBS	National Bureau of Standard
22. NOAA	National Oceanographic and Atmospheric Agency
23. ^{o}C	degrees Celsius
24. *P. abrupta*	*Panopea abrupta*
25. *P. reflexa*	*Panopea reflexa*
26. psu	practical salinity units
27. RWI	Ring width index
28. *S. confraga*	*Spisula confraga*
29. *S. modicello*	*Spisula modicello*
30. *S. s. similis*	*Spisula solidissima similis*
31. *S. s. solidissima*	*Spisula solidissima*
32. SGI	Standardized growth index
33. SHW	Shelf Water
34. SLW	Slope Water
35. *spp.*	*Species pluralis* or Genus, species unidentified
36. SST	sea surface temperature
37. T	temperature
38. USGS	United States Geological Survey
39. VBGM	Von Bertalanffy growth model
40. VPDB	Vienna Pee Dee Belemnite
41. VMNH	Virginia Museum of Natural History
42. VSMOW	Vienna Standard Mean Ocean Water
43. $\delta\,^{13}C$	carbon isotope ratio
44. $\delta\,^{18}O$	oxygen isotope ratio

45. $\delta^{18}O_W$	oxygen isotope ratio of water
46. $\alpha^{13}C$	carbon isotope 13 fractionation factor
47. μg	microgram, 10^{-6} gram

CHAPTER 1: INTRODUCTION, PURPOSE, DISSERTATION ORGANIZATION

1.1 Introduction

The Intergovernmental Panel on Climate Change (IPCC) projects a future warmer climate through the 21st century (IPCC WG1,2007). The predicted increase in air temperature is related to the observed and forecasted increases in anthropogenic greenhouse gases. The potential effects of a future warmer climate include sea level rise, extreme weather events, migrating ecosystems, and changing resources. Climate scientists and policy makers responsible for making decisions on the mitigation of and adaptation to human-induced climate change have determined that understanding past warm climate states is critical to evaluate its response to increasing greenhouse gas concentrations (IPCC WG1, 2007). Determining mitigation and adaptation strategies to lessen the resulting worldwide socio-economic stresses requires efforts to reduce the uncertainties associated with the nature and rate of projected climate change (IPCC, 2007; Robinson and Dowsett, 2010). To reduce the uncertainties, geologists and paleoclimatologists use proxy records to extend the instrumental record and study analogs to projected future warm climate.

Instrumental records can only assess large-scale climate changes over roughly the past century, whereas proxy-based reconstructions appear to explain relatively well the major surface temperature changes of the past millennium. The expansion and improvement in the networks of available proxy data sets that can be used to develop spatial maps (with associated errors) for each season of the last few millennia is essential (Jones and Mann, 2004). There is a need to develop high-resolution reconstructions as templates for calibrating the longer, lower resolution proxy data networks. To achieve this goal, reliable proxies must be "calibrated" and independently "validated" against instrumental records. Tree rings and coral isotopic data are currently the most widespread sources of annually and sub-annually resolved proxies, but both proxies are limited in spatial and temporal coverage. Early successes in the development of annual chronologies using the long-lived bivalve *Arctica islandica* (Wiedman and Jones, 1994) demonstrate that molluscan shell records are effective high-resolution proxy indicators that can potentially serve as useful data sets to develop multi-proxy climate reconstructions.

Over the last 30 years, many scientific papers have asserted that intervals in Earth history can be used as an analogue for future climate change. To be considered an appropriate analogue, the warm climate interval must result from increased concentrations of atmospheric greenhouse gases due to a transient forcing and have similar regional and global climate patterns due to continental configuration and orogenic effects. Studies of potential analogues have focused on warm intervals during the Cenozoic including the early Holocene, last interglacial, early Pliocene, early Miocene, and early Eocene. (e.g. Zubakov and Borzenkova, 1988; Crowley, 1991; Zachos et al., 2001).

The warm intervals of the Quaternary (early Holocene and the Pleistocene interglacials) all have the same position of continents and mountain ranges. However, evidence from trace gas records in ice cores indicate that atmospheric concentrations of CO_2 are already higher than at any time during the last 800,000 years (Siegenthaler et al., 2005; Loulergue et al., 2008). Evidence from new alkenone-based, boron isotope-based and stomatal density-based CO_2 proxy data indicate that the current concentration of CO_2 (394.45 ppm recorded in 2012; data from the National Oceanic and Atmospheric Administration's (NOAA) Earth System Research Laboratory, Mauna Loa Observatory) in the atmosphere may not have been reached in the last 3 million years. There is oceanic and terrestrial evidence for a transient forcing-induced warming during the Paleocene-Eocene Thermal Maximum (PETM) (Kennett and Stott, 1991; Zachos et al., 2005). However, the rate of climatic and ocean geochemical change is likely to have been an order of magnitude slower (Rigwell, 2007; Zeebe et al., 2009) and the configurations of continents, ocean gateways, and orogenic belts are widely dissimilar for intervals in Earth history earlier than the late Miocene (23.3-5.3 Ma). The search for an appropriate analogue of future global warming continues even though research concluded that no satisfactory warm intervals in Earth history could be used as a frame of reference or even a possible analogue for future atmospheric CO_2-induced warming (Crowley, 1991; Haywood et al., 2011).

Current research indicates that the mid-Pliocene Warm Period (MPWP; 3.3-3.0 Ma), representing warm interglacials during the Piacenzian Stage of the Pliocene Epoch, serves as the most robust analog to predicted climate changes (IPPC, 2007; Haywood et al., 2011). The Pliocene was remarkably similar to modern climate when compared to other geologically recent warm intervals in terms of positions of the continents, the thermal isolation of Antarctica (Zachos et al., 2001), and atmospheric CO_2 concentrations (Haywood et al., 2009). Even so, Pliocene interglacials reflected long-term equilibrium for a given ambient CO_2 level following the long-term negative trend in atmospheric CO_2 through the Cenozoic and not a rapid transient forcing on climate (Haywood et al., 2011). Evidence from faunal-based transfer functions and isotopic proxies of paleotemperature show the MPWP was approximately 2-3ºC warmer than today (Robinson et al., 2008). Moreover, the spatial distribution of global sea surface temperature (SST) during the MPWP was different from today because northern high latitudes were warmer, while temperatures in the tropics were similar (Dowsett et al., 2010; Federov et al., 2006).

General circulation models (GCM) using MPWP boundary conditions produce surface temperature anomalies in the range of late twenty-first century climate projections (Haywood et al., 2001). Still, discrepancies exist between proxy evidence and GCM simulations (Dowsett et al., 2009). For example, hypotheses for both permanent El Niño and La Niña conditions have been modeled and documented in alkenone-based SST reconstructions (Lawrence et al., 2006; Dowsett and Robinson, 2010). A Pliocene climate dominated by either permanent state is significantly different from modern climate conditions. The discrepant results are likely due to proxy resolution. The temporal resolution of the paleoceanographic data based on microfossil analyses to determine MPWP boundary conditions is at best one sample spanning 10,000 years (Wara et al., 2005). High-resolution (annual to multi-decadal) paleoclimate records potentially provide SST variability at a resolution capable of testing the environmental response to interannual atmospheric/oceanic phenomena.

1.2 Research Purpose

The purpose of this dissertation is to develop and employ classic and new high-resolution bivalve proxy records to reconstruction oceanic conditions in the near and distant past. In this series of studies, high-resolution records from live-collected clams from the Mid Atlantic Bight (MAB) and fossil Pliocene bivalves from fossiliferous units along the US Mid Atlantic Coastal Plain (MACP) are examined and compared to modern instrument records. High-resolution data sets recorded in bivalve shells are more analogous to instrumental observations than fossil assemblage data. Comparing modern climate records to Pliocene data series is necessary to better constrain uncertainties of future climate prediction. The estimation and comparison of past sea water temperatures to modern records allow the study of other larger questions about global warming intervals, such as: (1) are significant changes in interannual variability experienced along the western Mid Atlantic Shelf; (2) are there shifts in the boundaries of shelf province waters due to these changes; and (3) are past natural (pre-industrial) ocean-atmospheric interactions similar to baseline anthropogenically-altered modern analogues.

Previous research using faunal assemblages of ostracodes, foraminifera, molluscs, bryozoans, and echinoids have established that SST along the western mid-Atlantic shelf was warmer than the present throughout most of the Cenozoic (Dowsett et al., 2009). Mean SST decreased from Early to Late Pliocene, following the Cenozoic cooling trend into the Pleistocene. While previous research has examined Pliocene SST variation and seasonality in MACP deposits, little is known about interannual variability in the Pliocene and how it compares to present conditions. Interannual variability of modern SST in the MAB is related to a combination of local atmospheric processes and advection of water masses into the shelf area (Mountain, 2003). Warmer SST in the Pliocene may result from more frequent and northern penetration of warm water masses, a decline in the influence of northern cold waters, and/or different tropical perturbations to atmospheric circulation.

Much warmer winter SST during the Pliocene indicates reduced seasonality in MACP shelf waters, suggesting more stable warming mechanisms and diminished interannual variability (Krantz, 1990; Cronin, 1991). However, this scenario conflicts with colder winter and summer MPWP temperatures and a larger seasonal range in Virginia (Goewert and Surge, 2008). A more likely scenario is that winter SST along the MACP was warmer, but that the large interannual variability exhibited in the modern MAB also existed in the Pliocene. This hypothesis agrees with observed faunal data from the MACP. A reconstruction of interannual to decadal trends in SST provides evidence to test the validity of previously conflicting results.

1.3 Dissertation Organization

This research uses fossil bivalves as seawater temperature proxies for a Pliocene paleoenvironmental reconstruction capable of examining interannual to decadal trends in MAB shelf water variability. Bivalve proxies were used to explore aspects of climate change along the coastal shelf regions of the eastern United States. This research is based on modern analog techniques. All methods and data are compared to instrumental data from the late Holocene, but the overall goal is investigating the climate of the Pliocene (5.4-1.8 Million years ago (Ma)). The MACP is an ideal location for this research. The present MAB shelf is well instrumented, and the modern bivalve proxies are well studied due to commercial exploitation. Also, MACP shell beds contain numerous well-preserved molluscs and well-documented biostratigraphy and chronology. This work provides much needed proxy data for models attempting to reconstruct environmental and climatic changes in shallow marine settings along the low to mid-latitudal gradient of the western Atlantic shelf and those evaluating the response of regional teleconnections such as North Atlantic Oscillation.

Chapter 2 provides the background to the dissertation. This includes a brief review of the geologic history and large physiographic provinces of the eastern United States, modern oceanographic setting, and instrumental records and studies used to examine average and anomalous climate conditions in and along the MAB. A review of the North Carolina and Virginia fossil beds is also provided. Chapter 2 details the known ecology of the selected bivalve proxies, basic sclerochronological methods and assumptions, and previous works using growth increment and/or isotopic methods to investigate these proxies.

Chapter 3 is the first of the original research studies. It addresses precision of a single shell reader and how the lack of a second experienced shell reader is dealt with by means of computer-assisted quality control. Age determination for live-caught bivalves is simple, but labor intensive if there is a large number of samples. Good practices assume that each sample must be examined by several readers, several times for age determination to be considered accurate, and thus requires time. This challenge is addressed by using a novel image analysis-based method of discriminating annual increments in the shell.

Chapter 4 is a reexamination of the infaunal bivalve species *Spisula (Hemimactra) solidissima* (Dillwyn, 1817), the archetype for contemporary increment and isotope sclerochronology experiments. *S. s. solidissima* studies by Jones (1983) set standard sclerochronological practices that remain unchanged, but the potential applications expressed in those earlier works are currently possible with the expanded number and range of new *S. (s). solidissima* specimens. Using isotope sclerochronology, this work investigates the periodicity of growth intervals in the species *S. s. solidissima*, *S. s. similis* (Say, 1822), and *S.(Hemimactra) confraga* (Conrad, 1833)(Pliocene), and estimates paleoenvironmental conditions during the Recent and the Pliocene using isotope and increment comparisons to instrumental records. These data increase our knowledge of Pliocene climate along the MACP, and are compared to modern environmental conditions.

Chapter 5 is an investigation of the periodicities in growth-lines for aging two species of bivalves, *Glycymeris americana*, the American bittersweet, and *Panopea reflexa*, a geoduck. The purpose of the study is to identify whether these species, both large and abundant in MACP fossiliferous units, can be useful in constraining climatic variables of the Pliocene. *G. americana* is currently found in the waters off North Carolina, but no previously published research has confirmed age or paleoenvironmental calibration. Studies on the extant species *G. glycymeris* show annual growth-lines and maximum lifespans of ~100 years (Ramsay et al., 2009). Previous work on extant species of geoduck (*P. zelandica* (Quoy & Gaimard, 1835), *P. abbreviate* (Valenciennes, 1839) and *P. abrupta* (Conrad, 1849)) indicate the genus has annual growth-lines, is long-lived with maximum lifespans of 34 to 146 years, and is suitable for regional SST reconstructions (Black et al., 2009).

LITERATURE CITED

Chandler, M., D. Rind, and R. Thompson. (1994). Joint investigations of the middle Pliocene climate: II. GISS GCM Northern Hemisphere. *Global Planetary Change*, 9:197-219.

Cronin, T.M. (1991). Pliocene shallow water paleoceanography of the North Atlantic Ocean based on marine ostracodes. *Quaternary Science Review*, 10: 175-188.

Crowley, T. J. (1991). Are there any satisfactory geologic analogs for a future greenhouse warming. *Journal of Climatology*. 3, 1282–1292.

Dowsett, H. J., Robinson, M., Haywood, A. M., Salzmann, U., Hill, D. J., Sohl, L., Chandler, M. A., Williams, M. Foley, K. and Stoll, D. (2010). The PRISM3D paleoenvironmental reconstruction. *Stratigraphy,* 7, 123–139.

Dowsett, H.J., M.A. Chandler, T.M. Cronin, and G.S. Dwyer. (2005). Middle Pliocene sea surface temperature variability. *Paleoceanography*, 20: 1-8.

Dowsett, H.J., J.A. Barron, R.Z. Poore, R.S. Thompson, T.M. Cronin, S.E. Ishman, and D.A.Willard. (1999). Middle Pliocene paleoenvironmental reconstruction: PRISM2. U.S.Geological Survey Open File Report, 99-535: 1-33.

Dowsett, H.J. and R.Z. Poore. (1991). Pliocene sea surface temperatures of the North Atlantic Ocean at 3.0 Ma. *Quaternary Science Review*, 10: 189-204.

Dowsett, H.J. and T.M. Cronin (1990). High eustatic sea level during the middle Pliocene: Evidence from the southeastern U.S. Atlantic Coastal Plain. *Geology*, 18: 435-438.

Fedorov, A. V., Brierley, C. M. & Emanuel, K. (2010). Tropical cyclones and permanent El Niño in the early Pliocene epoch. *Nature* , 463, 1066–1070.

Fedorov, A. V., P. S. Dekens, M. McCarthy, A. C. Ravelo, P. B. deMenocal, M. Barreiro, R. C. Pacanowski, and S. G. Philander, (2006). The Pliocene paradox (mechanisms for a permanent El Niño). *Science,* 312, 1485–1489.

Goewert, A.E. and D. Surge. (2008). Seasonality and growth patterns using isotope sclerochronology in shells of the Pliocene scallop, *Chesapecten madisonius*. *Geo-Marine Letters* 28: 327–338.

Goman, M., Ingram, B.L., Strom, A., (2008). Composition of stable isotopes in geoduck (*Panopea abrupta*) shells: A preliminary assessment of annual and seasonal paleoceanographic changes in the northeast Pacific. *Quaternary International*, 188: 117-125.

Haywood, AM, Ridgwell, A, Lunt, DJ, Hill, DJ, Pound, MJ, Dowsett, HJ, Dolan, AM, Francis, JE and Williams, M (2011). Are there pre-Quaternary geological analogues for a future greenhouse warming? Philos. *Trans. R. Soc. A-Math. Phys. Eng. Sci*., 369, 1938.

Haywood, A. M., Chandler, M. A., Valdes, P. J., Salzmann, U., Lunt, D. J. & Dowsett, H. J. (2009). Comparison of Mid-Pliocene climate predictions produced by the HADAM3 and GCMAM3 general circulation models. *Glob. Planet. Change*, 66, 208–224.

Haywood, A.M., Valdes, P.J., Sellwood, B.W., Kaplan, J.O. Dowsett, H.J. (2001). Modelling Middle Pliocene warm climates of the USA. *Palaeontologia Electronica*, v.4, art.5. (available at: http://palaeo electronica.org/2001_1/climate/issue1_01.htm)

Haywood, A.M., P.J. Valdes, and B.W. Sellwood. (2000). Global scale palaeoclimate reconstruction of the middle Pliocene climate using the UKMO GCM: initial results. *Global and Planetary Change*, 25: 239-256

International Panel on Climate Change (2007), Climate change 2007: The physical science basis. In Contribution of Working Group I to the Fourth Assessment Report of the Intergovernmental Panel on Climate Change (eds S. Solomon, D. Qin, M. Manning, Z. Chen, M. Marquis, K. B. Averyt, M. Tignor & H. L. Miller). Cambridge, UK: Cambridge University Press.

Jones, D.S. and I.R. Quitmyer. (1996). Marking time with bivalve shells: oxygen isotopes and season of annual increment formation. *Palaios*, 11: 340-346.

Jones, D.S. (1983). Sclerochronology: reading the record of the molluscan shell. *American Scientist*, 71: 384-391.

Jones, D.S., D.F. Williams, and M.A. Arthur (1983). Growth history and ecology of the Atlantic surf clam Spisula solidissima (Dillwyn), as revealed by stable isotopes and annual shell increments. *J. Exp. Mar. Biol. Ecol*., 13: 225-242.

Jones, D.S. (1981). Annual growth increments in shells of Spisula solidissima record marine temperature variability. *Science*, 211, 4478: 165-167.

Jones, D.S. (1980). Annual cycle of shell growth increment formation in two continental shelf bivalves and its paleoecologic significance. *Paleobiology*, 6(3): 331-340.

Jones, D.S., I. Thompson, and W. Ambrose (1978). Age and growth rate determinations for the Atlantic surf clam Spisula solidissima (Bivalvia: Mactracea), based on internal growth lines in shell cross-sections. *Marine Biology*, 47: 63-70.

Jones, P.D., K.R. Briffa, T.P. Barnett and S.F.B. Tett (1998). High-resolution palaeoclimate records for the last millennium: interpretation, integration and comparison with General Circulation Model control-run temperatures. *The Holocene*, 8(4). 455-471

Jones, P. D., and M. E. Mann (2004), Climate over past millennia, *Rev. Geophys*., 42, RG2002

Krantz, D.E. (1990) Mollusk-Isotope Records of Plio-Pleistocene Marine Paleoclimate, U.S. Middle Atlantic Coastal Plain. *Palaios*, 5: 317-335.

Kennett, J. P. and Stott, L. D. (1991), Abrupt deep-sea warming, palaeoceanographic changes and benthic extinctions at the end of the Paleocene. *Nature* 353, 225–229.

Meehl, G.A., T.F. Stocker, W.D. Collins, P. Friedlingstein, A.T. Gaye, J.M. Gregory, Kitoh, R.Knutti, J.M. Murphy, A. Noda, S.C.B. Raper, I.G. Watterson, A.J. Weaver, Z.-C. Zhao. (2007). Global climate projections. In: S. Solomon, D. Qin, M. Manning, Z. Chen, M. Marquis, K.B. Averyt, M. Tignor, and H.L. Miller (Eds.), The Physical Science Basis. Contribution of Working Group I to the Fourth Assessment Report of the Intergovernmental Panel on Climate Change, Cambridge University Press, Cambridge, United Kingdom, and New York, NY, USA.

Lawrence KT, Liu ZH, Herbert TD (2006). Evolution of the eastern tropical Pacific through Plio-Pleistocene glaciation . *Science* , 312 5770:79-83

Loulergue, L. et al. 2008 Orbital and millennial-scale features of atmospheric CH_4 over the past 800,000 years. *Nature*, 453, 383–386.

Molnar, P. and M.A. Cane. (2002). El Niῆo's tropical climate and teleconnections as a blueprint for pre-Ice Age climates. *Paleoceanography*, 17: 11.1-11.12

Mountain, D. G. (2003). Variability in the properties of Shelf Water in the Middle Atlantic Bight, 1977–1999, *Journal of Geophysical Research*, 108(C1), 3014

Ridgwell, A. (2007). Interpreting transient carbonate compensation depth changes by marine sediment core modeling. *Paleoceanography*, 22, PA4102.

Robinson, M. M., Dowsett, H. J., Dwyer, G. S. & Lawrence, K. T. (2008). Re-evaluation of mid-Pliocene North Atlantic sea-surface temperatures. *Paleoceanography*, 23, PA3213

Siegenthaler, U. et al. 2005 Stable carbon cycle-climate relationship during the Late Pleistocene. *Science*, 310, 1313–1317.

Wara, M. W., A. C. Ravelo, and M. L. Delaney, (2005). Permanent El Niño–like conditions during the Pliocene warm period. *Science*, 309, 758–761.

Weidman, C.R., Jones, G.A. and Lohmann, K.C. (1994). The long-lived mollusk *Arctica islandica*- A new paleoceanographic tool for reconstruction of bottom temperatures for the continental shelvs of the northern North-Atlantic Ocean. *Geophys. Res.-Oceans*, 99: C9, 18305.

Zachos, J. C. et al. (2005), Rapid acidification of the ocean during the Paleocene–Eocene Thermal Maximum. *Science*, 308, 1611–1615.

Zachos, J., M. Pagani, L. Sloan, E. Thomas, and K. Billups. (2001). Trends, rhythms, and aberration in global climate 65 Ma to present. *Science*, 292: 686-693.

Zeebe, R. E., Zachos, J. C. and Dickens, G. R. (2009). Carbon dioxide forcing alone insufficient to explain Palaeocene–Eocene Thermal Maximum warming. *Nat. Geosci.* 2, 576–580.

Zubakov, V. A. and Borzenkova, I. I. (1988). Pliocene palaeoclimates: past climates as
possible analogues for mid-twenty-first century climate. *Palaeogeogr. Palaeoclimatol. Palaeoecol.* 65, 35–49.

CHAPTER 2: BACKGROUND

2.1 PURPOSE

The study of climate in the past, present and future is essential to society This dissertation focuses on using bivalve proxies to explore aspects of climate change along the coastal shelf regions of the eastern United States. All of the methods and data are anchored in late Holocene/Anthropocene climate studies, but the overall goal is investigating the climate of the Pliocene (5.4-1.8 Million years ago (Ma)). The Pliocene represents the last epoch before the Earth shifted completely into an icehouse world after the long Cenozoic transition from the late Mesozoic greenhouse. There is well-documented evidence that global temperature and atmospheric CO_2 levels are directly related, and that both steadily declined through the Cenozoic. They reached their lowest levels during the Quaternary. However, in the last decades of the Holocene, atmospheric CO_2 levels rose and are now projected to reach levels not present in the atmosphere since the Pliocene.

The mechanisms driving atmospheric CO_2 levels in the late Holocene are different than the mechanisms altering atmospheric CO_2 concentrations during the Pliocene. Natural forcing mechanisms operating on timescales of thousands to millions of years forced CO_2 levels to rise and fall during the Pliocene. In comparison, atmospheric CO_2 concentrations are rising in the late Holocene in hundreds of years.

However, some conditions during the Pliocene are similar to today or the probable near future. For example, the distribution of continents and ocean basins are in similar configurations. Estimates of mid-ocean spreading and continental collision rates are unchanged since Pliocene times, so mountain ranges are in the same locations and similar in elevation, ocean basins are similar in width, and volcanic activity is likely comparable. The physical and biological processes that sculpt our dynamic planet (insolation, wind and ocean circulation patterns, weather, erosion, respiration, photosynthesis, bioturbation, etc.) remain unchanged, though the exact biological species and topography do vary. Most importantly for society (at least for government planners), though the rate of cause and effects are different, the concentrations of CO_2 and the expected temperatures are similar.

Methods successful in deciphering shell isotopic data from the mid Pliocene Warming Period (MPWP; 3.2-2.5 Ma) and various Quaternary intervals demonstrate that marine bivalve fossil records potentially provide a unique opportunity to study environmental trends during climate change episodes prior to the instrumental record. Results from this dissertation research provides much needed proxy series data for modelers attempting to reconstruct environmental and climatic changes in shallow marine settings along the low to mid-latitudal gradient of the Atlantic Coastal Plain. These proxy time series also have temporal resolution high enough to investigate interannual to decadal climate phenomenon.

Earth's climate is a result of incoming solar radiation interacting with the dynamic earth systems of the hydrosphere, lithosphere, atmosphere, asthenosphere and biosphere. Today's climate is the outcome of the complex interactions and feedbacks between all of these systems, integrated over the billions of years of Earth history. For scientists to accomplish the essential societal task of predicting future climate, an understanding of present day and past climate is necessary. The continuing debate over future climate change stems from the temporal limitations of the instrumental record. The paleo-scientific community, espousing uniformitarian idealism, asserts that effective proxies can expand the instrumental record into the past and reduce the large uncertainties in future climate projections. But if to say that the study of climate since ~1900 (global instrumental record) is difficult and marginally adequate, then the study of much earlier climate is even more demanding and uncertain. Paleoclimatology, paleoceanography and paleoecology are based on robust physical and chemical geologic principles, (e.g., the movement of continents, distribution of ocean basins, etc.) and plausible assumptions underlying proxy estimations (e.g., biological uniformitarianism, climate effects on biologically induced mineralization, etc.). To effectively study present and past regional climate along the coastal regions of the eastern United States, it is important to distinguish between these extremes by summarizing what is known and what is assumed.

2.2 BACKGROUND

2.2.1 Physical Geographic Setting

The western North Atlantic continental margin is a passive margin junction between the continent and the ocean basins. The secondary physiographic features on the continent include the mountains, hills, plateaus, plains, and shelves. These physiographic features are separated by major faults, systems of folds and faults, and measurable differences in elevation and relief (Figure 2.1). Smaller physiographic features are formed through irregular erosion and deposition by geologic agents such as glaciers, streams, marine currents, waves and mass movements. Most of the Atlantic continental margin has been smoothed by sediments brought to the ocean by streams that eventually become eroded by wave action. These sediments prograde seaward across the continental shelf and slope and have constructed continental rises and abyssal plains, burying the irregular underlying topography.

The oldest and largest physiographic province, extending from the Arctic Circle to the St. Lawrence Valley and the Great Lakes, is the Laurentian Upland. The Laurentian Upland is the shield of Precambrian igneous and metamorphic rocks that was originally a mountainous region that has since eroded and produced the great quantities of sediment that were deposited in surrounding areas to form most of the other land area of North America. Glaciation during the Pleistocene Epoch produced surface erosional features on the bedrock and depositional features of glacial excavation and drift.

The Interior Plains province lies south of the Laurentian Upland and forms the broad saddle between the Appalachian Mountains and the Rocky Mountains. The central and southern portions of the Interior Plains consist of Paleozoic basins and domes of terrigenous beds, carbonate rocks, and evaporites overlain by Cenozoic alluvium. The northern edge is occupied by the Great Lakes, depressions carved by Pleistocene glaciers by way of the St. Lawrence River. Glaciers also had a considerable effect on the sedimentary regime of the continental shelf throughout the Susquehanna River to the Chesapeake Bay and the Mohawk and Hudson Rivers to the New York area of the Mid-Atlantic Bight. The northeasterly extension of the Interior Plains, the St. Lawrence Lowland, was depressed as much as 180 m during the glaciations. During glacial retreat drainage shifted from the Mississippi River to the northeastern river basins, sometimes with catastrophic outburst floods (Lewis and Teller, 2007).

The Appalachian Highlands occur on the Atlantic side of the Interior Plains. They extend from New England about 1,900 km to the southeastern United States and consist of the Adirondacks, Valley and Ridge, Blue Ridge, Appalachian Plateau, and Piedmont provinces. While well exposed in the northeast, the Appalachians dip and are buried beneath the coastal plain in the southeast. The Appalachian Plateau is the westernmost province, where the rocks consist mainly of late Paleozoic terrigenous sedimentary units, are nearly horizontal and undisturbed. The province is bounded on all sides by in-facing slopes that reflect a general synclinal structure. The Plateau province has undergone considerable fluvial erosion, and the northern part has been altered by glaciation.

The Piedmont is the easternmost province of the Appalachian Highlands and is the least mountainous. Its elevation above modern sea level ranges from about 60 m in the north to about 550 m in the south. The Piedmont is the expression of uplands with moderate relief containing several lowlands floored with Triassic sedimentary rocks. These Triassic basins, which represent fault troughs, extend from Canada to Florida and demarcate the rift zone of the early Atlantic basin. The boundary between the Piedmont and the Atlantic coastal plain is known as the Fall Line, where differences in the hardness of rocks on either side cause the rivers descending onto the coastal plan to drop over a series of rapids and waterfalls.

The coastal plain along the Atlantic coast of the eastern United States consists of one carbonate plateau (the Florida platform) and two terrigenous embankments (the Atlantic and Gulf coasts). The Atlantic terrigenous embankment extends from Cape Cod to northern Florida, and the one in the Gulf of Mexico lies between Florida and the Yucatan platforms. The Atlantic embankment is divided into a northern embayment, the Mid-Atlantic Bight (MAB),that extends from Cape Cod to Cape Hatteras, and the South Atlantic Bight (SAB) that extends from Cape Hatteras to northern Florida. These embayments are characterized by estuaries that extend inland as far west as the Fall Line, and narrow peninsulas (called arches) separate the embankments (Figure 2.2). The coastal plain consists of Cenozoic silisiclastic and carbonate strata overlaying Cretaceous evaporites and Paleozoic basement. East of New York City, the coastal plain is completely submerged except for a chain of islands formed by moraines and glacial outwash deposited during the latest glacial advance. These islands are part of an escarpment (the Orangeburg Scarp, Figure 2.3-cross-section) that can be traced from the Grand Banks as far south as the Chesapeake Bay. The crest of the Orangeburg Scarp consists of Upper Cretaceous strata that are overlain seaward by Tertiary beds. The SAB portion of the Atlantic coastal plain differs from the MAB by its lesser submergence.

The escarpment topography (Figure 2.3-cross-section) is less well developed than farther north.

The Florida platform is a region dominated by carbonate deposits and consisting of a high central area (the Ocala uplift-Peninsular arch) surrounded by extensive marine terraces, swampland, karst topography, and active and inactive coral reefs. The Ocala high is the major surface structural feature of the Florida peninsula, and uplift appears to have begun during the Eocene and continued into the Miocene. Prior to the Ocala uplift, the ancestral Gulf Stream (Florida Current) flowed through the Gulf Trough and Suwannee Strait of northern Florida and Georgia resulting in the warm current flowing across portions of the Carolina shelf, facilitating subtropical skeletal carbonate deposition (Coffey and Read, 2007). The Florida platform also displays a well-developed artesian system, having springs that discharge along the shore and on the continental shelf. These features formed during the lower sea level of glacial episodes of the Plio-Pleistocene (Swart and Price, 2002).

Topographic and sedimentary studies indicate that the surface of the coastal plain is indented by broad, flat areas termed “terraces” (Figure 2.3-cross-section). Various workers have used these coastal terraces to reconstruct former shorelines, former sea levels, and the complex stratigraphic sequences of marine and continental deposits along the Atlantic coastal plain (Blackwelder, 1981; Cronin, 1988; Krantz, 1991). As many as nine of these features, ranging in elevation from 3 to 82 m, exist along the Atlantic coast. They dip gently seaward and commonly are separated by distinct changes in slope that are escarpments probably carved by marine erosion. The most prominent are the Surry and Suffolk scarps (elevations 27-30 m and 6-9 m, respectively). These coastal scarps likely indicate interglacial stages when sea level was higher than at present. The recovery of Pleistocene-aged micro- and macrofossils indicate that the linear features and flat surfaces below the Surry scarp are marine in origin and Pleistocene in age. Features above the Surry scarp are the result of late Miocene to late Pliocene marine erosion and deposition followed by preglacial alluvial and estuarine deposition (Cronin, 1981; Gibson, 1983; Dowsett and Cronin, 1991). Analogous features, like Block Island (-40 m) and Fortune Shores (-80), are subtidal terraces that represent the position of a stillstand sea level during the Pleistocene (Krantz, 1991).

The continental shelf off the eastern United States can be divided into three major sections and associated with the chief process that shaped their topography. These three sections are Georges Bank-Scotian Shelf (GBS; glacial, meltwater, and marine deposition), MAB shelf (glacial, meltwater and marine deposition), and SAB shelf (marine deposition). The average width of the shelf is about 200 km, with the widest lengths to the shelf break in the northern GBS section (~500 km). Along the MAB section, the shelf is again widest in the northern portion and narrows to less than ~25 km adjacent to Cape Hatteras. After Cape Hatteras the SAB shelf widens but again narrows to less than a kilometer along the southern Florida coast.

2.2.2 Sedimentology

The continental shelf is dominated by siliciclastics (deposition of eroded Laurentian terrains) with a transition zone to a mixed carbonate–siliciclastic system south of the Carolinas (Figure 2.4, sediment sand percentage). The surficial sediments are primarily Tertiary in age and are overlain in locations by Quaternary alluvium (Reid et al., 2005). Glacial till and outwash deposits are present in both the GBS and MAB sections. Along the GBS section glacial deposits are less than 30 m thick, occurring along the shallowest bank tops, while in the MAB glacial deposits form the irregular island chain (end moraines, Long Island to Block Island) atop the Orangeburg escarpment.

Moving south along the MAB and into the SAB, coarse sediments (sands and shell hash) form waves and ridges nearly perpendicular to the shore. Near shore sand waves and ripples are altered by tides and major storm events and move generally southeastward along the shelf. Modern movement of deeper water sand waves on the continental shelf is less likely than in shallow water. Studies have found that the coarse-grained features are rather persistent, and there is little evidence of onshore sediment transport from deep waters (Gutierrez et al., 2005). These studies indicate that near shore deposits are likely former barrier beaches, while deeper sandy areas on the continental shelf are relicts from times of lower sea level.

Most all subtidal sediments are covered with a thin (millimeters) fluffy and easily re-suspended layer of fine-grained particles dominated by calcium carbonate (foraminifera) and lesser amounts of illite and chlorite clays (glacial and terrigenous in origin) (Walsh et al., 1988; Biscaye et al., 1994). This easily re-suspended sediment layer is underlain by a tens of centimeters thick layer of compacted sediment with the same biologically dominated components. Large-scale sediment surveys using cores and grab samples, such as those deployed by the USGS (usSEABED) and the Shelf Edge Exchange Processes (SEEP) experiments, indicate that this fine sediment is a late Holocene accumulation (since the flattening of post glacial sea level rise). Though easily transported along the MAB shelf, only a small portion escapes the shelf and is transported to the slope (Biscaye et al., 1994; Reid et al., 2005).

2.2.3 Oceanographic Setting

Shelf Water (SHW) is the primary water mass in the MAB (Chapman et al., 1986; Mountain 2003). It is generally cooler and lower in salinity than the oceanic waters seaward of the shelf, commonly termed the Slope Water (SLW). The boundary between these two water masses occurs in a narrow transition region, the shelf/slope front. Much of SHW in the MAB is formed as a water mass in the Gulf of Maine. Cold, low-salinity Scotian Shelf water (SSW) enters the gulf in the surface layer around Cape Sable, and the warmer, more saline SLW enters the gulf at depth through the Northeast Channel (Fairbanks, 1982). These two water masses mix as they circulate around the gulf. From the western gulf the product of this mixing enters onto the northern side of Georges Bank to flow clockwise around the bank and then westward from the bank’s southern flank past Nantucket Shoals and into the MAB. Once in the MAB, the properties of the SHW are modified locally by seasonal heating and cooling, by local precipitation and river runoff, and by mixing with the offshore SLW. However, much of the freshwater component of the SHW in the MAB is part of a large scale, buoyant coastal current system that extends from Labrador to Cape Hatteras (Fairbanks, 1982; Chapman et al., 1986; Chapman and Beardsley, 1989).

SHW leaves the MAB through several processes. Some SHW traverses the length of the MAB and leaves the shelf near Cape Hatteras, where it flows eastward along the northern edge of the Gulf Stream (GS) (Churchill et al., 1989, 1993). Warm core GS rings can entrain SHW when they impinge upon the edge of the shelf. Smaller scale mixing and exchange also occur between the SHW and SLW at the shelf/slope front. The SEEP I (Walsh et al., 1988) and SEEP II (Biscaye et al., 1994) did extensive studies of the cross frontal exchange in the MAB. While the transport of SHW into the MAB can be directly measured (e.g., Beardsley et al., 1985, Lentz, 2005b), the processes removing SHW from the MAB are much more difficult to measure and act along the entire length of the shelf. Quantitative estimates of the rate SHW is removed by the various processes listed above and of seasonal or interannual variations in those rates are not well documented.

The hydrography of the southern Mid-Atlantic Bight (MAB) has many features that are characteristic of the entire bight (Beardsley et al., 1976; Csandv and Hamilton, 1988; Mountain, 2001). The overall drift of the shelf waters is to the southwest (Mountain, 2001; Lentz, 2008a). A permanent thermohaline front exists between the relatively fresh shelf surficial waters and the more marine waters of the slope. The SHW undergoes large seasonal variations and stratification fluctuations from winter to summer. Large direct runoff into the MAB is primarily by fresh water discharge from the Hudson, Delaware, and Susquehanna Rivers. Freshwater discharges are modified through wave and tidal mixing as they pass through their associated embayments (New York, Delaware and Chesapeake Bays), and SHW salinity is also modified by the proximity of the GS and eddies shed from it (Figure 2.3).

The vigorous vertical and horizontal mixing in the MAB is caused by cooling and storms that occur during the late winter-early spring that resets the shelf each year(Beardsley et al., 1976; Csandv and Hamilton, 1988; Mountain, 2001). At this time the shelf is vertically well mixed and the mid-shelf horizontal property gradients are at a minimum. The shelf, because of its relatively shallow depths, is colder as well as fresher than the SHW offshore. Mid-shelf temperatures reach their seasonal minima between 5 and 7°C, while mid-shelf salinities are about 34 psu (practical salinity units). Offshore of the shelfbreak front, slope water temperatures and salinities for the same depth range are typically about 12°C and 35.3 psu, respectively (Csandy and Hamilton, 1988). The low salinity water flows southward close to shore because the prevailing winds during this period are from the northeast.

In late spring, the decrease in wind forcing, combined with increased insolation, causes the near-surface waters to warm, forming a 10-15 m thick seasonal thermocline at a depth of about 20 m. Below the thermocline, remnant winter water is isolated from the seasonal warming. This substantial body of cold water is referred to as the "cold pool" and is regularly found along the outer half of the shelf (Houghton et al., 1982). The water within the cold pool flows southward and is replenished from farther north, causing the annual minimum bottom temperatures on the outer shelf to occur in summer. The cold pool waters along the shelf warm gradually through heat flux from above (Wallace, 1994) and through the shelf-slope front (Houghton et al., 1994). These cold pool waters remain enriched in nutrients as surficial waters become depleted, resulting in a near constant supply of food to bottom-dwelling fauna (Wood and Sherry, 1993). The constant density of this chlorophyll-rich water may contribute to the nutrient budget of Atlantic surface waters through a long loop of circulation that transports deep water from the Labrador Sea to Cape Hatteras (Wood and Sherry, 1993).

Surface water salinity is also lower in the summer, partly as a result of increased freshwater discharge from the bays and the Hudson River. Contributing to the lower surface salinities are the prevailing summertime winds from the south. These upwelling-favorable winds tend to retard the southward, near-shore flow of the fresh water and drive the surface water offshore. The seasonal thermocline dominates the density structure of the upper water column, diffusing the intensity of the shelf-slope front at the surface. Even though the shelf surface temperatures reach 20-25°C, surface temperatures tend to increase offshore due to the impact of the warm Gulf Stream waters on the slope sea (Mountain and Holzwarth, 1989).

2.2.4 Geologic Setting and Stratigraphy

This study focuses on unconformity-bound marine deposits of the Pliocene of North Carolina and Virginia (Figure 2.2). These locations were chosen because of their proximity to important oceanographic and atmospheric circulation features. For example, the GS, which strengthened during the Miocene, became enhanced with the closure of the Panama Isthmus during the Pliocene (Cronin 1988; Cronin and Dowsett, 1996; Haug and Tiedemann, 1998, Haug et al., 2001). Moreover, as stated in the 2007 IPCC report, the mid Pliocene is important because it is similar to projections of future 21st century climate change (Meehl, et al., 2007). Similarities include: the continents and oceans have similar configurations, the interior of the continents were and are expected to be arid, estimated temperature ranges are similar, atmospheric CO_2 levels were and are expected to be higher than today, and sea and continental ice were and are expected to be reduced. The report explicitly states that the mid Pliocene "presents a view of the equilibrium state of a globally warmer world."

Pliocene sampling focused on the unconsolidated Tertiary sediments of the US Middle Atlantic Coastal Plain (MACP). The lithostratigraphy, biostratigraphy, and chronostratigraphy of the MACP have been extensively studied since the 19th century (Figure 2.5). The MACP was also the first study area that Pliocene Research, Interpretation and Synoptic Mapping project (PRISM) used to test the feasibility of their transfer function (Dowsett and Poore, 1990). PRISM was initially devised to reconstruct surface conditions from a focused stratigraphic interval (3.264 - 3.025 Ma = PRISM interval). The PRISM2 reconstruction (Dowsett et al, 1999) represents the most complete and detailed global reconstruction of climate and environmental conditions older than the last glacial maximum (18-21 ka) (CLIMAP, 1982). Bivalve shells were collected from the Rushmere (3.5-3.1 Ma) and Moore House (3.1-2.5 Ma) Members of the Yorktown Formation (Fm) (PRISM Mid-Pliocene Warm period (MPWP)) of Hampton Roadstead and the Edenhouse Member of the Chowan River Fm (2.5-1.9 Ma) of North Carolina (Mansfield, 1931; Petuch, 1982; Krantz, 1990). The litho- and biostratigraphy of the Yorktown and Chowan River Fms indicate open-marine conditions with normal-marine salinity (Ward and Strickland, 1985). The Yorktown Fm represents tropical to warm-temperate climatic conditions and has been dated using nannofossil assemblages (Hazel, 1971; Cronin and Hazel, 1980; Cronin et al., 1984) and molluscan biozones (Ward and Blackwelder, 1976; Blackwelder, 1981b). The Rushmere and Moore House Members contain molluscan assemblages (including *Strigilla* and *Dinocardium*), which indicate a pronounced episode of warming reflecting tropical conditions (Ward, 1998). The Chowan River Fm contains a molluscan assemblage entirely warm-temperature in nature, and therefore represents cooling conditions (Ward and Gilinsky, 1993). These different assemblages represent the shifting influence between warm tropical waters penetrating more northward during the middle Pliocene and cool boreal waters reaching Cape Hatteras, North Carolina post-Yorktown.

2.2.5 Sclerochronology

Sclerochronology is the study of shell and skeletal growth lines and increments, and provides a means to investigate differences in growth rates, life history, ecology, and environmental conditions (Jones, 1983; Jones and Quitmyer, 1996; Marchitto et al., 2000;

Schöne et al., 2002; Schöne et al., 2003; Walker and Surge, 2006; and many others). The discipline is based on the long accepted knowledge that most bivalves precipitate their shells in isotopic equilibrium with the ambient water, and accrete their shells in response to certain environmental and biological factors. The prominent annual growth lines and increments formed during seasonal temperature stresses are identified from the exterior and cross-section of the shell and are regularly used to determine age of an individual. In long-lived species (e.g. *Arctica islandica, M. mercenaria,* and *Spisula s. solidissima*), aging is done by counting the annual increments. Dates can be assigned to increments, if the time of death is known (Jones, 1979; Jones et al, 1983; Jones, 1989). If the animal was collected alive, articulated and/or the time of death known, then a precise chronology can be constructed. Multiple animals can be cross-dated to extend a chronology past the lifetime of a single individual. Constructing such master chronologies is similar to dendrochronology or 'tree-ring' records.

Most bivalve shells grow in isotopic equilibrium with the waters they inhabit (Williams et al., 1982). Shell growth is primarily related to temperature, but is also related to species fractionation, nutrient supply, and other environmental and biological parameters (Figure 2.6). Shell records of annual growth widths have been used to construct a master chronology along a latitudinal transect and to determine the spatial sensitivity of bivalve individuals to environmental parameters (Schöne et al., 2002). Using variations in the oxygen isotope ratio of shell carbonate ($\delta^{18}O$) between annual growth lines, sea surface temperature (SST) can be estimated with sub-annual or mean annual resolution assuming the $\delta^{18}O_{water}$ value is known or can be constrained (Jones, 1983; Jones and Quitmyer, 1996; Marchitto et al., 2000; Surge et al., 2001; Schöne et al, 2002). Therefore, the combination of sclerochronology and stable isotopes can be used to investigate the physical, chemical, and thermal oceanographic divisions in the MACP primarily caused by the changing intensity and penetration of the tropical and boreal waters.

Two socially important implications of this type of research are: (1) the effective management of on- and offshore commercial fisheries and shellfisheries; and (2) ecosystem and environmental monitoring. Fisheries managers keep track of catch amounts and ages to ensure that overfishing will not be the leading cause of a fish stock collapse. This is an essential task to ensure a stable commercial fishing market and the jobs, consumers, and communities associated with fishing. The purpose of ecosystem and environmental monitoring can refer to either tracing pollutants, for example human-made runoff into Chesapeake and Florida Bays that kill oyster bars and reef tracks, or to using bivalve biological responses to monitor long-term variations like those from climate change.

Two geological important implications of growth lines are sources of paleoecology and paleoenvironment information. For example, periodic lines can provide evidence on the time of year an organism was born, its lifespan, rate of growth, breeding periodicity, and season of death. Applied to fossil populations, similarity in the patterns of disturbance lines or of periodic lines can potentially determine which members of the population had lived (and died) at the same place and time. In some circumstances it may be possible to overlap the records of individuals in a population and construct a chronology of events far exceeding any single lifespan. The presence of disturbance lines or the variation in the spacing of periodic lines can provide paleoenviromental information (e.g., evidence for a variable environment and variability argues for relatively shallow water). Similarly, the presence of an annual growth line may suggest a subtidal habitat or a climate with well-defined seasons, while tidal periodicity lines imply a habitat in or near the intertidal zone. Differences between growth increment series recorded in adjacent populations can be interpreted as there being a physical or chemical barrier between the populations.

2.3. CONCLUSIONS

Climate scientists, science managers, and policy makers responsible for making policy decisions on the intervention and mitigation of human-induced climate must understand the past states of Atlantic circulation to determine its response to increasing greenhouse gas concentrations (IPCC WG1, 2007). To do this, they must understand the geologic boundary settings that permit present conditions. Much of the geologic and hydrologic information about the MAB and MACP region is well documented. Properly using this knowledge to in interpret past conditions is essential in the following studies.

The methods used in this dissertation produce long, sub-annually resolved climate reconstructions of significantly important intervals during the late Cenozoic along the western margin of the North Atlantic basin. Successfully deciphering shell isotopic data from the Recent and MPWP endemic species allow further investigation of various

Quaternary events (e.g. Little Ice Age, Young Dryas, and the Holocene extinction), and demonstrate that marine bivalve fossil records permit a unique opportunity to study physical ocean trends during climate change episodes on long time scales. The results of this work provide much needed proxy series data for modelers attempting to reconstruct environmental and climatic changes in shallow marine settings along the low to mid-latitude gradient of the MACP.

This research is innovative because it incorporates both increment and isotope sclerochronology, and paleoclimatology to understand, reconstruct and compare variations in environmental patterns during warming climate intervals. The estimations and comparisons of past parameter values to modern records allow the study other larger questions about global warming intervals, such as: (1) are there changes in the intensity of geostrophic and thermohaline circulation experienced along the western boundary of the North Atlantic; (2) are there shifts in the boundaries of shelf provinces waters due to these changes in intensity; and (3) are past natural (pre-industrial) ocean-atmospheric interactions similar to the baseline anthropogenically-altered modern analogs or are they radically different?

REFERENCES

Abbott, R.T., (1974), American Seashells, second edition. New York, Van Nostrand Reinhold Company, 663 p.

Abbott, R.T., (1984), Collectible Florida Shells: Melbourne, FL, American Malacologists, Inc., 64 p.

Andrews, Jean, (1971). Shells and shores of Texas: Austin, TX, University of Texas, 365 p.

Arthur, M.A., D.F. Williams and D. S. Jones (1983). Seasonal temperature-salinity changes and thermocline development in the mid-Atlantic Bight as recorded by the isotopic composition of bivalves. *Geology,* 11: 655-659

Bailey, R. H., (1973).Paleoenvironment, Paleoecology, and Stratigraphy of Molluscan Assemblages from the Yorktown Formation (Upper Miocene – Lower Pliocene) of North Carolina; Thesis, University of North Carolina at Chapel Hill

Bane, J.M and D.A. Brooks (1979). Gulf Stream meanders along the continental margin from the Florida Straits to Cape Hatteras. *Geophysical Research Letters*, 6(4). 280-282.

Baringer, M. O. (2001), Sixteen years of Florida current transport at 27 N, *Geophys. Res. Lett., 28,* 3179-3182

Black, B.A., (2009). Climate driven synchrony across tree, bivalve, and rockfish growth increment chronologies of the northeast Pacific. *Marine Ecology*. Progress Series 378, 37–46.

Black, B.A., Boehlert, G.W., Yoklavich, M.M., (2008). A tree-ring approach to establishing climate-growth relationships for yelloweye rockfish in the northeast Pacific. *Fisheries Oceanography* 5, 368–379.

Black, B.A., Gillespie, D., MacLellan, S.E., Hand, C.M., (2008). Establishing highly accurate production-age data using the tree-ring technique of crossdating: a case study for Pacific geoduck (Panopea abrupta). *Canadian Journal of Fisheries and Aquatic Sciences.*

Blackwelder, B.W. (1981a). Late Cenozoic stages and molluscan zones of the middle U.S. Atlantic Coastal Plain. *Journal of Paleontology, Memoir,* 12: Part II.

Blackwelder, B.W. (1981b). Stratigraphy of upper Pliocene and lower Pleistocene marine and estuarine deposits of northeastern North Carolina and southeastern Virginia. *U.S. Geological Survey Bulletin*, 1502-B: B1-B16.

Brunner, C. A. (1983). Evidence for increased volume transport of the Florida Current in the Pliocene and Pleistocene, *Mar. Geol., 54*, 223-235.

Bunn, A.G. (2007). dplR: Dendrochronology Program Library in R. R package version 1.0 URL http://www.R-project.org.

Bunn, A.G. (2008). A dendrochronology program library in R (dplR). *Dendrochronologia*, 26: 115-124

Campbell, L.D. (1976). Paleoecology of the Lone Star Industries Pit, Yorktown Formation (Pliocene), Chuckatuck, Virginia. Ph.D Dissertation: University of South Carolina, XII +184.

Campbell, L.D. (1993). Pliocene molluscs from the Yorktown and Chowan River Formations in Virginia, *Virginia Division of Mineral Resources*. 127: 1-259.

Campbell, Matthew R., (1998), Plio-Pleistocene Bivalvia of the Western Atlantic Ocean: Temporal and Taxonomic Resolution and the Anatomy of an Extinction; Thesis, University of North Carolina at Chapel Hill

Carter, J. G., T. J. Rossbach, Z. P. Mateo, and M. J. Badiali. (2003). Summary of lithostratigraphy and biostratigraphy for the Coastal Plain of the southeastern United States. *Biostratigraphy Newsletter*, 4: 1 chart

Chapman, D.C., J.A. Barth, R.C. Beardsley, and R.G. Fairbanks (1986). On the continuity of mean flow between the Scotian Shelf and the Middle Atlantic Bight. *Journal of Physical Oceanography*, 16: 758

Chiang, T., C. Wu, and S. Chao (2008). Physical and geographical origins of the south China Sea Warm Current. *Journal of Geophysical Research*, 113: C08028

Chintala M.M. and Grassle J.P. (2001). Comparison of recruitment frequency and growth of surfclams, *Spisula solidissima* (Dillwyn, 1817), in different inner-shelf habitats of New Jersey. *Journal of Shellfish Research*, 20: 1177–1186.

Cronin, T.M. (1981). Rates and possible causes of neotectonic vertical crustal movements of the emerged southeastern United States Atlantic Coastal Plain. *Geological Society of America Bulletin*, 92 : 812-833.

Cronin, T.M. (1988). Evolution of marine climates of the U.S. Atlantic coast during the past four million years. *In:* Shackleton, N.J., West, R.G., Bowen, D.Q. (Eds.), The Past Three Million Years; Evolution of Climatic Variability in the North Atlantic Region; a Discussion, *Philosophical Transactions of the Royal Society of London. Series B*: *Biological Sciences*, 318, Royal Society of London, London, 411-430.

Cronin, T.M. (1991). Pliocene shallow water Paleoceanography of the North Atlantic Ocean based on marine ostracodes. *Quaternary Science Review*, 10: 175-188.

Cronin, T.M. and H.J. Dowsett. (1996). Biotic and oceanographic response to the Pliocene closing of the central American Isthmus. *In:* Jackson, J.B.C., Budd, A.F., Coates, A.G. (Eds.), Evolution and Environment in Tropical America. University of Chicago, IL, 76-104.

Cronin, T.M. and J.E. Hazel. (1980). Ostracode biostratigraphy of Pliocene and Pleistocene deposits of the Cape Fear Arch region, North and South Carolina. *U.S. Geological Survey Professional Paper*, 1125-B: B1-B25.

Cronin, T.M., H.J. Dowsett, G.S. Dwyer, P.A. Baker, and M.A. Chandler. (2005). Mid-Pliocene deep-sea bottom-water temperatures based on ostracode Mg/Ca ratios. *Marine Micropaleontology*, 54: 249-261.

Cronin, T.M., L.M. Bybell, R.Z. Poore, B.W. Blackwelder, J.C. Liddicoat, and J.E. Hazel. (1984).Age and correlation of emerged Pliocene and Pleistocene deposits, U.S. Atlantic Coastal Plain. *Palaeogeography, Palaeoclimatology, Palaeoecology*, 47: 21-51.

Dowsett, H.J. and L.B. Wiggs. (1992). Planktonic foraminiferal assemblages of the Yorktown Formation, Virginia, USA. *Micropaleontology*, 38: 75-86.

Dowsett, H.J. and T.M. Cronin (1990). High eustatic sea level during the middle Pliocene: Evidence from the southeastern U.S. Atlantic Coastal Plain. *Geology*, 18: 435-438.

Elliot, M., P.B. deMenocal, K.L. Braddock, S.S. Howe. (2003). Environmental controls on the stable isotopic composition of <u>Mercenaria mercenaria</u>: potential application to paleoenvironmental studies. *Geochemistry, Geophysics, Geosystems*, 4: 1056–1072

Emery, K.O. and E. Uchupi (1972). Western North Atlantic Ocean: Topography, rocks, structure, water life, and sediments. Tulsa, Oklahoma., American Association of Petroleum Geologists, p 532.

Fenger, T., D. Surge, B.R. Schöne, and N. Milner. (2007). Sclerochronology and geochemical variation in limpet shells (*Patella vulgata*). A new tool to reconstruct Holocene coastalsea surface temperature. *Geochemistry Geophysics Geosystems*, 8.

Fritts, H.C., 1976. Tree Rings and Climate. Academic Press, New York. 567 pp.

Gardner, J. (1944). Mollusca from the Miocene and Lower Pliocene of Virginia and North Carolina, Part 1: Pelecypoda. *United States Geological Survey Professional Paper*, 199-A: 1-178.

Gardner, J. (1948). Mollusca from the Miocene and Lower Pliocene of Virginia and North Carolina, Part 2: Scaphopoda and Gastropoda. *United States Geological Survey Professional Paper*, 199-B: 1-310.

Gibson, T.G., (1983), Stratigraphy of Miocene through lower Pleistocene strata of the United States central Atlantic Coastal Plain, in Ray, C.E., ed., Geology and paleontology of the Lee Creek mine, North Carolina, I: Smithsonian Contributions to Paleobiology 53, p. 35–80.

Gibson, T.G., and Bybell, L.M., (1984), Foraminifers and calcareous nannofossils of Tertiary strata in Maryland and Virginia; A summary, in Frederiksen, N.O., and Krafft, Kathleen, eds., Cretaceous and Tertiary stratigraphy, paleontology, and structure, southwestern Maryland and northeastern Virginia; Field trip volume and guidebook (for field trip held October 17, 1984): Reston, Va., American Association of Stratigraphic Palynologists, p. 181–189.

Goewert, A.E. and D. Surge. (2008). Seasonality and growth patterns using isotope sclerochronology in shells of the Pliocene scallop, *Chesapecten madisonius*. *Geo-Marine Letters* 28: 327–338.

Grossman, E.L., and T. Ku. (1986). Oxygen and carbon isotope fractionation in biogenic aragonite: temperature effects. *Chemical Geology*, 59: 705 59–74.

Haug, G.H. and R. Tiedemann. (1998). Effect of the formation of the Isthmus of Panama on Atlantic Ocean thermohaline circulation. *Nature*, 393: 673-676.

Haus, B.K., H.C. Graber, L.K. Shay, and T.M. Cook (2003). Alongshelf Variability of a Coastal Buoyancy Current during the relaxation of downwelling favorable winds. *Journal of Coastal Research*, 19(2). 409-422

Hazel, J.E. (1971). Ostracode biostratigraphy of the Yorktown Formation (upper Miocene and lower Pliocene) of Virginia and North Carolina. *U.S. Geological Survey Professional Paper*, 704:1-13.

Hogg, N.G., (1992). On the transport of the Gulf Stream between Cape Hatteras and the Grand Banks. *Deep-Sea Research*, 39, 1231-1246.

Hogg, N.G., R.S. Pickart, R.M. Hendry, and W.J. Smethie Jr., (1986), The Northern Recirculation Gyre of the Gulf Stream. *Deep-Sea Research*, 33, 1139-1165.

Johns, W.E., T.J. Shay, J.M. Bane, D.R. Watts, (1995). Gulf Stream structure, transport, and recirculation near 68° W. *Journal of Geophysical Research*, 100, 817-838.

Jones, D.S. (1980). Annual cycle of shell growth increment formation in two continental shelf bivalves and its paleoecologic significance. *Paleobiology*, 6(3): 331-340.

Jones, D.S. (1981). Annual growth increments in shells of Spisula solidissima record marine temperature variability. *Science*, 211, 4478: 165-167.

Jones, D.S. (1983). Sclerochronology: reading the record of the molluscan shell. *American Scientist*, 71: 384-391.

Jones, D.S. and I.R. Quitmyer. (1996). Marking time with bivalve shells: oxygen isotopes and season of annual increment formation. *Palaios*, 11: 340-346.

Jones, D.S., B.J. MacFadden, S.D. Webb, P.A. Mueller, D.A. Hodell, and T.M. Cronin. (1991). Integrated geochronology of a classic Pliocene fossil site in Florida: linking marine and terrestrial biochronologies. *Journal of Geology*, 99: 637-648.

Jones, D.S., D.F. Williams, and M.A. Arthur (1983). Growth history and ecology of the Atlantic surf clam *Spisula solidissima* (Dillwyn), as revealed by stable isotopes and annual shell increments. *J. Exp. Mar. Biol. Ecol.*, 13: 225-242.

Jones, D.S., I. Thompson, and W. Ambrose (1978). Age and growth rate determinations for the Atlantic surf clam *Spisula solidissima* (Bivalvia: Mactracea), based on internal growth lines in shell cross-sections. *Marine Biology*, 47: 63-70.

Jones, D.S., M.A. Arthur, and D.J. Allard (1989). Sclerochronological records of temperature and growth from shells of *Mercenaria mercenaria* from Narragansett Bay, Rhode Island. *Marine Biology*, 102: 225-234.

Jossi, J.W. and R.L. Benway (2003) Variability of temperature and salinity in the middle Atlantic bight and Gulf of Maine based on data collected as part of the MARMAP Ships of Opportunity Program, 1978-2001. NOAA Tech Memo NMFS NE 172; 1-92.

Krantz, D.E. (1990) Mollusk-Isotope Records of Plio-Pleistocene Marine Paleoclimate, U.S. Middle Atlantic Coastal Plain. *Palaios*, 5: 317-335.

Krantz, D.E. (1991). A chronology of Pliocene sea-level fluctuations: the U.S. Middle Atlantic Coastal Plain record. *Quaternary Science Reviews*, 10: 163-174

Lentz, S.J. (2008a). Observations and a model of the mean circulation over the Middle Atlantic bight continental shelf. *Journal of Physical Oceanography*, 30(6), 1203-1221.

Lentz, S.J. (2008b). Seasonal variation in the circulation over the Middle Atlantic bight continental shelf. *Journal of Physical Oceanography*, 38(7), 1486-1500.

Lewis, M.F.C. and J.T. Teller (2007). North American late-Quaternary meltwater and floods to the oceans: Evidence and impact – Introduction, *Palaeogeography, Palaeoclimatology, Palaeoecology,* 246, 1, 1-7.

Lund, D. C. and W. B. Curry (2006), Florida Current surface temperature and salinity variability during the last millennium, *Paleoceanography, 21,* PA2009.

Lund, D.C. and W. B. Curry (2004), Late Holocene variability in Florida Current surface density; patterns and possible causes, *Paleoceanography, 19,* 17.

Lynch-Stieglitz, J., W. B. Curry, and N. Slowey (1999), A geostrophic transport estimate for the Florida Current from the oxygen isotope composition of benthic Foraminifera, *Paleoceanography, 14,* 360-373.

Ma, H., J.P. Grassle, and J.M. Rosario (2006). Initial recruitment and growth of surfclams (*Spisula solidissima* Dillwyn) on the inner continental shelf of New Jersey. *Journal of Shellfish Research,* 25(2): 481- 489.

Marchitto, T.M., D.S. Jones, G.A. Goodfriend, and C.R. Weidman. (2000). Precise temporal correlation of Holocene mollusk shells using sclerochronology. *Quaternary Research,* 53(2). 236-246.

Marine Resources Monitoring, Assessment, and Prediction website: http://www.nefsc.noaa.gov/nefsc/publications/crd/crd0408/#dt

Mountain, D. G. (2003). Variability in the properties of Shelf Water in the Middle Atlantic Bight, 1977–1999, *Journal of Geophysical Research,* 108(C1), 3014.

Mountain, D.G. and T.J. Holzwarth. (1989). Surface and bottom temperature distribution for the northeast continental shelf. NOAA Tech. Mem. NMFS-F/NEC-73; 32 p.

Mountain, D.G.; Taylor, M.H.; Bascuñán, C. (2004). Revised procedures for calculating regional average water properties for Northeast Fisheries Science Center cruises. Northeast Fisheries Science Center Reference Document 04-08; 53 p. Available from: National Marine Fisheries Service, 166 Water St., Woods Hole, MA 02543.

Olsson, A.A., and Petit, R.E., (1964), Some Neogene Mollusca from Florida and the Carolinas: Bulletins of American Paleontology, v. 47, no. 217, p. 509-567.

Peterson, C.H., P.B. Duncan, H.C. Summerson, and G.W. Safrit Jr. (1983). A mark-recapture test of annual periodicity of internal growth band deposition in shells of hard clams, Mercenaria Mercenaria, from a population along the southeastern United States. *Fishery Bulletin,* 81:765-779.

Popenoe, P. (1985). Cenozoic Depositional and Structural History of the North Carolina Margin from Seismic-Stratigraphic Analyses. *In*: C.W. Poag (Eds.), Geologic evolution of the United States Atlantic margin. New York, Van Nostrand Reinhold Company. 87-123.

Reid, J.M., Reid, J.A., Jenkins, C.J., Hastings, M.E., Williams, S.J., and Poppe, L.J, (2005). usSEABED: Atlantic coast offshore surficial sediment data release: U.S. Geological Survey Data Series 118, version 1.0. Online at http://pubs.usgs.gov/ds/2005/118/

Schöne, B.R (2003). A ‘clam-ring’ master-chronology constructed from a short-lived bivalve mollusk from the northern Gulf of California, USA. *The Holocene*., 13(1). 39-49.

Schöne, B.R., Castro, A.D.F, Fiebig, J., Houk, S.D., Oschmann, W., Kröncke, We., (2004), Sea surface water temperatures over the period 1884-1983 reconstructed from oxygen isotope ratios of a bivalve mollusk shell (*Arctica islandica*, southern North Sea). *Palaeogeography, Palaeoclimatology, Palaeoecology* 212, p. 215-232.

Strom, A., Francis, R.C., Mantua, N.J., Miles, E.L., Peterson, D.L., (2004). North Pacific climate recorded in growth rings of geoduck clams: a new tool for paleoenvironmental reconstruction. *Geophysical Research Letters* 31, L06206.

Sverdrup, H.U., M.W. Johnson, and R.H. Fleming, 1942: *The Oceans*, Englewood Cliffs, NJ Prentice Hall, 1087 pp.

Walker R.L., Heffernan P.B. (1994). Age, growth rate, and size of the southern surfclam, *Spisula solidissima similis* (Say, 1822). *Journal of Shellfish Research*, 13:433–441

Ward, L.W. and B.W. Blackwelder. (1980). Stratigraphic revision of upper Miocene and lower Pliocene beds of Chesapeake Group, middle Atlantic Coast Plain. *U.S. Geological Survey Bulletin*, 1482-D: 1-61.

Ward, L.W. and Blackwelder, B.W. (1987). Late Pliocene and Early Pleistocene Mollusca From the James City and Chowan River Formations at the Lee Creek Mine, *In*: Ray, C.E., ed. Geology and Paleontology of the Lee Creek Mine, North Carolina, II, *Smithsonian Contributions to Paleobiology*, 61: 1-283.

Ward, L.W. and G.L. Strickland. (1985). Outline of Tertiary stratigraphy and depositional history of the U.S. Atlantic Coastal Plain. *In*: C.W. Poag (Eds.), Geologic evolution of the United States Atlantic margin. New York, Van Nostrand Reinhold Company. 87-123.

Ward, L.W. and Powars, D.S. (1989). Tertiary stratigraphy and paleontology, Chesapeake Bay Region, Virginia and Maryland: Chesapeake Bay Region, Virginia and Maryland, July 15-July 1. Washington, D.C., American Geophysical Union.

Weinberg, J.R. (1998). Density-dependent growth in the Atlantic surfclam, *Spisula solidissima*, off the coast of the Delmarva Peninsula, USA. *Marine Biology*, 130: 621-630.

Weinberg, J.R. (1999). Age-structure, recruitment, and adult mortality in populations of the Atlantic surfclam, *Spisula solidissima*, from 1978 to 1997. *Marine Biology*, 134: 113-125.

Weinberg, J.R. (2005) Bathymetric shift in the distribution of atlantic surfclams: response to warmer ocean temperature. *ICES journal of Marine Science*, 62: 1444-1453.

Weinberg, J.R. and T.E. Helser (1996). Growth of the Atlantic surfclam, *Spisula solidissima*, from Georges bank to the Delmarva Peninsula, USA. *Marine Biology*, 126: 663-674.

Wigley, T.M.L., Briffa, K.R., Jones, P.D., (1984). On the average value of correlated timeseries, with applications in dendroclimatology and hydrometeorology. Journal of Climate and Applied Meteorology 23, 201–213.

Williams, D.F., M.A. Arthur, D.S. Jones, and N. Healy-Williams (1982). Seasonality and mean annual sea surface temperatures from isotopic and sclerochronological records. *Nature*, 269: 432-434.

Witbaard, R., M.I. Jenness, K. van der Borg, and G. Ganssen (1994). Verification of annual growth increments in *Arctica islandica* L. from the North Sea by means of oxygen and carbon isotopes. *Netherlands Journal of Sea Research*, 33(1). 91-101.

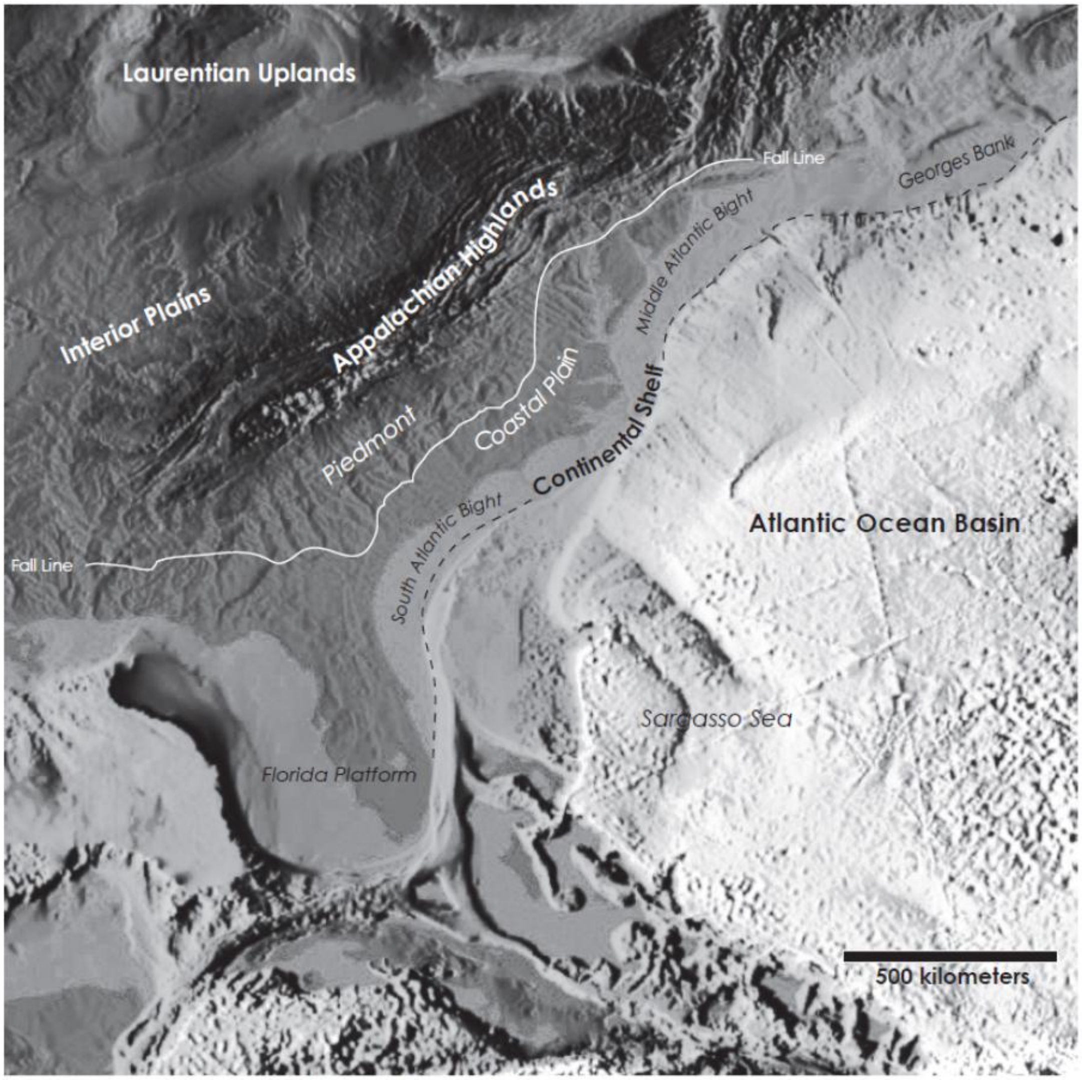

Base map is from the ETOPO2v2 Global Gridded 2-minute Database, National Geophysical Data Center, National Oceanic and Atmospheric Administration, U.S. Dept. of Commerce, http://www.ngdc.noaa.gov/mgg/global/etopo2.html.

Figure 2.1. Physical Setting of eastern North America and the western Atlantic Ocean Basin.

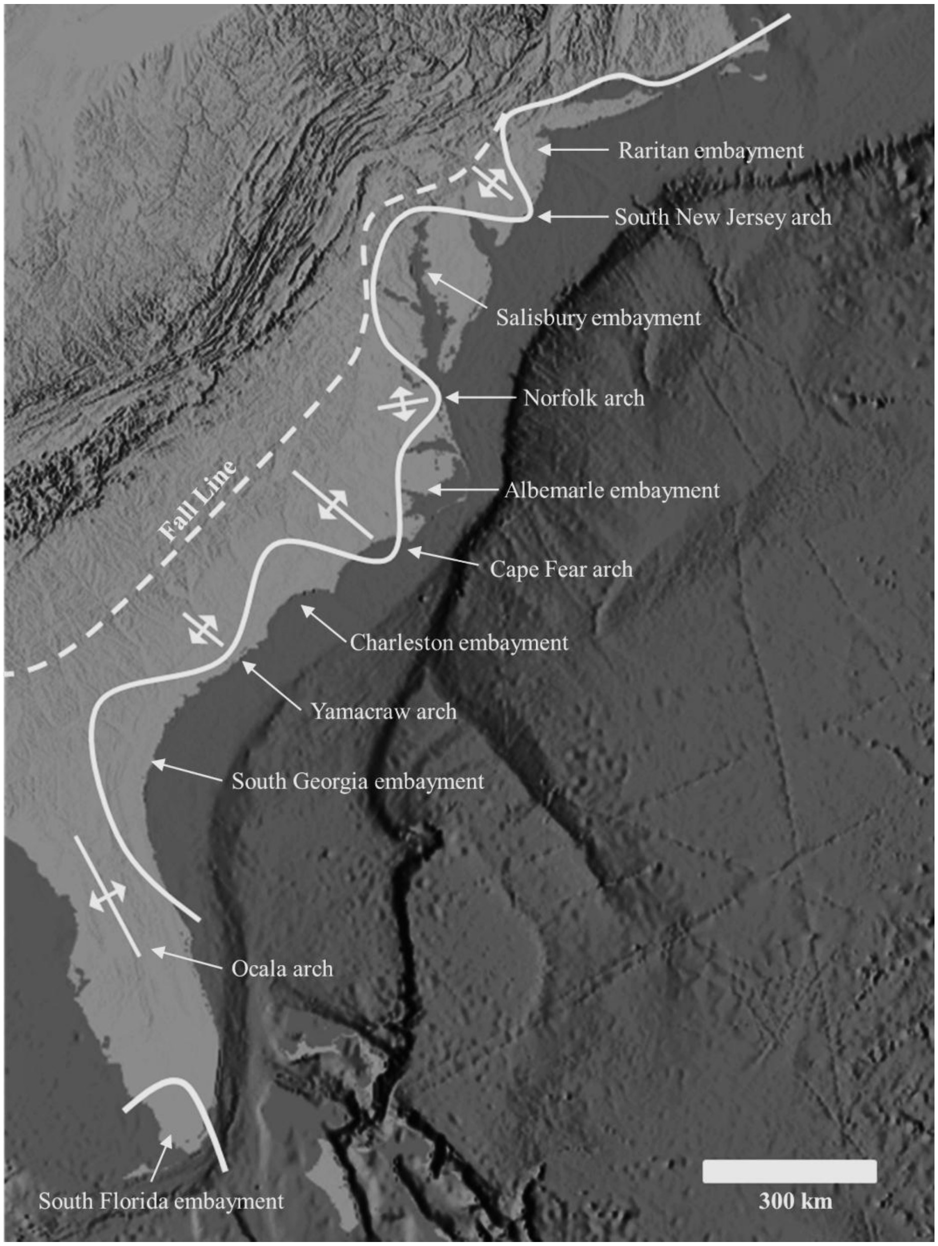

Figure 2.2 Generalized onshore embayment and major structural features map othe Atlantic Coastal Plain (after Ward et al., 1991).

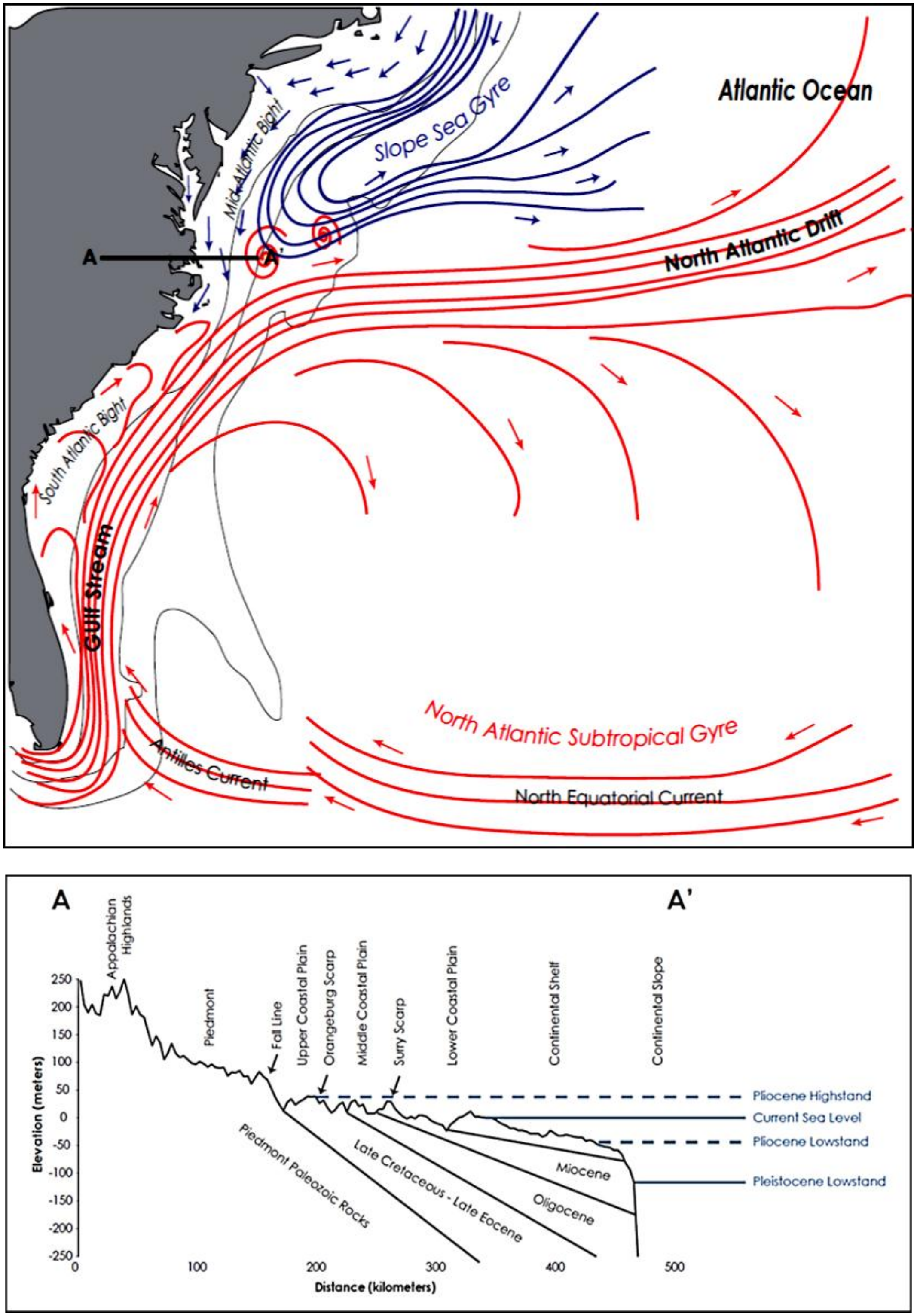

Figure 2.3. Schematic map and cross-section of the eastern North American coastal plain and western Atlantic basin. Upper panel shows cold (blue) and warm water (red) surface currents. Lower panel is a cross-section through Virginia from the Appalachian Highlands to the 250 meter bathymetric line (500× vertical exaggeration).

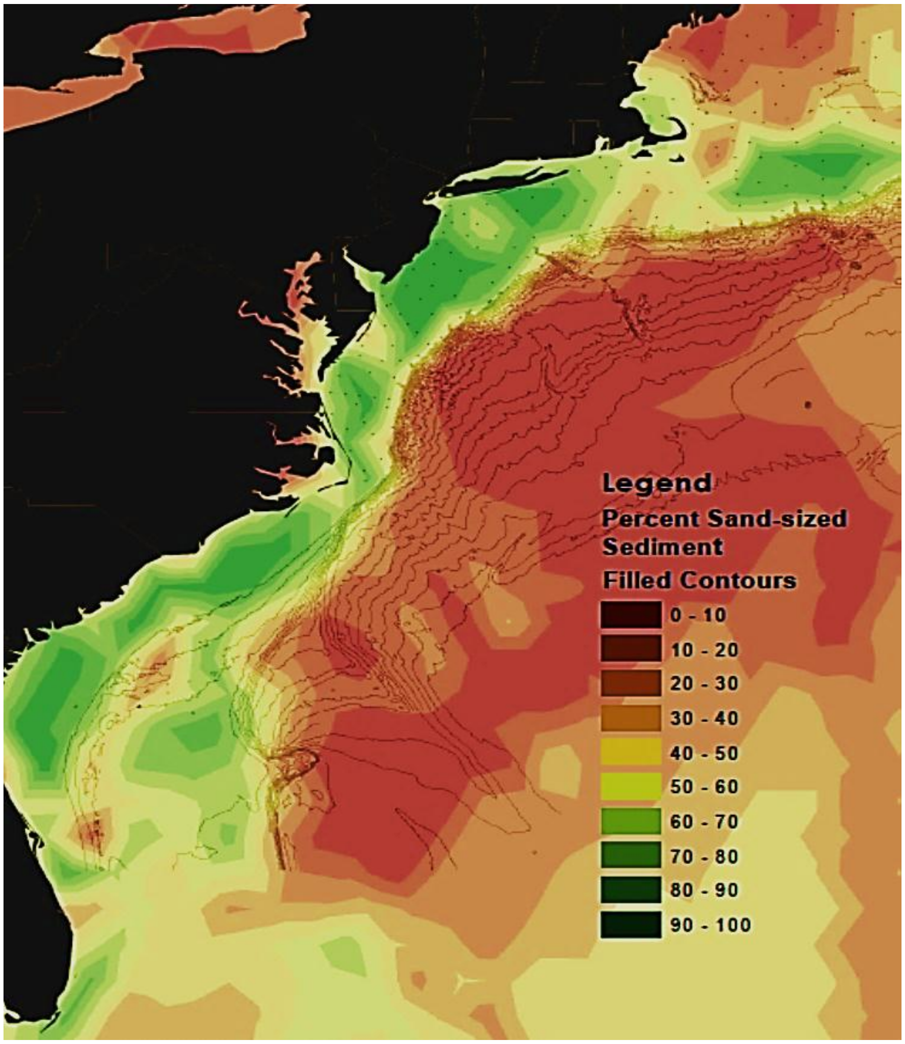

Figure 2.4. Filled contour map showing the percent sand-sized sediment along the eastern North American continental shelf and slope. (USGS usSEABED Data Series 118 (2005)).

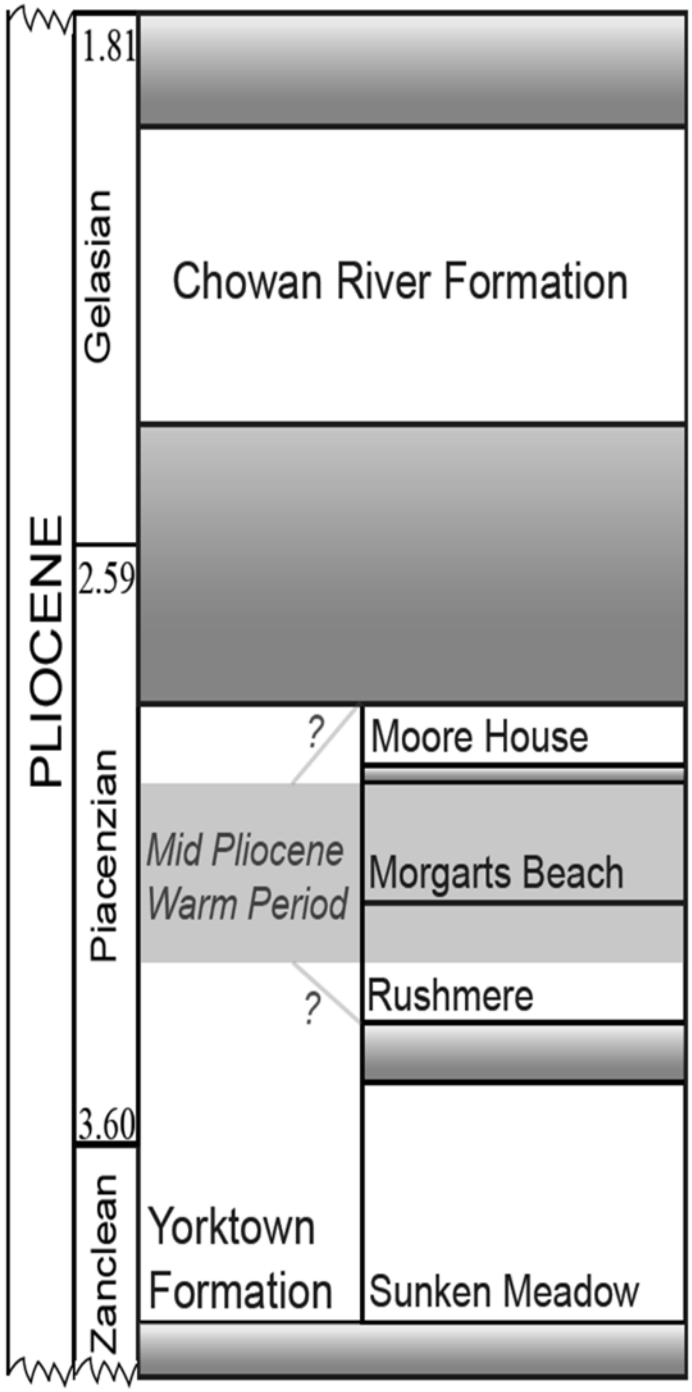

g

Figure 2.5. Pliocene stratigraphic nomenclature for the coastal plain of a combined North Carolina and Virginia. Column also shows the mid Pliocene Warm Interval slab according to the PRISM Reconstruction.

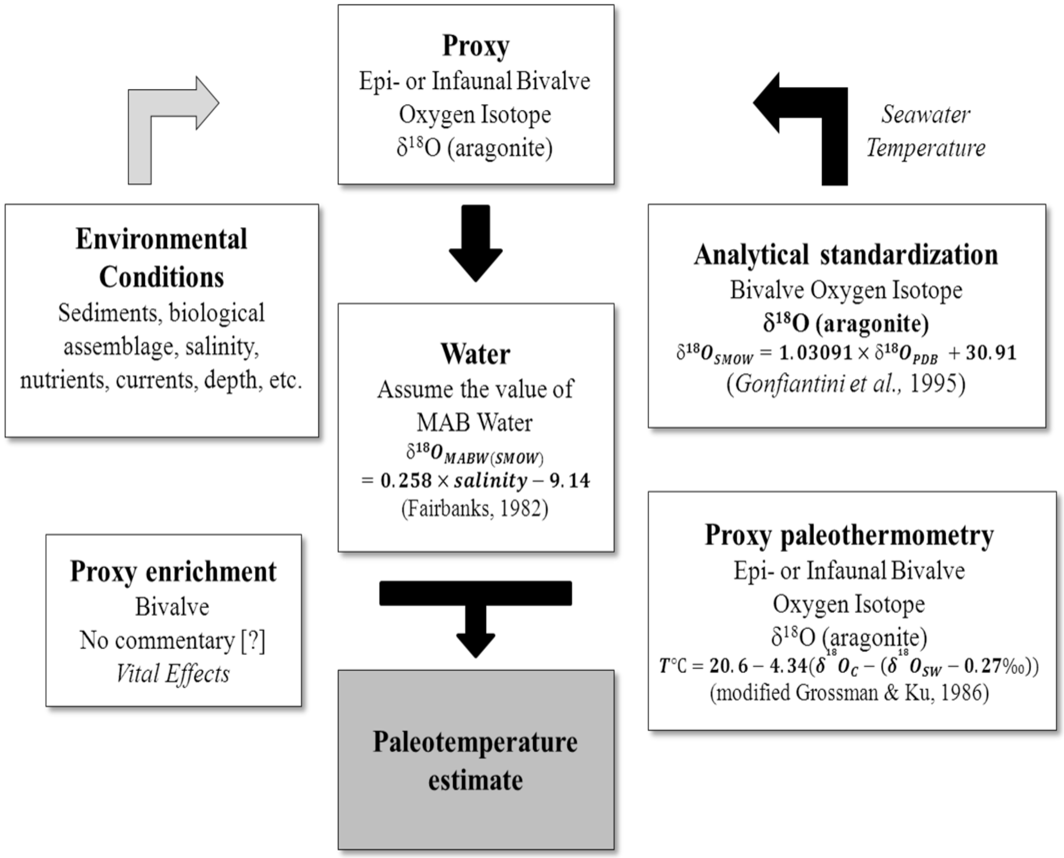

Figure 2.6. Flow chart showing the conventional methods employed in isotope paleothermometry.

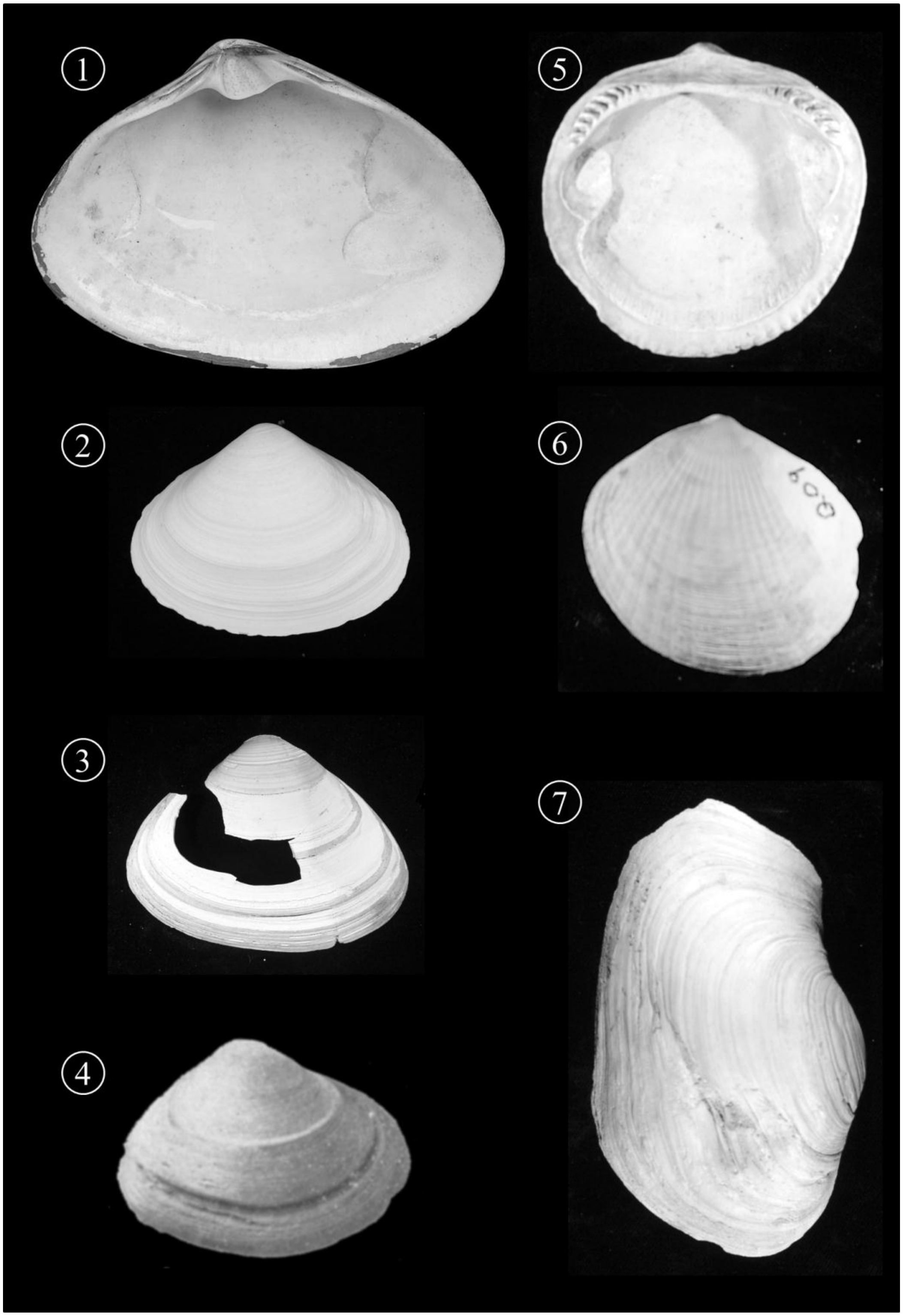

Figure 2.7 Bivalves examined for this study. 1) *Spisula (Hemimactra) solidissima* (Dillwyn, 1817), 2) *Spisula (Hemimactra) solidissima similis* (Say, 1822), 3) *Spisula (Hemimactra) confraga* (Conrad, 1833), 4) *Spisula modicella* (Conrad, 1833), 5) *Glycymeris americana* (DeFrance, 1826), 6) *Costaglycymeris subovata* (Say, 1824), and 7) *Panopea reflexa* (Say, 1824).

CHAPTER 3: ADDRESSING THE SINGLE COUNTER PROBLEM USING A COMPUTER-ASSISTED IMAGE AGING METHOD

Joel Hudley and Donna Surge

Department of Geological Sciences, University of North Carolina, Chapel Hill, 104 South Rd., CB#3315, Chapel Hill, NC 27599-3315, USA email: jhudley@unc.edu

Short running title: Computer-assisted Image Aging

Keywords: age determination, image analysis, *Spisula (Hemimactra) solidissima*

(As submitted to *Journal of Shellfish Research*)

ABSTRACT

The ages of individual specimens of the surf clam, *Hemimactra (Spisula) solidissima,* (Dillwyn, 1817) collected from the Middle Atlantic Bight, were estimated by visual inspection (traditional method) and computer-assisted image analysis. The traditional method employed a non-expert age reader examining shell chondrophore under a microscope. The computer-assisted method used standard imaging software to acquire a grayness intensity profile across each chondrophore, and then used a mathematical model to determine peak intensity values significantly different from the rest of the profile. The precision between the methods was 10% with a coefficient of

variance of 16.84. The precision of the computer-assisted method proved below that of the non-expert reader, and systematically underestimated ages of the surf calm population.

3.1 INTRODUCTION

Early seminal works by Hudson et al. (1976) and Jones and Ambrose (1978) showed that the internal growth lines in corals and clams chronicled both growth history and environmental information, similar to tree rings chronologies. Calling this new sub-discipline of geosciences “sclerochronology”, Jones (1983) claimed that bivalve chronologies were the marginal marine answer to dendrochronology and dendroclimatology. However, following Williams et al. (1982) who reported on methods to employ both increment and isotopes to reconstruct sea surface temperature, most sclerochronology studies are more analogous to dendrochemistry, purely dependent on isotopic results. Few sclerochronology paleo-studies report reconstructions derived from increment records, independent of isotopes.

One explanation for the lack of increment-based experiments is that no systematic methodologies and common practices exist for such experiments. In a review of fisheries management aging programs worldwide, Campana and Thorrold (2001) reported that 1–2 million fish were aged globally in 1999. The number of otoliths is massive in comparison to the tens of thousands of shellfish aged annually, and suggests that the majority of sclerochronologists are employed in successful increment programs. These increment programs employ basic quality monitoring techniques such as multiple examinations of the same specimen multiple times by various expert readers. These laboratories train age readers and keep aged reference collections of the species they examine. Many of these government run aging laboratories develop and exchange aging methods, validate growth curves, and verify daily to annual resolution of taxa growth increments without the use of isotopes. The use of non-isotope methods is often practical, as costs can be enormously prohibitive for large-scale isotopic analysis.

Another possible explanation for the dearth of increment sclerochronology studies in academic, geologic and marine science departments is the laboratory research structure. Most paleoclimate sclerochronology labs are administered by a single Principle Investigator (PI) overseeing a transient caste of graduate and undergraduate research assistants. The PIs must balance their time between teaching, research and mentoring, and then endeavor to find time to train, monitor, and recheck all the shells being processed in their laboratory. The monitoring and rechecking problem might be answered by an exchange of materials with another laboratory to compare measurements. However, cost and time may be prohibitive, and standard methods are comparable between academic laboratories.

Another possible explanation is the materials used for sclerochronological paleoclimate studies. Many researchers acquire specimens from fossiliferous deposits, museum collections, archeological sites, and fisheries research cruises. Since many of these acquisitions are through happenstance, the number of specimens is often small, the preservation dubious, and the proxies short-lived. Also, if the specimens are from a time prior to the instrumental record, then using important environmental factors related to bivalve growth to verify growth increment interpretations is suspicious. By using isotope analysis, past environmental information can be gathered from any well-preserved specimens.

The Single Counter Problem refers to the errors of one reader's bias. This bias is an introduction of human error due to difficulties recognizing and inconsistently counting (aging) and measuring growth increment series. The purpose of this study is to determine if a novel image analysis method previously employed for shellfish fisheries management could be used to: (1) reduce the labor and time consumed by age estimation, and (2) act as a computer guide for age monitoring. Harding et al. (2008) presented a method for using standard computer imaging software to estimate ages of *Artica islandica* (Linnaeus, 1767). We employed those methods, and then compared a single, non-expert age reader to the image analysis method. For comparison, we calculated the precision to describe the agreement ratio between readings by the two different readers. On the basis of our results, we discuss the validity of the computer-assisted aging method.

3.2 MATERIALS AND METHODS

3.2.1 Materials

Live caught specimens for this study were acquired from the NOAA Fisheries Service Northeast Regional Fishery Science Center (NEFSC): Fishery Biology Program which until recently conducted stock assessments of commercial bivalves in the Mid-Atlantic Bight (ranging from George's Bank to just south of Cape Hatteras) every 3-4 years. Specimens of *Spisula (Hemimactra) solidissima solidissima* (Dillwyn, 1817) came from surveys conducted from 1992 through 2005. Each specimen came from a NOAA sampling station with associated location, depth, salinity, and bottom and surface temperatures (Figure 1). Pliocene specimens of *S. confraga* [Mactra fragosa] (Conrad, 1833), *S. modicella* (Conrad, 1833), *Panopea reflexa* (Say, 1824) and *Glycymeris americana* (DeFrance, 1826) were collected from various Pliocene Mid-Atlantic Coastal Plain (MACP) fossiliferous deposits in southern Virginia and acquired from the Virginia Museum of Natural History (VMNH) (Figure 1).

All bivalve specimens were cleaned in a dilute bleach solution and rinsed with water. One valve from each shell was radially sectioned along the maximum axis of growth using a lapidary saw, ground down using 600 grit, and polished down to 6 micron diamond suspension grit on a variable speed grinder-polisher (Buehler). Depending on their fragility, some shells were coated with fast-hardening epoxy resin before cutting (JB Kwik Weld). When paired-valves were available, the left valve was employed because many of the NOAA specimens had only one remaining valve (the left) after original aging (Ropes, 1985). Once dried, shells were affixed to a slide using epoxy and thick sections were cut again a Buehler IsoMet slow speed saw. Slides were labeled with unique sample identification, and the remaining shell valves returned to storage for reference. Slides were ground and polished following the methods outlined above. A cross section of the hinge region for each polished valve was photographed, using an Olympus stereomicroscope with a 12.5 megapixel DP71 digital camera connected to a Windows-based computer.

3.2.2 Visual aging method

The standard visual aging method used to determine a clam's age the hinge plate (chondrophore) is by counting couplets of alternating patterns of translucent (dark = slow growth) and opaque (light = rapid growth) segments representing one year's growth (Arnold et al. 1991; Jones, 1996) (Figure 2). It is generally recognized that in bivalves the opaque increments form under good growth conditions and the dark increment under poor conditions (Rhoads and Lutz, 1980). Jones (1983) demonstrated that the dark zones of *Spisula* shells begin to form in late summer, followed by slow growth during the coldest winter months. Full color images of each hinge were used to visually age each specimen. Increment widths were measured using the Olympus Imaging Solutions Software. The determination of age by visual counter method was made by one reader (Reader 1). Reader 1, with limited experience determining the age of the multiple species, aged each specimen twice. The second count was made several months after the first count. Ages of live-caught *S. s. solidissima* were better constrained using patterns in the growth lines to cross-date the chronologies, a standard practice in both dendro- and sclerochronology. Cross-dating could not be used on the floating Pliocene increment series. In total, 343 *S. s. solidissima*, 17 *S. confraga*, 4 S. *modicella*, 12 *P. reflexa*, and a 134 *G. americana* were aged. 172 *S. s. solidissima*, 17 *S. confraga*, 4 *S. modicella*, 7 *P. reflexa*, and 3 *G. americana* chondrophores were used to compare our standard method to a computer-assisted aging method.

3.2.3 Computer-assisted aging

We used the 30 *S. s. solidissima* live caught as the example for this method because of the manageable number and the shells' easily readable growth lines. Using the Olympus Imaging Software, the full color images of each hinge were converted into gray scale, and the 'smooth' command was used to remove fine fluctuations in the image. The image was processed by optimizing the contrast to better distinguish the dark and light increments of the shell. Using the 'Intensity Profile' tool in the 'Measurements' menu of the Olympus Imaging Solutions Software, a single line 1 pixel wide was drawn across the length of the shell section from the dorsal end of the umbo to the ventral along the curvature of growth. The intensity profile command produced a graph of grayness values along the selected line, divided into intensity level from 0 to 255. In this grayness scale, level 255 is white and level 0 is black. The x-axis of the graph represents the distance from the umbo and the y-axis is grayness intensity at each pixel. Each graph's grayness was then inverted to make zero white and increasing intensity darker. Inversion was not necessary, but was done to aid visual interpretation of the intensity profiles.

After we imported all the intensity profiles series into MS Excel, we began following the methods and assumptions outlined by Harding et al. (2008). The underlying principle of Harding's method is that significant line types, such as annual growth bands, should be distinctly darker than other growth lines (Thompson et al. 1980b) and should exist as a distinctive group of uniform grayness within the array of growth lines observed from the lightest to the darkest grayness level. In order to identify yearly growth bands, Harding et al. (2008) presented a method to test if some groups of growth lines are distinctly more uniform in darkness than other growth lines, and to detect peaks on the intensity profile that intersected those predetermined intensity levels. Harding's method was performed as follows. The data set was composed of chondrophore length and a series of intensity profiles at grayness intensities of 0–225 for (30) *S. s. solidissima* between 1.403 and 2.470 mm in length. Line counts were initially evaluated in 5-intensity-unit intervals (I_i) from 5–120 grayness units, with I_1 = 5-10 and I_{23}=115-120. Intensity levels outside this range were either too sensitive and thus produced unreasonably high line counts or not sensitive enough and thus produced unreasonably low line counts. We plotted the average rate of change in line count (LC) as a function of change in intensity step (I), wherein the number of lines from one intensity step to another declines in magnitude with increasing grayness, and found a regression line for that series . We noted local minima intensities ranges. We plot a frequency diagram of zero differences between the numbers of lines counted from one 5-intensity-unit level to the next and found local maxima and minima intensities. Using the regression equation from Step 3, we obtained a series of residuals for each of the 30 shells and grayness intensities in the range of 25–140 grayness units, plotted the mean residual against grayness intensity and revealed which intensity levels the most negative mean residuals occurred. After we ranked the residuals, we perform a one-way ANOVA and a Tukey's HSD (honestly significant difference) to test the null hypothesis that the means of the residuals were equal across a range of grayness intensities. Finding the null hypothesis false, we displayed the results of how frequently one set of residuals differed significantly from another, and then assessed the likelihood that each difference might have occurred by chance. We then used analyses from the previous steps to show unique ranges of grayness in the grayness spectrum. Those unique ranges on each of the 172 surf clam intensity profiles were graphed, and the location of where intensity peaks intersected those predetermined intensity levels were recorded . Ages from the Visual Count (VC) of Reader 1 and the ages for the corresponding specimen's Intensity Profile (IP) Count were recorded and compared using their descriptive statistics (mean age, minimum and maximum age, standard deviation, counts, number of samples, and confidence level)(Table 1).

3.2.4 Comparison of aging methods

Valid comparisons between our aging methods can be made because we used the two methods on the same individual clams. We assumed that the computer-assisted method represents a valid second reader. To automate the calculations of the various measurements of age precision, we used the NOAA Fishery Biology Programs Templates for Calculating Aging Precisions (http://www.nefsc.noaa.gov/fbp/age-prec/#bow). The templates were designed to calculate various measurements of aging precision, including percent agreement between agers and the total coefficient of variance (CV, Chang, 1982). Templates from NOAA were also used to generate an age-bias plot (Figure 3) and an age matrix table (Hoenig et al., 1995). In these precision calculations, VC Age is considered to be the final (first-and-second count) age attached to a clam, as age Reader 1 worked twice with the entire sample set. IP Age is a single aging of each clam by the computer-assisted method.

3.3 RESULTS

3.3.1 Visual aging

After two counts of 172 *S. s. solidissima* shells by Reader 1, the mean and median ages of the clams were 14.0±4.1 years old. Ages ranged from a minimum of 4 years to a maximum of 26 years (range, 22 years). The agreement between Reader 1's first and second count was high (97%, 4 non-agreements).

3.3.2 Computer-assisted aging

The mean age of the IP aging method were 11.5±3.7 years, with ages ranging from 2 years to a maximum of 20 years. These 172 ages were based on grayness intensity levels 65–70, derived from the 30 clam test set. That intensity range was found following the methods in Harding et al. (2008). Local minima were identified at intensities 35-45, 65-70, 85-90, and 115-120. Overall minima are found at the two intensities 35-40 and 65-70 along the continuously decreasing section of the relationship between Intensity Range and Average Rate of Change. The fewest lines are lost in increments across these two ranges of grayness intervals. One might expect that annual bands would be of sufficient strength compared to other growth lines that a step in grayness intensity would not change the line count. Where the number of cases in which an increment of 5 grayness units produced the same line count for these 30 clams, local maxima were observed at grayness intensities of 20-25, 35-40 and 55–60. Local maxima are succeeded by minima at 30-35, 40-45, and 60–75. Using the regression equation, the most negative mean residuals are encountered at the 40-45 and 70-75 grayness intensities. This is consistent with Figures 3.4A and 3.4B, indicating that, for most shells, the rate of change in line count is distinctly lower in the two grayness ranges from 35-45 and 65-75 than elsewhere in the grayness spectrum. We anticipated that these grayness ranges are associated with significant life history events, such as yearly shifts in growth. The null hypothesis that all grayness intensities were the same was tested false when grayness intensities 45-50, 65-70, and 85-90 exhibit significant divergence from chance ($P < 0.001$). Collectively, the analyses identified two unique ranges of grayness at 45-50 and 65-70. Grayness ranges >80 resulted in lower than acceptable ages. The average line count for the lower grayness intensity is about double that of the higher grayness intensity. Following the assumptions in Harding et al. (2008), this ratio suggests that annual bands are detected at intensities of 65-70 and seasonal bands or spawning breaks are detected at intensities of 45-50. However, this was not proven. The 65-70 intensity level (the one chosen for the entire population count) does consistently match with many of the annuliseen in the images (Figures 3.2). However, the 45-50 grayness intensity matches growth checks in the early years (Figure 3.2, Area B), but also annual growth marks near the ventral end of the chondrophore (Figure 3.2, Area C). By disregarding the lower grayness intensity level, we systematically underestimate the ages of the shells. If we combine the counts of both intensity levels, thus incorporating the missed annual growth marks and the early growth checks, we will grossly overestimate ages.

3.3.3 Comparison of aging methods

The percent agreement between the visual and the computer-assisted aging methods is 10.5%, with only 18 agreements out of the 172 clams aged. The CV, a measure of precision, was 16.84%. This result being greater than the reference point of

5%, suggests that the ages are relatively imprecise (Campana, 2001). On the age-agreement table (Figure 5), the main diagonal represents the frequency for which the two methods obtained the same age, and cells off the diagonal represent differences in ages between methods. IP Age (the computer-assisted method), in the upper space, shows systematically underestimated ages of clams after year 4 or 5 (Figure 5). The same result of IP age underestimation is shown in the age-bias plot (Figure 6), where the average test age moved away from a 1:1 agreement between the more accurate counter (Reader 1) and the computer-assisted method.

3.3.4 Other Bivalve Proxy Results

We followed the same procedures from Harding et al. (2008), for Pliocene surf clams *S. confraga* and *S. modicella*, the geoduck *P. reflexa,* and bittersweet cockle *G. americana.* These bivalves were chosen as potentially useful proxies of environmental variations on subannual to decadal resolution because they were considered abundant in Pliocene localities (Ward, 1994) and well preserved.

The results from the 17 *S. confraga* chondrophore indicated that significant grayness intensities were found at 65-70 and 105-110, with 65-70 representing the annulus. The maximum IP age of *S. confraga* was 10 years, with a mean age of 6±2 years. From the 4 *S. modicella*, the maximum aged specimen was 12 years old, with mean of 7±3 years old for the small population. Statistically different grayness intensities were indicated at 65-70 and 120-125, and again 65-70 represented the annulus. The average age of the geoduck *P. reflexa* was 21±6 years, with a maximum IP Age of 33 years. Grayness intensity levels along the geoduck hinge plate of 35-40 and 120-125 were indicated as significantly different, with 35-40 representing the annulus. Only 3 Pliocene *G. americana* were aged using the hinge. The annual growth lines were represented by the 35-40 grayness intensity level. The maximum cockle aged using the computer-assisted method was 45 years old.

3.4 DISCUSSION

Image analysis is often employed for detecting and measuring the growth widths of trees (Guay et al., 1990; WinDENDRO©) and was recently used on otoliths (Calliet et al., 1996; Takashima et al., 2000). These image analyses are used as supplementary tools for age determination and not for automatic reading. In this study, we used a method that determines significantly different grayness intensities from intensity profiles of clam shells to develop a computer-assisted method to age the entire population. Both counting methods, the standard visual aging and the computer-assisted, were considered consistent between repeat counts. However, the accuracy and precision of the computer-assisted method constantly underestimated the age of cross-dated live caught specimens.

The IP aging method proves inferior to a non-expert age estimation (Reader 1) for multiple reasons. One explanation is that the method, though simple, probably fails to detect peaks just outside the identified the grayness intensities. The significantly different intensities work for most of the 30 shells used in the test set. However, many shells (Specimens 3, 7, 8, 13, 16, 22, 24, 27 and 29) had extremely low line counts when using the 45-50 and 65-70 intensity levels. This outcome may result from variations in the quality of the images, not only in the test set, but in the entire population. Shadows, light reflection angles, and lighting intensity could not be held constant throughout the entire image collection process. Light areas and closer spaced annuli may have missed certain growth lines or clumped older ages, hence the systematic underestimates of age. Even with improved imaging software, the causes of image quality variation (due to the processes of cutting, grinding, polishing, and mounting) are inherently unavoidable. The Harding et al. (2008) method seemed effective at creating a power function for an age-at-length relationship for *A. islandica* less than 80 mm, but using the method to age an entire population proves inadequate. If the computer method used in Harding et al. (2008) could be improved, it might be useful in age determination studies. The computer is acceptable to use for early growth, but it is not calibrated to read older growth lines accurately. In this study, the method was used as a supplement for finding and confirming the earliest (1-3 years) growth lines in all the taxa aged.

3.5. CONCLUSIONS

In this study, we addressed the challenges of relying on a single non-expert age reader for sclerochronological analysis by using a novel image analysis method for differentiating significant grayness intensities in the shell grayness profile. This method was relatively rapid, only taking 2 days to age and measure 172 chondrophore, compared to the standard visual aging method, which took 4 weeks total time. It is especially rapid when comparing ages after second processes like acetate peels and staining.

Unfortunately, the image analysis method systematically underestimates ages compared to ages counted using cross-dating of the visual aging. Therefore, though subjective and potentially biased, the standard visual aging and measuring methods employed by researchers to interpret the periodic features of calcified structures must continue for the foreseeable future.

ACKNOWLEDGEMENTS

We thank Jay Burnett (NOAA-retired) and the Northeast Fisheries Science Center (NEFSC) Fishery Sampling Branch. Thank you also to Lauck Ward (VMNH) for the use of specimens, species identification, and directions to collecting localities. Many Pleistocene and late Holocene shells that were used as references were donated and identified by Lynn Wingard (USGS). Funding was provided in part by the Preston Jones and Mary Elizabeth Frances Dean Marin Trust (UNC) and National Science Foundation Grants #ATM-0455974 to DS and #HRD-0450099 to Valerie Ashby (UNC).

REFERENCES

Beamish, R. J. & G. A. McFarlane. 1983. The forgotten requirement for age validation in fisheries biology. Trans. Am. Fish. Soc. 112:735-743.

Blackwelder, B. W. 1981. Late Cenozoic stages and molluscan zones of the united-states middle Atlantic coastal-plain. J. Paleontol. 55:1-34.

Blackwelder, B.W. 1981b. Stratigraphy of upper Pliocene and lower Pleistocene marine and estuarine deposits of northeastern North Carolina and southeastern Virginia. U.S. Geological Survey Bulletin, 1504-B: B1-B16.

Cailliet, G. M., L. W. Botsford, J. G. Brittnacher, G. Ford, M. Matsubayashi, A. King, D. L. Watters & R. G. Kope. 1996. Development of a computer-aided age determination system: Evaluation based on otoliths of bank rockfish off California. Trans. Am. Fish. Soc. 125:874-888.

Campana, S. E. 2001. Accuracy, precision and quality control in age determination, including a review of the use and abuse of age validation methods. J. Fish Biol. 59:197-242.

Campana, S. E., M. C. Annand & J. I. McMillan. 1995. Graphical and statistical-methods for determining the consistency of age-determinations. Trans. Am. Fish. Soc. 124:131-138.

Campana, S. E. & J. D. Neilson. 1985. Microstructure of fish otoliths. Can. J. Fish. Aquat. Sci. 42:1014-1032.

Campana, S. E. & S. R. Thorrold. 2001. Otoliths, increments, and elements: Keys to a comprehensive understanding of fish populations? Can. J. Fish. Aquat. Sci. 58:30-38.

Chang, W. Y. B. 1982. A statistical-method for evaluating the reproducibility of age-determination. Can. J. Fish. Aquat. Sci. 39:1208-1210.

Elliot, M., P. B. deMenocal, B. K. Linsley & S. S. Howe. 2003. Environmental controls on the stable isotopic composition of *Mercenaria mercenaria*: Potential application to paleoenvironmental studies. Geochem. Geophys. Geosyst. 4.

Fenger, T., D. Surge, B. Schöne & N. Milner. 2007. Sclerochronology and geochemical variation in limpet shells (*Patella vulgata*): A new archive to reconstruct coastal sea surface temperature. Geochem. Geophys. Geosyst. 8.

Goewert, A. E. & D. Surge. 2008. Seasonality and growth patterns using isotope sclerochronology in shells of the Pliocene scallop *Chesapecten madisonius*. Geo-Mar. Lett. 28:327-338.

Guay, R. G., R. J. Gagnon & H. Morin. 1992. A new automatic and interactive tree ring measurement system based on a line scan camera. The Forestry Chronicle 68:138-141.

Harding, J. M., S. E. King, E. N. Powell & R. Mann. 2008. Decadal trends in age structure and recruitment patterns of ocean quahogs *Arctica islandica* from the mid-Atlantic bight in relation to water temperature. Journal of Shellfish Research 27:667-690.

Hoenig, J. M., M. J. Morgan & C. A. Brown. 1995. Analyzing differences between 2 age-determination methods by tests of symmetry. Can. J. Fish. Aquat. Sci. 52:364-368.

Jones, D. S. 1983. Sclerochronology - reading the record of the molluscan shell. Am. Scientist 71:384-391.

Jones, D. S., B. J. Macfadden, S. D. Webb, P. A. Mueller, D. A. Hodell & T. M. Cronin. 1991. Integrated geochronology of a classic Pliocene fossil site in Florida - linking marine and terrestrial biochronologies. J. Geol. 99:637-648.

Jones, D. S. & I. R. Quitmyer. 1996. Marking time with bivalve shells: Oxygen isotopes and season of annual increment formation. Palaios 11:340-346.

Marchitto Jr., T. M., G. A. Jones, G. A. Goodfriend & C. R. Weidman. 2000. Precise temporal correlation of Holocene mollusk shells using sclerochronology. Quaternary Research 53:236-246.

Quitmyer, I. R., D. S. Jones & W. S. Arnold. 1997. The sclerochronology of hard clams, mercenaria spp., from the south-eastern USA: A method of elucidating the zooarchaeological records of seasonal resource procurement and seasonality in prehistoric shell middens. J. Archaeol. Sci. 24:825-840.

Robinson, W.J., Evans, R. 1980. A microcomputer-based tree-ring measuring system. Tree-Ring Bulletin 40:59-64.

Schöne, B. R., A. D. F. Castro, J. Fiebig, S. D. Houk, W. Oschmann & I. Kroncke. 2004. Sea surface water temperatures over the period 1884-1983 reconstructed from oxygen isotope ratios of a bivalve mollusk shell (*Arctica islandica*, southern North Sea). Paleogeogr. Paleoclimatol. Paleoecol. 212:215-232.

Schöne, B. R., D. H. Goodwin, K. W. Flessa, D. L. Dettman & P. D. Roopnarine. 2002. Sclerochronology and growth of the bivalve mollusks *Chione (chionista) fluctifraga* and *C. (chionista) cortezi* in the northern gulf of California, Mexico. Veliger 45:45-54.

Surge, D., K. Lohmann & G. Goodfriend. 2003. Reconstructing estuarine conditions: Oyster shells as recorders of environmental change, southwest Florida. Estuarine, Coastal and Shelf Science 57:737.

Ward, L. W. 1992. Molluscan biostratigraphy of the Miocene, middle Atlantic coastal plain of North America /. Martinsville Virginia Museum of Natural History. Pages pp.

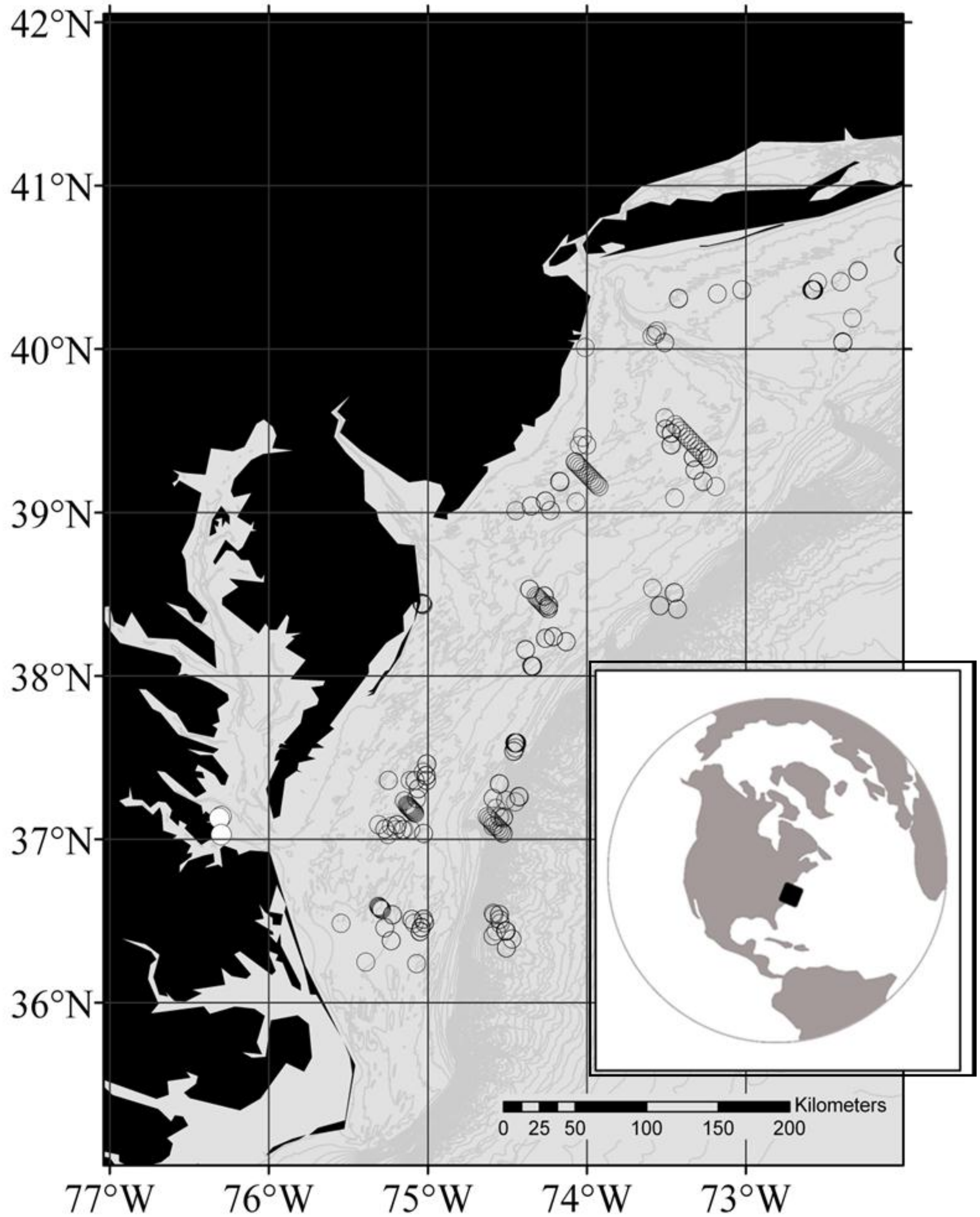

Figure 3.1. Collection localities (open circles) for *Spisula spp.* collected alive on the continental shelf, and Pliocene fossil specimens (white circles) collected from coastal plain deposits.

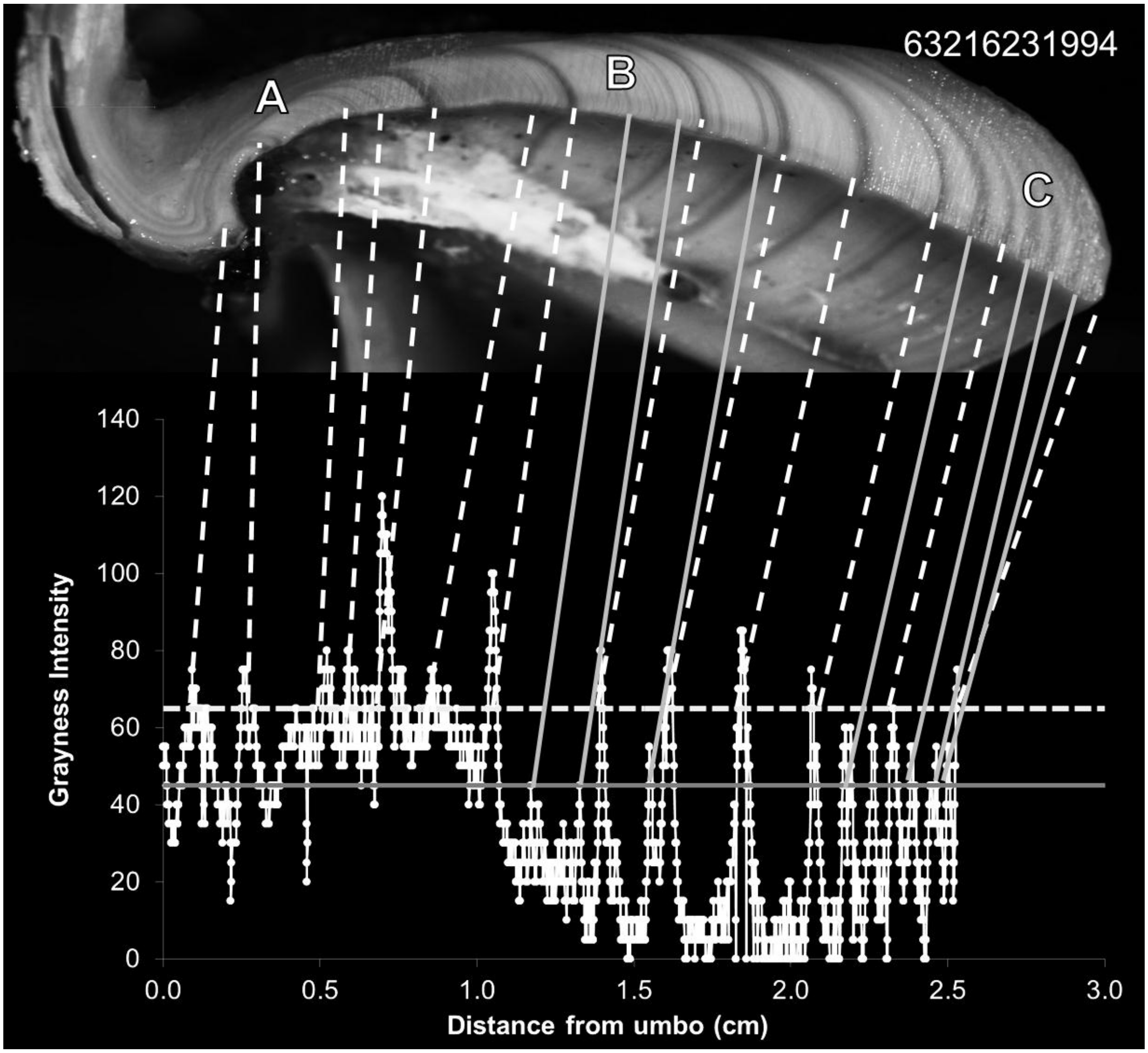

Figure 3.2. Example comparison of visual count versus computer-assisted count picks on sample number 6321621994. The horizontal dashed-white line at 65 grayness intensity represents first choice intensity level used by the computer counter. The horizontal gray line at 45 grayness intensity represents the best alternative intensity level for a computer count. Dashed and solid lines connect the 65 and 45 intensity levels to growth lines matches on the chondrophore. Areas around letters A, B, and C are areas of early, middle, and late growth.

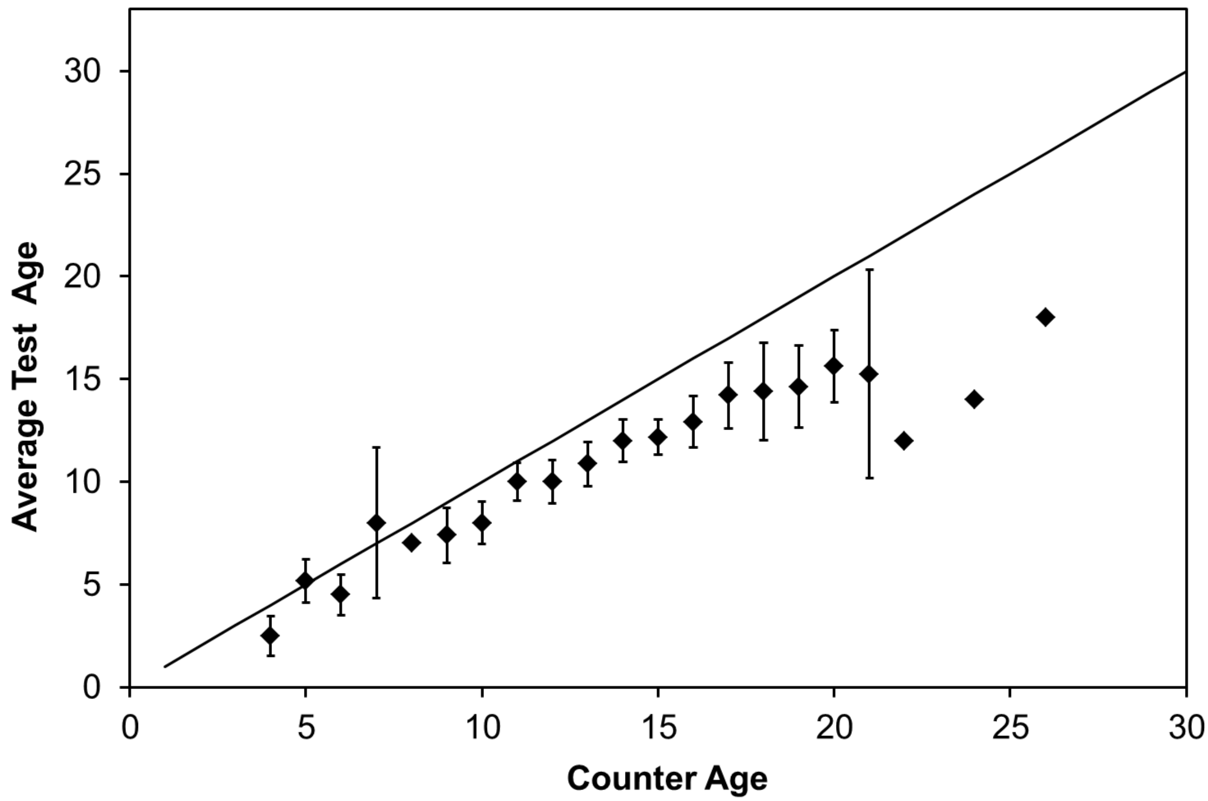

Figure 3.3. Age-bias plot. Counter age versus average test age. Error bars indicate 95% confidence intervals and solid line is the 1:1 line.

Table 3.1 Descriptive statistics of the Visual and Computer counters.

	Mean Age	SD	Min Age	Max Age	Count	Samples	CL (95.0%)
Visual Counter	13.88	4.10	4	26	2388	172	0.62
Computer Counter	11.38	3.68	2	20	1958	172	0.55

CHAPTER 4: COMPARATIVE SCLEROHRONOLOGY OF MODERN AND MID-PLIOENE SURF CLAM (MACTRIDAE) ALONG THE WESTERN MID-ATLANTIC: THE ARCHETYPE REVISITED

Joel Hudley and Donna Surge

Department of Geological Sciences, University of North Carolina, Chapel Hill, 104 South Rd., CB#3315, Chapel Hill, NC 27599-3315, USA email: jhudley@unc.edu

Keywords: Sclerochronology, climate, Pliocene, Yorktown, *Hemimactra*, *Spisula*

(To be submitted to the journal *Palaios*)

ABSTRACT

Modern and fossil species of the genus *Spisula* potentially serve as the archetype bivalve proxy record for contemporary increment and isotope sclerochronology studies. However, this genus has not been sufficiently utilized as paleoclimate and paleoecologic indicators of past temperature regimes in mid- to low-latitude marine realms. Previous studies have limited specimen sampling to small spatial and temporal ranges and focused on the importance of long-lived species. Here, we review and expand the sclerochronologic data for *Spisula* along the western Atlantic margin across a greater portion of its natural range, ecologic amplitude, and deeper into geologic time. This was accomplished by comparing growth parameters, standardized increment time series and

stable isotope data series from *Spisula* populations. This study tests the conclusions of some of the foundational sclerochronologic studies and confirms the usefulness of *Spisula* as annual to multi-decadal environmental proxies.

4.1 INTRODUCTION

The early pioneering studies by Jones (1980 and 1981) and Williams et al. (1982) proposed that the combination of growth increment and isotopic time-series records in the shells of long-lived bivalves are useful subannual climate proxies in modern and ancient shallow-marine environments through geologic time, in regions and on time scales unresolvable by more traditional proxy records from corals or trees (Jones, 1983). Over the last three decades, bivalve sclerochronology has been a powerful tool for paleoenvironmental reconstruction, equivalent to and possibly exceeding its longer established sister-field, dendrochronology (Schöne and Surge, 2005; 2012). Time-series data from dozens of marine and freshwater bivalve taxa, have demonstrated the value of bivalve shell records to reconstruct environmental and climate changes.

Jones (1983) predicted that the ocean quahog, *Arctica islandica* (Linnaeus, 1767), would become the exemplar species for marine sclerochronology because of it's reported longevity (over 150 years Thompson et al., 1980; over 700 years, Richardson and Wannamaker, 2011). Almost three decades later, this prediction holds true. However, it is unexpected that the genus *Spisula* (e.g. *Spisula (Hemimactra) solidissima solidissima* (Dillwyn, 1817))), the archetype bivalve proxy for contemporary increment and isotope sclerochronology procedures (Jones 1978; Jones et al., 1981, Williams et al., 1982; Stecher et al., 1996; Ivany et al., 2003), has not been more utilized. *Spisula* is present in many important geologic settings where *A. islandica* absent, such as along the western Atlantic margin prior to the Holocene.

The Mid Pliocene Warm Period (MPWP, ~3.3 to 3.0 Ma) is among the most critical geologic intervals for studying the Earth during a warm, relatively high atmospheric CO_2 state (Jansen et al., 2007; Salzmann et al., 2011). Moreover, the 2007 report by the Intergovernmental Panel on Climate Change (IPCC, 2007) stated that the middle Pliocene may be an analogue to projections of future 21st century climate change (Meehl, et al., 2007). Similarities include: the continents and oceans have similar configurations, the interior of the continents were and are expected to be arid, estimated temperature ranges are similar, atmospheric CO_2 levels were and are expected to be higher than today, and sea and continental ice were and are expected to be reduced. The report explicitly states that the mid Pliocene "presents a view of the equilibrium state of a globally warmer world." Paleoclimate data available from the United States Geological Survey (USGS) Pliocene Research, Interpretation, and Synoptic Mapping (PRISM) project and a variety of independent studies enable modeling of global climatic conditions during the Pliocene (Dowsett et al., 2011). Lacking in these data are sufficiently high-resolution time series that can potentially provide more detailed information about annual temperature cyclicity (seasonality) and regional climate variability. Unlike *A. islandica, Spisula* are present in the early PRISM deposits investigated by USGS researchers (Dowsett, H.J. and L.B. Wiggs, 1992; Dowsett et al., 1992), and they represent a proxy capable of providing important high-resolution data.

In this study we review and significantly add to the sclerochronologic data for *Spisula* along the eastern coast of North America using modern examples of *S.s. solidissima* and *S. s. similis* (Say, 1822) collected alive and Pliocene aged fossil *Spisula spp*. from mid-Atlantic coastal plain (MACP) formations. This study employs growth increment methods (using the von Bertalanffy growth equation constants and regionally standardized growth increment time series) and stable isotope ratios ($^{18}O/^{16}O$, $^{13}C/^{12}C$) as independent paleoenvironmental proxies. In conjunction with the data from previously published works, this combination of techniques enables a comparative investigation of changes in sea water temperature, depth, seasonality, and interannual variability during modern and mid-Pliocene globally warm conditions. The objectives of this study are to: (1) supplement previous increment and isotope sclerochronologic data on modern *Spisula spp.* by examining shell growth patterns across a greater portion of its natural range and across its ecologic amplitude; (2) test if modern *Spisula spp.* shells consistently record regional environmental patterns when compared to instrumental records across its natural range; and (3) assess whether fossil *Spisula* collected from MACP high stands deposited during the MPWP are useful paleoclimate archives of seasonal variability in seawater temperature. We tested the following hypotheses: (1) *S. s. solidissima* living in shelf waters exhibit increment width growth and isotopic patterns that more significantly reflect local seawater conditions in which they grow than those not living in the same region; (2) estimated regional sea water conditions derived from live-collected bivalve growth patterns are significantly similar to conditions based on direct instrumental measurements; and (3) fossil *Spisula* from the MACP can be used as paleoclimate archives by comparing patterns in fossil shells to patterns in shells found living along the region today.

4.1.1 Ecology of modern Atlantic surf clam

Large *Spisula*, such as the Atlantic surf clam *S. s. s. solidissima*, are commercially important molluscs (Bivalvia: Mactridae) occurring in abundance in the North Atlantic since at least the Eocene. In the North Atlantic basin, commercially exploited species include *S. s. s. solidissima* and *Mactromeris polynyma* (Stimpson, 1860) along the western margin, and *S. elliptica* (Brown, 1827), *S. solida* (Linnaeus, 1758), and *S. subtruncata* (da Costa, 1778) along the eastern margin. Along the western shelf, *S. s. s. solidissima* is found in continental shelf waters along North America between the Gulf of St. Lawrence and North Carolina (the western Atlantic boreal biogeographic province; Briggs and Bowen, 2012) and commercially harvested between Cape Cod and New Jersey (the mid-Atlantic Bight (MAB)) (Weinberg and Helser, 1996; Hare and Weinberg, 2005). Smaller subspecies, *S. s. similis* (Say, 1822) and *S. s. raveneli* (Conrad, 1832) (synonyms), are primarily found in shallower waters south of Cape Hatteras and into the Gulf of Mexico (Carolinian province; Briggs and Bowen, 2012), but also occupy a narrow range of coastal habitats as far north as Long Island Sound (Walker and Heffernan, 1994; Hare et al., 2010). A similar distribution occurs along the eastern Atlantic margin with *S. solida* and *S. subtruncata* ranging south of Iceland to Spain and Morocco, while *S. elliptica* extends north from Ireland to the Barents Sea. Though surf clams are morphologically convergent, DNA variations display net divergence, indicating long-term reproductive isolation of all species and subspecies (Hare and Weinberg, 2005).

Spisula are infaunal, siphonate suspension feeders occupying water depths extending from approximately 5 to 65 m (Cargnelli et al., 1999) and inhabit sand-dominated sediments in high-energy neritic, subtidal zones (Snelgrove et al., 1998). Surf clams are found primarily in marine waters, in salinities higher than 28 psu, but are capable of surviving in salinities as low as 12.5 psu and as high as 52 psu (Castagna and Chanley, 1973). The optimal temperature for burrowing activity is between 16-26°C. The lethal temperature in laboratory experiments is 37°C, though surf clams in the field survive in temperatures between 2°C and 26°C with adult upper limits of 28-30°C (Goldberg and Walker, 1990).

Growth rate in MAB surf clams is not uniform throughout the year (Jones, 1978; Jones, 1980; Cargnelli et al., 1999). Though shell growth is potentially affected by various environmental conditions, growth is most significantly correlated with temperature. Shell accretion rate is positively correlated with warmer temperatures and negatively correlated with variations in temperature with optimal shell accretion centered around 11°C (Jones 1980; Ivany et al., 1999). Studies measuring conditional indices of meat dry weight to shell length indicate that optimal growth is at bottom water temperature around 20°C (Weinberg, 2005). Individual *S. s. solidissima* are reported to attain significant longevity, estimates of 37 years, and a maximum shell length (dorsal to ventral) of 226 mm (Ropes and Jerald 1987). *S. s. similis* is shorter lived, 5-10 years (significant longevity in the animal kingdom), and grows to a smaller maximum size of 121 mm (Walker and Heffernan, 1994).

4.1.2 Modern Location

The MAB is commonly defined as the continental shelf region extending from Cape Hatteras to Nantucket Shoals (Figure 4.1). It has a temperate climate and a broad continental shelf adjacent to a coast dominated by micro-tidal, inshore estuaries, with three major river inputs. These river inputs include the Hudson and Delaware Rivers, and large estuaries of the Chesapeake Bay. This area is characterized by a cold and warm season as shown by instrumental records of daily air temperature (1976-2008) at the Ambrose Light, NY (C-MAN ALSN6) and Cape Hatteras (MB 41001) (http://www.ndbc.noaa.gov/). The warmest average monthly sea surface temperature (SST) at the Ambrose Light is 22±1.4ºC and 26.2±1.2ºC at Cape Hatteras, while the coldest SST is 4.2±1.4ºC off New York and 14.9±3.8ºC off North Carolina. Maximum warm SSTs are reached in July off New York and August off North Carolina, while coldest SSTs are reached February and March, respectively.

Recent scientific interests in the region is expansive,and studies from the preceding decades that focus mostly on mean circulation and dynamics as overviews include (Bumpus (1973); Beardsley et al. (1976); Beardsley and Boicourt (1981); and Lentz (2008)). The character of MAB water is generally cooler and lower in salinity than the oceanic waters seaward of the shelf (~30-35 psu, MARMAP, Appendix A, Figures 3 and 4). MAB water is the product of a cold, low salinity water mass originating from along the southern coast of Greenland (Chapman and Beardsley, 1988), flowing through the Gulf of Maine and then locally modified by inter-annually variable seasonal heating and cooling, precipitation and river runoff, and mixing with oceanic waters (Fairbanks, 1982; Mountain, 2003). Though there are few long-term records of currents, the mean circulation direction over the MAB shelf is equatorward along the shelf, and the speed generally increases with distance from shore (Beardsley et al. (1976); Lentz (2008)

Recent observations demonstrate that MAB circulation is subject to both seasonal and interannual variability due to through-flow flux. This flux relates to the time a volume of water enters the MAB from the north and exits either through the Gulf Stream (GS) or through an unknown pathway to the south. MAB circulation is, therefore, directly connected to both northern cold, freshwater areas via buoyant, southward surface currents and thermohaline driven meridional overturning mechanisms via the cold, bottom currents and the GS (Häkkinen and Rhines, 2004;Shoosmith, 2005; Hamilton, 2005; Lund, 2006). This includes features such as distinctive bands of cold bottom water located over the mid- and outer shelf, colloquially named the “cold pool”. The cold pool persists from the winter throughout the summer until the thermocline deepens in the fall to allow water column mixing, and this modulates annual nutrient compositions across the shelf (Mountain, 2003). Observations also indicate that the MAB, with its adjacent oceanic gyre regions, should be considered as a complex system rather than the generally accepted straight “pipes”.

4.1.3 Geologic context

The US MACP is the low-lying area between the Appalachian Highlands and Piedmont regions and the MAB. Geologically, the MACP is a tectonically stable area with numerous emergent marine deposits of Cenozoic age that provide evidence for regional marine climates and relative sea level positions. Emergent Pliocene age marine deposits from Virginia (Figure 4.1) were chosen for their proximity to important oceanographic and atmospheric circulation features. Such features include the surficial (GS) and deep western boundary currents which became enhanced with the closure of the Panama Isthmus during the Pliocene (Keigwin, 1982; Cronin 1988; Haug et al., 2001; Molnar and Cane, 2002) and Labrador Current water system, which developed during the Pliocene (~2.5 Ma) (Berggren and Hollister, 1977).

Radiometric chronologies indicate the Yorktown Formation (Fm) in Virginia and North Carolina is restricted in age to 4.8-2.4 Ma (Cronin et al., 1993). According to litho- and biostratigraphy evidence, the Yorktown Fm of Virginia represents tropical to temperate climatic conditions and has been dated using nannofossil assemblages (Hazel, 1971; Cronin and Hazel, 1980; Cronin et al., 1984) and molluscan biozones (Ward and Blackwelder, 1976; Blackwelder, 1981). Paleoecological evidence also indicates open marine conditions with normal marine salinity (Mansfield, 1931; Petuch, 1982; Ward and Strickland, 1985; Krantz, 1990). The Yorktown Fm contains molluscan assemblages (including *Dinocardium*) which indicate a pronounced episode of warming (MPWP) reflecting a mixture of warm-temperate to tropical conditions (Ward, 1998). This assemblage, different from today's, represents either a northward shift of warm tropical waters during the early to mid- Pliocene and/or less cool boreal waters reaching the current physiographic and biogeographic divide at Cape Hatteras, NC. Presently, the Yorktown Fm is at the southern limit of the cold-temperate zone (Briggs and Bowen, 2012).

4.2 MATERIALS AND METHODS

4.2.1 Collection and growth increments

Modern *S. s. solidissima* shells were collected by the National Oceanic and Atmospheric Administration (NOAA) Fisheries Service Northeast Regional Fishery Science Center (NEFSC): Fishery Biology Program located at Woods Hole, MA. This unit conducts stock (i.e., population) assessments of commercial bivalves. Modern *Spisula* were collected alive from adjacent shelf waters (~50-200 meters (m) depth). NOAA surveys shellfish every 3 years. They collected individuals from 5 surveys during 1992 through 2002 in 10 NOAA statistical areas(Figure 4.1). The NOAA-NEFSC employs a random stratified survey sampling technique where they have no fixed-stations but a wide sampling distribution within the 1º×1º statistical areas along the shelf (Azarovitz, 1981). Data comprising the dates of harvest and spatial characteristics (e.g. latitude, longitude, depth, etc.) for the surf clams used are available in NEFSC Resource Survey Reports (http://www.nefsc.noaa.gov/esb/rsr.html) (this study subset in Appendix A, Table 1). A change in dredge opening size from earlier (1980s) surveys limited the capture of smaller individuals (<4 years old). Twenty five *S. s. similis* specimen provided by G.L Wingard (USGS) and 4 additional *S. s. similis* shells were collected by hand in the near shore sub-tidal zone from Playa Linda Beach, eastern coast of Florida.

Specimens were cleaned in a dilute bleach solution, rinsed with water, and allowed to dry. Once clean, shells were photographed and weighed (using a Sartorius electronic balance, accurate to 0.0001 g). The length of the maximum growth axes (width, length, and height) of each shell was measured across the valve and chondrophore using digital calipers (0.01 mm) and grade of preservation recorded (Figure 4.2; Appendix A, Table 1). Pliocene *Spisula* shells were collected from the Yorktown Fm (Yorktown locality) and provided by the Virginia Museum of Natural History (VMNH). All fossil specimens were selected based on taxonomy, similarity of paleoenvironments (e.g. fully marine, depth, and salinity) and physical and chemical preservation. Shells collected and identified by Lauck Ward (USGS, VMNH retired) are from the Yorktown Monument, Rice's and Zook's Pit localities in southeastern Virginia (Figure 4.1). Pliocene specimens were identified by Ward as *S. (Hemimactra) confraga* (Conrad) and *S. modicello* (Conrad). Due to the ancient and fragile nature of the shells, all fossil specimens were broken. Shells with both dorsal and ventral margins were measured for length. Only fragments with intact umbonal regions were examined for age and growth rate, totaling 17 specimens.

All well preserved shells with unbroken chondrophores from NOAA live collections and Pliocene locations underwent standard sclerochronologic increment analysis (Williams et al., 1982; Jones et al., 1983). One valve from each shell (either the only remaining or most complete valve) was radially sectioned from umbo to ventral margin, along the axis of maximum length (height), using a Lortone Model FS6 lapidary saw equipped with a diamond blade. Prior to cutting, fast-hardening epoxy was applied to the exteriors of the shells to reduce breakage. Half of each sectioned shell was affixed to a slide using epoxy and cut into thick sections with a Buehler IsoMet low speed saw. The thick sections were ground down using 600 grit and polished down to 1 μm suspended diamond polish, on a variable speed grinder-polisher (Buehler). Shells were again cleaned, rinsed and allowed to dry. The thick sections were digitized using an Olympus stereomicroscope with a 12.5 megapixel DP71 digital camera. Using the Discover image analysis software, shell length, age, and annual growth increment width were measured and recorded (Appendix A, Tables 2 and 5). Age was determined by counting alternating patterns of translucent (dark = slow growth) and opaque (light = rapid growth) segments under reflected light (Jones et al., 1978; Ropes and O'Brien, 1979). Dark/light couplets in relatively long-lived *Spisula* represent annual growth (Jones, 1996). The reference *S. s. simils* were not sectioned; however, aging was determined by counting couplets using light transmitted through the intact shell (Walker and Heffernan, 1994).

Using the growth increment measurements, growth curves were plotted to determine whether comparisons between modern and Pliocene populations serve as a proxy for paleoenvironmental conditions, specifically SST and depth. Latitudinal variations in growth, related to temperature and subspecies, have been examined in modern surf clam population along the Canadian and United States shelf (Jones et al., 1978; Walker and Heffernan, 1994, up to age 3 years; Weinberg and Hessler, 1996, MAB region). The modern growth versus depth relationship is consistently noted in population studies, but tested in inshore versus offshore populations (Jones et al., 1978; Ambrose et al., 1980; increments) and in Pleistocene fossil populations (Jones, 1980, increments; Krantz et al., 1987, isotopes). Neither connection has been tested in Pliocene *Spisula* populations. The von Bertalanffy growth model (VBGM) was employed to quantitatively test this relationship (von Bertalanffy, 1957):

$$E_t = L_\infty\left[1 - e^{-k(t-t_0)}\right]$$

where E_t = the expected or mean length at time (or age) t, L_∞ = the asymptotic average length, k = the Brody growth rate coefficient (yr^{-1}), and t_o = the time or age when the average length was zero. The VBGM is commonly used in *Spisula* growth studies (Jones, 1978; Cerratto and Keith, 1992; Castro and Monteiro, 1995; etc.) and many other bivalve growth studies for population comparisons. The parameters L_∞ and k enabled direct comparisons between the growth of modern and fossil populations. However, for comparisons to be significant, according to Cerrato (1990) VBGM analyses require sample sizes in excess of 300 measurements to produce k and L_∞ parameter values that do not violate curvature effects and inaccurate outcomes. In addition to our data, modern growth data were compiled from previous publications with large measurement data sets, similar processing methods, and available VBGM parameters and arranged by species from north to south (Jones et al. 1978; Serchuk and Murawski, 1980; Cerrato and Keith, 1992; Walker and Heffernan, 1994; Weinberg and Helser, 1996; Weinberg et al., 2005). Though some previous studies used slightly different curve-fitting methods (computer programs) or VBGM equations incorporating non-zero t_o values, reported L_∞ and k were accepted as-is because minor differences among studies should not affect qualitative interpretation of the parameter trends as the non-zero t_o values are very small and methods so similar.

Using standard dendrochronologic techniques, individual specimen growth was detrended (Briffa et al., 1992). Growth trends due to phylogeny were detected by first examining the average growth model curve of shell population series (Briffa et al., 1992) (Appendix A, Figure 1). The mean species growth trend is used to detrend and standardize all the individual ontogenic growth patterns. A dimensionless index is used to visually and statistically cross-date the live-collected specimens to form a chronology for the 8 NOAA statistical areas and the MAB as a whole. Pliocene *Spisula* could not be cross-dated, thus their chronology was based on stratigraphic evidence. The models for ontogenetic curves of all the shells were modeled using the standard individual-based detrending developed by Cook and Peters (1981) and employed by various bivalve studies (e.g. Schöne et al., 2003; Ivany et al., 2011). In this individual-based detrending method, the raw increment data series from each individual shell was formatted using the decadal-format CASE program in the University of Arizona's Dendrochronology Program Library (DPL) (Holmes, 1999) and loaded into dendrochronology program library in R (dplR). The dendrochronology program library in R (dplR) was developed by Bunn (2008) to emulate the DPL programs such as COFECHA and ARTSAN. For each individual, a cubic smoothing spline was fitted to the series of measured growth increments I_t (t = 1, 2…n) using the detrend command (series, method= 'Spline) in dplR with a spline frequency response of 50% to obtain a series of expected increment growth G_t. Using dplR, individual growth ring width indices (RWI) for all shells and regional chronologies for modern shells were computed and recorded. Standardized growth indices (SGI) were computed using the residuals of the splines and the means of the residual population. SGI increment width series are an expression of the number of standard deviations away from zero (zero represents expected growth from the VBGM) with thinner bands being less than and wider bands being greater than expected growth.

4.2.2 Stable isotopes

Two *S. s. solidissima* (identification number: SS0190702, live-collected June 4, 2002, and SS3070299, live-collected June 27, 1999), one *S. s. similis* (SSFLA1, collected articulated July 1997), and two Pliocene Yorktown Fm. *S. confraga* (SC001A and SC003) were analyzed isotopically to compare shell records to present marine environmental conditions (Appendix A, Figure 2). Specimen SS0190702 was collected from the shelf off the southeastern shore of Long Island (NOAA statistical area 613, depth ~24.5 m) and SS3070299 from the shelf east of the Albemarle Sound (NOAA statistical area 631, depth ~36.0 m). These specimens were chosen because of their locations, near the apparent entry and exit points of MAB shelf water, depths, their size and age (~112 mm length, 17 and 15 years respectively). Subannual oxygen and carbon isotope records from the young portions (4-7 annuli) of these two shells should capture shelf water characteristics at the ends of the MAB and overlap temporally.

S. s. similis was examined to determine if there were any species-specific differences in isotopic ratios. Commonly found in the SAB and near shore, modern specimen SSFLA1 was collected dead, but articulated, in the intertidal zone along Playa Linda Beach, Florida (28.6°N, 80.6°W). *S. s. similis* was examined because of its morphological similarity to *S. confraga* and *S. s. solidissima* when found in the field along the MAB and MACP. A recent study using mitochondrial DNA markers found *S. s. similis* in Long Island Sound (41ºN) well north of its typically reported range (Hare et al., 2010). This range extension northward past the modern physiographic and biogeographic boundary at Cape Hatteras calls into question the taxonomy of some specimens used in previous near shore S. solidissima studies (Jones 1978; 1980; 1981; Cerrato and Keith,

1992) and demonstrates that: 1) some *Spisula* in the shallow waters of the MAB are potentially *S. s. similis* misidentified as *S. s. solidissima*; and/or 2) *Spisula* (e.g. *S. confraga* and *S. modicello*) in Yorktown MACP deposits may be compared to these "southern" surf clams that breach the Cape Hatteras biogeographic boundary in the past.

S. confraga specimens SC001A and SC003 were collected at Rice's Borrow Pit in Hampton County, VA (Yorktown Fm, USGS locality 26112, 37.0°N, and 76.4° W). The exposed surficial deposit is part of the Morgarts Beach Member (3.6-2.6 Ma) of the Yorktown Fm, corresponding to Molluscan Zone 5 (M5, Burwellian Stage) (Blackwelder, 1981) and within the MPWP (Dowsett, 1992; Haywood et al., 2009).

To acquire high-resolution, subannual samples, sectioned *Spisula* chondrophores were microsampled across the visible growth lines. Before microsampling, the microstructures of all shells were screened under a stereomicroscope to evaluate preservation of original aragonite (Appendix A, Figure 2). If original aragonite was present, then it was assumed the specimen was not diagenetically altered. Sampling strategy was guided by the dark increments, whose locations were noted during sampling. For *S. s. solidissima* shells, microsamples were collected from the younger portions of the shells because growth rates throughout the populations are rapid for the first 2 years of growth and the individual growth diverge from the rest of the population depending on water depth (Jones et al., 1980; Jones et al., 1983). The chondrophore of modern specimens SSFLA1, SC001A, and SC003 were sampled across their entire lengths. Shells were microsampled at 5-14 samples per year, depending on the width of the increment, to achieve subannual resolution. The sampling resolution was lower for these smaller chondrophore (SSFLA1, SC001A, and SC003) because of the smaller area and sampling strategy. Microsampling was performed on a Merchentek micromill fitted with a 0.3 mm dental burr. Each digitized drilling path produced approximately 50 µg of carbonate powder for isotopic analysis. Oxygen and carbon isotope ratios of the powdered shell carbonate samples were measured using a gas-ratio mass spectrometer (Finnigan MAT 252) coupled to an automated carbonate preparation device (Kiel-III) housed at the Environmental Isotope Laboratory at the University of Arizona. Powdered samples were reacted with dehydrated phosphoric acid under vacuum at 70°C for one hour. Isotopic ratios were calibrated based on repeated measurements of NBS-19 (National Bureau of Standard) and NBS-18. The precision of the measurements was ±0.1 ‰ for $\delta^{18}O$ (1σ, 1 standard deviation) and ±0.06‰ for $\delta^{13}C$ (1σ). The results are reported in per mil units (‰) relative to the VPDB (Vienna Pee Dee Belemnite) standard. Reported $\delta^{18}O$ and $\delta^{13}C$ values were plotted against distance from umbo along with annotations showing the locations of the dark growth increments.

To evaluate whether $\delta^{18}O$ and $\delta^{13}C$ values in *Spisula* shells can be used to estimate MAB and MACP seawater, we compared: 1) $\delta^{18}O$, $\delta^{13}C$, and estimated temperatures between modern and Pliocene shells; and 2) estimated temperatures based on $\delta^{18}O$ measurements of *Spisula* shells to modern instrument records. Estimated temperature was calculated following procedures from Williams et al. (1982) and using the equation reported by Grossman and Ku (1986):

$$T°\mathrm{C} = 20.6 - 4.34(\delta^{18}O_C - (\delta^{18}O_{SW} - 0.27‰))$$

where $\delta^{18}O$ (VPDB) is the isotope ratio from the shell carbonate (aragonite) and $\delta^{18}O_{SW}$ is the oxygen isotope ratio of sea water (VSMOW; Vienna-Standard Mean Ocean Water). Note that the original equation subtracted −0.2‰ from the $\delta^{18}O_{SW}$ value to account for the different scales on which carbonate and water are measured (i.e., VPDB and VSMOW, respectively). Gonfiantini et al. (1995) has since reported this correction as −0.27‰. To estimate seawater temperature from $\delta^{18}O$ values of modern shells, regional MAB $\delta^{18}O_{SW}$ values were estimated using the $\delta^{18}O_{water}$-salinity mixing equation reported by Fairbanks (1982):

$$\delta^{18}O_{MABW(VSMOW)} = 0.258 \times salinity - 9.14$$

where $\delta^{18}O_{MABW(VSMOW)}$ is the oxygen isotope ratio of MAB water. Based on the mean annual bottom salinity from NEFSC-MARMAP corresponding to the period of growth for the specimens investigated, a $\delta^{18}O_{MABW}$ value of −0.88±0.5‰ (32.02±1.92 psu) was used for specimen SS0190702 and a value of −0.6±0.55‰ (32.02±1.92 psu) was used for specimen SS3070299. MARMAP salinity data displayed a range of average annual salinity values between 27.69 and 33.81 psu for both locales. For modern specimen SSFLA1, a $\delta^{18}O_{SW}$ value of +0.9‰ was used. Oxygen isotope ratios of seawater along central and south Florida range between 0‰ and +1‰ depending on the proximal location of the GS (regionally called the Florida Current) and seasonal to interannual precipitation patterns (Swart et al., 1989). The 0.9‰ value was based on a compilation and distribution of global $\delta^{18}O_{W}$ values reported by Biggs and Rohls (2000) and consistent with values from Levitus (1993). No standard deviations were reported in these references. A $\delta^{18}O_{SW}$ value of +1.1‰ was used for Pliocene aged *Spisula* based on model predictions reported by Williams et al. (2009) for all members of the Yorktown Formation.

4.3 RESULTS

4.3.1 Shell Ages and Growth Parameters

The median age of all live collected *S. s. solidissima* is 11 years, the modal age is 6 years, and the mean age is 10.7±4.4 years. The youngest modern *S. s. solidissima* is 3 years old, while the 2 oldest specimens are 23 years old. Fossil *S. confraga* from the Yorktown Fm had minimum age of 4 years and a maximum age of 10 years with a mean age of 6±2 years. Pliocene *S. modicello* has a mean age of 7±3 years, with a minimum age of 4 years and a maximum age of 12 years.

Calculated k and L_∞ parameter values from all modern MAB *S. S. s. solidissima* populations are 0.150 and 163.00 mm, respectively. Calculated k and L_∞ parameter values for *S. s. similis* from the Florida Atlantic coast are 0.43 and 72.34 mm, respectively. Pliocene *S. modicello* and *S. confraga* from the Yorktown Fm have calculated k-values of 0.62 and 0.24, respectively, and maximum lengths of 44.32 mm and 43.23 mm, respectively.

4.3.2 Variations in growth increments

Calculated annual mean SGIs for the statistical areas used in our study are given in Tables 4 and 5. The SGIs for areas 621 and 626 (off the Delmarva Peninsula; Figure

4.1) were excluded because of low numbers of individuals that can be used for cross-dating. The cross-dated individuals provided a time series of SGIs from 1972 to 200, longer than most RWI and on similar timescale to the continuously sampled MARMAP record (Tables 4 and 5). In comparison, individual RWIs that includes those individuals that could not be used for cross-dating extended back to 1969 (Appendix A, Tables 3 and 4). The maximum length of the SGIs was 30 years (Area 613; Table 4) with a mean time range of 23±3 years. The number of cross-dated individuals in each SGI increases from 1972 to 2001. Individual SGIs, MAB-wide, and MAB-regional chronologies were plotted along with mean annual surface and bottom SST and salinity measurements from the NEFSC Marine Resources Monitoring, Assessment, and Prediction (MARMAP) program (http://www.nefsc.noaa.gov/nefsc/publications/crd/crd0408/#dt) (Appendix A, Figures 5 and 6.

4.3.3 Variations in stable isotopes

All *Spisula* exhibited temporal variations of δ^{18}O values following a relatively sinusoidal trend. Oxygen isotope ratios for *S. s. solidissima* SS0190702 ranged from −1.0‰ to +1.6‰ with a mean of +0.2±0.7‰ (*n*=49; Figure 4.5, Table 4.2). Values from specimen SS3070299 ranged from +0.4‰ to +2.3‰ with a mean of 1.5±0.5‰ (*n*=40; Figure 4, Table 2). Values of δ^{18}O recorded in *S. s. similis* SSFLA1 ranged from −1.0‰ to +0.8‰ with a mean of 0.1±0.5‰ (*n*=27; Figure 4.5, Table 4.2). Specimen SS190702 exhibited the largest range of δ^{18}O values (2.6‰). SS3070299 and SSFLA1 displayed similar ranges of 1.8‰ and 1.9‰, respectively. Oxygen isotope ratios for Pliocene age *S.*

confraga SC001A ranged from +1.4‰ to +2.9‰ with a mean of +2.1±0.4‰ (*n*=28; Figure 4.9, Table 4.2), and SC003 ranged from +1.6‰ to +3.2‰ with a mean of 2.5±0.4‰ (*n*=31; Figure 4.9, Table 4.2). Both shells displayed similar ranges of 1.6‰ and 1.5‰, respectively.

Like $\delta^{18}O$ values, the temporal variation of $\delta^{13}C$ values recorded in modern and fossil *Spisula* shells displayed a more or less sinusoidal pattern. However, the patterns were not in phase with and were smaller than the associated $\delta^{18}O$ values. Carbon isotope ratios of modern *Spisula* ranged from +0.6‰ to +2.4‰ with a mean of +1.7±0.4‰ (SS0190702), +1.2‰ to +2.7‰ with a mean of +1.9±0.4‰ (SS3070299), and −0.4‰ to +1.0‰ with a mean of +0.5±0.4‰ (SSFLA1) (Figure 4.5, Table 4.2). Pliocene shells ranged from +0.7 to +2.0‰ (SC001A) and +0.3‰ to +1.7‰ (SC003) with both having a mean of +1.2±0.3‰ (Figure 4.9, Table 4.2). No clear secular trend was exhibited by the modern *Spisula* $\delta^{13}C$ value series; however, the Pliocene *S. confraga* series SC001A and SC003 displayed $\delta^{13}C$ values that noticeably decreased with ontogenetic age (i.e., away from the umbo). No significant correlation was observed between $\delta^{18}O$ and $\delta^{13}C$ values in either modern or Pliocene species of *Spisula* (Figure 4.8, Table 4.3).

4.4 DISCUSSION

4.4.1 Comparison of growth parameters

VBGM parameters measured from western North Atlantic surf clams reveal trends within and among species related to latitude and depth. L_∞ values from the modern MAB *S. s. s. solidissima* populations show a difference in the maximum length attained between shallow (inshore) and deeper (offshore) populations south of New Jersey (statistical areas 614 and 615), but there is no clear latitudinal trend (Figure 4.4). Following Richardson et al. (1999), we evaluated whether there are morphological differences between inshore and offshore populations. When comparing the linear relationship between chondrophore and valve length reveals slopes of the trend lines are influenced by depth (Figure 4.3). Shells from depths greater than 50 m have the steepest slope, whereas those from less than 25 meters fall along the most shallow slope. The apparent difference in slope is, however, small. For all depth bins, the measured lengths is a 1:1 relationship and f-tests for variance between the regressions indicate the greatest variance between the shallowest and deepest bins. However, the f-tests fail to reject the null hypothesis that the populations are significantly different ($f = 0.362$, $f_{crit} = 0.591$, <25m vs. > 50m). L_∞ values of *S. s. s. solidissima* from this study are also shorter than previous studies with the notable exception of Jones et al. (1978; inshore). These values are very similar to the St. Joseph Bay population (Walker and Heffernan, 1994), but our samples did not attain the same maximum length.

Unlike L_∞ values, *k*-values generally decrease with decreasing latitude for populations of *S. S. s. solidissima,* both on- and offshore with notable exceptions near the New Jersey shelf region. That same latitudinal trend is shown with *S. s. similis k*-values and generally for maximum shell length. There is no latitudinal difference between Pliocene *Spisula* samples/species. Our values are indistinguishable from NOAA-NEFSC studies that analyzed many of the same individuals but used the right instead of the left valve. (Weinberg and Hesler, 1996; Weinberg et al., 2005) (Table 4.1). MAB sub-region parameters are also very similar. The differences in k-values between adjacent sub-regions (inshore versus offshore) in our study are 0.002 to 0.107 with the largest difference occurring in the New Jersey shelf region.

Our observations are consistent with previous Atlantic surfclam growth studies that propose that both decreasing latitude and water depth result in higher *k*-values, earlier age of maturity, and shorter lifespans likely occur under natural conditions (Ropes, 1980; Jones, 1980; Walker and Heffernan, 1994; Chintala and Grassle, 2001; and others). Intraspecific (*S. S. s. solidissima)* variations of these *k*-value occurrences (small sized, shorter life span, etc.) are largely related to latitudinal temperature and depth related temperature variations across the species' natural range. Assuming that *Spisula* inhabiting the more marginal environments of their natural range likely experience and exhibit less than optimal growth conditions than individuals in the center of range will experience more ideal growth conditions, then using *k*-values allows us to infer where within the range an individual grew. If *k*-value trends are viewed on the three range dimension axes (latitude, distance from shore, and depth), trend lines should have high *k*-values on the ends with a low in middle as in instead of a simple linear trend. High ends of the latitude axis are seen at Georges Banks (GB) and southern Delmarva with the low near northern New Jersey (Figure 4). The anomalously high *k*-values that dominate where the low should be on the latitude axis are consistent if they represent the shallow end of depth axis. This interpretation is consistent with a map view of offshore conditional indices for *S. S. s. solidissima* (Marzec et al., 2010, Figures 1, 3, and 5) where highest conditions are along the -20 to -30 isobaths and diminish as they move farther offshore. As in the present study, Marzec et al. (2010) sample populations in federal waters (offshore), but inshore (Chang et al., 1976; Chintala and Grassle, 2001) growth and length-weight studies are consistent with Jones' (1980) high *k*-value.

The same growth parameter relationship trends should hold true for interspecific (Mactridae) growth trends. Polar and equatorial species should have populations where larger growth and greater longevity are common, and variations in depth modulate these characteristics. The narrow ecological amplitude and depth ranges of the warm water surfclam species (*S. s. similis, S. modicello*, and S. *confraga*) we investigated enables us to best related lower latitude (biogeographic province) to k-values and longevity, but paleodepth effects are difficult to determine because of the limited sample ranges. *S. s. similis* parameters show a similar trend over a large latitude range (Long Island Sound to Florida). Unfortunately, all populations are shallow, either collected by dredges or divers (<15 m) or as articulated beach drift. Consistent with our prediction of trends, the end members of the range (LIS and FL Gulf) are on average older (age 7-12 years) than those found in middle (example Walker and Heffernan, 1994, Figure 4).

The calculated *k*-values for the Yorktown shell populations fall within the variable ranges for modern *S. S. s. solidissima* populations living at the warm-temperate latitude margin, or the deeper or cold-temperate latitude margin of *S. s. similis*. Pliocene *Spisula* growth parameters are challenging to compare since they were sampled at the same latitude and display very different *k*-values. This may be due to different shell thicknesses. Thin *S. confraga* look very similar to *S. s. similis,* and were measured to have a maximum age of 10 years with a mean age of 6±2 years. All of the *S. modicello* shells were very worn, but their original thickness and shell shape is similar to the modern, tropical *Mactrellona alata* (Spengler). The more robust *S. modicello* had a mean age of 7±3 years, with a maximum aged of 12 years. These ages are comparable to shallow, northern *S.s. similis* ages (Cerrato and Keith, 1992; Hare et al., 2010, Long Island Sound). The high *k*-values and relative abundance and longevity of both these species lead us to reason that they are "warm" water species living either near the center of their conditional range or closer to the colder (northern and/or deeper) margin of that range. Listed occurrences of *S. confraga* and *S. modicello* are limited to the Pliocene Virginia localities, but *S. subparilis* and *Spisula spp.* are found in more southern localities (Florida). Paleodepth estimates for our sample localities place them on a fully marine shell (>25 m) (Ward and Blackwelder, 1976; Blackwelder, 1981). This is consistent with succeeding estimates of emergent Pliocene deposits paleodepth (Cronin et al., 1989; Dwyer and Chandler, 2005). However, all of our samples are worn and broken (evidence of transport) and may have migrated either along or down isobaths. Previous studies indicated that a high ratio of Plio-Pleistocene *Spisula* fossils exhibited morphology of modern individuals living above the seasonal thermocline (Jones, 1980; Arthur et al., 1983). Anomalously high VBGM *k*-value, in terms of both inter- and intra-specific variations, are most likely related to decreasing depths (larger SST variation, lower salinities, and higher predation) but are inseparable associated with decreasing latitude (warmer average temperatures).

4.4.2 SGI Comparisons

A plot of the population-wide SGI indices from the MAB indicated that *S. s. solidissima* growth displayed interannual variation over the interval 1972-2001 (Figure 4.10, bottom panel; Statistical Areas, Appendix A, Figures 5 and 6). SGIs were plotted along with regional NEFSC-MARMAP bottom temperature and salinity anomaly instrumental records which initiated in 1977. The SGIs series are expressed as the number of standard deviations away from zero, with an SGI of 0.0 equaling the expected growth in *S. S. s. solidissima* in an area or the entire MAB. Yearly SGI values >0.0 denoted years of higher than expected growth, whereas years with SGI values <0.0 represented years of poorer than expected growth. All SGI time series within the MAB contain similar clusters of years having greater than expected growth: years 1980-1984, 1993-1996, and 2001 (Tables 4.3 and 4.4, Figure 4.10; Appendix A, Tables 3 and 4, Figures 5 and 6). Between these clusters were several years of slightly above or slightly below expected growth, except for a lower than predicted episode between 1975 and 1980.

SGI time series and yearly NEFSC-MARMAP instrumental records for the period 1977-2001 appeared closely related (Figure 4.10; Appendix A Figures 5 and 6). Most

SGI increments of significantly greater than expected growth coincide with years of colder than normal bottom water temperatures, and slower than expected growth occurs during years with higher than normal bottom water temperatures. Least-squares regressions were used to test the relationship between mean annual bottom water temperatures, mean annual salinity anomaly, and the SGI profiles. A weak correlation exists between shell increment growth in *S. s. solidissima* and MAB water temperatures (r=0.15, p-value =4.5×10^{-14}). Separated into statistical areas, linear regressions showed correlations were weak to insignificant, and ranged between r=0.05, p =4.7×10^{-14} (Area 625) and r=0.43, p =2.8×10^{-16} (Area 613). The observed negative relationship between SGI and water temperature consistently occurs between 1985 and 1997, but diverges at the beginning and ends of the chronologies where the number of cross-dated individuals was low. The relationship between SGI series and MAB salinity was insignificant (r=0.01, p =0.06), as was the relationship between measured MAB bottom water temperature and salinity (r=0.01, p =2.11×10^{-29}).

The strong correlation between temperature and SGI reported by Jones (1980) and (1983) for inshore (0-25 m) specimens is consistent with the known influence of temperature on the growth of S. *S. s. solidissima*, but is not consistently demonstrated in the SGIs of the populations from this study. However, positive correlations exist during the years 1977-1982 and 1985-1989. The lack of significant correlation between growth and temperature in this study does not reject previous findings nor does it invalidate our conclusions.

Our growth parameter results indicate that most of the offshore specimens sampled are experiencing the high to medium growth conditions near the center of their range and ecological amplitude. This is demonstrated by relatively flat (low interannual variability) SGIs in 4 of regions in the mid-1990s to 2000, during intervals with large numbers of cross-dated individuals. The offshore SGIs, producing complacent (i.e., low amplitude) time series, should be rejected due to poor site selection for producing bivalve-increment time series sensitive to local environmental variability. The SGI for all MAB S. *S. s. solidissima* demonstrate a weak correlation, and most though weak likely represents a time series capable of capturing MAB-wide anomalies in volume, temperature, and salinity related to larger physical oceanographic variations (Mountain, 2003).

4.4.3 Species stable isotope distinctions

Estimated SST from modern specimens were plotted using mean, maximum, and minimum $\delta^{18}O_W$ values (Figure 4.6). Modern *Spisula* temperature estimate ranges were plotted against instrumental records in proximity to their collection locations (Figure 4.6). Pliocene estimates were graphed along with modern instrumental and bivalve proxy-based seawater temperature ranges for adjacent shelf and corresponding Yorktown deposits. *Spisula* $\delta^{18}O$, $\delta^{13}C$, and estimated temperatures were also compared to each other (Table 4.2).

Our study is consistent with previous studies that isotopic proxy data from *Spisula* shells can be used for paleotemperature reconstruction (Jones et al., 1983; Krantz et al., 1987). The clear annual cycles in both modern and fossil shell is strong evidence that there were minimal effects of diagenesis on the data and that shell growth in the early years of ontogeny were consistent. In all the shells observed, dark increments corresponded with the coldest recorded temperatures. This is consistent with previous studies on *Spisula* growth that indicate these marks are annual (Jones 1978; 1980; etc.)),though the actual timing of marks likely varies slightly through the range due to the small offset in annual shelf water temperature cycles.

Estimated temperatures, based on $\delta^{18}O$ values, for *S. s. solidissima* in the MAB showed a general range of 6.8 ºC to 19.9 ºC (Figure 4.4, Table 4.2). Estimated temperature for SS0190702 ranged from 8.6 ºC to 19.9 ºC with a mean of 14.6±3.2 ºC (Figure 4.4, Table 4.2). The warmest estimated temperatures in SS0190702 (at $\delta^{18}O$ lows within the light growth increments) ranged from 14.6 ºC to 21.11 ºC with a mean of 18.1±2.7 ºC (n=7; Figure 4.4, Table 4.2). Coldest estimated temperatures (near dark increments) ranged from 8.6 to 12.6 with a mean of 10.1±1.3 ºC (n=8; Figure 4.4, Table 4.2). The estimated temperature range for SS0190702 encompassed almost all of the range in seawater temperature measured at the Ambrose Light (NOAA-ALSN6, water depth: 21 m) during 1986-1993 (Figure 4.6). Two periods of >24 ºC were not captured. SS3070299 estimated temperature values ranged from 6.8 ºC to 15.0 ºC with a mean of 10.3±2.1 ºC (Figure 4.4, Table 4.2). The warmest estimated temperatures in SS3070299 ranged from 11.53 ºC to 15.1 ºC with a mean of 13.8±1.6 ºC (n=4), while the coldest ranged from 6.8 ºC to 8.5 ºC with a mean of 7.5±0.7 ºC (n=4; Figure 4.4). Plotted against SST measurements from NOAA buoy 44009 (water depth: 28 m, sampling depth: 0.6 m), SS3070299 estimated temperatures failed to capture measured SST <5 ºC and >16 ºC.

However, when compared to NEFSC-MARMAP bottom temperatures (mean: 9.77±2.16 ºC, range: 6.34-14.08 ºC), SS3070299 estimated temperatures enclosed that entire range.

SSFLA1 estimated temperature values ranged from 20.0 ºC to 27.7 ºC with a mean of 23.1±2.3 ºC (Figure 4.4, Table 4.2). The warmest estimated temperatures in SSFLA1 were 27.7 ºC and 26.9 ºC with a mean of , while the coldest estimated temperatures calculated were 19.9 ºC and 20.7 ºC (Figure 4.4). SSFLA1 temperature estimates only captured the warmest measured SST from the nearest active shoreline NOAA meteorological station (SAUF1; depth 0 m) during its lifespan. Station 41009, the an offshore buoy 20 nautical miles (37.4 km) east of Cape Canaveral (depth 44.2 m) exhibited measured SSTs range from 23.0 ºC to 27.6 ºC (Q_3) with a mean of 25.2±2.7 ºC, corresponding well to the estimated temperature range (Figure 4.6).

Estimated temperature for *S. confraga* SC001A ranged from 11.5 ºC to 18.3 ºC with a mean of 15.1±1.8 ºC (Figure 4.8, Table 4.2), and SC003 values ranged from 10.4 ºC to 17.1 ºC with a mean of 15.5±1.9 ºC (Figure 4.8, Table 4.2).The *S. confraga* displayed similar ranges of 6.8 ºC and 6.7 ºC. The warmest estimated temperatures in SC001A ranged from 17.5 ºC to 18.3 ºC with a mean of 18.8±0.4 ºC (n=3), while the coldest ranged from 8.6 ºC to 13.2 ºC with a mean of 11.6±2.1 ºC (n=4; Figure 4.4). The warmest estimated temperatures in SC003 ranged from 15.8 ºC to 17.1 ºC with a mean of 16.5±0.6 ºC (n=5), while the coldest ranged from 10.3 ºC to 11.8 ºC with a mean of 11.1±0.7 ºC (n=5; Figure 4.4). When compared to previously published bivalve $\delta^{18}O$ temperature estimate data from the MACP Yorktown Fm (Krantz, 1990; Goewert and Surge, 2008), only the warmest *S. confraga* temperature estimates overlapped the published range (Figure 4.9). *S. confraga* mean estimated temperatures of 14.2±1.0 ºC straddled the mean SST and standard deviation (15.5±7.0 ºC) of the NOAA station CHLV2 (Chesapeake Light, http://www.ndbc.noaa.gov/) (Figure 4.9).

The largest modern estimated temperature range of 11.3 ºC was exhibited by SS0190702, the most northern MAB surf clam, and the smallest (7.7 ºC) by SSFLA1, collected off Florida. The largest standard deviation of all *Spisula* estimated temperature series was recorded by SS0190702 (±3.2 ºC), while the smallest standard deviations (±1.8-1.9 ºC) were displayed and the *S. confraga* (SC001A and SC003; MACP, Yorktown Fm). Similar standard deviations about their means were recorded by *S. s. solidissima* SS30702 and *S. s. similis* SSFLA1 (±2.1 ºC and ±2.3 ºC, in that order).

The live-collected *S. s. s. solidissima* shells did not have a similar $\delta^{18}O$ ranges. This offset of about 0.5‰ reduced the range of temperature estimates captured by SS3070299 below the full range of the continuous SST buoy record but close to southern MARMAP bottom temperature values. Yorktown *Spisula* displayed similar $\delta^{18}O$ ranges, but these ranges are just above previously published $\delta^{18}O$ values for the Yorktown and smaller in range than the $\delta^{18}O$ recorded by modern *S. s. similis*. The colder than previously published bivalve $\delta^{18}O$ temperature estimate data from the MACP Yorktown Fm might be: (1) an artifact of low shell sampling not resolving the warmest portions of the year, (2) a systematic difference between the aragonite shell mineralization in the surfclam and the calcite in the scallops, or (3) the actual temperatures recorded, just during different times and at different depths within the Pliocene. Overall, estimated temperature profiles from Yorktown Fm *Spisula* shells document greatly reduced seasonality, similar to the modern *S. s. similis*, but with similar average temperatures relative to modern SST at the same latitude.

4.5 CONCLUSIONS

With their abundance, size, relative longevity, easily measured growth marks, wide distribution, and good preservation species of *Spisula* remain excellent archetypes for bivalve sclerochronology. *Spisula* is a consistently useful environmental recorder of sea water temperature, depth, seasonality, and interannual variability during modern and ancient shelf conditions, and along their entire western Atlantic coast range, it consistently records annual growth marks during the coldest season and dependably displays regional environmental patterns within its shells when compared to instrumental records. Further comparison of growth parameters across wide natural ranges should enable more reliable paleoecological interpretations and site selection for the increment derived time series.

ACKNOWLEDGEMENTS

Thanks to the Virginia Museum of Natural History for providing the fossil shells picked and identified by Dr. Lauck Ward. Thanks to Dr. Jay Burnett (NOAA-retired) and the Northeast Fisheries Science Center (NEFSC) Fishery Sampling Branch for the live-collected surf clams. Thanks to Dr. G. Lynn Wingard (USGS) for providing shells from South Florida and fossil references. Dr. David Dettman at the Environmental Isotope Laboratory at the University of Arizona performed isotopic analysis of carbonate samples. This paper is largely derived from a dissertation written under the guidance of DS, and made possible by the stimulus and support of the Preston Jones and Mary Elizabeth Frances Dean Martin Trust (UNC-Chapel Hill) and National Science Foundation Grants #AGS-0602422 (DS) and #HRD-0450099 (Valerie Ashby, UNC-AGEP).

REFERENCES

Azarovitz, TR. (1981). A brief historical review of the Woods Hole Laboratory trawl survey time series. In: Doubleday, WG and Rivard, D, eds. Bottom trawl surveys. Canadian Special Publication of Fisheries and Aquatic Sciences 58, p. 62-67

Bailey, R. H. and S. A. Tedesco. (1986). Paleoecology of a Pliocene coral thicket from North Carolina: an example of temporal change in community structure and function. Journal of Paleontology 60(6):1159-1176.

Blackwelder, B.W. (1981a). Late Cenozoic stages and molluscan zones of the middle U.S. Atlantic Coastal Plain. Journal of Paleontology, Memoir, 12: Part II.

Blackwelder, B.W. (1981b). Stratigraphy of upper Pliocene and lower Pleistocene marine and estuarine deposits of northeastern North Carolina and southeastern Virginia. U.S. Geological Survey Bulletin, 1502-B: B1-B16.

Briggs, J.C. and B.W. Bowen (2012). A realignment of marine biogeographic provinces with particular reference to fish distributions. Journal of Biogeography, 39, 12-30.

Cargnelli, L.M., S.J. Griesbach, D.B. Packer, and E. Weissberger (1999). Essential fish habitat source document: Atlantic surfclam, *Spisula* solidissima, life history and habitat characteristics. NOAA Tech. Memo. NMFS-NE-142.

Cronin, T.M. (1991). Pliocene shallow water paleoceanography of the North Atlantic Ocean based on marine ostracodes. Quaternary Science Review, 10: 175-188.

Cronin, T.M. and H.J. Dowsett. (1996). Biotic and oceanographic response to the Pliocene closing of the central American Isthmus. In: Jackson, J.B.C., Budd, A.F., Coates, A.G. (Eds.), Evolution and Environment in Tropical America. University of Chicago, IL, 76-104.

Cronin, T.M. and J.E. Hazel. (1980). Ostracode biostratigraphy of Pliocene and Pleistocene deposits of the Cape Fear Arch region, North and South Carolina. U.S. Geological Survey Professional Paper, 1125-B: B1-B25.

Cronin, T.M., H.J. Dowsett, G.S. Dwyer, P.A. Baker, and M.A. Chandler. (2005). Mid-Pliocene deep-sea bottom-water temperatures based on ostracode Mg/Ca ratios. Marine Micropaleontology, 54: 249-261.

Cronin, T.M., L.M. Bybell, R.Z. Poore, B.W. Blackwelder, J.C. Liddicoat, and J.E. Hazel. (1984). Age and correlation of emerged Pliocene and Pleistocene deposits, U.S. Atlantic Coastal Plain. Palaeogeography, Palaeoclimatology, Palaeoecology, 47: 21-51.

Dowsett, H.J. and L.B. Wiggs. (1992). Planktonic foraminiferal assemblages of the Yorktown Formation, Virginia, USA. Micropaleontology, 38: 75-86.

Dowsett, H.J. and R.Z. Poore. (1991). Pliocene sea surface temperatures of the North Atlantic Ocean at 3.0 Ma. Quaternary Science Review, 10: 189-204.

Dowsett, H.J. and T.M. Cronin (1990). High eustatic sea level during the middle Pliocene: Evidence from the southeastern U.S. Atlantic Coastal Plain. Geology, 18: 435-438.

Dowsett, H.J., J.A. Barron, and R.Z. Poore. (1996). Middle Pliocene sea surface temperatures: a global reconstruction. Marine Micropaleontology, 27: 13-25.

Dowsett, H.J., J.A. Barron, R.Z. Poore, R.S. Thompson, T.M. Cronin, S.E. Ishman, and D.A. Willard. (1999). Middle Pliocene paleoenvironmental reconstruction: PRISM2. U.S. Geological Survey Open File Report, 99-535: 1-33.

Dowsett, H.J., M.A. Chandler, T.M. Cronin, and G.S. Dwyer. (2005). Middle Pliocene sea surface temperature variability. Paleoceanography, 20: 1-8.

Dowsett, H.J., T.M. Cronin, R.Z. Poore, R.S. Thompson, R.C. Whatley, and A.M. Wood. (1992). Micropaleontological evidence for increased meridional heat transport in the North Atlantic Ocean during the Pliocene. Science, 258: 1133-1135.

Elliot, M., P.B. deMenocal, K.L. Braddock, S.S. Howe. (2003). Environmental controls on the stable isotopic composition of Mercenaria mercenaria: potential application to paleoenvironmental studies. Geochemistry, Geophysics, Geosystems, 4: 1056–1072.

Fairbank, R.G. (1982). The origin of continental-shelf and slope water in the New York Bight and Gulf of Maine –Evidence from δ18O/ δ16O ratio measurements. Journal of Geophysical Research: Oceans and Atmospheres, 87: 5796-5808.

Gardner, J. (1944). Mollusca from the Miocene and Lower Pliocene of Virginia and North Carolina, Part 1: Pelecypoda. United States Geological Survey Professional Paper, 199-A: 1-178.

Gardner, J. (1948). Mollusca from the Miocene and Lower Pliocene of Virginia and North Carolina, Part 2: Scaphopoda and Gastropoda. United States Geological Survey Professional Paper, 199-B: 1-310.

Gaspar, M B, M Castri and C C Monteiro (1995). Age and growth rate of the clam, *Spisula solida* L., from a site off Vilamoura, south Portugal, determined from acetate replicas of shell sections. Scientia Marina 59 (supl. 1): 87-93

Goewert, A.E., Surge, D., (2008). Seasonality and growth patterns using isotope sclerochronology in shells of the Pliocene scallop Chesapecten madisonius. Geo-Marine Letters 28, 327–338.

Goodwin, D.H., Schöne, B.R., Dettman, D.L., (2003). Resolution and fidelity of oxygen isotopes as paleotemperature proxies in bivalve mollusk shells: models and observations. Palaios 18, 110–125.

Gonfiantini, R., Stichler, W., Rozanski, K., (1995). Standards and intercomparison materials distributed by the International Atomic Energy Agency for stable isotope measurements, Reference and intercomparison materials for stable isotopes of light elements. I.A.E.A., pp. 13-29

Grossman, E.L., and T. Ku. (1986). Oxygen and carbon isotope fractionation in biogenic aragonite: temperature effects. Chemical Geology, 59: 705 59–74.

Hare, M.P. and J.R. Weinberg (2005). Phylogeography of surfclams, *Spisula* solidissima, in the western North Atlantic based on mitochondrial and nuclear DNA sequences. Marine Biology, 146: 707-716.

Hare, M.P., J. Weinberg, O. Peterfalvy, and M. Davidson (2010). The “southern” surfclam (*Spisula* solidissima similis) found north of its reported range: A commercially harvested population in Long Island Sound, New York. Journal of Shellfish Research, 29, 4, 799-807.

Haug, G.H. and R. Tiedemann. (1998). Effect of the formation of the Isthmus of Panama on Atlantic Ocean thermohaline circulation. Nature, 393: 673-676.

Haug, G.H., R. Tiedemann, R. Zahn, and A.C. Ravelo. (2001). Role of Panama uplift on oceanic freshwater balance. Geology, 29: 207-210.

Haus, B.K., H.C. Graber, L.K. Shay, and T.M. Cook (2003). Along shelf Variability of a Coastal Buoyancy Current during the relaxation of downwelling favorable winds. Journal of Coastal Research, 19(2): 409-422

Haywood, A.M. and P.J. Valdes (2004). Modelling Pliocene warmth: contribution of atmosphere, oceans and cryosphere. Earth and Planetary Science Letters, 218: 363-377.

Haywood, A.M., P. Dekens, A.C. Ravelo, and M. Williams. (2005). Warmer tropics during the mid-Pliocene? Evidence from alkenone paleothermometry and a fully coupled ocean-atmosphereGCM. Geochemistry, Geophysics, and Geosystems, 6: 1-20.

Haywood, A.M., P.J. Valdes, and B.W. Sellwood. (2000). Global scale palaeoclimate reconstruction of the middle Pliocene climate using the UKMO GCM: initial results. Global and Planetary Change, 25: 239-256

Haywood, A.M., Valdes, P.J., Sellwood, B.W., Kaplan, J.O. Dowsett, H.J. 2001. Modelling Middle Pliocene warm climates of the USA. Palaeontologia Electronica, v.4, art.5. (available at: http://palaeoelectronica.org/2001_1/climate/issue1_01.htm)

Hazel, J.E. (1971). Ostracode biostratigraphy of the Yorktown Formation (upper Miocene and lower Pliocene) of Virginia and North Carolina. U.S. Geological Survey Professional Paper, 704:1-13.

Helama, S. and J.K. Nielsen (2008). Construction of statistically reliable sclerochronology using subfossil shells of river pearl mussel. Journal of Paleolimnology, 40: 247-261.

Johns, W.E., T.J. Shay, J.M. Bane, D.R. Watts, (1995). Gulf Stream structure, transport, and recirculation near 68° W. Journal of Geophysical Research, 100, 817-838.

Jones, D.S. (1980). Annual cycle of shell growth increment formation in 2 continental-shelf bivalves and it paleoecologic significance. Paleobiology, 6 (3)m 331-340.

Jones, D S (1981). Reproductive cycles of the Atlantic surf clam *Spisula solidissima* and the ocean quahog *Arctica islandica* off New Jersey. Journal of Shellfish Research 1(1): 23-32

Jones, D.S., D.F. Williams and M.A. Arthur (1983). Growth history and ecology of the Atlantic surf clam, *Spisula solidissima* (Dillwyn), as revealed by stable isotopes and annual shell increments. J. Exp. Mar. Biol. Ecol, 73: 225 - 242

Jones, D.S., I. Thompson and W. Ambrose (1978). Age and growth rate determinations of the Atlantic surf clam *Spisula solidissima* (Bivalvia: Mactracea), based on internal growth lines in shell cross-sections. Marine Biology 47: 63-70

Jones, D.S. (1983). Sclerochronology: reading the record of the molluscan shell. American Scientist, 71: 384-391.

Jones, D.S., B.J. MacFadden, S.D. Webb, P.A. Mueller, D.A. Hodell, and T.M. Cronin. (1991). Integrated geochronology of a classic Pliocene fossil site in Florida: linking marine and terrestrial biochronologies. Journal of Geology, 99: 637-648.

Jones, P. D., and M. E. Mann (2004), Climate over past millennia, Rev. Geophys., 42, RG2002.

Jones, P.D., K.R. Briffa, T.P. Barnett and S.F.B. Tett (1998). High-resolution palaeoclimate records for the last millennium: interpretation, integration and comparison with General Circulation Model control-run temperatures. The Holocene, 8(4): 455-471.

Jossi, J.W. and R.L. Benway (2003). Variability of temperature and salinity in the middle Atlantic bight and Gulf of Maine based on data collected as part of the MARMAP Ships of Opportunity Program, 1978-2001. NOAA Tech Memo NMFS NE 172; 1-92.

Kelly, K.A., (1991). The meandering Gulf Stream as seen by the Geosat altimeter: surface transport, position and velocity variance from 73° to 46°W. Journal of Geophysical Research, 96, 16721-16738.

Krantz, D. E., Williams, D. F. and Jones, D. S., (1987). Ecological and paleoenvironmental information using stable isotope profiles from living and fossil molluscs. Palaeogeography, Palaeoclimatology, Palaeoecology, 58:249 266.

Krantz, D.E. (1990) Mollusk-Isotope Records of Plio-Pleistocene Marine Paleoclimate, U.S. Middle Atlantic Coastal Plain. Palaios, 5: 317-335.

Krantz, D.E. (1991). A chronology of Pliocene sea-level fluctuations: the U.S. Middle Atlantic Coastal Plain record. Quaternary Science Reviews, 10: 163-174.

Krauss, W., (1986). The North Atlantic Current. Journal of Geophysical Research, 91, 5061-5074.

Lentz, S.J. (2008a). Observations and a model of the mean circulation over the Middle Atlantic bight continental shelf. Journal of Physical Oceanography, 30(6), 1203-1221.

Lentz, S.J. (2008b). Seasonal variation in the circulation over the Middle Atlantic bight continental shelf. Journal of Physical Oceanography, 38(7), 1486-1500.

Lunt, D.J., Valdes, P.J., Haywood, A., Rutt, I.C., (2008). Closure of the Panama Seaway during the Pliocene: implications for climate and Northern Hemisphere glaciation. Climate Dynamics 30, 1–18.

Marchitto, T.M., D.S. Jones, G.A. Goodfriend, and C.R. Weidman. (2000). Precise temporal correlation of Holocene mollusk shells using sclerochronology. Quaternary Research, 53(2):236-246.

Marine Resources Monitoring, Assessment, and Prediction website: http://www.nefsc.noaa.gov/nefsc/publications/crd/crd0408/#dt

McConnaughey, T.A., Gillikin, D.P., (2008). Carbon isotopes in mollusk shell carbonates. Geo-Marine Letters 28, 287–299.

Meehl, G.A., T.F. Stocker, W.D. Collins, P. Friedlingstein, A.T. Gaye, J.M. Gregory, A. Kitoh, R. Knutti, J.M. Murphy, A. Noda, S.C.B. Raper, I.G. Watterson, A.J. Weaver, Z.-C. Zhao. (2007). Global climate projections. In: S. Solomon, D. Qin, M. Manning, Z. Chen, M. Marquis, K.B. Averyt, M. Tignor, and H.L. Miller (Eds.), The Physical Science Basis. Contribution of Working Group I to the Fourth Assessment Report of the Intergovernmental Panel on Climate Change, Cambridge University Press, Cambridge, United Kingdom, and New York, NY, USA.

Mountain, D. G. (2003). Variability in the properties of Shelf Water in the Middle Atlantic Bight, 1977–1999, Journal of Geophysical Research, 108(C1), 3014.

Mountain, D.G. and T.J. Holzwarth. (1989). Surface and bottom temperature distribution for the northeast continental shelf. NOAA Tech. Mem. NMFS-F/NEC-73; 32 p.

Mountain, D.G.; Taylor, M.H.; Bascuñán, C. (2004). Revised procedures for calculating regional average water properties for Northeast Fisheries Science Center cruises. Northeast Fisheries Science Center Reference Document 04-08; 53 p. Available from: National Marine Fisheries Service, 166 Water St., Woods Hole, MA 02543.

National Research Council. (2002). Abrupt Climate Change: Inevitable Surprises. Washington, DC, National Academy Press.

O'Hare, G., Johnson, A., Pope, R., (2005). Current shifts in abrupt climate change: the stability of the North Atlantic Conveyor and its influence on future climate. Geography 90, 250–266.

Raymo, M.E., B. Grant, M. Horowitz, and G.H. Rau. (1996). Mid-Pliocene warmth: stronger greenhouse and stronger conveyor. Marine Micropaleontology, 27: 313-326.

Ropes J W and L O'Brien (1979) A unique method of aging surf clams. ICES C.M. 1979/K:28

Ropes, J W (1968) Reproductive cycle of the surf clam, *Spisula solidissima*, in offshore New Jersey. Biological Bulletin (Woods Hole) 135: 349 – 365.

Schöne, B.R, (2003). A 'clam-ring' master-chronology constructed from a short-lived bivalve mollusc from the northern Gulf of California, USA. The Holocene, 13, 39–49.

Schöne, B.R., D.H. Goodwin, K.W. Flessa, D.L. Dettman, and P.D. Roopnarine. (2002). Sclerochronology and growth of the bivalve mollusks Chione (Chionista) fluctifraga and Chione (Chinista)cortezi in the northern Gulf of California, Mexico. Veliger, 45: 45-54.

Schöne, B.R., Surge, D. (Eds.), (2005). Looking back over skeletal diaries — high-resolution environmental reconstructions from accretionary hard parts of aquatic organisms. Palaeogeography, Palaeoclimatology, Palaeoecology, vol. 228, pp. 1–192.

Stecher, H.A, III, Krantz, D.E., Lord, C.J. III, Luther, G.W III, and K.W. Bock (1996). Profiles of strontium and barium in Mercenaria mercenaria and *Spisula* solidissima shells, Geochimica et Cosmochimica Acta, Volume 60, Issue 18, Pages 3445-3456

Surge, D., Kelly, G., Arnold, W. S., Walker, K. J., and A. Goewert (2008). Isotope sclerochronology of Mercenaria mercenaria, M. campechiensis, and their natural hybrid form (Bivalvia): Does genotype matter? Palaios, 23:559–565.

Ward, L.W. (1992). Molluscan biostratigraphy of the Miocene, Middle Atlantic Coastal Plain of North America, Virginia Museum of Natural History Memoir 2: pp. 159.

Ward, L.W. (1998). Mollusks from the lower Miocene Pollack Farm Site, Kent County, Delaware: a preliminary analysis, In: Benson, R.N., ed. Geology and paleontology of the lower Miocene Pollack Farm Fossil Site, Delaware: Delaware Geological Survey Special Publication, 21: 59-131.

Ward, L.W. and B.W. Blackwelder. (1980). Stratigraphic revision of upper Miocene and lower Pliocene beds of Chesapeake Group, middle Atlantic Coast Plain. U.S. Geological Survey Bulletin, 1482-D: 1-61.

Ward, L.W. and Blackwelder, B.W. (1987). Late Pliocene and Early Pleistocene Mollusca From the James City and Chowan River Formations at the Lee Creek Mine, In: Ray, C.E., ed. Geology and Paleontology of the Lee Creek Mine, North Carolina, II, Smithsonian Contributions to Paleobiology, 61: 1-283.

Ward, L.W. and G.L. Strickland. (1985). Outline of Tertiary stratigraphy and depositional history of the U.S. Atlantic Coastal Plain. In: C.W. Poag (Eds.), Geologic evolution of the United States Atlantic margin. New York, Van Nostrand Reinhold Company. 87-123.

Ward, L.W., Bailey, R.H., Carter, J.G., (1991). Pliocene and Early Pleistocene stratigraphy, depositional history, and molluscan paleobiogeography of the coastal plain. In: Horton, J.W., Zullo, V.A. (Eds.), The geology of the Carolinas: Carolina Geological Society fiftieth anniversary volume. University of Tennessee Press, Knoxville, TN, pp. 274–289.

Weinberg J R (1999) Age-structure, recruitment and adult mortality in populations of the Atlantic surfclam, *Spisula solidissima*, from 1978 to 1997. Marine Biology 134: 113-125

Weinberg, J R (1998) Density-dependent growth in the Atlantic surfclam, *Spisula solidissima*, off the coast of the Delmarva Peninsula, USA Marine Biology 130: 621 – 630.

Weinberg, J R and T E Helser (1996) Growth of the Atlantic surfclam, *Spisula*

Williams, M., Haywood, A.M., Harper, E.M., Johnson, A.L.A., Knowles, T., Leng, M.J., Lunt, D.J., Okamura, B., Taylor, P.D., Zalasiewicz, J., (2009). Pliocene climate and seasonality in North Atlantic shelf seas. Philosophical Transactions of the Royal Society. London A367, 85–108.

Williams, M., Haywood, A.M., Hillenbrand, C.D., Wilkinson, I.P., (2005). Efficacy of δ18O data from Pliocene planktonic foraminifer calcite for spatial sea surface temperature reconstruction: comparison with a fully coupled ocean-atmosphere GCM and fossil assemblage data from the mid Pliocene. Geological Magazine 142 399–417.

Zachos, J., M. Pagani, L. Sloan, E. Thomas, and K. Billups. (2001). Trends, rhythms, and aberration in global climate 65 Ma to present. Science, 292: 686-693.

Zachos, J.M., L.D. Stott, and K.C Lohmann. (1994). Evolution of early Cenozoic marine temperatures. Paleoceanography, 9: 353-387.

Table 4.2. VBGM parameters from natural populations of modern and fossil *Spisula* along the Atlantic coast of the United States.

Location	*k*	L_{∞}	Source
S. s. s. solidissima			
George's Bank	0.242	154.10	Weinberg and Helser, 1996
S. New England	0.300	164.70	Weinberg and Helser, 1996
Long Island	0.251	161.00	Weinberg and Helser, 1996
New Jersey	0.217	163.70	Weinberg and Helser, 1996
New Jersey	0.273	158.70	Serchuk and Murawski, 1980
Delmarva	0.177	164.00	Weinberg and Helser, 1996[1]
Delmarva	0.298	163.80	Serchuk and Murawski, 1980
Point Pleasant, NJ (Offshore)	0.249	148.69	Jones et al. 1978
Chincoteague Inlet, VA (Inshore)	0.456	108.36	Jones et al. 1978
Long Island	0.209	152.74	This study
New York Bight	0.133	152.70	This study
N. New Jersey, < 25 m	0.148	149.31	This study
N. New Jersey, > 25 m	0.110	144.10	This study
N. Delmarva, < 25 m	0.132	163.00	This study
N. Delmarva, > 25 m	0.173	144.55	This study
S. Delmarva, < 25 m	0.175	147.95	This study
S. Delmarva, > 25 m	0.110	137.27	This study
Mid-Atlantic Bight	0.150	163.00	This study
Mid-Atlantic Bight	0.156	163.00	Weinberg et al., 2005 NEFSC
S. s. similis			
Long Island Sound, NY	0.46	84.09	Cerrato and Keith, 1992[2]
Wassaw Island, GA	0.74	75.77	Walker and Heffernan, 1994
St. Joseph Bay, FL	0.46	121.50	Walker and Heffernan, 1994
Playa Linda, FL	0.43	72.34	This study
Spisula modicello (Pliocene)			
Yorktown Fm, MACP	0.62	44.32	This study
Spisula confraga (Pliocene)			
Yorktown Fm, MACP	0.24	43.23	This study

[1] Samples collected from shallower strata, < 27 m, were excluded because of the presence of south subspecies and morphs.

[2]Original reported as multiple populations of *S. s. s. solidissima*, but evidence from recent studies suggest that western LIS populations are *S. s. similis* (Hare et al, 2010).

Table 4.3. Isotopic composition of shells. Samples taken from the *Spisula* were micro-milled from the chondrophore. Samples were run at the University of Arizona's Environmental Isotope Laboratory

Sample ID	min.	Distance (mm)	d13C VPDB	d18O VPDB	C std dev	O std dev	Voltage
SS190702-01	arag	0.383	1.32	1.61	0.038	0.033	1.48
SS190702-02	arag	0.765	1.74	0.25	0.026	0.050	1.57
SS190702-03	arag	1.148	1.96	-0.81	0.013	0.031	1.55
SS190702-04	arag	1.53	1.94	-0.75	0.011	0.055	1.49
SS190702-05	arag	1.913	1.93	0.04	0.016	0.070	1.48
SS190702-06	arag	2.295	1.55	1.58	0.024	0.031	1.66
SS190702-07	arag	2.678	1.61	1.25	0.049	0.029	1.80
SS190702-08	arag	3.06	1.64	1.23	0.019	0.004	2.34
SS190702-09	arag	3.443	1.64	0.49	0.011	0.021	1.70
SS190702-10	arag	3.825	1.87	0.03	0.070	0.018	1.32
SS190702-11	arag	4.208	1.89	-0.26	0.047	0.039	1.34
SS190702-12	arag	4.59	1.97	-0.57	0.014	0.039	2.84
SS190702-13	arag	4.86	1.83	-0.53	0.013	0.015	2.24
SS190702-14	arag	5.071	2.01	-0.46	0.064	0.030	2.91
SS190702-15	arag	5.281	2.10	-0.55	0.008	0.041	2.03
SS190702-16	arag	5.492	2.35	-0.39	0.032	0.228	1.89
SS190702-17	arag	5.703	2.30	-0.20	0.006	0.033	1.48
SS190702-18	arag	5.914	2.39	0.19	0.042	0.016	2.45
SS190702-19	arag	6.125	1.90	1.04	0.023	0.054	1.42
SS190702-20	arag	6.335	1.91	0.88	0.046	0.012	1.71
SS190702-21	arag	6.546	1.50	0.01	0.013	0.041	1.74
SS190702-22	arag	6.757	1.65	-0.52	0.012	0.066	2.36
SS190702-23	arag	6.968	1.84	-0.86	0.056	0.038	1.99
SS190702-24	arag	7.179	2.10	-0.99	0.013	0.033	2.28
SS190702-25	arag	7.389	2.03	-0.99	0.005	0.083	1.37
SS190702-26	arag	7.6	2.24	-0.37	0.015	0.096	1.60
SS190702-27	arag	7.983	2.11	-0.13	0.063	0.027	1.86
SS190702-28	arag	8.365	1.97	1.17	0.008	0.037	2.67
SS190702-29	arag	8.747	1.91	1.23	0.016	0.039	2.52
SS190702-30	arag	9.13	1.86	0.24	0.042	0.009	2.82
SS190702-31	arag	9.512	1.78	0.50	0.094	0.062	2.14
SS190702-32	arag	9.894	2.18	-0.66	0.018	0.025	1.43
SS190702-33	arag	10.277	2.13	-0.06	0.051	0.024	2.40
SS190702-34	arag	11.299	2.17	0.03	0.041	0.088	1.45
SS190702-35	arag	11.609	1.75	0.55	0.014	0.033	2.03
SS190702-36	arag	11.919	1.84	0.68	0.024	0.028	2.37
SS190702-37	arag	12.229	1.06	0.31	0.055	0.018	1.92

Sample ID	min.	Distance (mm)	d13C VPDB	d18O VPDB	C std dev	O std dev	Voltage
SS190702-40	arag	12.534	1.27	0.28	0.014	0.044	2.08
SS190702-38	arag	12.539	0.95	0.78	0.018	0.031	1.94
SS190702-41	arag	12.880	1.56	1.37	0.023	0.066	1.57
SS190702-42	arag	13.188	1.24	0.59	0.023	0.070	2.32
SS190702-43	arag	13.496	1.16	0.04	0.022	0.018	2.76
SS190702-44	arag	13.805	0.65	0.67	0.035	0.024	1.55
SS190702-45	arag	14.113	0.88	1.25	0.017	0.033	2.29
SS190702-46	arag	14.421	1.46	0.83	0.013	0.030	1.42
SS190702-47	arag	14.729	1.69	0.24	0.011	0.062	2.39
SS190702-48	arag	15.038	1.50	0.67	0.015	0.074	1.46
SS190702-49	arag	15.346	1.13	1.43	0.026	0.077	1.62
SS30702-01	arag	0.297	1.21	2.12	0.010	0.030	2.7
SS30702-02	arag	0.593	2.05	2.01	0.063	0.042	1.42
SS30702-03	arag	0.89	1.52	1.78	0.032	0.029	2.14
SS30702-04	arag	1.186	2.47	1.56	0.099	0.156	0.94
SS30702-05	arag	1.482	2.58	1.90	0.049	0.008	2.77
SS30702-06	arag	1.779	2.33	1.79	0.026	0.066	1.87
SS30702-07	arag	2.075	2.70	1.34	0.036	0.057	1.54
SS30702-08	arag	2.372	2.52	1.39	0.049	0.039	2.24
SS30702-09	arag	2.669	2.33	1.17	0.027	0.060	1.03
SS30702-10	arag	2.965	2.29	0.88	0.081	0.033	1.35
SS30702-11	arag	3.523	2.04	0.55	0.077	0.039	1.76
SS30702-12	arag	3.871	1.96	0.38	0.034	0.076	2.53
SS30702-13	arag	4.368	1.94	0.55	0.018	0.050	2.94
SS30702-14	arag	4.684	2.11	1.38	0.023	0.080	1.46
SS30702-15	arag	5	2.42	1.30	0.016	0.023	1.85
SS30702-16	arag	5.316	2.41	1.65	0.042	0.028	2.11
SS30702-17	arag	5.632	2.17	1.78	0.005	0.039	2.59
SS30702-18	arag	5.948	2.10	1.87	0.073	0.050	2.08
SS30702-19	arag	6.264	1.91	1.86	0.009	0.056	2.14
SS30702-20	arag	6.58	1.98	1.50	0.012	0.020	1.52
SS30702-21	arag	6.895	2.05	1.23	0.057	0.058	2.42
SS30702-22	arag	7.211	2.24	1.04	0.055	0.026	2.05
SS30702-23	arag	7.527	2.00	1.24	0.014	0.071	1.76
SS30702-24	arag	7.827	1.84	1.00	0.022	0.034	1.53
SS30702-25	arag	8.021	1.58	0.59	0.005	0.068	2.25
SS30702-26	arag	8.215	1.86	1.09	0.034	0.049	2.58
SS30702-27	arag	8.409	1.79	1.47	0.086	0.062	1.65
SS30702-28	arag	8.603	1.71	2.11	0.011	0.094	1.83
SS30702-29	arag	8.797	1.60	2.11	0.005	0.021	2.26
SS30702-30	arag	8.991	1.62	1.91	0.010	0.032	1.44

Sample ID	min.	Distance (mm)	d13C VPDB	d18O VPDB	C std dev	O std dev	Voltage
SS30702-31	arag	9.184	1.63	1.58	0.045	0.018	2.20
SS30702-32	arag	9.39	1.52	0.88	0.039	0.042	1.42
SS30702-33	arag	9.589	1.17	1.53	0.045	0.050	2.15
SS30702-34	arag	9.789	1.73	1.75	0.037	0.013	1.96
SS30702-35	arag	9.989	1.65	1.85	0.014	0.031	1.42
SS30702-36	arag	10.188	1.70	2.26	0.033	0.063	1.97
SS30702-37	arag	10.388	1.68	2.05	0.033	0.060	2.73
SS30702-38	arag	10.588	1.81	1.48	0.041	0.082	1.63
SS30702-39	arag	10.787	1.48	1.40	0.026	0.020	2.56
SS30702-40	arag	10.791	1.17	1.21	0.019	0.013	1.5
SSFLA1-01	arag	0.055	0.21	0.07	0.025	0.009	1.95
SSFLA1-02	arag	0.111	0.14	0.18	0.016	0.070	2.54
SSFLA1-03	arag	0.166	0.28	0.06	0.026	0.010	1.50
SSFLA1-04	arag	0.221	0.29	0.60	0.016	0.052	2.46
SSFLA1-05	arag	0.277	0.27	0.76	0.050	0.058	1.74
SSFLA1-06	arag	0.332	0.41	-0.03	0.033	0.034	1.64
SSFLA1-07	arag	0.387	0.52	0.40	0.031	0.049	1.92
SSFLA1-08	arag	0.443	0.23	0.66	0.048	0.062	1.42
SSFLA1-09	arag	0.498	0.95	0.10	0.009	0.051	1.65
SSFLA1-10	arag	0.553	1.04	0.33	0.057	0.074	1.93
SSFLA1-11	arag	0.609	0.85	0.61	0.054	0.026	1.48
SSFLA1-12	arag	0.98	0.91	0.71	0.026	0.048	1.23
SSFLA1-13	arag	1.04	0.45	0.18	0.035	0.026	1.95
SSFLA1-14	arag	1.099	0.05	-0.23	0.028	0.036	1.61
SSFLA1-15	arag	1.159	0.35	-0.92	0.050	0.048	1.54
SSFLA1-16	arag	1.219	0.79	-0.25	0.057	0.065	1.61
SSFLA1-17	arag	1.278	0.56	-1.02	0.014	0.024	1.31
SSFLA1-18	arag	2.195	1.00	-0.44	0.022	0.024	1.63
SSFLA1-19	arag	2.421	1.03	0.23	0.077	0.036	2.48
SSFLA1-20	arag	2.647	0.71	0.60	0.028	0.012	1.96
SSFLA1-21	arag	2.873	0.59	0.40	0.033	0.032	1.81
SSFLA1-22	arag	3.099	0.60	0.42	0.015	0.083	1.66
SSFLA1-23	arag	3.325	0.51	0.32	0.028	0.010	1.82
SSFLA1-24	arag	3.551	0.52	-0.10	0.048	0.045	2.13
SSFLA1-25	arag	3.777	0.25	-0.36	0.009	0.008	2.03
SSFLA1-26	arag	4.002	-0.18	-0.82	0.015	0.016	2.57
SSFLA1-27	arag	4.227	-0.44	-0.83	0.034	0.040	1.97
SC001A-01	arag	0.319	1.44	2.48	0.069	0.042	2.48
SC001A-02	arag	0.638	1.38	2.51	0.036	0.078	2.49
SC001A-03	arag	0.958	1.26	2.22	0.038	0.041	1.69
SC001A-04	arag	1.277	1.48	1.85	0.027	0.055	1.84

Sample ID	min.	Distance (mm)	d13C VPDB	d18O VPDB	C std dev	O std dev	Voltage
SC001A-05	arag	1.596	1.48	1.63	0.008	0.062	1.29
SC001A-06	arag	1.915	1.88	1.53	0.012	0.046	2.27
SC001A-07	arag	2.253	1.95	2.47	0.021	0.055	2.77
SC001A-08	arag	2.59	1.71	2.93	0.003	0.067	2.69
SC001A-09	arag	2.928	1.59	2.56	0.013	0.010	2.31
SC001A-10	arag	3.266	1.52	2.27	0.004	0.010	2.37
SC001A-11	arag	3.604	1.51	1.69	0.032	0.021	1.52
SC001A-12	arag	3.941	1.26	1.36	0.016	0.032	2.83
SC001A-13	arag	4.279	1.16	1.39	0.059	0.019	1.74
SC001A-14	arag	4.546	0.93	1.60	0.013	0.064	1.98
SC001A-15	arag	4.813	1.03	2.24	0.009	0.016	2.63
SC001A-16	arag	5.08	1.09	2.61	0.020	0.009	2.78
SC001A-17	arag	5.347	1.25	2.17	0.037	0.030	1.70
SC001A-18	arag	5.614	1.24	1.92	0.029	0.046	2.10
SC001A-19	arag	5.881	1.27	1.75	0.061	0.046	2.48
SC001A-20	arag	6.148	1.07	1.54	0.061	0.030	1.67
SC001A-21	arag	6.529	0.96	1.90	0.006	0.033	1.74
SC001A-22	arag	6.911	1.07	2.27	0.037	0.036	1.97
SC001A-23	arag	7.293	0.88	2.41	0.025	0.071	1.84
SC001A-24	arag	7.675	0.87	2.30	0.003	0.031	1.48
SC001A-25	arag	8.057	0.81	2.16	0.036	0.043	2.37
SC001A-26	arag	8.314	1.15	2.17	0.054	0.025	2.23
SC001A-27	arag	8.55	0.88	2.53	0.013	0.038	2.16
SC001A-28	arag	8.865	0.67	2.34	0.016	0.081	1.62
SC003-01	arag	0.319	1.30	2.32	0.012	0.033	1.74
SC003-02	arag	0.638	1.41	2.67	0.069	0.071	1.38
SC003-03	arag	0.958	1.05	2.77	0.031	0.067	1.59
SC003-04	arag	1.277	1.42	2.93	0.030	0.012	1.60
SC003-05	arag	1.596	1.57	2.81	0.015	0.024	2.03
SC003-06	arag	1.915	1.71	2.41	0.047	0.031	1.44
SC003-07	arag	2.253	1.59	1.86	0.027	0.024	1.88
SC003-08	arag	2.59	1.69	2.51	0.051	0.061	1.77
SC003-09	arag	2.928	1.28	2.92	0.031	0.021	1.35
SC003-10	arag	3.266	1.34	2.83	0.025	0.066	2.68
SC003-11	arag	3.604	1.38	2.45	0.039	0.059	1.52
SC003-12	arag	3.941	1.57	2.18	0.030	0.022	2.29
SC003-13	arag	4.279	1.35	1.80	0.008	0.022	1.9
SC003-14	arag	4.546	1.52	1.66	0.021	0.027	2.80
SC003-15	arag	4.813	1.54	2.01	0.026	0.042	1.58
SC003-16	arag	5.08	1.34	2.45	0.054	0.040	1.62
SC003-17	arag	5.347	1.55	3.04	0.019	0.031	2.65

Sample ID	min.	Distance (mm)	d13C VPDB	d18O VPDB	C std dev	O std dev	Voltage
SC003-18	arag	5.614	1.21	3.19	0.011	0.056	1.92
SC003-19	arag	6.148	1.07	3.06	0.065	0.039	1.69
SC003-20	arag	6.529	1.19	2.34	0.032	0.009	1.51
SC003-21	arag	6.911	0.83	1.74	0.053	0.010	1.68
SC003-22	arag	7.293	1.23	2.40	0.047	0.047	1.67
SC003-23	arag	7.675	1.16	2.83	0.021	0.033	2.15
SC003-24	arag	8.057	0.77	2.85	0.015	0.080	1.48
SC003-25	arag	8.314	0.61	2.23	0.046	0.022	2.02
SC003-26	arag	8.55	0.90	1.65	0.028	0.035	1.88
SC003-27	arag	8.865	1.22	2.33	0.051	0.044	1.73
SC003-28	arag	9.18	1.16	2.74	0.034	0.008	1.90
SC003-29	arag	9.495	0.69	2.72	0.032	0.022	2.01
SC003-30	arag	9.81	0.33	1.93	0.033	0.035	2.05
SC003-31	arag	10.125	1.11	2.51	0.042	0.012	1.64

Table 4.4. Summary statistics for $\delta^{18}O$, $\delta^{13}C$, and $\delta^{18}O$ based temperature estimates preserved in modern and Mid-Pliocene aged *Spisula* shells. Temperature estimates calculated using the equation reported by Schöne et al. (2005) as modified from Grossman and Ku (1986).

	Summary Statistics	**$\delta^{13}C$ (‰ VPDB)**	**$\delta^{18}O$ (‰ VPDB)**	**Temperature (°C)**
SS190702	Mean	1.7	0.2	14.6
	S.D.	0.4	0.7	3.2
	Range	1.7	2.6	11.3
	Minimum	0.6	-1.0	8.6
	Maximum	2.4	1.6	19.9
	Count (*n*)	49	49	49
SS30702	Mean	1.9	1.5	10.3
	S.D.	0.4	0.5	2.1
	Range	1.5	1.9	8.2
	Minimum	1.2	0.4	6.8
	Maximum	2.7	2.3	15.0
	Count (*n*)	40	40	40
SSFLA1	Mean	0.5	0.1	23.1
	S.D.	0.4	0.5	2.3
	Range	1.5	1.8	7.7
	Minimum	-0.4	-1.0	20.0
	Maximum	1.0	0.8	27.7
	n	27	27	27
SC001A	Mean	1.2	2.1	15.1
	S.D.	0.3	0.4	1.8
	Range	1.3	1.6	6.8
	Minimum	0.7	1.4	11.5
	Maximum	2.0	2.9	18.3
	Count (*n*)	28	28	28
SC003	Mean	1.2	2.5	13.5
	S.D.	0.3	0.4	1.9
	Range	1.4	1.5	6.7
	Minimum	0.3	1.6	10.4
	Maximum	1.7	3.2	17.1
	Count (*n*)	31	31	31

Table 4.5. Correlation by simple linear regression between δ ^{13}C and δ^{18}O in each shell.

Shell	**r^2**	**F-statistic**	***n***	***p*-value**
SS190702	0.257	16.242	49	2.03E-04
SS30702	0.018	0.691	40	0.411
SSFLA1	0.135	3.905	27	0.059
SC001A	1.17E-04	0.003	28	0.956
SC003	0.007	0.213	31	0.648

Table 4.5. Standardize growth indices (SGI) from around the New York Bight and along the New Jersey shore with sample depth (S.D.)

	Area 612		Area 613		Area 614		Area 615	
Year	SGI	S.D.	SGI	S.D.	SGI	S.D.	SGI	S.D.
1972			1.14	2				
1973			-0.46	2				
1974			-0.25	2				
1975			0.20	2				
1976			-1.33	6				
1977			0.50	7				
1978	-2.552	2	0.19	7	-1.55	2		
1979	2.186	4	-0.43	8	0.20	3		
1980	-1.393	4	0.14	9	-0.59	4		
1981	1.14	7	0.55	11	2.86	4		
1982	0.717	8	0.60	11	1.95	6		
1983	1.028	9	0.55	12	-0.94	8	-1.74	2
1984	-1.324	11	0.40	13	-1.44	8	1.00	3
1985	-0.769	14	0.34	16	0.40	9	1.01	4
1986	-0.273	16	0.39	18	0.03	10	-0.96	5
1987	-0.332	17	0.16	19	-0.42	11	-0.22	6
1988	-0.29	19	0.24	21	-0.94	11	0.08	6
1989	0.801	19	0.22	23	-0.63	12	0.17	6
1990	0.132	21	0.27	24	-0.25	12	0.12	7
1991	0.072	22	0.27	24	-0.06	12	0.06	7
1992	-0.479	16	0.36	25	0.92	12	-0.30	7
1993	-0.004	18	0.29	25	0.10	12	0.30	7
1994	0.43	13	0.39	13	0.20	12	-0.46	6
1995	-0.616	13	0.21	13	-0.04	12	-0.14	6
1996	0.606	13	0.21	13	0.05	12	0.05	6
1997	0.271	6	0.23	9	0.21	8	0.69	5
1998	0.026	6	0.37	9	0.11	8	0.99	5
1999			0.27	9	-0.39	3	0.16	5
2000			0.23	9	-1.00	3	0.35	5
2001			0.21	9	1.21	3	0.62	5

Table 4.6 Standardize growth indices (SGI) from off the Delmarva peninsula and Hampton roadstead with sample depth (S.D.).

	Area 625		Area 626		Area 631		Area 632	
Year	SGI	S.D.	SGI	S.D.	SGI	S.D.	SGI	S.D.
1972								
1973								
1974								
1975								
1976								
1977								
1978	0.76	3			-0.02	2	-1.88	7
1979	0.39	4			-2.06	4	-0.28	16
1980	0.01	6			1.21	4	0.83	20
1981	-0.68	9			-0.77	7	0.20	30
1982	1.09	9			0.71	13	0.19	32
1983	-0.16	9	0.59	2	-1.41	17	0.24	35
1984	0.39	9	1.22	2	-1.35	19	-0.23	37
1985	-1.75	11	0.14	2	0.35	22	-0.18	37
1986	-1.48	12	-0.14	2	0.12	24	0.06	39
1987	0.42	13	-0.44	6	0.55	28	-0.08	39
1988	0.15	14	-0.39	7	0.02	31	-0.15	40
1989	-0.26	15	0.25	7	-0.48	33	-0.06	40
1990	0.12	15	-0.51	8	-0.33	36	0.90	40
1991	0.71	16	0.34	9	-0.24	38	0.56	41
1992	0.22	16	-0.17	11	-1.12	35	-0.29	17
1993	1.11	16	0.82	11	0.92	38	0.57	17
1994	-0.45	13	0.48	12	0.24	27	0.51	13
1995	-0.73	13	0.07	13	-0.33	27	0.49	10
1996	0.57	13	0.30	16	0.45	27	0.02	10
1997	0.74	8	-0.14	18	-1.22	16	-0.77	5
1998	-0.92	8	0.15	19	0.98	16	-0.12	5
1999	0.68	3	0.34	21	-0.10	6	2.26	3
2000	0.34	3	0.16	23	-0.02	6	1.47	3
2001	1.64	3	1.32	24	2.10	6	-1.68	3

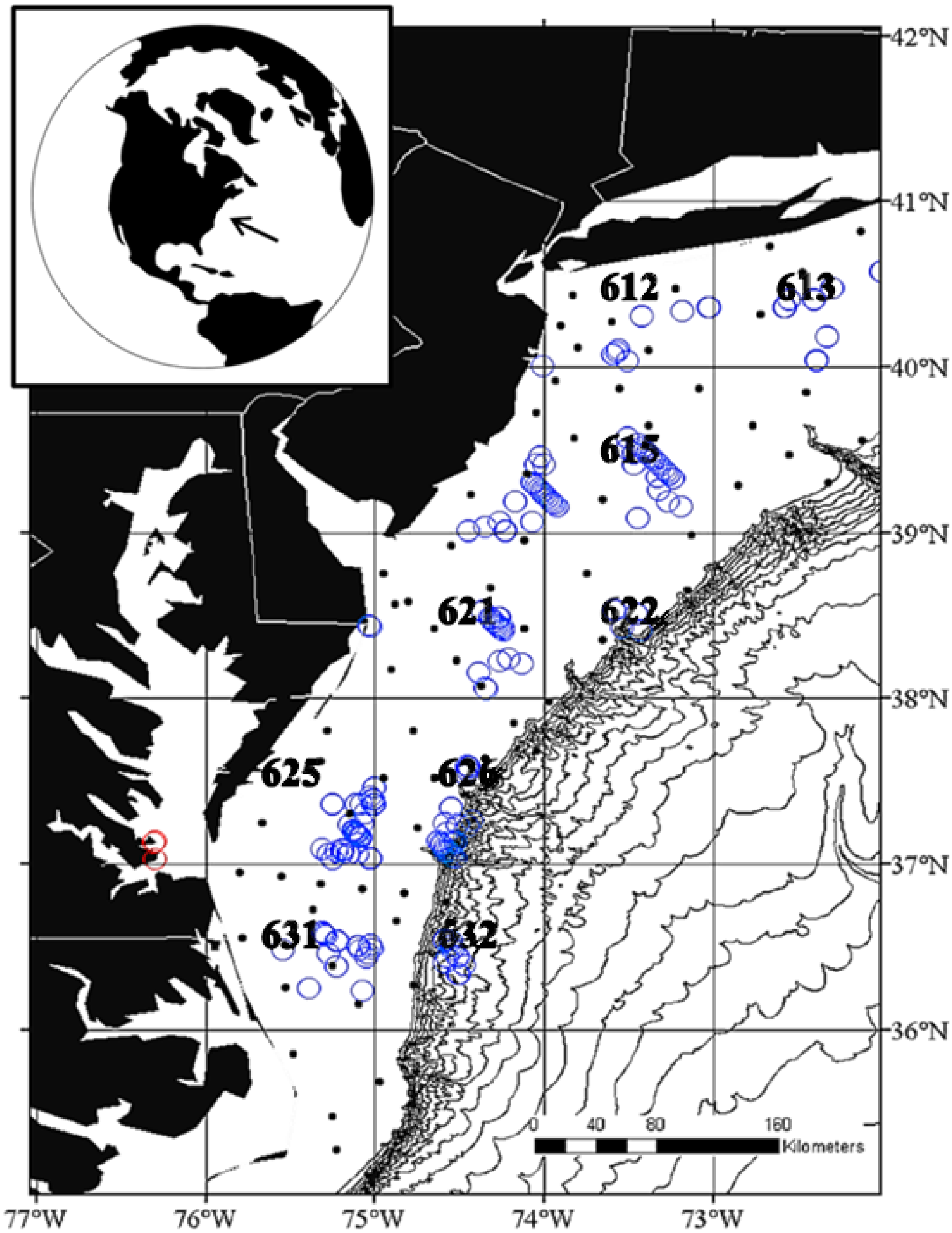

Figure 4.1 Collection localities for modern and Pliocene specimens. *Spisula solidissima* collected alive on the continental shelf (blue circles). Mid-Pliocene age *Spisula* specimens were collected from the Yorktown Formation (red circles). Black circles are the locations of standard MARMAP stations in Middle Atlantic Bight. The map has a bathymetric contour interval of 250 meters.

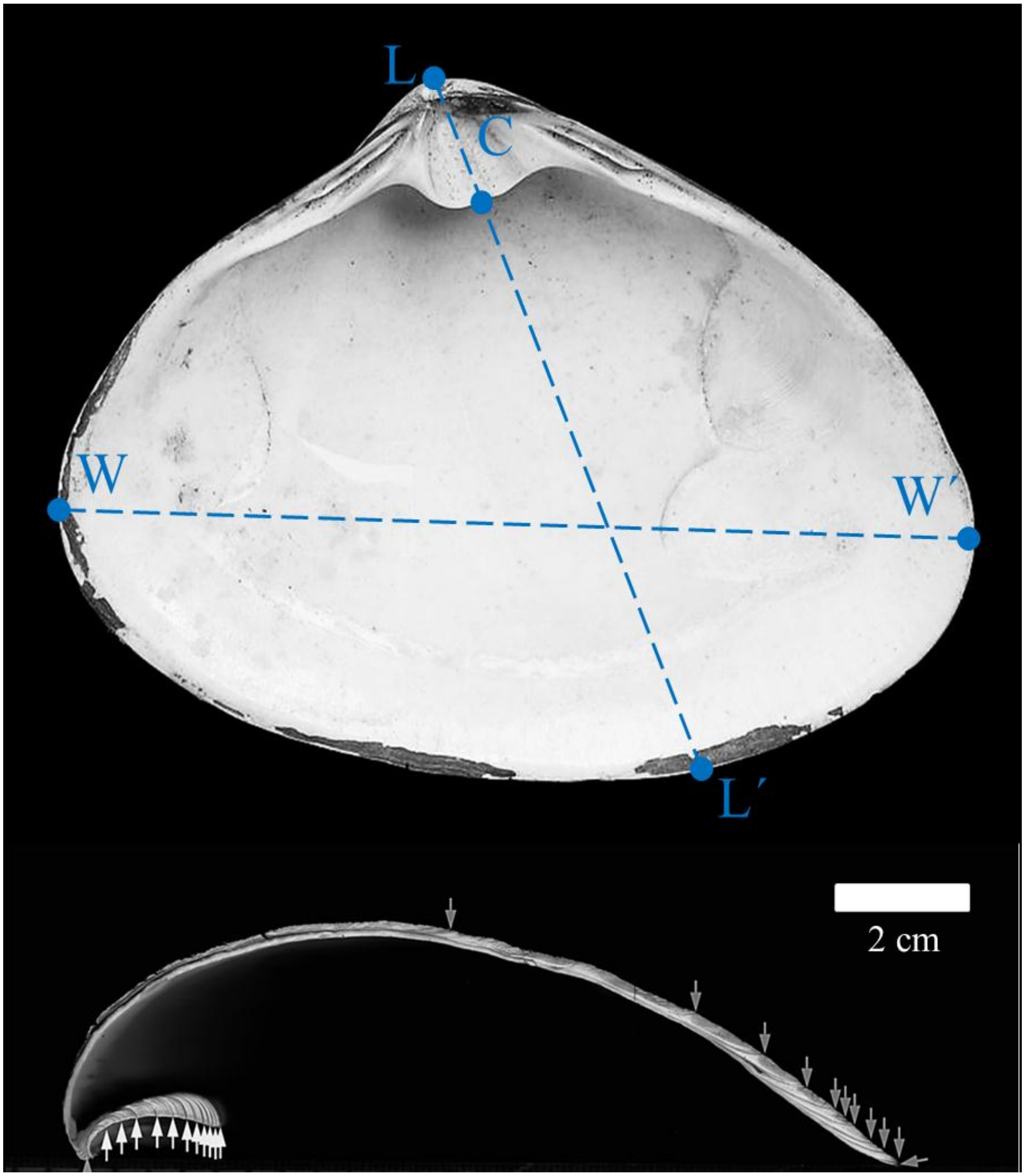

Figure 4.2 Example of how Spisula shells were measured and sectioned. Measurements of maximum length (L-L'), width (W-W'), and chondrophore length (L-C). Aging used growth increment lines along both the chondrophore and valve (arrows).

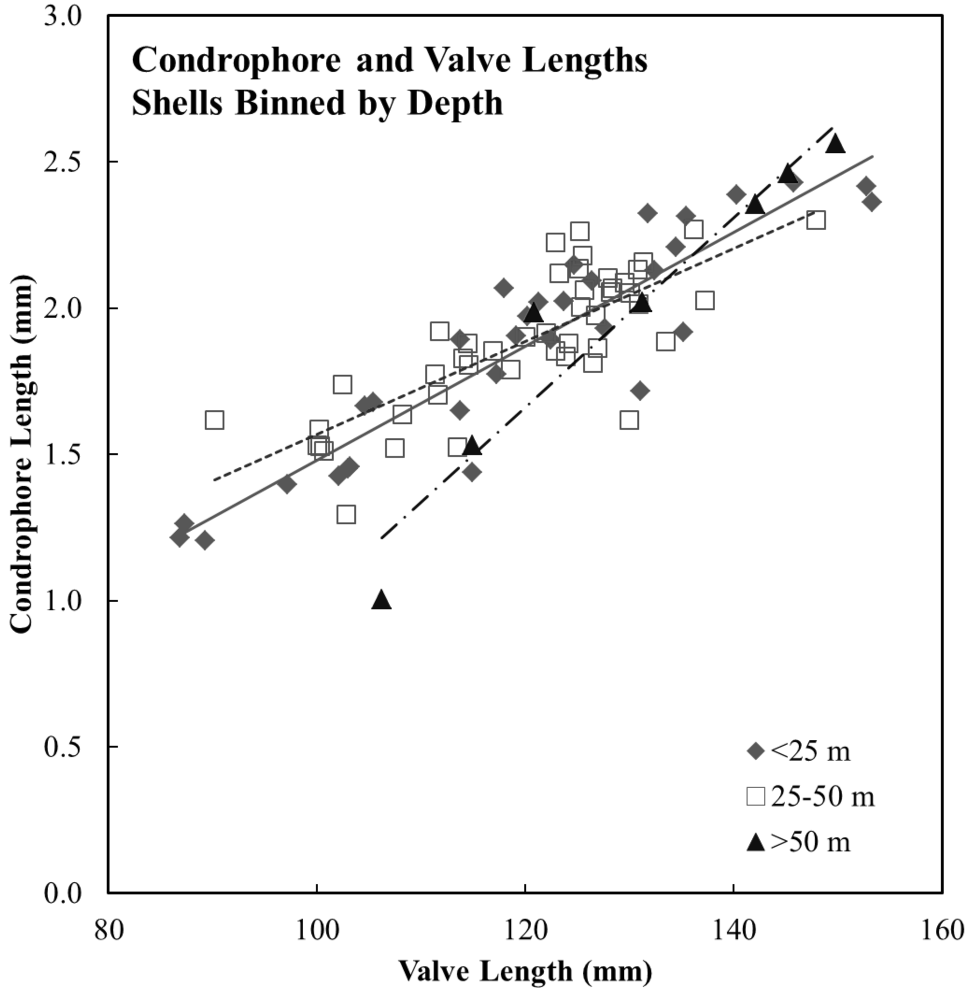

Figure 4.3 Graph of valve length (mm) versus chondrophore length (mm). Shell populations separated into depth bins of <25 m (gray diamonds, solid linear regression line), 25-50 m (open squares, dashed linear regression line), and >50 m (black triangles, dashed-dotted linear regression line).

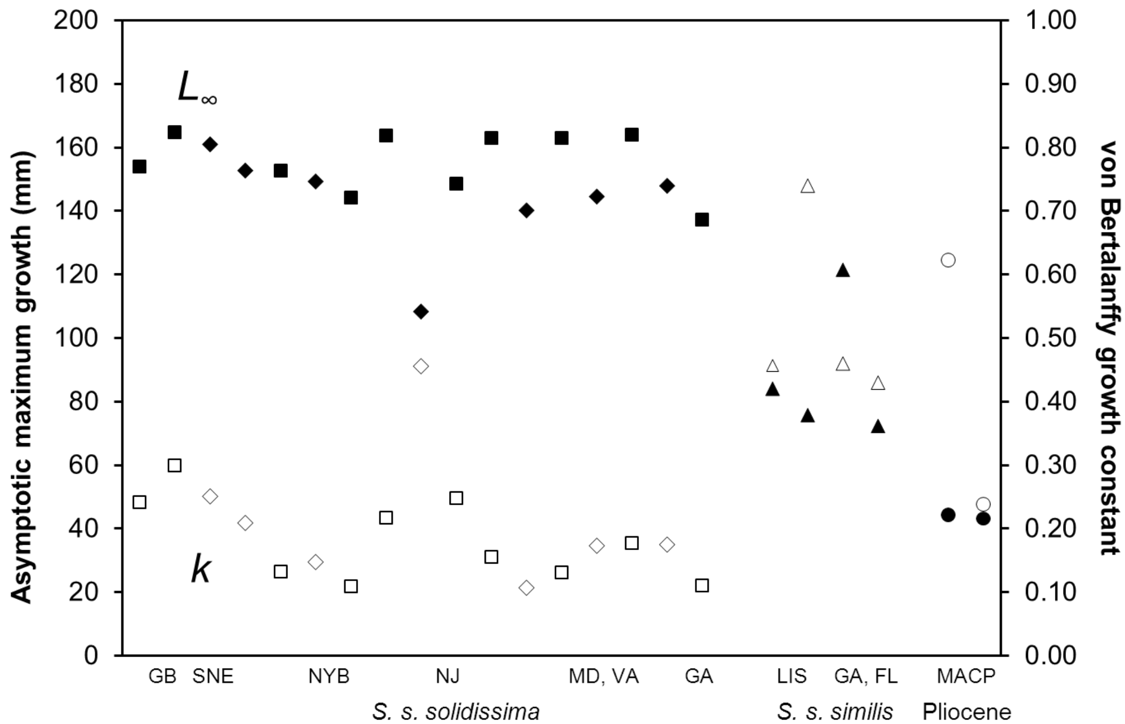

Figure 4.4 Plot comparing von Bertalanffy growth model parameters *k* (growth constant, clear shapes) and L_∞ (maximum shell length in mm, black shapes) of MAB and MACP *Spisula* arranged by species and region. Species include live collected *S. s. solidissima* are separated into offshore (squares) and inshore (diamonds), *S. s. similis* (triangles), and Pliocene aged *S. modicello* and *S. confraga* (circles).

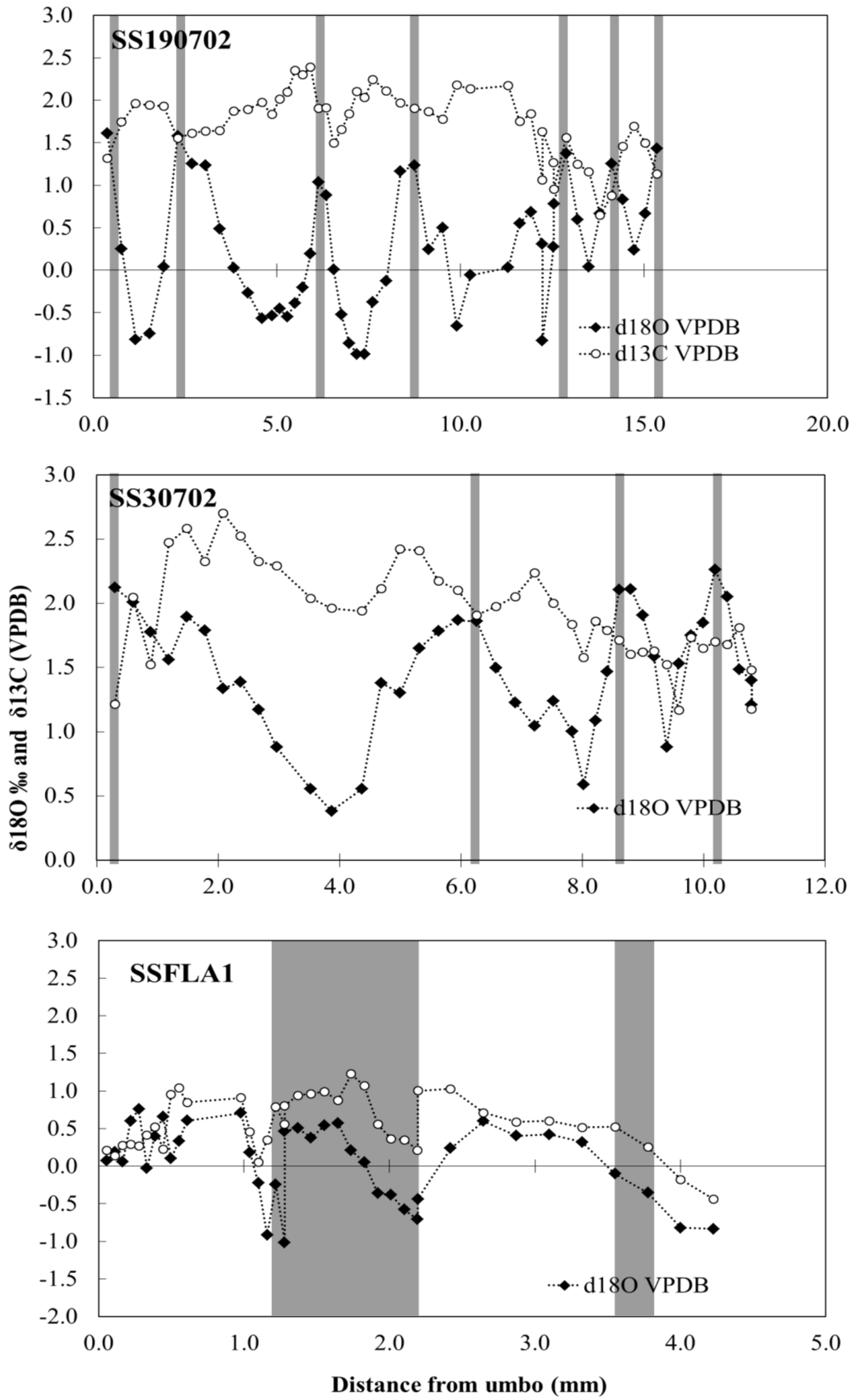

Figure 4.5 Oxygen (black circles) and carbon (white circles) isotopic profiles from *Spisula solidissima* specimens SS190702 (top), SS30702 (middle), and *S. s. similis* specimen SSFLA1 (bottom). X-axis displays distance from umbo (mm) with direction of growth toward higher values. Gray vertical lines approximate location and widths of dark growth increments.

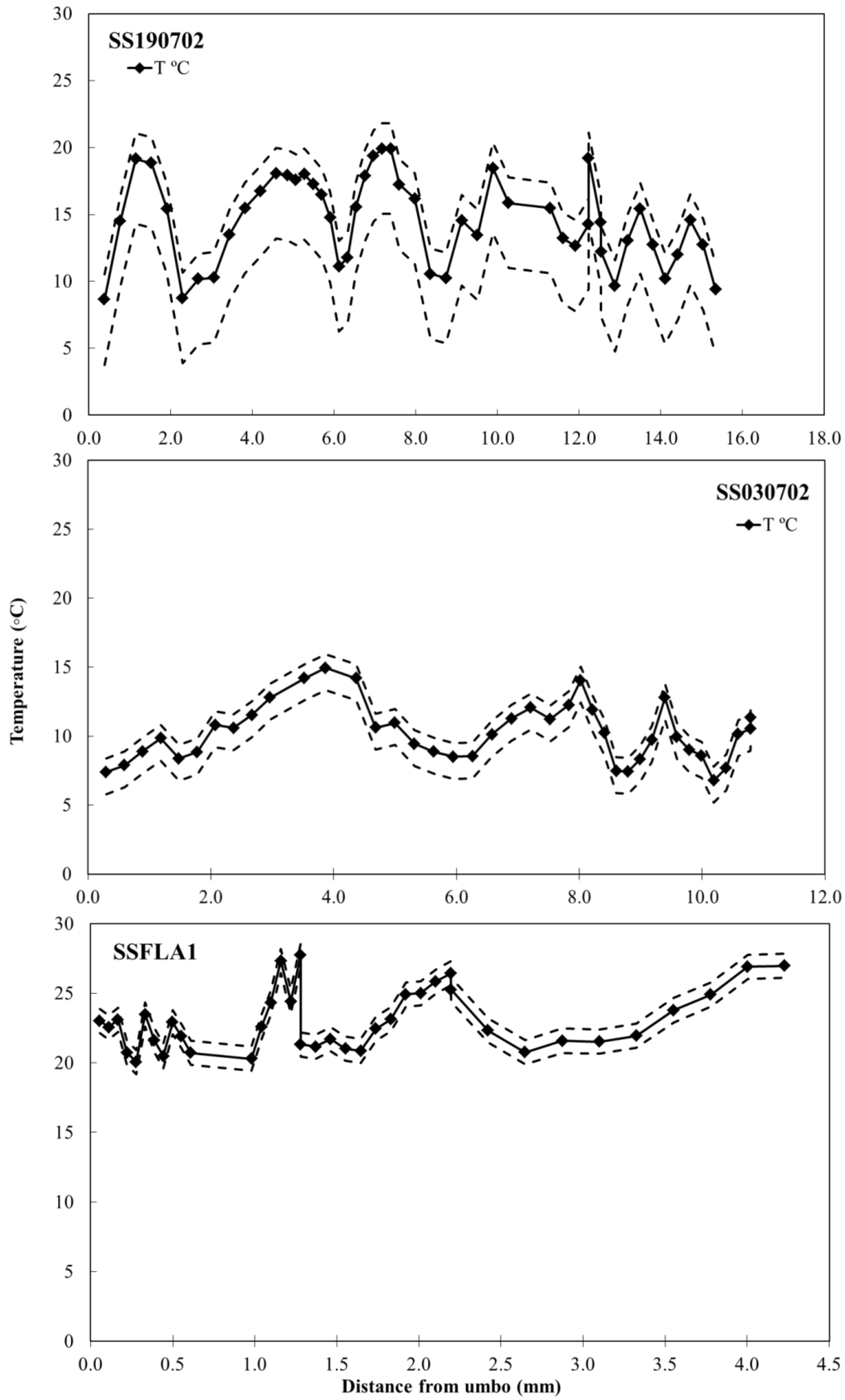

Figure 4.6 Temperature (ºC) estimates for *Spisula S. s. solidissima* and *S. s. similis* (SSFLA1) specimens. Dashed lines represent the ranges of values calculated using the maximum and minimum $\delta^{18}O$ seawater values at each location over the time interval corresponding to shell growth.

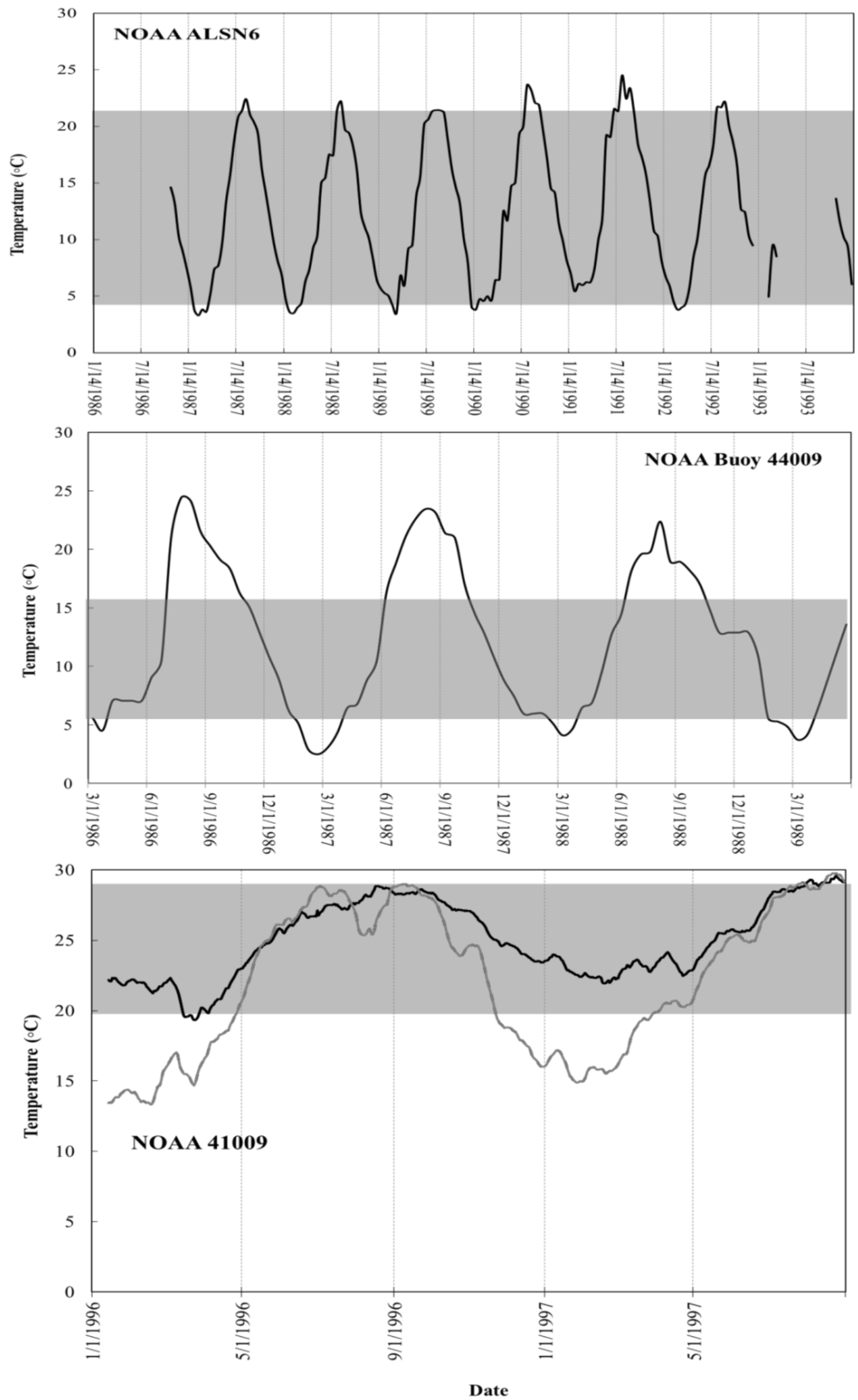

Figure 4.7 Sea water temperatures (black/gray sinusoidal lines) records from nearby NOAA stations during the growth of *Spisula s. solidissima* specimens SS190702/ALSN6 (top), SS30702/44009 (middle), *and S. s. similis* specimen SSFLA1/41009 (black) and SAUF1(gray) (bottom). Horizontal gray bands denote temperature estimate range from the corresponding shell.

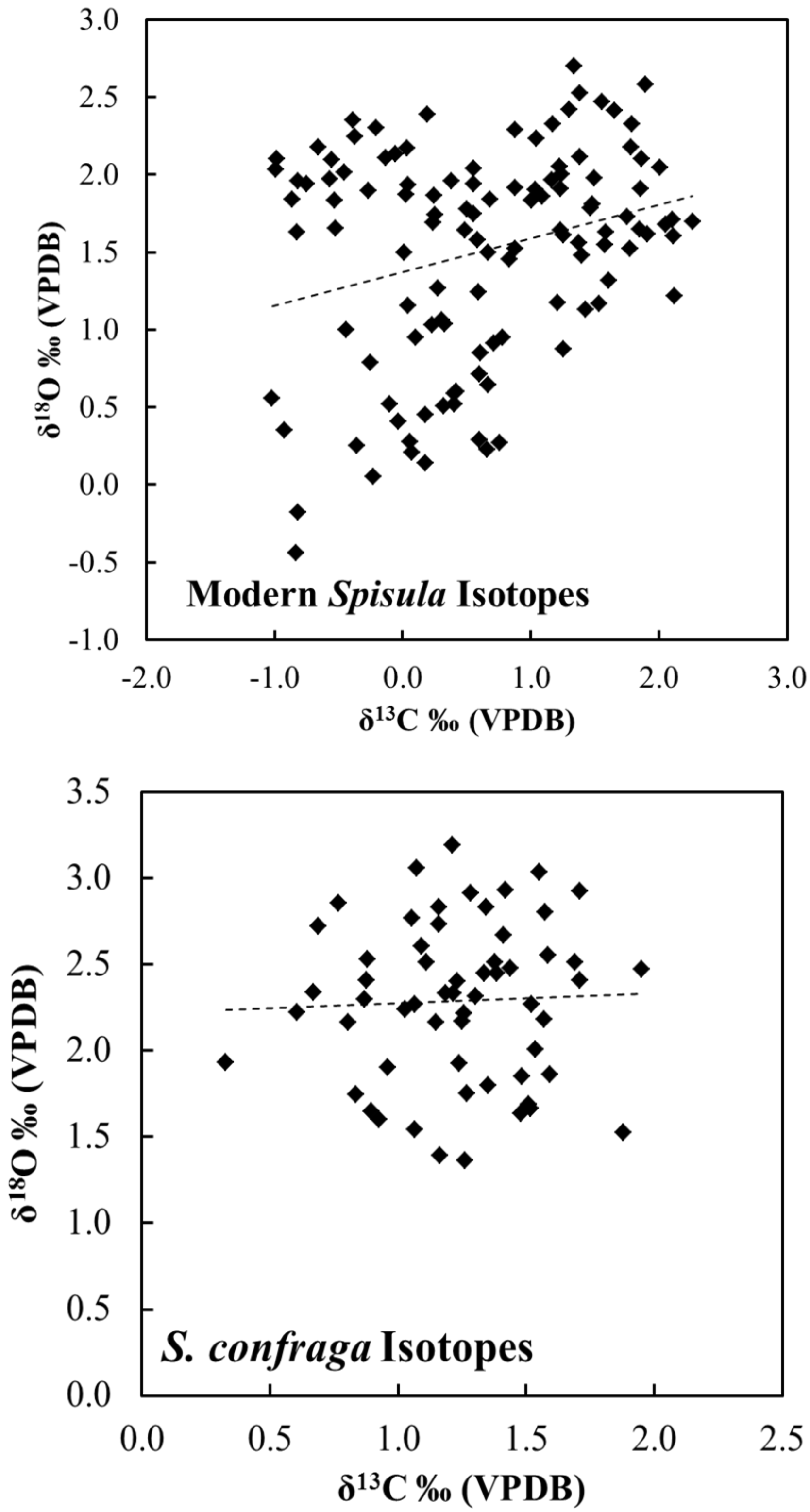

Figure 4.8 Covariance of $\delta^{18}O$ and $\delta^{13}C$ values from modern Spisula spp. (top) and Pliocene *S. confraga* (bottom).

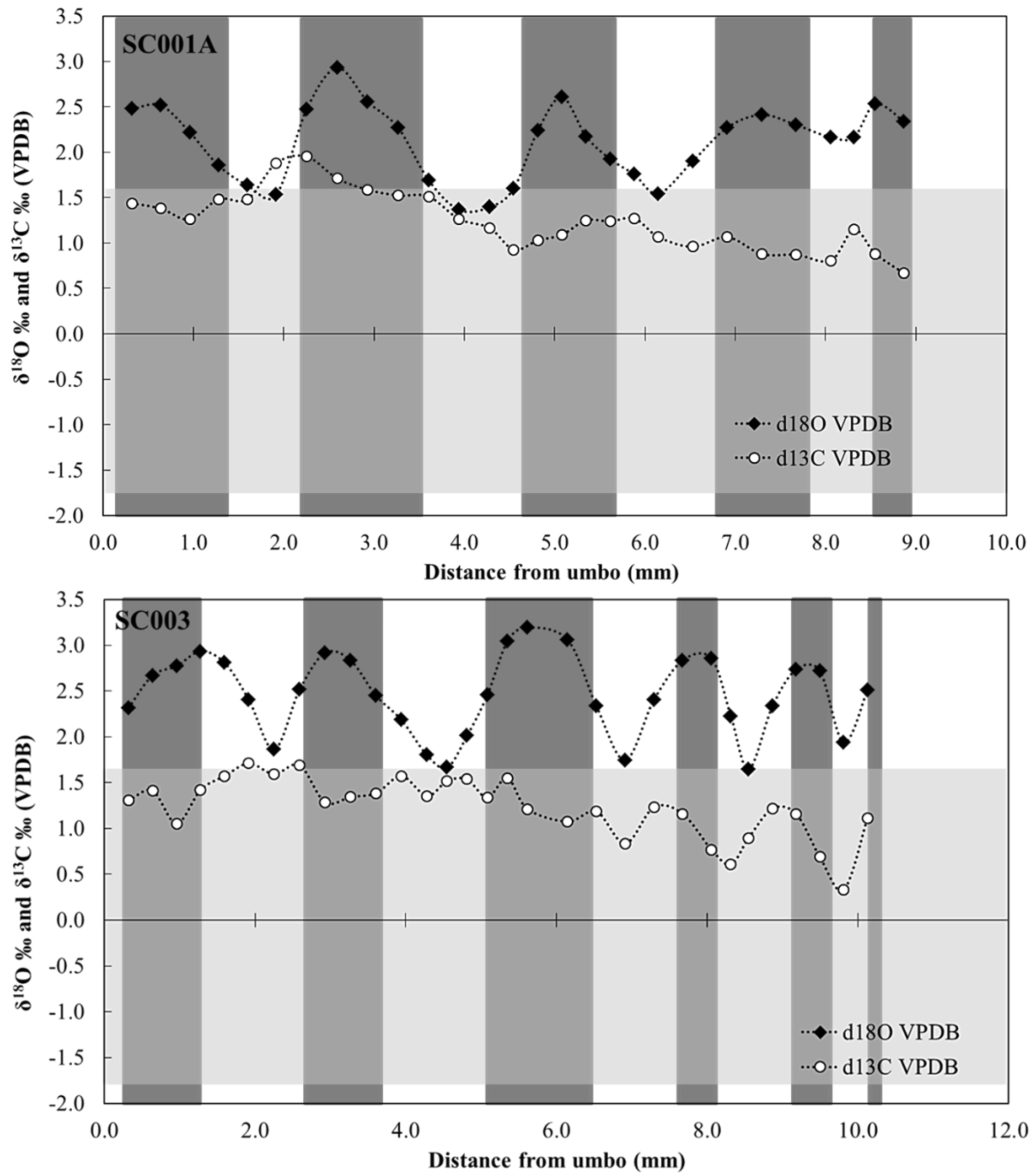

Figure 4.9 Oxygen (black circles) and carbon (white circles) isotopic profiles from *S. confraga* specimens SC001A (top) and SC003 (bottom). X-axis displays distance from umbo (mm) with direction of growth toward higher values. Gray vertical lines approximate location and widths of dark growth increments. Light gray horizontal band indicates the $\delta^{18}O$ value range of published Pliocene *Chesapecten* from the Yorktown Fm (Williams et al., 2009).

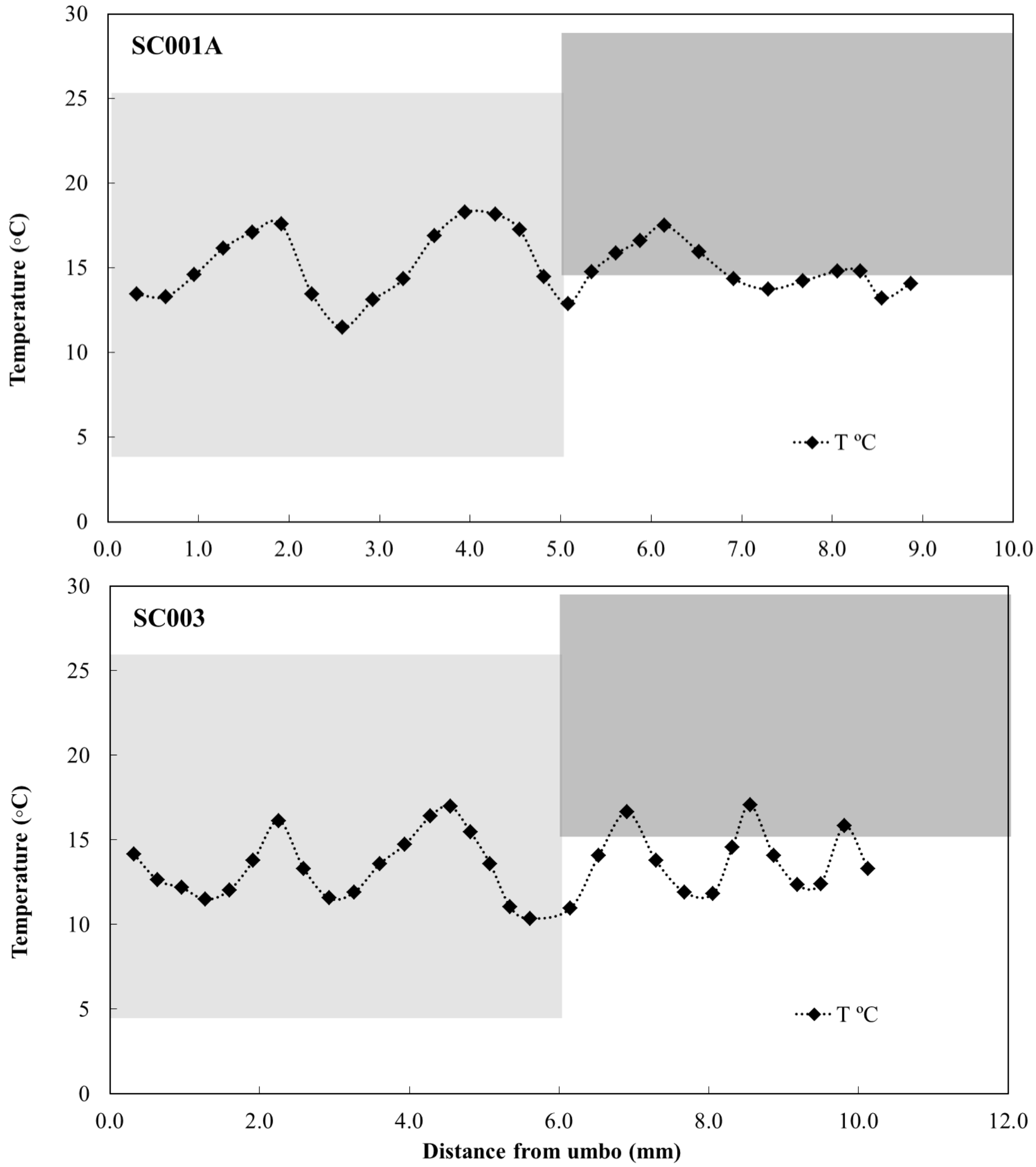

Figure 4.10 Temperature (ºC) estimates (black line with circles) for *S. confraga* specimens SC001A (top) and SC003 (bottom). Light gray horizontal band denotes the instrumental temperature range of the Chesapeake Light station (NOAA-CHLV2, http://www.ndbc.noaa.gov), while the darker gray horizontal band represents estimated temperature range for the Pliocene Yorktown Fm based on *Chesapecten* (Williams et al., 2009).

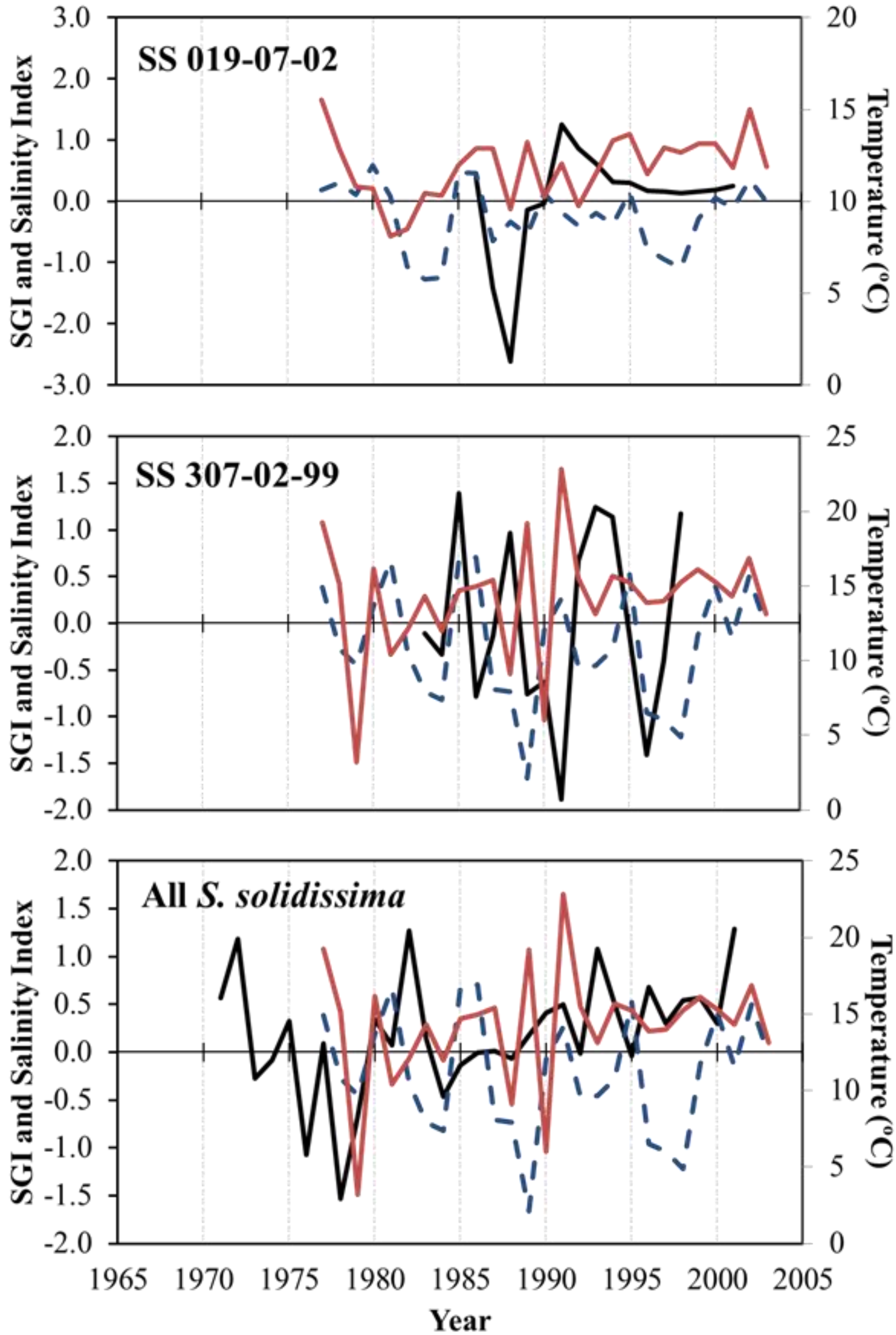

Figure 4.11 Comparison of individual and all annual standardized growth indices (black line) to mean annual temperature (red line) and salinity index (dashed blue line) (MARMAP). The two indices are plotted on the same axes.

CHAPTER 5: IN SEARCH OF LONG-LIVED BIVALVES FROM THE PLIOCENE MID-ATLANTIC: STABLE ISOTOPE AND INCREMENT ANALYSIS OF LARGE MARINE BIVALVES, VIRGINIA & NORTH CAROLINA, U.S.A

Joel W. Hudley and Donna Surge

Department of Geological Sciences, University of North Carolina, Chapel Hill, 104 South Rd., CB#3315, Chapel Hill, NC 27599-3315, USA email: jhudley@unc.edu

Keywords: Pliocene, isotopes, increments, *Glycymeris*, *Panopea*, Yorktown

(To be submitted to the journal *Palaeogeography, Palaeoclimatology, Palaeoecology*)

ABSTRACT

The Pliocene was the last time in Earth's history when reduction in polar ice sheets and higher sea levels were a consequence of higher atmospheric carbon dioxide concentrations comparable to levels projected for the late 21^{st} century. To investigate the climate variability during the Pliocene, variations in isotope ratios in shells of the bivalves *Glycymeris americana* (DeFrance, 1826) and *Panopea reflexa* (Say, 1824) were assessed. The purpose of this study is to identify whether these species, both large and abundant in United States Atlantic coastal plain fossiliferous units, exhibit annually resolved primary growth increments. Previous work on extant species of geoduck (*P. abrupta*) (Conrad, 1849)and dog cockles (*G. glycymeris* (Linnaeus, 1758)) shells indicate the genera have annual growth lines and reach maximum lifespans of 40 to 160 years.

Fossil bivalves were collected from the Pliocene Yorktown Formation in Virginia and the Chowan River Formation in North Carolina. Most specimens of *G. americana* and *P. reflexa* were collected articulated and unaltered by diagenesis. Sclerochronological studies of the growth patterns and the oxygen isotope ratios clearly exhibited annual cycles confirming periodic formation in shells of *G. americana*. Several specimens of *G. americana* reached ontogenetic ages of more than 70 years. *P. reflexa* growth increments could not be verified as annual. Oxygen isotope ratios of fossil *G. americana* and *P. reflexa* shells were consistent with previous bivalve studies of modern genera. Spectral analysis of long-lived *G. americana* showed that shell growth indices exhibit periodicities related to the North Atlantic Oscillation (NAO). The bivalve shells investigated here provide high-resolution data on seasonal to decadal climate variation and may therefore serve as an ancient analogue for predicted climate shifts along the United States Atlantic coastal plain.

HIGHLIGHTS

- *Glycymeris americana* form annual increments and exhibit significant longevity
- *Panopea reflexa* growth resolution could not be verified using isotope methods
- Shell growth indexes exhibit periodicities similar to the NAO

5.1 INTRODUCTION

Our current knowledge of past climate variability is based primarily on the use of short-lived, seasonal to annually resolved biological proxies. CLIMAP (Climate: Long range Investigation, Mapping, and Prediction) (CLIMAP, 1981), PRISM (Pliocene

Research, Interpretation and Synoptic Mapping) (Dowsett et al., 1996), and the Cenozoic oxygen isotope curve (Zachos et al., 2001) are cornerstones of paleoclimate research and remain the most used and/or only global temperature reconstructions for the three most important time periods (the Last Glacial Maximum, the mid-Pliocene, and the Cenozoic) prior to the late Holocene and modern instrumentation. Assuming the Intergovernmental Panel on Climate Change estimates of a 2-4.5ºC increase in global mean temperature is likely for the late twenty-first century (Jansen et al. 2007), then the Pliocene is the most appropriate past analogue for future climate conditions (Hansen et al., 2006; Dowsett, 2007; Chandler et al., 2008; Haywood et al., 2011). The PRISM framework (see Dowsett et al., 1996, 1999), with continents basically in their current positions and atmospheric CO_2 similar to projected late twenty-first century values, represents the most robust and only alternative for evaluating future climate scenarios using coupled atmosphere and ocean general circulation models (GCM). However, coupled climate models do not reproduce conditions indicated by PRISM data, and these unresolved discrepancies have led researchers to raise concerns about model estimates of future climate change.

To address these concerns, over the last decade groups of Pliocene researchers have used innovative tools, developed new proxies, and practiced multi-proxy methods incorporating faunal-based transfer functions with isotope and organic molecule paleothermometry to develop synoptic boundary conditions at seasonal and 12-month resolutions (Dowsett et al., 2006; Robinson et al., 2007; Dowsett and Robinson, 2009; Dowsett et al., 2009). The records derived from microfossils in the PRISM slab represent a static picture of the mid Pliocene, encompassing ~300,000 years and multiple glacial/interglacial cycles. Though mean annual and monthly temperatures can be displayed (see http://geology.er.usgs.gov/eespteam/prism/), little is known about continuous subannual to multi-decadal interannual temperature variability. Neogene paleoclimatology is based on long, continuous, high-resolution time series that provide millennial to sub-millennial resolution (Niemitz and Bilups, 2005; Williams et al., 2009). However, these data are inadequate to address important issues associated with multi-decal phenomena such as global or regional teleconnections like the El Niño Southern Oscillation (ENSO) or the North Atlantic Oscillation (NAO). Williams et al. (2009) state that many Pliocene studies acknowledge this lack of high-resolution data, and have portended that shell carbonate of long-lived fauna will provide data capable of addressing these issues and fill the current dearth of well-calibrated, high-resolution proxies in important Pliocene deposits.

Long-lived bivalves potentially represent the most widespread sources of annually and sub-annually resolved proxies that are not limited in spatial (latitudinal) or temporal coverage. In modern-day climate studies, the molluscan shell record bridges the gap between well-developed and cross-dated tree-ring networks (terrestrial, high-latitude) and continuously sampled coral skeleton geochemical records (low-latitude, shallow shelf) (Mann, 2002; Jones and Mann, 2004)(see Helma et al., 2007; Black et al., 2009 for examples). Only a dozen non-colonial animals have a lifespan >100 years (Ziuganov et al., 2000). Many of them are bivalves including the longest lived, *Arctica islandica* (Linnaeus, 1767) with a reported maximum lifespan of >500 years (Schöne et al., 2005; Wanamaker et al., 2012), and *Margaritifera margaritifera* (Ršding,1798) at 190 years

(Ziuganov et al., 2000). The freshwater mussel, *M. margaritifera*, and the marine quahog, *A. islandica*, are the archetypes for isotopic and increment sclerochronology studies. *A. islandica* studies show that long-lived individuals are capable of reliably recording environmental variables (e.g. seawater temperature, salinity, ocean productivity, and the NAO) on daily to centennial scales (Schöne et al., 2003; -2004; -2005; Wannamaker et al., 2009). Unfortunately, most long-lived bivalves, including the hard clam, *Eurhomalea exalbida* (Lomovasky et al., 2002), and the fossil ark clam, *Cucullea raea*, from Eocene Antarctic deposits (Buick and Ivany, 2004) inhabit high-latitude, cold water environments and are not found in Pliocene deposits of the Mid-Atlantic Coastal Plain (MACP). In order for sclerochronology to provide critical information about the Pliocene and other important Cenozoic climate intervals, more long-lived bivalve proxies must be found.

The aim of this study is to determine if the extant cockle, *Glycymeris americana* (Defrance, 1829), and the extinct geoduck, *Panopea reflexa* (Say, 1824), both common and abundant in MACP Neogene deposits, exhibit the resolution and longevity to preserve environmental records of Pliocene interannual to multi-decadal variability. Our objectives are to: (1) employ isotope sclerochronology to verify regular timing of primary growth lines; (2) compare the synchronicity of oxygen isotope ratios in this study to previously published bivalve $\delta^{18}O$ values and modern instrumental ranges; and (3) and compare growth models derived from increment widths to growth models of related species. We also used increment sclerochronology and spectral analysis to investigate and interpret interannual to multi-decadal periodicity of the Pliocene MACP. We selected *G. americana* and *P. reflexa* because of their large and easily identifiable shells and because extant, cold-water species in their genera, *G. glycymeris* (Linnaeus, 1758) and *P. abrupta* (Conrad, 1849), are documented to reach ages of >100 years (Ramsay et al., 2000; 2011; Bureau et al., 2002).

5.2 Geological and Paleoenvironmental Setting

Specimens were collected from the upper early and middle Pliocene Rushmere-Morgarts Beach (3.5-3.1 Ma) and Moore House (3.1-2.5 Ma) Members of the Yorktown Formation at Petersburg, Virginia and the late Pliocene Edenhouse Member (2.5-1.9 Ma) of the Chowan River Formation at Colerain, North Carolina (Carter et al., 2003) (Figure 5.1). These two formations are shallow-marine successions comprised of unconsolidated sand, clay, and shell marls that accumulated in the basins along the continental passive margin. The lithology and biostratigraphy of the Yorktown and Chowan Formations indicate inner to outer neritic conditions with normal marine salinity (Ward and Strickland, 1985). The Yorktown Formation represents tropical climatic conditions based on nannofossil assemblages (Hazel, 1971; Cronin and Hazel, 1980; Cronin et al., 1984) and molluscan biozones (Ward and Blackwelder, 1976; Blackwelder, 1981b). The Rushmere and Moore House Members contain molluscan assemblages which indicate a pronounced episode of warming (Mid Pliocene Warm Interval, MPWP) reflecting tropical conditions (Ward, 1998). The Chowan Formation contains a molluscan assemblage entirely warm-temperature in nature, and therefore represents cooling conditions following the tropical assemblages of the early Pliocene (Ward and Gilinsky, 1993). These assemblages represent the shifting influence between warm tropical waters penetrating more northward during the early and mid- Pliocene and cool boreal waters reaching Cape Hatteras, North Carolina post-Yorktown. Paleontological studies suggesting a tropical to temperate temperature shift are supported by oxygen isotope paleothermometry (Krantz, 1990; Goewert and Surge, 2008; Williams et al., 2009).

Age control of the MACP is based primarily on well-developed regional biostratigraphy of molluscs and microfossils (Cronin and Hazel, 1980; Blackwelder, 1981b) and limited paleomagnetic and radiometric data (Cronin et al., 1984). Though few open-ocean specimens are present, Pliocene MACP formations are tied globally with planktonic foraminifera records from deep sea cores (Dowsett & Cronin, 1990; Dowsett & Wiggs, 1992). The time span of deposition for each member of the Pliocene MACP has been estimated by correlating each transgressive sedimentary unit with deep-ocean $\delta^{18}O$ records (Krantz, 1991). Individual shell specimen ages should be considered as 'floating' within and representative of the entire litho-stratigraphic unit. Relative ages of fossil specimens recovered were considered in stratigraphic order because many specimens were collected from beds with little evidence of post-depositional transport or bioturbation. Other studies have also noted specimens from the high-energy shell marls and deep-burrowers of the MACP deposits in excellent conditions of preservation (Thompson, 1970; Bailey and Tedesco, 1986; Ward et al., 1987). In this study, many specimens of *Glycymeris spp.* and all specimens of *Panopea* reflexa were found articulated, some in life position, slightly worn but overall well preserved.

5.3 METHODS

5.3.1 Fossil bivalve shell preparation and growth increment reading

Fossil shells of *Glycymerididae* (N=154) and *P. reflexa* (N=18) were picked from highstand deposits of the Yorktown and Chowan River Formations, and then processed at the University of North Carolina. Shells were cleaned, photographed, weighed (using a Sartorius electronic balance, accurate to the 0.0001 g) and the length and height measured using digital calipers to the 0.01 mm (Appendix B, Table 1). Multiple species of *Glycymerididae* are found in the deposits of the MACP (Thompson, 1970; 1975). Measurements of the physical characteristics of the *Glycymerididae* shells were used to properly differentiate small, worn, and/or asymmetric *G. americana* (DeFrance, 1826) from the rugose polymorph (Nicol, 1950) and the costate (ribbed) *Costaglycymeris subovata* (Ward, 1992) (Appendix Figure 1). Using an Olympus SZX7 microscope with an attached DP71 12 megapixel camera, the external shell surfaces of the *Glycymerididae* were magnified (15×) and digitally recorded along the maximum growth path. Following methods previously used to determine the resolution of *G. glycymeris* increments (Berthou et al., 1986; Reynolds, 2011a), photomicrographs of the external growth increments were digitally measured using the Olympus Imaging Solutions Software to the nearest (0.001 mm) (Figure 5.2, Appendix B Table 2). Abrasion and bioerosion can remove portions of the outer shell making it difficult to distinguish growth increments. External counts were not taken if too much of an individual specimen's outer shell was destroyed.

Fast-hardening epoxy was applied to the shells prior to sectioning. They were sectioned through the umbo and along the axis of maximum growth using a diamond band saw. Half of each sectioned shell was affixed to a slide using epoxy and cut again using a Buehler IsoMet low speed saw. The thinly sliced shells were ground down using 600 grit and polished using 6 μm and 1 μm diamond polish on a Buehler variable speed grinder-polisher. Shells were again cleaned, rinsed and allowed to dry. Each slide was stained using Mutvei's solution (Schöne et al, 2001) and inspected for diagenetic alteration under reflected light using the Olympus microscope setup. The purposes of staining were to: (1) identify microstructural layers and growth lines; and (2) evaluate the preservation of the original mineralogy.

Fossil aragonite shells were only lightly stained by the alcian blue during the staining process (Schöne et al., 2001), and the process better revealed microstructure and evaluate petrography. With the stain applied, shell microstructure was shown to consist of an outer and an inner crossed-lamellar layer separated by a thin layer of prismatic myostracum tracing the ontogenetic path of the pallial line (Figures 5.2b and d). *Glycymeris spp.* and *Panopea spp.* shell composition is entirely aragonite (Thompson, 1975; Strom et al., 2004; Hallman et al., 2008). Areas of secondary calcification, other debris, and heavily etched and cracked locations from handling, processing and staining were more darkly stained by the Mutvei's solution than the rest of the shell. Areas along the valve presumed to be annual bands, distinctly darker in color in the cross-lamellar part of the outer hinge in living shells (Thompson, 1970; Ramsay et al., 2000), appeared lighter than the surrounding stained area on some shells. These observations are consistent with other studies using fossil *Glycymerididae* from the Eocene (Zirkel and Schöne, 2010). These multiple lines of evidence indicate the exceptional preservation of the original material.

5.3.2 Isotope sclerochronology

To determine whether fossil shells of *G. americana* and *P. reflexa*: (1) deposit shell carbonate in regular annual intervals between visible growth increments; and (2) exhibit temperature representing the entire annual range, standard oxygen and carbon isotope sclerochronology methods were employed on four shells. Two fossil *G. americana* from the Yorktown Formation were microsampled at 8-12 samples per year across the fifth to tenth growth increments to achieve subannual resolution (N=69). Samples were taken from these growth increments because the large area of these increments enabled identification of different portions of the valve. The samples were taken from the outer cross-lamellar portion of each valve. The chondrophore of *Glycymerididae* was used for aging but not for isotopes because it is part of the inner shell layer and in continuous contact with inner extrapallial cavity fluids (Thompson, 1970). Two *P. reflexa* shells from the Yorktown Formation formation were microsampled along the chondrophore area following similar sampling strategies of Goman et al., (2007) and Hallman et al. (2008). Visible growth lines used to guide sampling were only distinguishable in the chondrophore. Microsamples were taken from the first twelve years of growth at sampling rates of 5-7 per year in fast-growing shell regions near the umbo and diminishing numbers of samples in slower growing, older shell portions (N=75). Microsampling was performed on a Merchentek micromill fitted with a 0.1 mm carbide scribe bit. Each digitized drilling path consisted of multiple passes to a drilling depth of approximately 10 to 50 μm. To obtain subannual resolution, drill paths were made parallel to the growth lines. Approximately 20-40 μg of carbonate powder was collected for each isotopic analysis. Isotopic analysis was performed at the University of Arizona's Environmental Isotopes Laboratory (Department of Geosciences). Oxygen and carbon isotope ratios of shell carbonate were measured using a Kiel-III automated sampler coupled to a Finnigan MAT 252 gas-ratio mass spectrometer. Powdered samples were reacted with dehydrated phosphoric acid under vacuum for one hour at 70ºC. The isotope ratio measurements were calibrated based on repeated measurements of National Bureau of Standard NBS-18 and NBS-19. Precision was ±0.1‰ for $\delta^{18}O$ and ±0.08‰ for $\delta^{13}C$. The results are reported in per mil units (‰) relative to the Vienna Pee Dee Belemnite (VPDB) standard (Table 1).

5.3.3. Temperature estimates

Estimated temperature was calculated using the equation reported by Grossman and Ku (1986):

$$T°\mathrm{C} = 20.6 - 4.34(\delta^{18}O_C - \delta^{18}O_{\mathrm{SW}})$$

where $\delta^{18}O_C$ (VPDB) is the isotope ratios from the shell carbonate. The regional seawater $\delta^{18}O_{SW}$ value of 1.1‰ (VSMOW) is from a model predicted Pliocene seawater value for all members of the Yorktown Formation as reported by Williams et al. (2009). To account for subtracting oxygen isotope ratios from the two different scales, 0.27‰ was subtracted from the $\delta^{18}O_w$ value (Gonfiantini et al., 1995). The Grossman and Ku (1986) equation does not account for possible differences in vital effects for different species of bivalves. We compared $\delta^{18}O$ values and estimated temperature in this study to modern instrumental records and previously published values of Pliocene bivalve shells from the same formations. Published stable isotope data of bivalves from the Pliocene MACP formations are based on the analyses of extinct pectinids *Chesapecten jeffersonius*, *C. madisonius* and *C. eboreus* (Krantz, 1990; Goewert and Surge, 2008). We used the revised temperature estimates for *Chesapecten spp.* based on the Williams et al. (2009) $\delta^{18}O_{SW}$ value of 1.10‰. The modern seawater temperature values and ranges are from the NOAA station CHLV2 - Chesapeake Light off Virginia (http://www.ndbc.noaa.gov/data/climatic/CHLV2.txt, download September 2011).

5.3.4 Growth analysis

All sectioned shells were aged and the internal growth increments measured using an Olympus SZX7 Microscope with a DP71 12.5 megapixel, 12-bit digital color camera setup with Olympus imaging software. *G. americana* shell increments (I_t) were measured between the consecutive couplets of dark increments (viewed under reflected light), starting at the ventral margin (commissure edge) and counted back along the valve to the umbo (Figure 5.2). Measurements were halted a few increments preceding broken ventral margins and later in ontogeny where increments became too difficult to discern because of slowed growth. *P. reflexa* shell counts were measured from the chondrophore (hinge plate, cardinal tooth) area (Figure 5.2). Previous work on live-caught specimens of *P. abrupta* (Shaul and Goodwin, 1982; Strom et al., 2004, 2005; Hallmann et al., 2008) found that cross-sections through the cardinal tooth provided the clearest and most reliable view of the growth increments. Measurements were made along a transect from the origin of growth to the farthest (ventral) edge of the cardinal tooth.

For each *G. americana* and *P. reflexa* shell measured, the sum of all growth increments widths in the chondrophore gave the length of the chondrophore. Chondrophore increments were converted to growth increment in shell height using the formula reported by Steíngrímsson, (1989):

$$SH_{inc} = \frac{SH_{tot}}{CL_{tot}} \times A$$

where SH_{inc}, = growth increment in shell width, A = the growth increment age in the chondrophore measured from the digital image, SH_{tot}, = the total shell height measured with calipers before sectioning, and CL_{tot} = the total length of the chonodrophore (the sum of A from the origin of growth to the farthest edge of the chondrophore). Directly measured increment widths from sectioned *G. americana* shells were used to construct growth curves for the entire 134 shells and separate Yorktown Formation and Chowan River Formation populations. The calculated growth data were used to construct growth curves for each usable *P. reflexa* in the population (15 shells) from the Yorktown Formation.

Growth curves of all the shells were modeled by fitting a von Bertalanffy (1957) growth function to the age-shell height data. This function is described by the equation (Ogle, 2011):

$$E_t = L_\infty\left[1 - e^{-K(t-t_0)}\right]$$

where E_t = the expected or mean length at time (or age) t, L_∞ = the asymptotic average length, K = the Brody growth rate coefficient (units are yr^{-1}), and t_o = is said to represent the time or age when the average length was zero ($L_o = 0$). The von Bertalanffy growth model (VBGM) was fitted to the data using fishR, a fisheries analysis tool performed in the R software environment (Ogle, 2011). This non-linear regression technique gives an estimate for L_∞, K, and a 95% confidence interval for the evaluated asymptotic shell height and rate constant. This method has been used to model shell growth in *G. americana* in the same Pliocene formations (Thompson, 1970, 1975) and *G. glycymeris, P. abrupta* and *P. zelandica* in late Holocene localities (Menesguen and Dreves, 1987; Steingrímsson, 1989; Gibben and Creese, 2005; Strom, 2006).

5.3.5 Increment analysis

Eight *G. americana* shells with long increment records were selected for spectral analysis to examine interannual variability and spectral frequencies. The selected shells included 4 from the Yorktown Formation (44, 49, 51, and 55 years) and 4 from the Chowan River Formation (68, 70, 70 and 74 years). There are two standard methods for removing the ontogenetic growth trend of decreasing increment widths with increasing age. The first detrending method is done by removing the VBGM curve (above section) from the raw increment series of the shells to get growth indices based on the population. Growth indices (GI_t) were computed by:

$$GI_t = I_t / E_t$$

This method is representative of the fixed logarithmic transformations used in a number of bivalve studies (e.g. Schöne, 2003; Butler et al., 2009) in which a large number of shells (>25) were measured. The second method employed is the standard individual-based detrending developed in dendrochronology (Cook and Peters, 1981) and employed by various bivalve studies (e.g. Schöne et al., 2003; Ivany et al., 2011) with limited numbers of long increment series. In this adaptive individual-based detrending method, the raw increment data series from each individual shell was recorded using the decadal-format CASE program in the University of Arizona's Dendrochronology Program Library (DPL) (Holmes, 1999) and loaded into 'dplR', a dendrochronology program library in R developed by Bunn (2008). For each individual, a cubic smoothing spline was fitted to the series of measured growth increments I_t (t = 1, 2…n; detrend (series, method= 'Spline)) command in dplR with a spline frequency response of 50% to obtain a series of expected increment growth G_t. Standardized growth indices (SGI) were plotted using the residuals of the spline and the mean of the residual population. SGI increment width series are expressed as the number of standard deviations away from zero with thinner bands being less than and wider bands being greater than expected growth.

5.3.6 Spectral analysis

Spectral analysis was used to identify any significant periodicities in the SGI series. Using a standard spectral analysis procedure, we compared the 8 *G. americana* growth indices to instrumental data from the middle Atlantic coast. These procedures were done to determine: (1) if the SGI records displayed oscillation patterns; and (2) if those patterns were similar to modern MACP seawater patterns. Instrument records representing the MACP included the winter NAO Index (1950-2011) from the NOAA Climate Prediction Center (http://www.cpc.ncep.noaa.gov/products/precip/CWlink/pna/nao, downloaded September 2011), NAO Reconstruction (1049-1995) (Trouet et al., 2009), mean monthly temperature data from Cape Hatteras, North Carolina (1874-2005), and the Long Branch Oakhurst, New Jersey (1907-1997) Global Historical Climatology Network (GHCN) stations (http://www.ncdc.noaa.gov/ghcnm/, downloaded September 2011). The Cape Hatteras and Long Branch Oakhurst monthly instrument records were converted into lower resolution summer (June-July-August) mean annual series so that all time series were annually resolved. A smoothed periodogram, i.e. a spectral plot, and a fast Fourier transform (FFT) plot were constructed for each times series to first check that the shell SGIs and the station data exhibited oscillation patterns. We employed a two-step procedure using the software package kSpectra by SpectraWorks Inc. following Ivany et al. (2011). A singular spectrum analysis (SSA) was first applied to each short time series [SSA; settings: window length 16, covariance estimation by Vautard & Ghil [Vautard and Ghil, 1989] approach, Monte Carlo significance test] to reduce the noise level in the time series. kSpectra output ranked the first ten SSA components. Following Ivaney et al. (2011), the first eight SSA components (which captured more than 65% of total variance in each SGI) were used to construct a "filtered" SGI time series. In the second step, these "filtered" SGI time series were subjected to a multi-taper method (MTM) [MTM; settings: significance = "red noise", 3 tapers, adaptive procedure, robust background noise]. This procedure allowed construction of a MTM spectrum with distinct peaks that could be verified against the corresponding FFT plots. Lastly, SSA-MTM spectrograms were plotted against previously proposed periods of the NAO, and the distinct structures and intervals of high confidence were compared to the FFT and periodogram. SSA-MTM and other low-pass filtering methods are common in paleoclimatology (Mann and Lees, 1996; Schöne et al., 2004), especially for relatively short time series.

[Spectral procedures were also performed using the “multitaper” (Rahim, 2010), “RSEIS” (Lees, 2008), “rssa” (Korobeynikov, 2010) and “stats” (R Core Team) packages in R. We applied SSA to reduce the noise in each time series and decompose each in to a trend (secular variation), cyclic and slow (irregular) component series (new SSA settings: window length 5, full singular value decomposition (SVD) method by Korobeynikov (2010)). The “slow” component of each time series, representing the filtered residuals of the original time series, underwent a general multi-taper spectral analysis method (spec.mtm; settings: 5 tapers, adaptive calculations, F-test, jackknife 95% confidence intervals).

5.4 RESULTS

5.4.1 Isotope sclerochronology

Oxygen isotope time series in *G. americana* shells exhibits a saw-tooth patterns and consistent amplitude between minimum and maximum values (Figure 5.3). Cuspate peaks occur at the most positive values and valleys coincide with the lowest values. Prominent growth lines are located at or just prior to the most positive $\delta^{18}O$ values at the peaks in the time series. The oxygen isotope ratios of GLY-A ranged from −0.57‰ to 2.04‰ with a mean of 0.62±0.18‰ (N=39). Specimen GLY-C ranged from 1.71‰ to 2.24‰ with a mean of 2.03±0.62‰ (N=3).

Unlike *G. americana*, the oxygen isotope time series in both *P. reflexa* specimens do not exhibit a saw-tooth pattern (Figure 5.4). Prominent growth lines did not regularly coincide with any particular features (i.e., peaks or valleys) within the time series; however, they did appear to form closer together with increasing age. The oxygen isotope ratios of PR-C ranged from 1.71‰ to 3.32‰ with a mean value of 2.32±0.04‰ (N=35). Specimen PR-D ranged from 0.92‰ to 2.38‰ with an average of 1.83±0.04‰ (N=40).

Variations in $\delta^{13}C$ values generally showed no consistent trend through time in either species. The carbon isotope ratios of GLY-A ranged from 1.78‰ to 2.77‰ with a mean of 2.17±0.03‰ (N=39). GLY-C recorded values that ranged from 1.71‰ to 2.24‰ with a mean of 2.03±0.3 (N=30). Both *G. americana* $\delta^{13}C$ values showed a slight decreasing trend through time (Figure 5.3). The carbon isotope ratios of *P. reflexa* specimen PR-C ranged from −1.04‰ to 0.89‰ with a mean of 0.07±0.03‰ (N=35). Specimen PR-D recorded values that ranged from −0.91‰ to 0.36‰ with a mean of −0.11‰±0.03‰ (N= 40). No significant correlation was observed between $\delta^{18}O$ and $\delta^{13}C$ values in either species (Figure 5.4, Appendix B, Figure 2).

5.4.2 Aging

Internal growth marks could clearly be identified and counted macroscopically along the valves of *G. americana* and hinge plates of *P. reflexa*. Marks near the ventral margins became faint and closely spaced, making counts and measurements increasingly subjective. However, even as growth increments thinned, it was clear that they continued to form throughout ontogeny. After isotopic verification that primary increments were annually resolved and likely preserved in *G. americana* (see discussion below), annual increments were used for age reading and growth measurements. We excluded *P. reflexa* from further growth increment and ontogenetic analysis because annual increment formation could not be verified in our isotopic study (see discussion below). No primary annual increment could be verified for *P. reflexa* (see above). The unverifiable counts of primary growth increments of 7 *P. reflexa* specimens (Appendix B, Table 3) resulted in a maximum count of 63 and a mean of 31 (Hudley and Surge, 2010).

G. americana from the Yorktown and Chowan River populations were aged from 15 to 75 years old with a mean and median age of approximately 38 and 36 years, respectively (N=134; Figure 5.5). There is a positive relationship between age and total shell length (r^2= 0.630, p=0.0004). Some individuals may have been longer lived than what was counted, especially those individuals whose ventral margins were eroded or exceptionally difficult to read due to closely spaced growth marks. About 37% (N = 37) of the population lived for >50 years. The maximum length measured was 93.4 mm. Previous studies showed that Pliocene specimens commonly reached 105 mm (Campbell, 1993) to 113.4 mm long (Nicol, 1953).

5.4.3 Growth models

The VBGM analysis of *G. americana* resulted in a growth pattern that had a clear sigmoidal form (Figure 5.6). This curve was exhibited for both the Yorktown and Chowan River populations. Growth rates revealed some variation among individuals and populations. The growth rate was exponential in the first eight to twelve years of life, and increment width decreased with age. After the early period of exponential growth, annual increments declined to a minimum of about 0.07 mm in the oldest animals (Appendix B, Tables 5 and 6). For the Yorktown and Chowan River populations, respectively, the VBGM results yielded asymptotic shell lengths (L_∞) of 82.4 mm and 79.1 mm and growth rate constants (k) of 0.106 and 0.086. The shape of the growth curve was similar to other studies of *Glycymeris* (*G. americana*-MACP, Thomas, 1970; *G. glycymeris*-Isle of Man, UK, Steíngrímsson, 1989) with high growth rates in the first eight years of life. All populations had similarly high infinite lengths (L_∞) but slight differences in growth rate constants (k), which likely relate to differences in shell curvature.

5.4.4 Increment analysis

Fixed logarithmic (VBGM) and adaptive individual-based detrending and standardization methods did not compare well to each other. Growth increment time-series that were detrended using population-specific VBGM all exhibited a similar pattern. The SGIs displayed high variation oscillations away from normal growth for the first ~10-12 years of life. After that point, the oscillations diminished and time-series flattened between ~20-50 years. The SGI developed using individual-based adaptive splines displayed greater variation, with continuous oscillations though ontogeny. This is the pattern more commonly plotted in increment studies, and presumes that the specimen's indeterminate growth rate should show variations throughout ontogeny, and does not become constant in senescence. The individual-based SGIs all exhibited different patterns. When both detrending methods were compared, the fraction of VBGM-SGI growth increments with less than normal growth was 59% while less than normal growth years comprises 58% of SGIs using the individual-base model (*N*=550). Only the individual-based detrending method resulted in time-series used for spectral analysis. Interestingly, both methods displayed patterns were ~60% of the SGI showed less than normal growth even though the stages where most of that growth was displayed was different for each method (Appendix B, Figures 3-8).

5.4.5 Spectral analysis

SSA-MTM analyses of the SGIs, SST (Jun–Aug), and NAO Index (Dec–Feb) time series revealed weak spectral structures at frequencies centered on 0.050, 0.109, 0.40 and 0.50 yr^{-1} corresponding to commonly reported frequencies of the NAO. The 1950-2011 NAO Index SSA-MTM exhibited power only at low frequencies but displayed structures high frequencies attributed to NAO. The NAO Reconstruction (1050-2011) only had significant power in the high frequencies. The Cape Hatteras and Long Branch Oakhurst observation records SSA-MTM displayed patterns similar to the instrument NAO. The SGI spectrum from Yorktown Formation (specimens GLY-LA02, GLY-LA03, GLY-LA04, and GLY-YKTC) exhibit a trend of maximum spectral power at the lowest frequencies (0.0-0.1 yr^{-1}) with and much lower relative power in the higher frequencies. Chowan River Formation SGIs SSA-MTM spectrum also displayed most of their power in the lower frequencies.

5.5 DISCUSSION

5.5.1 Oxygen Isotope ratios in Panopea

Estimated temperature in *P. reflexa* falls below the reported Pliocene paleotemperature range for the Yorktown Formation (13.6ºC–29.7ºC; Williams et al., 2009) and historic instrument records from the NOAA station Chesapeake Light off Virginia (Figure 5.7). Moreover, the lack of a sinusoidal pattern in the $\delta^{18}O$ time series of *P. reflexa* does not support that the primary growth marks found in the umbo are annual increments. One explanation for our findings is that the cardinal tooth region of *P. reflexa* is out of isotopic equilibrium. although other isotope sclerochronology studies indicate that *Panopea* is sensitive to environmental variables (e.g., temperature, food resources, and habitat topography) at seasonal and annual scales (Strom et al., 2004; Goman et al., 2008; Black et al., 2009; Nielsen and Nielsen, 2009), we cannot verify this for *P. reflexa*. In Strom et al. (2004) and Goman et al. (2007), temperature estimates derived from oxygen isotopic measurement in the cardinal teeth of *P. abrupta* were found to correlate well with local instrumental records. Contrary to the findings of these previous studies, Hallman et al. (2008) indicated that interpretation of isotopic time series in modern *P. abrupta* hinge plates is problematic, which is consistent with our findings. Hallman et al. (2008) sample the cardinal tooth and corresponding growth intervals in the inner and outer layer of the valve. Although growth patterns (age) were similar in all areas of the shell, results suggest that the $\delta^{18}O$ data from the cardinal tooth and inner valve layer were shifted away from equilibrium by up to approximately 0.7–0.9‰ toward less positive values in most years. Hallman et al. (2008) proposed that the cardinal tooth is precipitated from the inner extrapallial fluid (EPF) and is not in elemental or isotopic equilibrium with either the outer EPF or environmental waters. They further determined the outer prismatic layer is more appropriate for isotopic analysis and aging studies. However, sampling *P. reflexa* along the outer prismatic layer is difficult as shells often have damaged surfaces and cracks throughout the interior of the valve despite that they may have been found articulated and well preserved (Figure 5.2).

We considered two alternative explanations: (1) an introduction of a systematic sampling error (i.e., time averaging bias) and/or; (2) misidentification of the paleoenvironment. Time averaging bias can occur during intervals of slowed growth (e.g., advanced ontogenetic age). Such time averaging biases with increasing ontogenetic age has been documented by decreasing amplitudes and periods in the isotopic time series of several bivalve taxa (Jones 1980; Thompson et al. 1980; Weidman et al. 1994; and many others). This explanation does not best explain the lack of a clear sinusoidal pattern in the $\delta^{18}O$ time series of *P. reflexa.* The decreasing amplitudes reported for other taxa seem to be present in the decreasing width of successive growth increments (space between dark lines indicated by black triangles along x-axis in Figure 5.7). However, neither PR-C nor PR-D exhibit a systematic change from high amplitude sinusoids in early growth to decreasing amplitude with advanced age (Figure 5.7). Misidentification of the paleoenvironment can potentially invalidate the assumed $\delta^{18}O_{seawater}$ value. Perhaps *P. reflexa* were not growing in fully marine conditions. Though we assumed that the Yorktown fossiliferous beds were outer neritic (Hazel, 1971; Blackwelder, 1981a; Cronin, 1991), some biostratigraphical and lithological interpretations of the Rushmere and Morgarts Beach Members imply estuarine influences (Ward, 1992). Estuarine influences may result in freshwater/seawater mixing complicating the constraint of the $\delta^{18}O$ value of ambient water. Therefore, our use of a constant Pliocene $\delta^{18}O_{seawater}$ value (1.1‰) may be unsuitable in this case. *Panopea spp.* has broad ecological amplitude and are found in sands, muddy-sands, and muddy sediment depositional environments (Strom, 1997; Alexander and Dietl, 2005; Gribben and Creese, 2005). Deep-burrowing *Panopea spp.* are found in various environments including inner-neritic, outer-neritic and deltaic deposits (Franz, 1982). This explanation is unlikely because *Chesapecten*, a fully marine genus, were abundant at the same localities. Extant scallops tolerate only small fluctuations in marine salinity and are not commonly found in sequences deposited under strong fluvial influences. Therefore, our preferred explanation is that the cardinal tooth region of *P. reflexa* is out of isotopic equilibrium and cannot be used as a reliable paleotemperature proxy capable of resolving seasonal and annual variations. Given the probable isotopic disequilibrium, oxygen isotope time series cannot be used to determine whether or not primary growth marks are annual in this species.

5.5.2 Interpretations of paleotemperature estimates from Glycymeris

The oxygen isotope time series of *G. americana* records seasonal variability. The regular saw-tooth patterns exhibited in the time series are generally interpreted as cycles displaying both a time of growth, when environmental conditions are within species-specific tolerances, and time of shutdown, when conditions fall outside of that range. Prominent growth lines occurring prior to or at the most positive $\delta^{18}O$ values formed in fall or winter, respectively (Figure 5.3). Our findings of winter growth cessation from *G. americana* is consistent with Steíngrímsson (1989) who indicated the populations of *G. glycymeris* in Irish Sea deposited dark growth lines in the winter months. Our findings are consistent with Goewert and Surge (2008), who reported winter growth cessation in *Chesapecten* shells from the Chuckatuck–Riddick's Pit locality in the same member (Moore House member) of Yorktown. Goewert and Surge (2008) found seasonal temperatures ranging from 3.2°C to 20.8°C (cooler than reported Yorktown temperatures), and concluded that the winter growth cessation lines might be ascribed to eddies and cold filaments of the Labrador Current that may have penetrated the marine environment during the deposition of the Yorktown Formation. However, recalculation of the Goewert and Surge (2008) *Chesapecten* estimates using $\delta^{18}O_w$ by Williams et al. (2009) indicates a revised temperature range from 10.1°C to 28.5°C. Both the Krantz (1990) and Goewert and Surge (2008) revised estimated temperatures of winter growth cessation in *Chesapecten* are similar to the winter cessation temperature of 8-9ºC of the extant scallops, *Pecten maximus* (Owen et al., 2002). The revised value of 10.1°C is lower than other Yorktown proxies (Williams et al. (2009) revised MPWI scenario Yorktown temperatures of 13.6°C to 30.1°C), but is not inconsistent with the leading scenario of greater influence of Gulf Stream waters transported onto the shelf during the time the Yorktown Formation was deposited (Figure 5.8).

Our finding of winter growth cessation is inconsistent with sclerochronology studies of molluscs from temperate provinces, which document growth cessation in warmer months (Jones, 1980; Jones and Quitmyer, 1996; Quitmyer et al., 1997; Arnold et al., 1998; Surge et al., 2008; Quitmyer and Jones, 2012; Jones et al., 2012; Surge et al., in review). Studies that document growth cessation during cooler seasons are from molluscan taxa inhabiting temperate regions (Jones and Quitmyer, 1996; Surge et al, in review). This pattern of seasonal timing of slowed growth is more complicated, however. Elliott et al. (2003) isotopically sampled *Mercenaria* shells from localities within the warm- and cold-temperate zone. All specimens formed dark increments during the summer regardless of location. More recently, Henry and Cerrato (2007) isotopically analyzed *M. mercenaria* shells from various locations in Narragansett Bay, Rhode Island, and compared their results to the earlier studies of Jones et al. (1989) and Bernstein (1993). Examining chronologically the seasonal timing of dark increment formation over several decades revealed a progression from slow growth only in winter to an annual pattern of slowed growth during summer, fall, and winter (Henry and Cerrato, 2006). Henry and Cerrato (2007) suggested that changes in the marine environment may have altered seasonal growth patterns and may have accompanied an increase in water temperature over time in Narragansett Bay.

Estimated seawater temperature from specimens GLY-A and GLY-C ranged from 14.1ºC to 26.7ºC (Figure 5.8). Averaging the coldest and warmest temperatures recorded across all years in both shells resulted in mean winter and summer temperatures of 16.2±1.4°C and 24.4±1.5°C, respectively, and an average seasonal temperature range of

~8.2°C. Reported Pliocene palaeotemperatures for the Yorktown Formation based on isotopic proxy records from *Chesapecten* shells (Krantz, 1990) fall within that range of 13.6–30.1ºC (Williams et al., 2009). Our winter and summer temperature estimates fall within the previously reported values, and the seasonal range in our study is lower than these previous studies. One explanation for our lower range is that *Glycymeris* and *Chesapecten* are recording seawater temperature from different regions on the shelf (Figure 5.8, darker areas). However, fossil *Chesapecten* and *Glycymeris* are both common and abundant in the same beds at most of our Pliocene sampling localities. Extant *Pectinidae* (i.e., *Aequipecten* and *Argopecten*) are also commonly found in abundance with *G. americana* in deep (>30 m) gravel-bottom assemblages in the South Atlantic Bight (Wolfe, 2008). Therefore, this explanation is unlikely. Another alternative explanation for the differences in temperature recorded in these two taxa is that neither species precipitates their shells in equilibrium with the water. An isotopic study of extant *Pectinidae (Pecten maximus)* by Owen et al. (2002) determined that at times of low shell growth rates (intervals of cessation) shell $\delta^{18}O$ deviated from equilibrium +0.6‰, a temperature equivalency of approximately −3°C. Similarly, a study of *G. glycymeris* by Royer et al. (in press) demonstrated oxygen isotope-derived temperatures closely related to bottom water temperatures but overestimated temperature from 0.1 °C to more than 2 °C when using the Grossman and Ku (1986) equation. These studies demonstrate the critical importance of a species-specific paleotemperature equation for each of these bivalve proxies. Unfortunately, *Chesapecten* is extinct and a species-specific calibration of *G. americana* has not yet been calibrated. The differences in temperature estimates between *Chesapecten* and *G. americana* may be a result of disequilibrium with water, but if calibrated *Glycymeris* species may capture the entire seasonal range of seawater temperature.

Compared to modern instrumental records reported in Williams et al. (2009), our temperature estimates record a more narrow range of seasonal amplitude with warmer winters and cooler summers (Figure 5.8). This observation is similar to other paleotemperature estimates from the Yorktown based on molluscan archives. Our findings are consistent with interpretations that during the Pliocene, warm southern waters penetrated north of what is now the physiographic and thermal barrier of Cape Hatteras and extended the biogeographic range to outer tropical (Carolinian) fauna (Ward and Strickland, 1985; Cronin 1988). Dowsett et al. (1999, 2005) documented intensification of the Gulf Stream, thus potentially enhancing the warmth of the Carolina Coastal Current. The northward flowing Carolina Current in the South Atlantic Bight (SAB) is influenced by a mixture of wind, seawater density, and Gulf Stream incursions (Atkinson et al., 1983). More incursions of vigorous, warm Gulf Stream filaments may explain warmer temperatures farther north along the Pliocene shelf than present day. However, a reduced latitudinal SST gradient implies weaker atmospheric forcing of surface oceanic circulation, and hence weaker oceanic heat transport from Equator to higher latitudes (Crowley 1996).

Another possible explanation is that cold, southward flowing waters (e.g., the Virginia Coastal Current and MAB modified Labrador Current waters) did not penetrate as far south as they do in present day winters. Cold, bouyant Labrador Current system water represents a significant water mass, reaching ~45ºN during the present day winter. Though the Labrador Current water system is reported to have developed during the Pliocene (~2.5 Ma) (Berggren and Hollister, 1977), the system was likely not as strong as today due to reduced sea cover and terrestrial ice sheet development. This weaker Labrador Current system is consistent with Pliocene simulations using the HadCM3 GCM with PRISM SST boundary conditions. Simulations predict both reductions in sea ice cover and greater Gulf Stream velocity compared to pre-industrial simulations along with weaker thermohaline circulation and a shallower depth for North Atlantic Deep Water formation (Haywood & Valdes, 2004).

5.5.3 G. americana as a multi-decadal climate archive.

To determine whether *G. americana* can potentially serve as a multi-decadal archive to reconstruct Pliocene marine climate, we evaluated whether this species is long lived using results from the VBGM analysis. Growth curves from this study were compared to previously published curves of: (1) populations of *G. americana* in the same stratigraphic formations; and (2) *Glycymeris* populations of the same genus in different localities and time (Figure 5.6). Counts based on internal growth marks show that ~80% of the Pliocene *G. americana* attained at least 30 years of age, and almost 40% reach an age 50 years (Figure 5.5). None our specimens are as large as those found in the Pliocene MACP localities (105 mm (Campbell, 1993); 113.4 mm long (Nicol, 1953)), thus Pliocene *G. americana* likely attain true ages at death greater than those we show here. Modern *Glycymeris* (e.g. *G. glycymeris*) populations from the Irish Sea show growth patterns and age distributions with individuals reaching ages >100 years (Ramsey et al, 2000; Reynolds, 2011b) with a lower L_∞ (Figure 5.6). *G. glycymeris* share the same boreal habitat and distribution as the long-lived ocean quahog, *Arctica islandica* (>500 years, Wanamaker et al., 2012). The long life span and slow growth of *A. islandica* are often associated with cold temperature and great depth. In contrast, *G. americana* occurs along the Atlantic coast from Virginia to Brazil. Cold temperatures cannot be associated with its longevity. However, some studies suggest that limited food supply is the more important factor for longevity in *A. islandica* (Witbaard et al., 1999; Schöne et al., 2004) and Eocene *Cucullaea raea*, (Buick and Ivany, 2004; Ivany et al., 2011). Our results from Pliocene *G. americana* support the hypothesis that physiological stress associated with limited food could be responsible for increase longevity in some bivalve species. Thomas (1970, 1975) noted that *Glycymeris spp.* are physiologically unspecialized bivalves, adapted to a relatively narrow range of environments, which are rather inhospitable to bivalves in general. If food limitation is a primary factor, then marginal living *Glycymeris spp.* likely exhibits this longevity throughout its range and, therefore, potentially serves as an important archive for multi-decadal proxies for paleoecologicial and paleoclimatic investigations in areas where traditional multi-decadal proxy records do not exist.

After we confirmed that *G. americana* lived for several decades, we evaluated results from our SGI analysis to assess their potential for recording interannual and multi-decadal climate variability along MACP during the Pliocene. Spectral densities originated from detrended increment series and instrument SST data show structures at the periods associated with the NAO: 20, 6-10, 4.8, and 2-3 years (Rogers, 1984; Hurrell and van Loon, 1997), but with most below the 95% significance level relative to the estimated red noise background (Figures 5.9 – 5.11). The NAO instrumental series (Figure 5.9A; Appendix B, Figure 3) and NAO reconstruction series (Figure 5.9B; Appendix B, Figure 3) both exhibit significant power at the period around 20 years, however only the NAO instrument SSA-MTM (Figure 5.9A) exhibits potential structures near the smaller reported NAO periodicities. The Long Branch Oakhurst (Figure 5.9C; Appendix B, Figure 4) and Cape Hatteras (Figure 5.9D; Appendix B, Figure 4) observation records SSA-MTM displayed structures at 0.109, 0.187, 0.414, and 0.402, corresponding to periods of 9.2, 5.3, 2.4, and 2.5 years all at or near reported NAO periods. In the Yorktown Formation, GLY-LA02 displayed weak but high-confidence structures at periods 20.0, 7.7, and 3.2 years (Figure 5.10A). The periodogram mean spectrum of GLY-LA02 is at period 7.3 years, and neither the periodogram nor the FFT showed significant structures other than the 20-year (0.054 yr^{-1}) period (Appendix B, Figure 5 lower left panel). GLY-LA03 SSA-MTM displayed power corresponding to periods of 20.0 to 7.0 years (Figure 5.10B). A mean spectrum at period 7.6 year was calculated and the most significant structure was at 18 years ($p = 0.016$), while The FFT displayed structures corresponding to 21.7, 10.7, and 2.3 years (Appendix B, Figure 5 lower right panel). GLY-LA04 SSA-MTM was the only series not to exhibit significant power at the 20 year period (Figure 5.10C). GLY-YKTC had distinct structures at period 20, 7.7, and around 4.8 years (5.10D). The Chowan River SSA-MTM time series (Figure 5.11; Appendix B, Figures 7 and 8) mostly followed the trend of displaying some power at NAO reported periods.

The periodicity at 20 years may not be significant because none of our growth increment series exhibit continuous sequences longer than 75 year. The same might be concluded about the NAO instrumental time series. Accepting the high frequency bands, SSA-MTM spectral analysis of shell increment records coincide with the primary periodicities found in the modern NAO and MACP shelf instrument records. A general comparison of modern records to SGIs from the Yorktown and Chowan River Formations shows that MACP seawater variability was likely similar in the both the mid- and late Pliocene. Our findings that the NAO remains relatively unchanged are similar to a MTM spectral analysis of tree-ring and isotope records from Pliocene Ellesmere Island (Ballantyne et al., 2006) and support model simulations of mid-Pliocene climate (Chandler et al., 1994; Haywood et al., 2000; Haywood & Valdes, 2004; Haywood et al., 2008).

5.6. CONCLUSIONS

Pliocene *G. americana* preserves records of growth and climate at seasonal to multi-decadal variation in $\delta^{18}O$ and growth increments, and exhibits longevity not often found in warm-temperate and tropical bivalves. Through isotope sclerochronology we determined the primary growth marks of *G. americana* are annually resolved, exhibiting both periodicity and synchronicity when compared against records from other Pliocene bivalves. *Glycymeris* paleotemperature estimates exhibit warmer than modern winter temperatures, supporting previous interpretations of diminished seasonality in Yorktown deposits. This work demonstrates that spectral analysis of long, standardized growth increment records from *G. americana* shells display periodicities similar to those of the modern NAO in both the mid- and late Pliocene.Using the isotope sclerochronology methods, oxygen isotope compositions of *P. reflexa* showed no periodicity or synchronicity and could not be verified as annual.

ACKNOWLEDGMENTS

Thanks to David Dettman at the University of Arizona's Environmental Isotopes Laboratory for isotopic analysis and to Joseph Carter (UNC) and Lauck Ward (VMNH) for their guidance on MACP collection localities. We thank Janice Edgerson for her proof reading of the early drafts of this paper. Thanks also to Melissa Hudley and Ian Winklestern for assistance in field collections. We would like to thank JH's doctoral committee for their constructive influences on this manuscript. This project is supported in part by the Preston Jones and Mary Elizabeth Frances Dean Martin Trust and National Science Foundation Grants # HRD-0450099 (V. Ashby) and # AGS-0602422 (DS).

Table 5.1: Isotopic composition of shells. Specimens were collected from the Morgarts Beach and Rushmere members of the Yorktown Formation, Pliocene Age. Samples from *Glycymeris* were taken from the valve and represent (4) annuals. Samples from the *Panopea* were micromilled from the umbo. Samples were run at the University of Arizona's Environmental Isotope Laboratory.

Shell	ID	Mineral	Sample	Distance	δ13C VPDB	δ18O VPDB	C std dev	O std dev	Voltage
GLY-A	GLY-A-001	aragonite	1-54	28.23	1.97	1.51	0.051	0.029	1.8
GLY-A	GLY-A-002	aragonite	2-54	28.82	2.48	1.27	0.043	0.085	1.88
GLY-A	GLY-A-003	aragonite	3-54	29.409	2.77	0.60	0.018	0.024	2.83
GLY-A	GLY-A-004	aragonite	4-54	29.999	2.42	0.06	0.007	0.004	2.54
GLY-A	GLY-A-005	aragonite	5-54	30.588	2.11	0.12	0.026	0.049	1.43
GLY-A	GLY-A-006	aragonite	6-54	31.177	1.98	0.26	0.017	0.079	1.74
GLY-A	GLY-A-007	aragonite	7-54	31.767	1.88	0.24	0.007	0.036	2.39
GLY-A	GLY-A-008	aragonite	8-54	32.357	1.88	0.21	0.034	0.055	2.65
GLY-A	GLY-A-009	aragonite	9-54	32.946	1.97	0.31	0.006	0.036	1.97
GLY-A	GLY-A-010	aragonite	10-54	33.536	2.15	0.92	0.030	0.030	2.13
GLY-A	GLY-A-011	aragonite	11-54	34.125	2.24	1.53	0.013	0.058	1.35
GLY-A	GLY-A-012	aragonite	12-54	34.715	2.28	2.04	0.011	0.031	2.50
GLY-A	GLY-A-013	aragonite	13-54	35.231	2.34	1.13	0.013	0.073	1.96
GLY-A	GLY-A-014	aragonite	14-54	35.747	2.49	0.90	0.050	0.076	2.70
GLY-A	GLY-A-015	aragonite	15-54	36.264	2.31	0.69	0.035	0.067	2.63
GLY-A	GLY-A-016	aragonite	16-54	36.78	2.25	0.04	0.022	0.063	2.44
GLY-A	GLY-A-017	aragonite	17-54	37.297	2.07	0.17	0.008	0.008	2.72
GLY-A	GLY-A-018	aragonite	18-54	37.813	1.94	0.25	0.045	0.042	1.45
GLY-A	GLY-A-019	aragonite	19-54	38.33	1.86	0.28	0.010	0.007	1.89
GLY-A	GLY-A-020	aragonite	20-54	38.846	1.92	0.62	0.006	0.055	1.71
GLY-A	GLY-A-021	aragonite	21-54	39.363	1.78	0.86	0.013	0.021	2.05
GLY-A	GLY-A-022	aragonite	22-54	39.879	2.09	1.66	0.026	0.084	1.42
GLY-A	GLY-A-023	aragonite	23-54	40.395	2.16	1.70	0.025	0.032	1.64
GLY-A	GLY-A-024	aragonite	24-54	41.033	2.16	0.98	0.021	0.013	2.19
GLY-A	GLY-A-025	aragonite	25-54	41.67	2.19	0.53	0.012	0.019	2.53
GLY-A	GLY-A-026	aragonite	26-54	42.307	2.28	0.18	0.014	0.053	2.06
GLY-A	GLY-A-027	aragonite	27-54	42.945	2.10	-0.30	0.039	0.036	2.56
GLY-A	GLY-A-028	aragonite	28-54	43.582	1.98	-0.57	0.021	0.049	1.55
GLY-A	GLY-A-029	aragonite	29-54	44.219	2.05	0.07	0.025	0.043	2.62
GLY-A	GLY-A-030	aragonite	30-54	44.856	2.48	0.67	0.019	0.021	1.66
GLY-A	GLY-A-031	aragonite	31-54	45.494	2.21	1.31	0.060	0.009	1.70
GLY-A	GLY-A-032	aragonite	32-54	46.001	2.03	0.90	0.047	0.021	1.63
GLY-A	GLY-A-033	aragonite	33-54	46.508	2.12	0.64	0.070	0.024	1.57

GLY-A	GLY-A-034	aragonite	34-54	47.016	2.24	0.23	0.047	0.080	2.15
GLY-A	GLY-A-035	aragonite	35-54	47.523	2.23	-0.38	0.013	0.046	1.47
GLY-A	GLY-A-036	aragonite	36-54	48.031	2.29	-0.26	0.067	0.053	1.91
GLY-A	GLY-A-037	aragonite	37-54	48.538	2.37	0.05	0.035	0.025	1.40
GLY-A	GLY-A-038	aragonite	38-54	49.046	2.40	0.91	0.028	0.047	2.66
GLY-A	GLY-A-039	aragonite	39-54	49.553	2.29	1.73	0.003	0.060	1.96
GLY-C	GLY-C-001	aragonite	1-66	44.815	2.17	2.34	0.035	0.047	1.46
GLY-C	GLY-C-002	aragonite	2-66	45.15	1.99	1.68	0.037	0.023	1.75
GLY-C	GLY-C-003	aragonite	3-66	45.485	2.22	1.20	0.032	0.046	2.75
GLY-C	GLY-C-004	aragonite	4-66	45.82	2.14	0.79	0.017	0.017	2.09
GLY-C	GLY-C-005	aragonite	5-66	46.155	2.24	0.88	0.009	0.023	2.95
GLY-C	GLY-C-006	aragonite	6-66	46.49	2.08	0.69	0.030	0.003	2.94
GLY-C	GLY-C-007	aragonite	7-66	46.825	2.18	0.32	0.021	0.042	2.73
GLY-C	GLY-C-008	aragonite	8-66	47.16	2.08	0.19	0.036	0.083	1.96
GLY-C	GLY-C-009	aragonite	9-66	47.495	2.11	0.61	0.069	0.085	1.65
GLY-C	GLY-C-010	aragonite	10-66	47.831	2.10	0.89	0.012	0.060	1.78
GLY-C	GLY-C-011	aragonite	11-66	48.166	2.02	1.38	0.019	0.017	2.25
GLY-C	GLY-C-012	aragonite	12-66	48.5	1.95	2.13	0.039	0.085	2.08
GLY-C	GLY-C-013	aragonite	13-66	48.835	2.02	1.60	0.096	0.016	2.62
GLY-C	GLY-C-014	aragonite	14-66	49.171	1.93	1.30	0.011	0.066	2.13
GLY-C	GLY-C-015	aragonite	15-66	49.506	2.12	0.99	0.020	0.048	2.01
GLY-C	GLY-C-016	aragonite	16-66	49.841	1.98	0.36	0.030	0.043	2.05
GLY-C	GLY-C-017	aragonite	17-66	50.176	2.04	0.13	0.028	0.013	2.27
GLY-C	GLY-C-018	aragonite	18-66	50.511	2.13	-0.05	0.050	0.009	2.93
GLY-C	GLY-C-019	aragonite	19-66	50.846	2.08	0.21	0.004	0.032	2.58
GLY-C	GLY-C-020	aragonite	20-66	51.181	2.00	1.01	0.020	0.048	2.57
GLY-C	GLY-C-021	aragonite	21-66	51.516	1.99	1.48	0.030	0.084	2.05
GLY-C	GLY-C-022	aragonite	22-66	51.851	1.98	2.05	0.045	0.040	2.36
GLY-C	GLY-C-023	aragonite	23-66	52.186	1.71	1.53	0.046	0.033	2.70
GLY-C	GLY-C-024	aragonite	24-66	52.521	1.78	1.10	0.017	0.010	1.63
GLY-C	GLY-C-025	aragonite	25-66	52.856	1.89	1.23	0.010	0.020	1.9
GLY-C	GLY-C-026	aragonite	26-66	53.191	1.83	0.66	0.093	0.047	2.05
GLY-C	GLY-C-027	aragonite	27-66	53.526	1.95	0.44	0.043	0.047	1.53
GLY-C	GLY-C-028	aragonite	28-66	53.861	2.14	0.73	0.028	0.038	2.35
GLY-C	GLY-C-029	aragonite	29-66	54.196	2.01	1.27	0.022	0.061	2.03
GLY-C	GLY-C-030	aragonite	30-66	54.531	2.02	1.84	0.038	0.060	1.66
PR-C	PR-C-001	aragonite	1-56	0.067	-0.17	2.16	0.046	0.047	1.32
PR-C	PR-C-002	aragonite	2-56	0.134	-0.21	2.17	0.030	0.056	1.48
PR-C	PR-C-003	aragonite	3-56	0.201	-0.11	1.87	0.032	0.025	1.56
PR-C	PR-C-004	aragonite	4-56	0.268	-0.22	2.15	0.017	0.063	1.58

PR-C	PR-C-005	aragonite	5-56	0.335	-0.16	2.30	0.035	0.007	2.69
PR-C	PR-C-006	aragonite	6-56	0.402	-0.29	2.40	0.029	0.028	1.96
PR-C	PR-C-007	aragonite	7-56	0.469	-0.52	2.39	0.016	0.074	2.20
PR-C	PR-C-008	aragonite	8-56	0.536	-0.44	2.41	0.011	0.022	2.2
PR-C	PR-C-009	aragonite	9-56	0.603	-0.07	2.35	0.066	0.021	1.83
PR-C	PR-C-010	aragonite	10-56	0.67	0.03	2.48	0.013	0.035	1.68
PR-C	PR-C-011	aragonite	11-56	0.737	0.18	2.26	0.016	0.019	2.34
PR-C	PR-C-012	aragonite	12-56	0.804	-0.10	2.11	0.026	0.024	1.47
PR-C	PR-C-013	aragonite	13-56	0.871	-0.02	2.65	0.025	0.056	1.44
PR-C	PR-C-014	aragonite	14-56	0.938	-0.43	2.11	0.019	0.012	1.44
PR-C	PR-C-015	aragonite	15-56	1.005	-1.04	2.25	0.040	0.058	1.91
PR-C	PR-C-016	aragonite	16-56	1.072	-0.82	2.67	0.021	0.034	2.80
PR-C	PR-C-017	aragonite	17-56	1.139	0.22	2.74	0.019	0.079	1.46
PR-C	PR-C-018	aragonite	18-56	1.206	0.35	2.07	0.031	0.051	1.39
PR-C	PR-C-019	aragonite	19-56	1.273	0.22	2.54	0.047	0.009	1.61
PR-C	PR-C-020	aragonite	20-56	1.34	0.47	2.51	0.033	0.048	2.72
PR-C	PR-C-021	aragonite	21-56	1.407	0.21	1.93	0.053	0.040	2.09
PR-C	PR-C-022	aragonite	22-56	1.474	-0.12	2.39	0.015	0.026	2.73
PR-C	PR-C-023	aragonite	23-56	1.541	-0.06	2.75	0.026	0.004	1.79
PR-C	PR-C-024	aragonite	24-56	1.608	0.28	3.32	0.010	0.053	2.35
PR-C	PR-C-025	aragonite	25-56	1.675	0.89	2.42	0.047	0.045	1.54
PR-C	PR-C-026	aragonite	26-56	1.742	0.48	1.71	0.031	0.079	1.72
PR-C	PR-C-027	aragonite	27-56	1.809	0.49	1.85	0.035	0.083	2.16
PR-C	PR-C-028	aragonite	28-56	1.876	0.39	2.07	0.012	0.016	1.69
PR-C	PR-C-029	aragonite	29-56	1.943	0.42	2.30	0.007	0.076	2.82
PR-C	PR-C-030	aragonite	30-56	2.01	0.39	2.53	0.041	0.010	2.69
PR-C	PR-C-031	aragonite	31-56	2.077	0.68	2.15	0.068	0.090	1.17
PR-C	PR-C-032	aragonite	32-56	2.144	0.49	2.22	0.026	0.042	2.52
PR-C	PR-C-033	aragonite	33-56	2.211	0.49	2.35	0.021	0.016	1.22
PR-C	PR-C-034	aragonite	34-56	2.278	0.29	2.44	0.052	0.022	2.71
PR-C	PR-C-035	aragonite	35-56	2.278	0.37	2.24	0.105	0.125	0.62
PR-D	PR-D-001	aragonite	1-48	0.113	-0.17	1.81	0.055	0.039	2.42
PR-D	PR-D-002	aragonite	2-48	0.227	-0.39	1.76	0.030	0.007	1.58
PR-D	PR-D-003	aragonite	3-48	0.34	-0.11	1.41	0.022	0.069	1.95
PR-D	PR-D-004	aragonite	4-48	0.454	0.04	1.25	0.079	0.035	2.06
PR-D	PR-D-005	aragonite	5-48	0.567	0.07	0.92	0.047	0.056	1.60
PR-D	PR-D-006	aragonite	6-48	0.681	0.26	0.96	0.022	0.041	1.92
PR-D	PR-D-007	aragonite	7-48	0.794	-0.05	1.28	0.027	0.056	2.20
PR-D	PR-D-008	aragonite	8-48	0.908	-0.59	1.58	0.076	0.052	1.45
PR-D	PR-D-009	aragonite	9-48	1.021	-0.44	1.41	0.042	0.023	1.32

PR-D	PR-D-010	aragonite	10-48	1.135	-0.22	1.91	0.036	0.072	1.71
PR-D	PR-D-011	aragonite	11-48	1.248	-0.61	1.81	0.029	0.044	2.20
PR-D	PR-D-012	aragonite	12-48	1.361	-0.91	2.12	0.039	0.042	1.82
PR-D	PR-D-013	aragonite	13-48	1.475	-0.82	2.14	0.015	0.085	2.46
PR-D	PR-D-014	aragonite	14-48	1.588	-0.38	1.66	0.024	0.029	1.46
PR-D	PR-D-015	aragonite	15-48	1.702	0.00	1.98	0.015	0.060	2.59
PR-D	PR-D-016	aragonite	16-48	1.815	-0.01	2.04	0.016	0.061	2.21
PR-D	PR-D-017	aragonite	17-48	1.929	0.01	2.10	0.021	0.042	2.12
PR-D	PR-D-018	aragonite	18-48	2.042	0.03	2.15	0.033	0.044	2.65
PR-D	PR-D-019	aragonite	19-48	2.156	-0.03	2.27	0.039	0.077	2.22
PR-D	PR-D-020	aragonite	20-48	2.269	-0.05	2.12	0.012	0.026	1.97
PR-D	PR-D-021	aragonite	21-48	2.383	0.06	2.10	0.005	0.028	2.57
PR-D	PR-D-022	aragonite	22-48	2.496	-0.23	2.38	0.071	0.030	2.13
PR-D	PR-D-023	aragonite	23-48	2.609	-0.15	1.92	0.024	0.018	1.73
PR-D	PR-D-024	aragonite	24-48	2.723	-0.13	2.07	0.043	0.071	2.25
PR-D	PR-D-025	aragonite	25-48	2.836	-0.01	1.91	0.025	0.018	2.46
PR-D	PR-D-026	aragonite	26-48	2.95	0.12	2.13	0.059	0.034	2.45
PR-D	PR-D-027	aragonite	27-48	3.063	-0.06	2.26	0.022	0.022	2.72
PR-D	PR-D-028	aragonite	28-48	3.177	-0.30	2.22	0.017	0.033	2.57
PR-D	PR-D-029	aragonite	29-48	3.29	-0.07	2.06	0.015	0.061	2.37
PR-D	PR-D-030	aragonite	30-48	3.404	-0.38	1.86	0.013	0.068	2.02
PR-D	PR-D-031	aragonite	31-48	3.517	-0.34	1.91	0.023	0.011	1.44
PR-D	PR-D-032	aragonite	32-48	3.631	-0.20	1.81	0.015	0.065	2.61
PR-D	PR-D-033	aragonite	33-48	3.744	0.14	1.76	0.018	0.033	2.43
PR-D	PR-D-034	aragonite	34-48	3.857	0.18	1.55	0.028	0.065	1.44
PR-D	PR-D-035	aragonite	35-48	3.971	0.17	1.63	0.011	0.027	1.73
PR-D	PR-D-036	aragonite	36-48	4.084	0.12	1.67	0.024	0.043	2.34
PR-D	PR-D-037	aragonite	37-48	4.198	0.23	1.72	0.037	0.010	3.03
PR-D	PR-D-038	aragonite	38-48	4.311	0.18	1.66	0.043	0.029	1.49
PR-D	PR-D-039	aragonite	39-48	4.425	0.36	1.80	0.009	0.037	1.92
PR-D	PR-D-040	aragonite	40-48	4.425	0.23	1.92	0.022	0.050	1.87

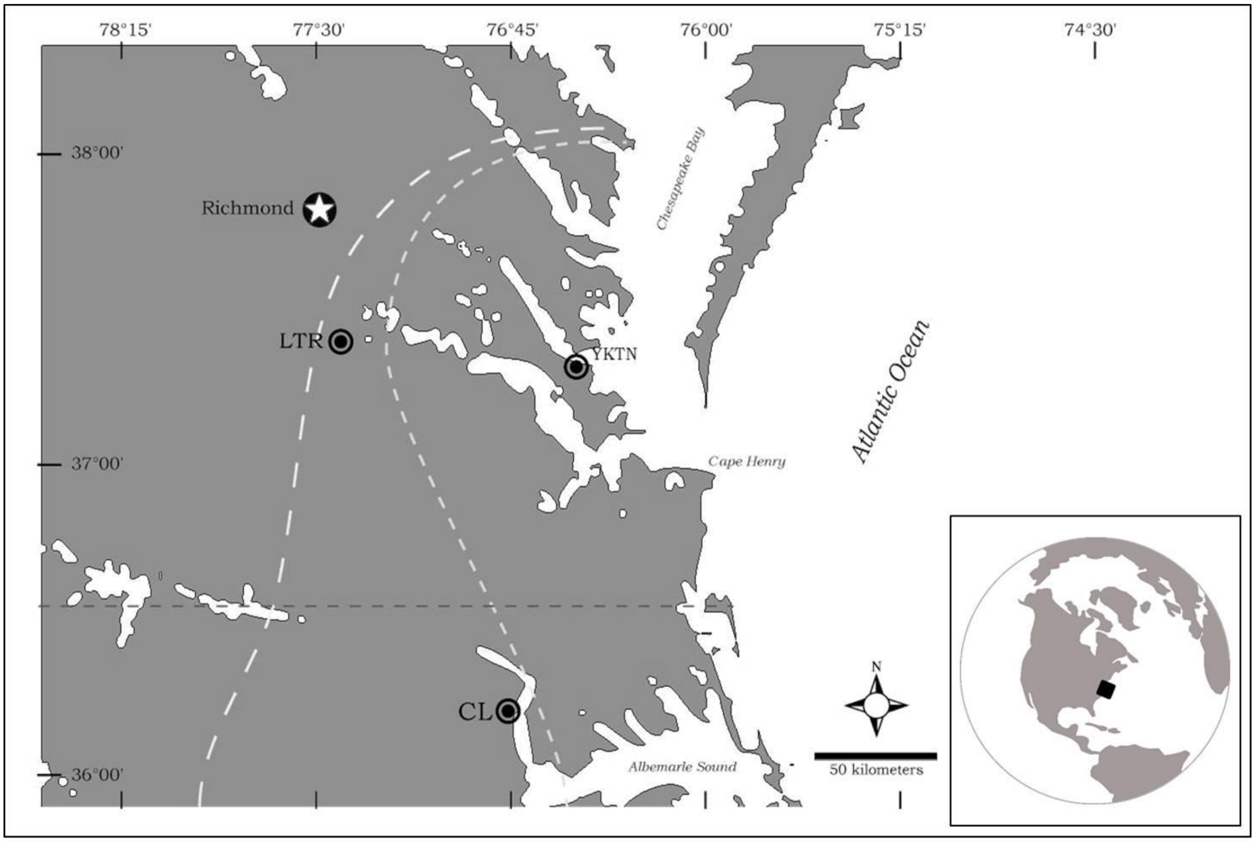

Figure 5.1. Location of collection sites along the Middle Atlantic Coastal Plain. Map shows the approximate limits of marine and marginal marine deposition during the Late Neogene along the mid-Atlantic Coast of the United States. Localities at Lieutenants Run (LTR), Yorktown Monument (YKTN), and Colerain Landing (CL) are denoted with bullets.The lighter more inland dashed line delineates Burwellian (M5) stage while the darker more shoreward dashed line delineates Wiltonian (M6) stage. Based on MACP chronostratgraphic stages (Blackwelder, 1981).

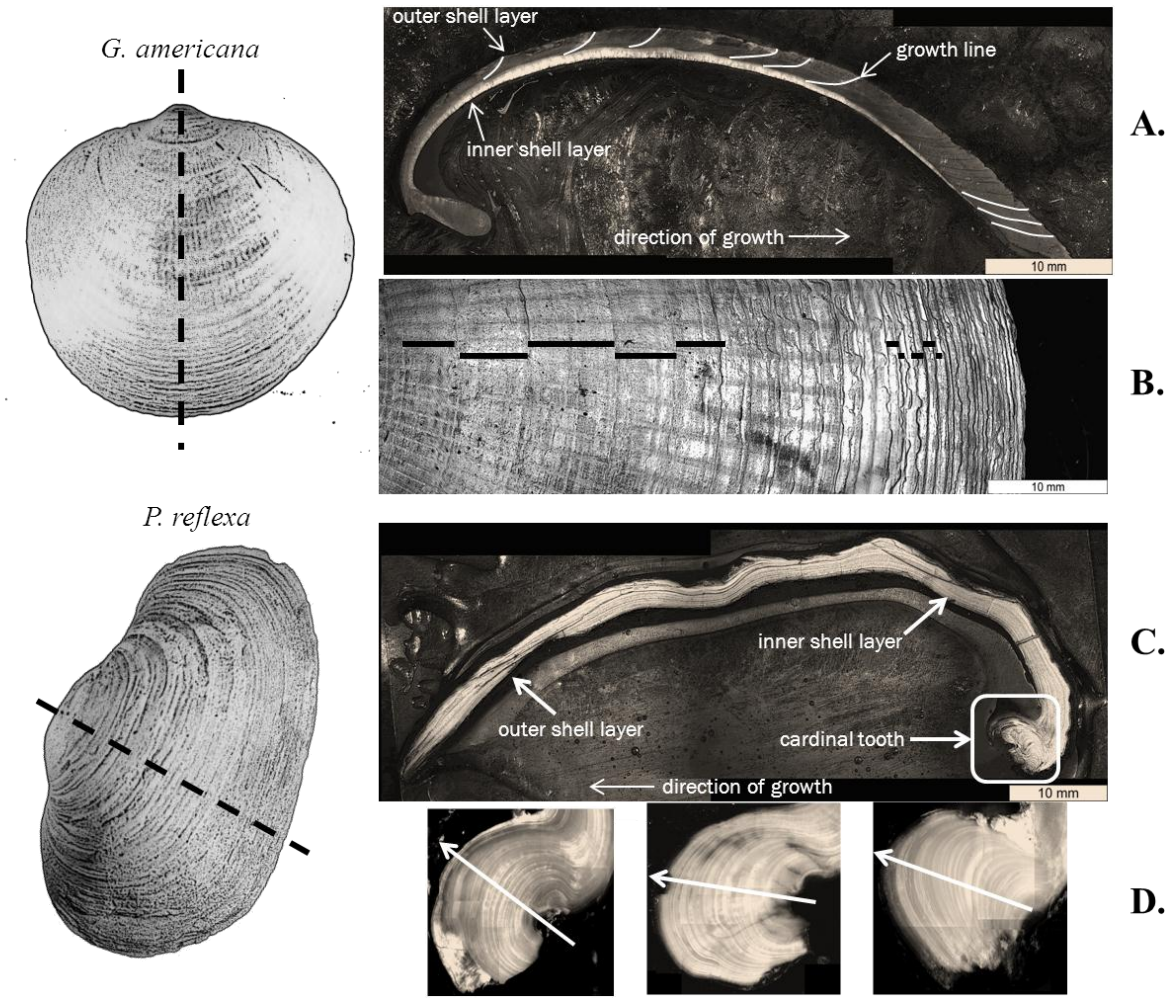

Figure 5.2 Shells of *Glycymeris americana* and *Panopea reflexa* cut through the axis of maximum growth to show annual growth increments. Panel A highlights the inner and outer shell layers and interior growth lines of *G. americana*. Panel B shows sample measurements of external growth lines. Panel C highlights the inner and out shell layers and cardinal tooth (umbo) of *P. reflexa*. Panel D illustrates the method of counting and sampling *P. flexa* along the longest growth axis of the hinge plate.

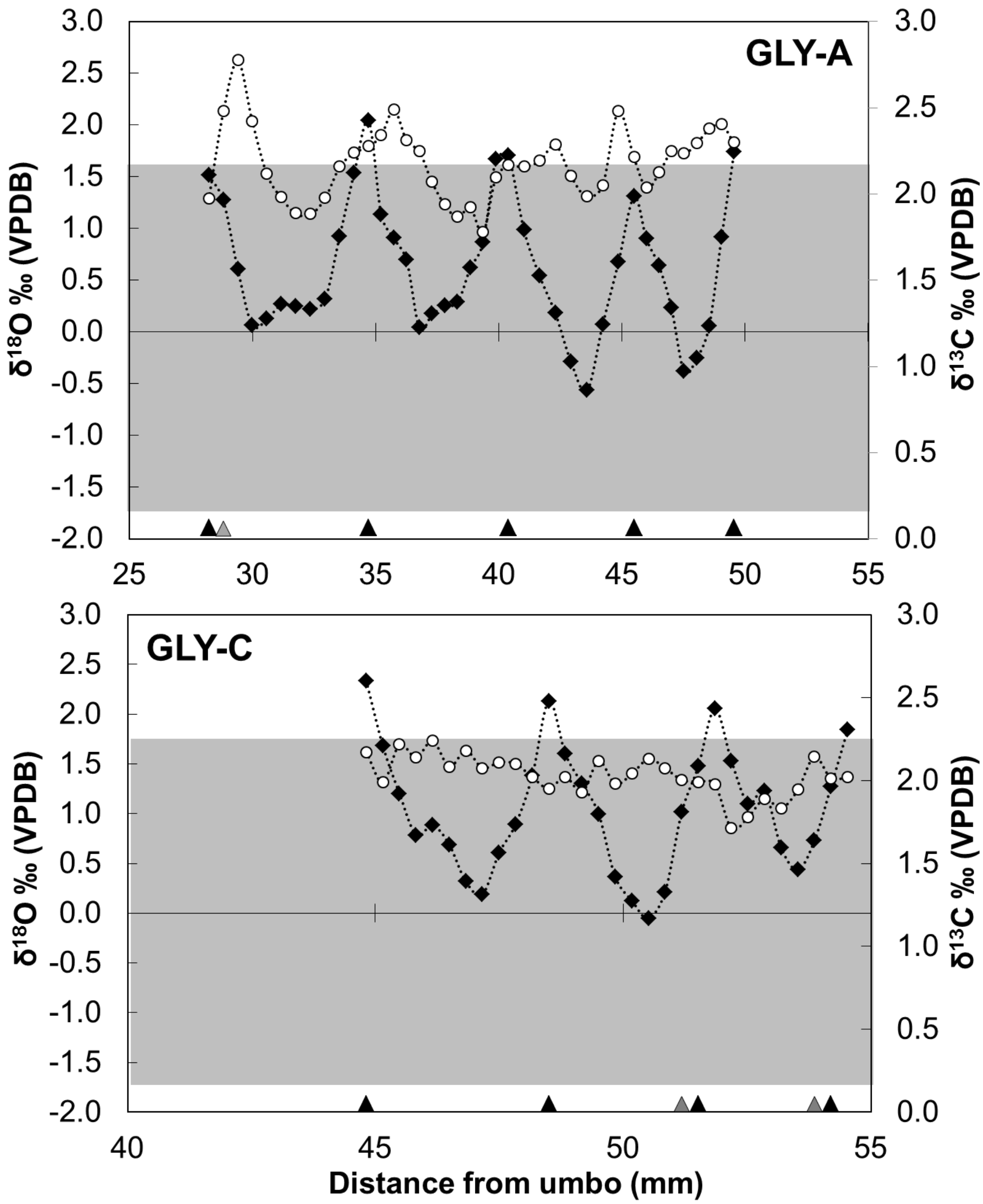

Figure 5.3 Variation of $\delta^{18}O$ (filled diamonds) and $\delta^{13}C$ (open circles) values (‰ VPDB) versus distance (in millimeters) from the umbo to the ventral edge in shells of *G. americana* (GLY-A & -C). Black triangles on the x-axis represent the location of prominent growth lines, and the gray triangles represent disturbance lines. The dark background area represents the range of $\delta^{18}O$ values previously published in Yorktown bivalves (from Williams et al., 2009).

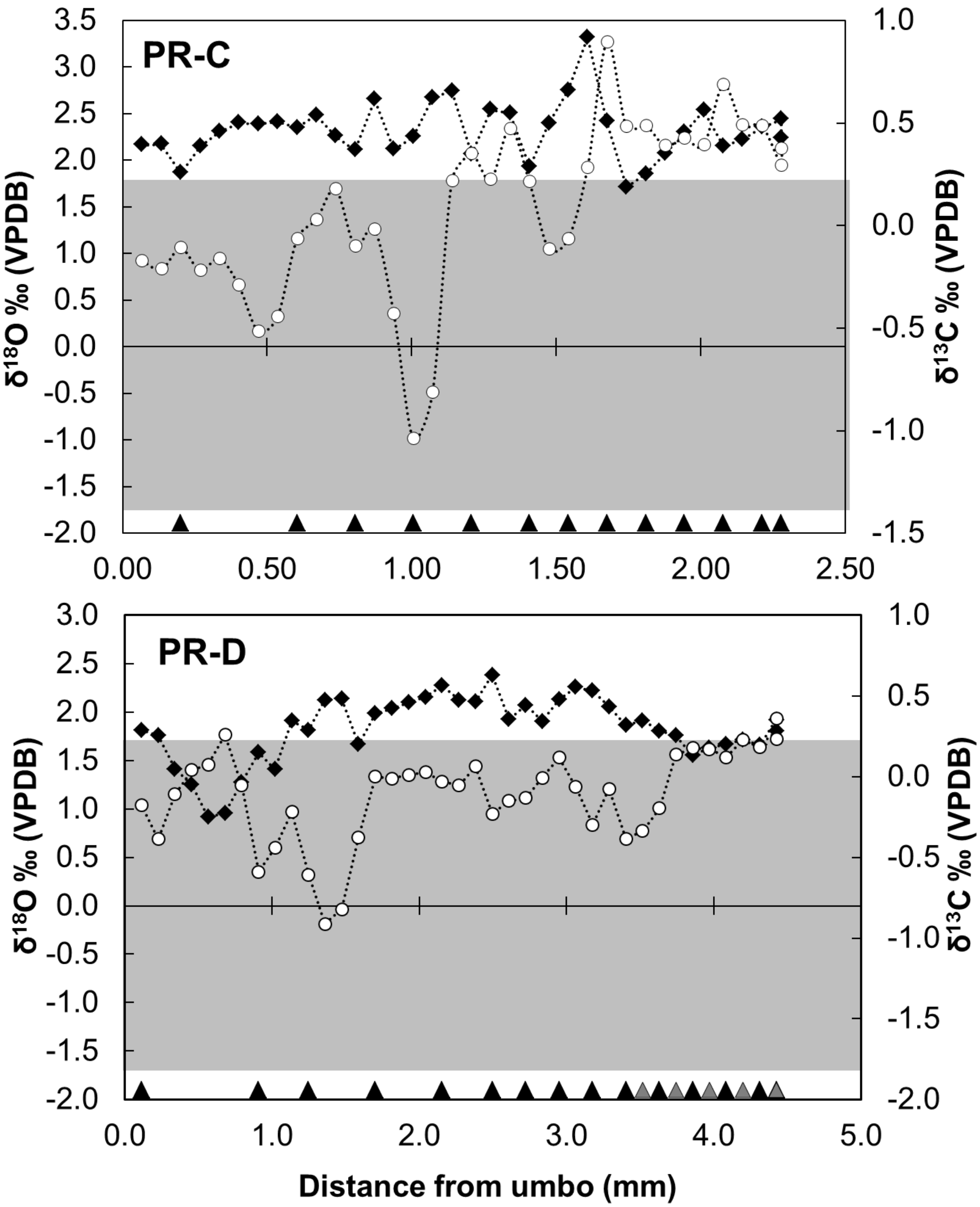

Figure 5.4 Variation of $\delta^{18}O$ (filled diamonds) and $\delta^{13}C$ (open circles) values (‰ VPDB) versus distance (in millimeters) from the umbo to the ventral edge in cardinal tooth of *P. reflexa* (PR-C & -D). Black triangles on the x-axis represent the location of prominent growth lines, and the gray triangles represent disturbance lines. The dark background area represents the range of $\delta^{18}O$ values previously published in Yorktown bivalves (from Williams et al., 2009).

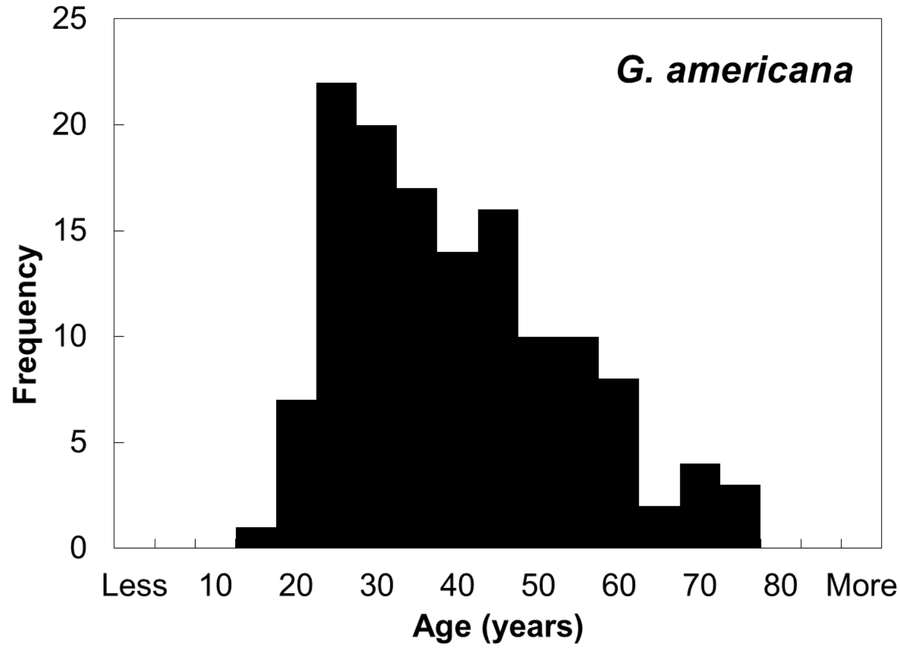

Figure 5.5 Histogram: Age versus frequency plot of Yorktown and Chowan River Formation *G. americana* populations (N=134).

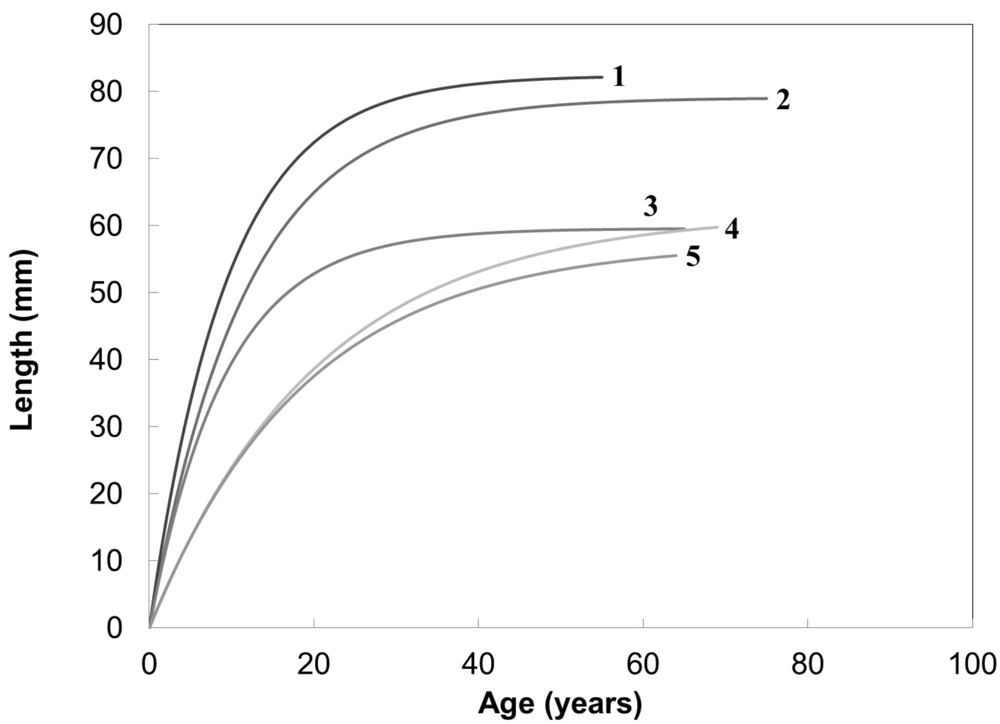

Figure 5.6 Growth model comparison: VGBM curves of Age (in years) versus expected Length (in millimeters). Curve (1) Yorktown Fm, (2) Chowan River Fm, (3) Duplin Fm (Thomas, 1970 curvature values), (4) Isle of Man, Port St. Mary, UK

(Steingrímsson, 1989), and (5) Isle of Man, Calf of Man, UK (Steingrímsson, 1989) populations.

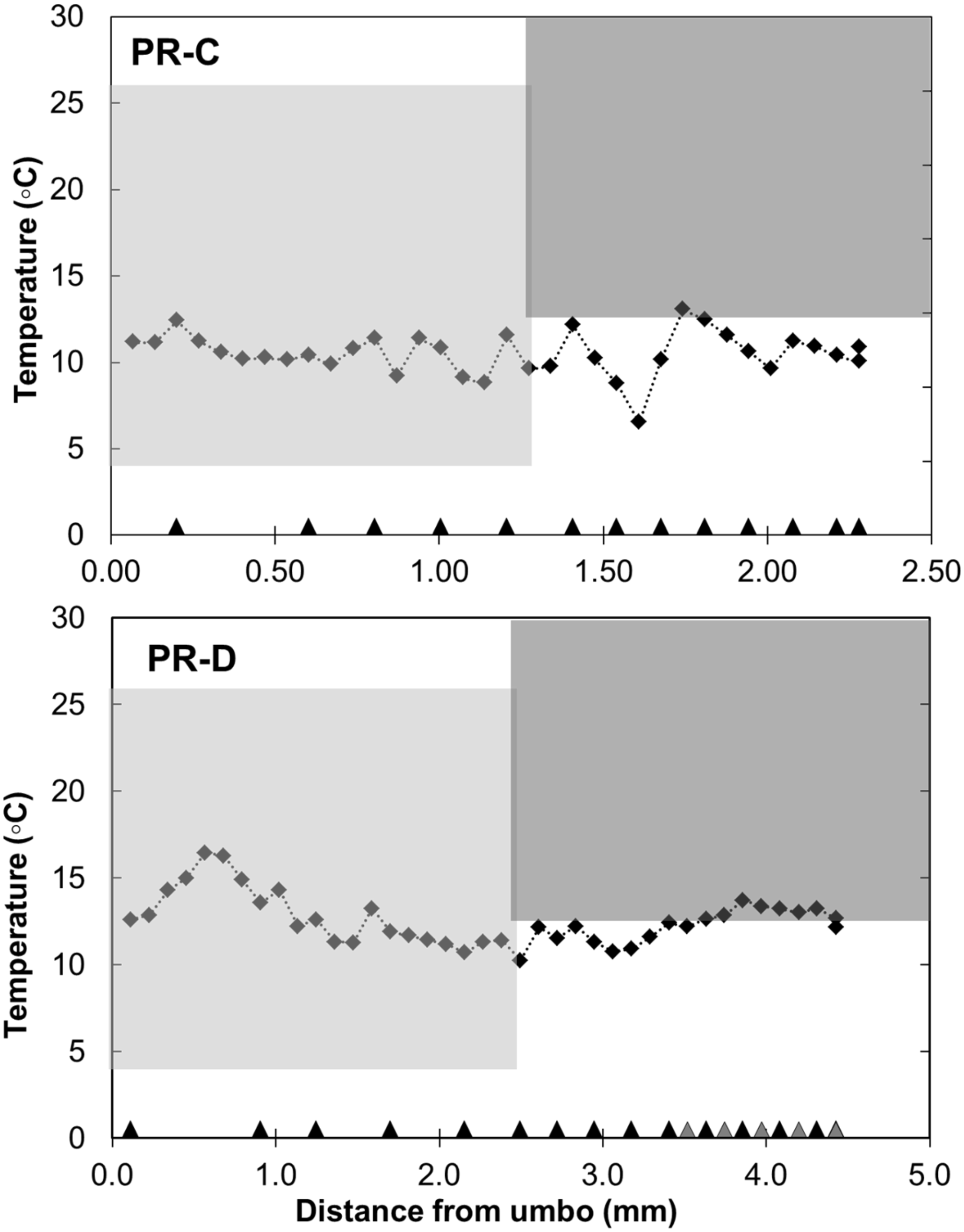

Figure 5.7 Temperature estimates (ºC) versus distance (in millimeters) from the umbo to the ventral edge of the cardinal tooth in *P. reflexa* (PR-C & -D) shells. Black triangles on the x-axis represent the location of prominent growth lines, and the gray triangles represent disturbance lines. The lighter highlighted background (on the left) represents the modern mean annual temperature range along the Virginia coast (NOAA station CHLV2). The darker highlighted background (on the

right represents) the currently accepted temperature range for the Pliocene Yorktown Formation based on multiple proxies (from Williams et al., 2009).

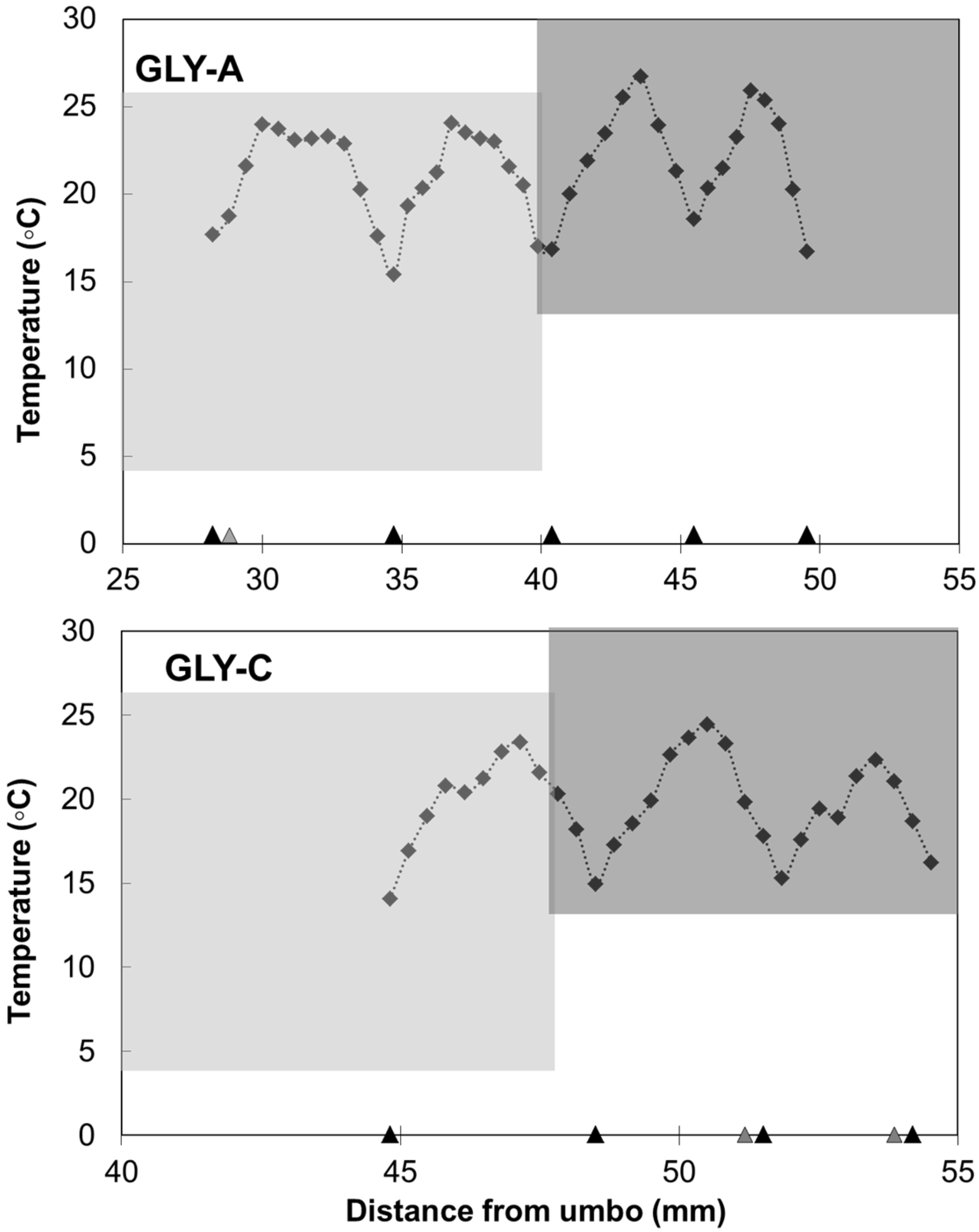

Figure 5.8 Temperature estimates (ºC) versus distance (in millimeters) from the umbo to the ventral edge of *G. americana* (GLY-A & -C) valves. Black triangles on the x-axis represent the location of prominent growth lines, and the gray triangles represent disturbance lines. The lighter highlighted background (on the left

represents) the modern mean annual temperature range along the Virginia coast (NOAA station CHLV2). The darker highlighted background (on the right) represents the currently accepted temperature range for the Pliocene Yorktown Formation based on multiple proxies (from Williams et al., 2009).

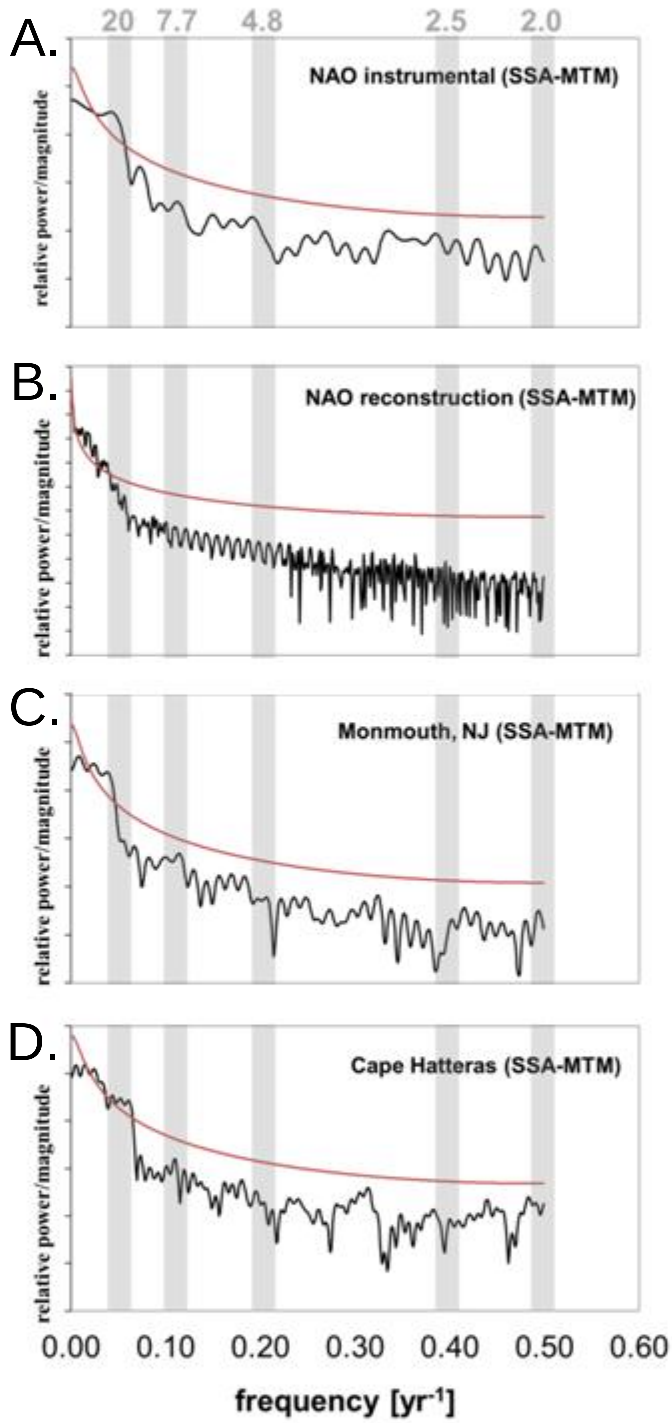

Figure 5.9 Spectral densities (black lines) for four time series as computed by the SSA-MTM method. (log_{10} y-axis scale versus frequency on the x-axis). (A)

Instrument record of winter NAO Index (1950-2011), (B) NAO Reconstruction (1049-1995) (Trouet et al., 2009), (C) Long Branch Oakhurst, New Jersey (1907-1997) NOAA-GHCN station, and (D) Cape Hatteras, North Carolina (1874-2005) NOAA-GHCN station. Gray bands with periodicities in years given at top indicate modern spectral power for NAO. Solid red line is the 95% significance level relative to the estimated red noise background.

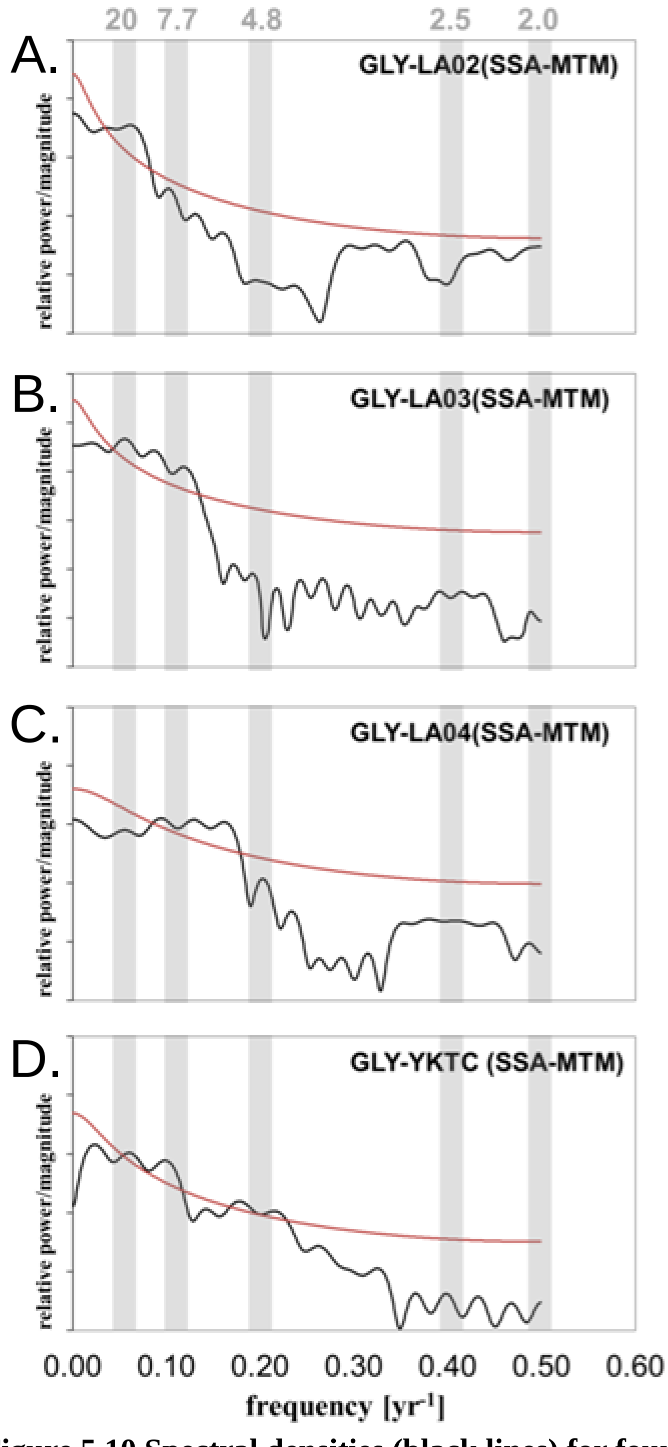

Figure 5.10 Spectral densities (black lines) for four SGI time series as computed by the SSA-MTM method. (log_{10} y-axis scale versus frequency on the x-axis). Panels (A-D) are SGIs of growth increments in fossil bivalve from the Yorktown Formation. Gray bands with periodicities in years given at top indicate modern spectral power for NAO. Solid red line is the 95% significance level relative to the estimated red noise background.

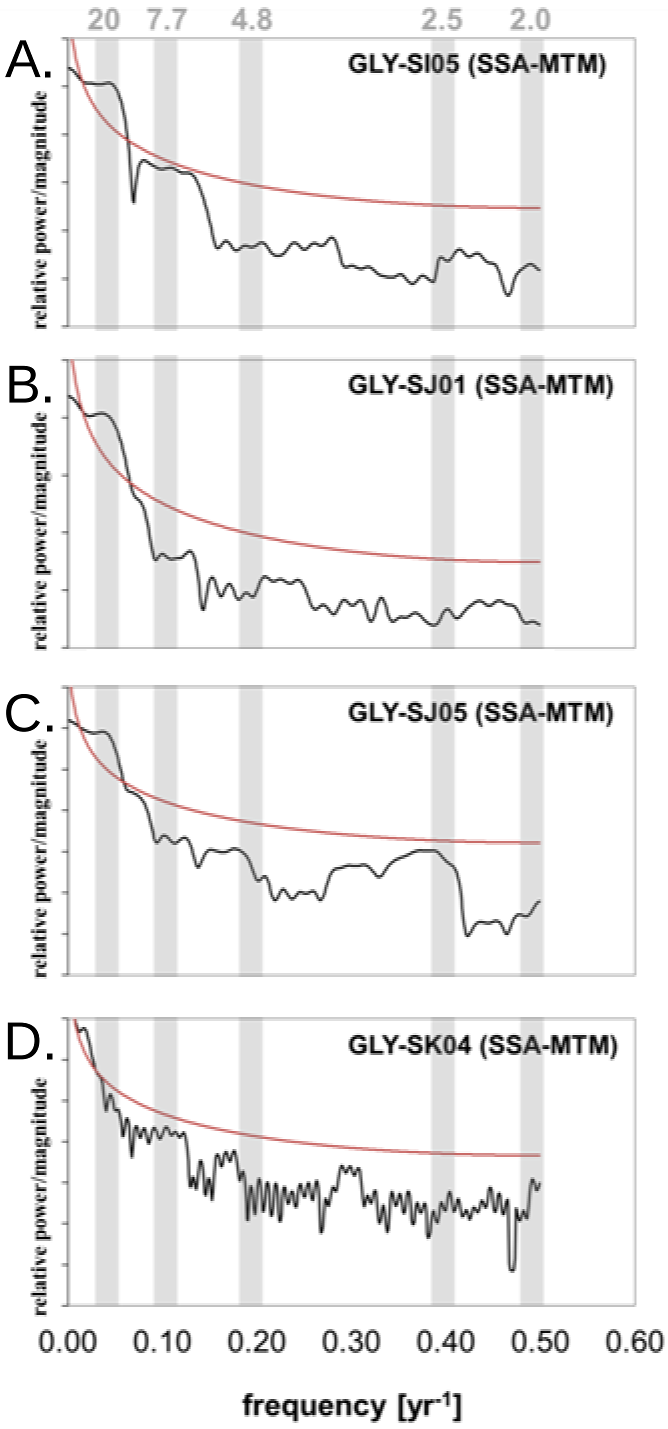

Figure 5.11 Spectral densities (black lines) for four time series as computed by the SSA-MTM method. (log_{10} y-axis scale versus frequency on the x-axis). Panels (A-D) are SGIs of growth increments in fossil bivalve from the Chowan River Formation. Gray bands with periodicities in years given at top indicate modern spectral power for NAO. Solid red line is the 95% significance level relative to the estimated red noise background.

APPENDIX A: SPISULA

Table 1. Data on live-collected *Hemimactra (Spisula) solidissima*. Data includes Unique Identification (UID), shell length (mm), width (mm), height (mm), valve, age counted through visual inspection of internal growth increments, date of harvest, NOAA-NEFSC Statistical Area, and location characteristics of latitude, longitude and ocean depth (m).

UID	Length (mm)	Width (mm)	Height (mm)	Valve	Age	Harvested	Area	Lat.	Long.	Depth (m)
001-01-94	115.48	152.88	38.80	LEFT	18	8/3/1994	613	4004.00	7239.00	57.0
001-02-94	106.17	140.55	35.67	LEFT	17	8/3/1994	613	4004.15	7239.02	57.0
001-03-94	124.47	164.77	41.82	LEFT	18	8/3/1994	613	4004.30	7239.03	57.0
033-08-94	124.72	165.11	41.90	LEFT	15	8/2/1994	612	4008.00	7359.00	20.5
033-09-94	117.07	154.97	39.33	LEFT	13	8/2/1994	612	4001.00	7401.00	20.5
033-23-94	120.43	159.42	40.46	LEFT	16	8/2/1994	612	4009.00	7357.00	20.5
120-11-94	78.00	103.25	26.20	LEFT	8	8/5/1994	625	3709.00	7531.00	17.5
161-01-94	108.22	143.26	36.36	LEFT	13	8/5/1994	632	3644.00	7457.00	35.0
162-01-94	85.95	113.78	28.88	LEFT	13	8/5/1994	632	3639.00	7447.00	61.0
162-02-94	106.78	141.35	35.87	LEFT	14	8/5/1994	632	3639.01	7447.01	61.0
162-03-94	102.46	135.64	34.42	LEFT	14	8/5/1994	632	3639.02	7447.02	61.0
162-04-94	82.89	109.73	27.85	LEFT	8	8/5/1994	632	3639.03	7447.03	61.0
162-4B-94	93.99	124.42	31.58	LEFT	11	8/5/1994	632	3639.04	7447.04	61.0
163-02-94	97.78	129.44	32.85	LEFT	14	8/5/1994	632	3644.00	7451.00	47.0
163-06-94	98.46	130.34	33.08	LEFT	11	8/5/1994	632	3654.00	7455.00	40.0

167-06-94	126.96	168.07	42.65	LEFT	13	8/5/1994	632	3654.01	7455.01	40.0
167-07-94	114.59	151.69	38.50	LEFT	14	8/5/1994	632	3654.02	7455.02	40.0
167-08-94	102.57	135.78	34.46	LEFT	13	8/5/1994	632	3654.03	7455.03	40.0
181-01-94	102.60	135.82	34.47	LEFT	17	8/5/1994	625	3706.00	7520.00	27.0
181-14-94	90.18	119.38	30.30	LEFT	13	8/5/1994	625	3706.00	7515.00	34.0
181-16-94	94.40	124.96	31.71	LEFT	13	8/5/1994	625	3703.00	7525.00	29.5
187-01-94	88.57	117.25	29.76	LEFT	10	8/5/1994	626	3708.00	7459.00	41.5
187-03-94	86.17	114.07	28.95	LEFT	11	8/5/1994	626	3719.00	7457.00	39.5
189-02-94	86.17	114.07	28.95	LEFT	12	8/5/1994	626	3725.00	7459.00	32.5
189-05-94	96.56	127.82	32.44	LEFT	12	8/5/1994	626	3723.00	7445.00	58.0
189-2B-94	118.96	157.48	39.97	LEFT	13	8/5/1994	626	3724.00	7451.00	44.0
190-01-94	109.38	144.79	36.75	LEFT	14	8/2/1994	615	3958.00	7351.00	24.5
305-01-94	111.02	146.96	37.30	LEFT	15	8/6/1994	621	3806.00	7434.00	39.0
305-02-94	86.66	114.71	29.11	LEFT	13	8/6/1994	621	3806.01	7434.01	39.0
305-03-94	109.79	145.34	36.88	LEFT	13	8/6/1994	621	3806.02	7434.02	39.0
305-04-94	107.21	141.92	36.02	LEFT	15	8/6/1994	621	3806.03	7434.03	39.0
311-02-94	120.45	159.45	40.47	LEFT	15	8/7/1994	621	3823.00	7426.00	42.5
311-05-94	91.92	121.68	30.88	LEFT	13	8/7/1994	621	3823.01	7426.01	42.5
311-06-94	121.07	160.27	40.68	LEFT	12	8/7/1994	621	3823.02	7426.02	42.5
323-01-94	116.06	153.64	38.99	LEFT	16	8/7/1994	622	3851.01	7345.01	46.5
323-04-94	92.27	122.14	31.00	LEFT	9	8/7/1994	622	3851.00	7345.00	46.5
004-05-97	103.79	137.40	34.87	LEFT	13	6/8/1997	612	4004.00	7351.00	27.0
005-01-97	90.38	119.65	30.37	LEFT	10	6/9/1997	612	4011.00	7356.00	15.0

005-12-97	117.19	155.13	39.37	LEFT	15	6/9/1997	612	4011.01	7356.01	22.5
041-01-97	133.75	177.05	44.93	LEFT	19	6/10/1997	614	3919.00	7417.00	19.0
048-01-97	98.18	129.97	32.99	LEFT	12	6/10/1997	614	3907.00	7426.00	19.0
048-03-97	111.16	147.15	37.34	LEFT	14	6/10/1997	614	3907.05	7426.05	23.0

UID	**Length (mm)**	**Width (mm)**	**Height (mm)**	**Valve**	**Age**	**Harvested**	**Area**	**Lat.**	**Long.**	**Depth (m)**
054-01-97	68.30	92.12	19.60	LEFT	5	6/10/1997	621	3844.18	7503.43	20.0
054-02-97	61.21	85.35	17.99	LEFT	5	6/10/1997	621	3844.28	7503.51	19.0
054-03-97	54.45	72.01	17.08	LEFT	4	6/10/1997	621	3844.38	7503.59	21.0
054-04-97	48.15	66.47	14.47	LEFT	3	6/10/1997	621	3844.48	7503.67	19.0
054-05-97	48.28	65.50	13.43	LEFT	3	6/10/1997	621	3844.58	7503.75	18.0
072-01-97	91.03	120.51	30.58	LEFT	9	6/16/1997	613	4058.01	7201.00	22.0
072-02-97	107.63	142.48	36.16	LEFT	12	6/16/1997	613	4058.00	7200.00	18.0
108-03-97	107.69	142.56	36.18	LEFT	11	6/19/1997	615	3926.00	7332.00	35.5
119-01-97	107.10	141.78	35.98	LEFT	10	6/19/1997	621	3843.00	7424.00	32.5
119-01-97	111.76	148.48	30.91	LEFT	11	6/19/1997	621	3843.01	7424.01	32.0
119-03-97	97.98	125.15	25.01	RIGHT	9	6/19/1997	621	3843.02	7424.02	31.5
119-04-97	109.33	142.96	27.91	LEFT	11	6/19/1997	621	3843.03	7424.03	31.0
119-06-97	112.63	151.66	28.84	LEFT	11	6/19/1997	621	3843.04	7424.04	30.5
119-07-97	111.03	154.83	30.58	RIGHT	11	6/19/1997	621	3843.05	7424.05	30.0
123-01-97	56.18	75.45	16.50	RIGHT	4	6/19/1997	621	3843.00	7354.00	47.5
123-02-97	73.06	98.40	21.74	LEFT	6	6/19/1997	621	3843.01	7354.01	47.0
123-04-	74.08	98.0	22.89	LEFT	6	6/19/19	621	3843.	7354.	46.5

97		2				97		02	02	
123-05-		11.5				6/19/19		3843.	7354.	
97	89.00	2	22.36	LEFT	8	97	621	03	03	46.0
123-06-		105.				6/19/19		3843.	7354.	
97	80.60	51	19.85	LEFT	7	97	621	04	04	45.5
123-07-		96.7				6/19/19		3843.	7354.	
97	73.93	2	21.44	LEFT	6	97	621	05	05	45.0
123-08-		96.5				6/19/19		3843.	7354.	
97	73.49	8	20.20	LEFT	6	97	621	06	06	44.5
123-09-		78.9				6/19/19		3843.	7354.	
97	63.41	6	17.90	LEFT	5	97	621	07	07	44.0
128-01-		100.				6/20/19		3821.	7413.	
97	78.92	08	20.62	LEFT	6	97	621	00	00	55.0
128-02-		96.2		RIG		6/20/19		3821.	7413.	
97	75.64	3	18.38	HT	6	97	621	03	03	55.5
128-03-		102.				6/20/19		3821.	7413.	
97	79.24	38	22.92	LEFT	6	97	621	05	05	55.0
129-01-		102.		RIG		6/20/19		3824.	7421.	
97	79.37	75	21.80	HT	6	97	621	02	02	45.5
129-02-	126.4	167.				6/20/19		3824.	7421.	
97	5	39	42.48	LEFT	18	97	621	00	00	45.0
129-02-	122.2	165.				6/20/19		3824.	7421.	
97	7	71	36.35	LEFT	13	97	621	04	04	44.5
129-03-	106.0	140.				6/20/19		3824.	7421.	
97	6	13	32.17	LEFT	10	97	621	06	06	44.0
129-04-		100.				6/20/19		3824.	7421.	
97	76.09	43	30.43	LEFT	6	97	621	10	10	43.0
129-07-	105.5	138.				6/20/19		3824.	7421.	
97	0	31	32.21	LEFT	10	97	621	08	08	46.0
154-02-	144.5	191.				6/21/19		3739.	7501.	
97	5	35	48.56	LEFT	19	97	625	00	00	32.0
155-03-		126.				6/21/19		3734.	7455.	
97	95.88	93	32.21	LEFT	11	97	626	00	00	32.0
164-04-	109.2	144.				6/21/19		3731.	7506.	
97	8	66	36.71	LEFT	19	97	625	00	00	28.5
165-05-	125.4	166.				6/21/19		3736.	7508.	
97	5	07	42.15	LEFT	20	97	625	00	00	27.0
165-06-	100.4	132.				6/21/19		3736.	7508.	
97	1	92	33.73	LEFT	12	97	625	05	05	28.0
233-02-		125.				6/24/19		3625.	7539.	
97	94.63	27	31.79	LEFT	14	97	631	00	00	24.0
255-01-	106.4	140.				6/25/19		3644.	7451.	
97	8	95	35.77	LEFT	15	97	632	00	00	46.0
255-01-		135.				6/25/19		3644.	7451.	
97	93.80	20	27.33	LEFT	8	97	632	00	00	47.0
255-02-	113.4	150.	38.11	LEFT	14	6/25/19	632	3644.	7451.	47.0

97	2	15				97		03	03	
255-02-97	87.65	119.45	23.63	LEFT	7	6/25/1997	632	3644.02	7451.02	46.5
255-03-97	99.97	132.35	33.59	LEFT	13	6/25/1997	632	3644.05	7451.05	48.0
255-03-97	94.11	125.43	25.31	LEFT	8	6/25/1997	632	3644.04	7451.04	47.5
255-04-97	67.33	91.89	21.11	LEFT	5	6/25/1997	632	3644.06	7451.06	46.0
255-05-97	66.48	90.96	18.89	LEFT	5	6/25/1997	632	3644.08	7451.08	48.0
255-06-97	57.91	77.80	18.44	LEFT	4	6/25/1997	632	3644.10	7451.10	47.0
255-07-97	62.79	82.08	17.40	RIGHT	5	6/25/1997	632	3644.12	7451.12	46.5
255-08-97	55.18	73.70	15.30	LEFT	4	6/25/1997	632	3644.14	7451.14	47.0
255-09-97	55.45	74.56	15.80	LEFT	4	6/25/1997	632	3644.16	7451.16	47.0

UID	**Length (mm)**	**Width (mm)**	**Height (mm)**	**Valve**	**Age**	**Harvested**	**Area**	**Lat.**	**Long.**	**Depth (m)**
275-04-97	116.94	154.81	39.29	LEFT	17	6/26/1997	626	3754.05	7446.05	34.0
276-01-97	134.04	182.29	36.18	LEFT	17	6/26/1997	626	3759.10	7445.50	30.0
276-02-97	136.62	185.92	33.12	LEFT	18	6/26/1997	626	3759.08	7445.25	31.0
276-03-97	77.86	102.80	19.90	RIGHT	6	6/26/1997	626	3759.00	7444.00	30.0
276-04-97	128.49	174.47	33.95	LEFT	15	6/26/1997	626	3759.06	7445.00	30.0
276-05-97	102.48	135.66	34.43	LEFT	12	6/26/1997	626	3759.00	7445.00	29.0
276-05-97	132.61	180.27	34.08	LEFT	16	6/26/1997	626	3759.04	7444.75	31.5
276-06-97	111.52	147.63	37.47	LEFT	13	6/26/1997	626	3759.05	7444.00	31.0
276-06-97	113.14	146.21	32.36	LEFT	12	6/26/1997	626	3759.02	7444.50	30.5
009-01-99	84.85	112.32	28.51	LEFT	9	6/4/1999	612	4036.35	7302.50	21.5
011-01-99	111.15	147.14	37.34	LEFT	14	6/4/1999	612	4031.03	7342.32	20.0

019-07-99	90.91	120.34	30.54	LEFT	8	6/4/1999	612	4031.07	7342.37	21.0
021-01-99	94.79	125.48	31.84	LEFT	10	6/5/1999	614	3941.29	7400.02	20.0
022-03-99	121.93	161.41	40.96	LEFT	16	6/5/1999	614	3941.15	7404.66	16.0
034-04-99	124.52	164.83	41.83	LEFT	17	6/5/1999	614	3918.78	7416.78	17.5
123-01-99	116.38	154.07	39.10	LEFT	14	6/9/1999	622	3853.66	7358.63	43.5
125-06-99	107.95	142.91	36.27	LEFT	13	6/9/1999	614	3901.24	7422.82	26.5
210-01-99	112.92	149.48	37.94	LEFT	19	7/7/1999	614	3901.17	7444.64	14.0
284-01-99	93.71	124.06	31.48	LEFT	10	6/26/1999	625	3723.63	7514.82	28.5
295-05-99	114.73	151.89	38.55	LEFT	12	6/26/1999	625	3708.96	7519.25	29.5
305-02-99	113.75	150.58	38.22	LEFT	12	6/27/1999	631	3646.01	7504.06	29.0
306-03-99	114.39	151.42	38.43	LEFT	16	6/27/1999	631	3646.05	7504.09	34.0
306-04-99	99.82	132.14	33.54	LEFT	9	6/27/1999	631	3646.15	7504.19	35.0
307-02-99	112.09	148.38	37.66	LEFT	15	6/27/1999	631	3646.20	7504.20	36.0
307-03-99	77.76	102.93	26.12	LEFT	9	6/27/1999	631	3646.25	7504.21	35.0
310-01-99	114.91	152.12	38.61	LEFT	15	6/27/1999	632	3653.81	7458.36	35.0
310-02-99	120.37	159.34	40.44	LEFT	13	6/27/1999	632	3653.86	7458.42	36.0
323-01-99	123.20	163.09	41.39	LEFT	14	6/27/1999	632	3654.86	7458.90	37.0
413-26-99	119.06	157.62	40.00	LEFT	19	7/9/1999	625	3741.09	7502.86	26.5
413-38-99	120.88	160.02	40.61	LEFT	18	7/9/1999	625	3736.12	7500.78	25.5
413-57-99	134.95	178.65	45.34	LEFT	20	7/9/1999	625	3736.03	7511.04	28.0
421-13-99	96.70	128.01	32.49	LEFT	8	7/9/1999	626	3713.86	7452.26	49.0
421-14-99	84.49	111.84	28.38	LEFT	6	7/9/1999	626	3713.08	7452.44	49.0
432-08-99	95.33	126.20	32.03	LEFT	11	7/10/1999	626	3726.34	7442.72	52.5

432-15-99	82.40	109.08	27.68	LEFT	10	7/10/1999	626	3726.04	7442.54	52.5
015-01-02	101.88	134.86	34.23	LEFT	12	6/4/2002	613	4047.85	7229.42	24.0
015-01-02	123.27	155.87	28.06	LEFT	14	6/4/2002	613	4047.79	7229.55	25.0
015-02-02	90.65	122.57	19.89	LEFT	8	6/4/2002	613	4047.79	7229.55	25.0
018-14-02	62.33	85.88	18.87	RIGHT	5	7/7/2002	613	4041.22	7240.31	31.0
019-01-02	117.65	154.89	27.44	LEFT	12	6/4/2002	613	4036.38	7258.21	26.0
019-02-02	129.03	170.81	43.35	LEFT	18	6/4/2002	613	4036.21	7257.20	23.5
019-02-02	144.42	196.91	33.68	LEFT	21	6/4/2002	613	4036.27	7257.54	24.0
019-06-02	117.84	159.47	31.33	LEFT	12	6/4/2002	613	4036.35	7258.04	24.0
019-07-02	113.19	149.84	38.03	LEFT	17	6/4/2002	613	4036.24	7257.37	24.5
019-07-02	134.13	182.42	33.51	LEFT	17	6/4/2002	613	4036.30	7257.71	25.0
019-09-02	83.39	114.68	23.32	LEFT	7	6/4/2002	613	4036.41	7258.38	24.0
019-10-02	111.28	145.50	26.98	LEFT	11	6/4/2002	613	4036.32	7257.87	23.0
019-11-02	69.64	94.88	17.40	RIGHT	5	6/4/2002	613	4036.44	7258.55	25.0
059-01-02	123.79	167.85	32.24	LEFT	14	6/6/2002	615	3951.05	7350.53	25.0

UID	**Length (mm)**	**Width (mm)**	**Height (mm)**	**Valve**	**Age**	**Harvested**	**Area**	**Lat.**	**Long.**	**Depth (m)**
059-03-02	123.48	154.93	31.41	LEFT	14	6/6/2002	615	3951.04	7350.52	25.5
059-04-02	89.72	123.14	24.94	LEFT	8	6/6/2002	615	3951.03	7350.52	24.5
059-05-02	108.65	143.32	29.93	LEFT	11	6/6/2002	615	3951.03	7350.51	24.5
059-06-02	111.04	132.01	29.61	LEFT	11	6/6/2002	615	3951.02	7350.51	25.5
059-07-02	74.58	99.03	20.91	LEFT	6	6/6/2002	615	3951.02	7350.50	25.0
059-08-	82.81	110.	19.31	LEFT	7	6/6/200	615	3951.	7350.	25.0

02		13				2		01	49	
059-09-02	65.16	89.21	15.98	LEFT	5	6/6/2002	615	3951.01	7350.49	25.0
059-10-02	63.02	85.40	17.51	LEFT	5	6/6/2002	615	3951.00	7350.48	25.0
060-01-02	127.63	173.26	32.15	LEFT	15	6/6/2002	615	3948.66	7346.93	28.0
060-01-02	133.92	177.28	44.99	LEFT	18	6/6/2002	615	3948.66	7346.93	28.0
060-02-02	117.84	144.56	30.87	LEFT	12	6/6/2002	615	3948.65	7346.92	28.5
060-03-02	120.15	154.92	31.40	LEFT	13	6/6/2002	615	3948.64	7346.91	27.5
060-04-02	59.35	84.69	17.84	LEFT	4	6/6/2002	615	3948.63	7346.90	28.0
060-05-02	93.97	122.36	25.93	LEFT	8	6/6/2002	615	3948.62	7346.89	28.0
060-06-02	80.92	105.19	21.67	LEFT	7	6/6/2002	615	3948.61	7346.87	28.5
060-07-02	70.78	97.77	20.82	LEFT	6	6/6/2002	615	3948.60	7346.86	27.5
060-08-02	125.02	169.58	35.42	RIGHT	14	6/6/2002	615	3948.59	7346.85	28.0
060-09-02	77.57	105.35	22.55	RIGHT	6	6/8/2002	615	3948.57	7346.84	27.0
062-01-02	134.84	183.42	33.47	LEFT	17	6/6/2002	615	3941.43	7346.92	18.0
062-02-02	111.26	151.18	26.84	LEFT	11	6/6/2002	615	3941.44	7346.94	19.0
062-03-02	93.05	133.63	22.75	LEFT	8	6/6/2002	615	3941.46	7346.95	17.0
062-04-02	58.23	78.20	13.50	LEFT	4	6/6/2002	615	3941.47	7346.96	18.0
062-05-02	93.47	129.73	21.50	LEFT	8	6/6/2002	615	3941.48	7346.97	19.0
062-06-02	92.76	126.83	21.98	LEFT	8	6/6/2002	615	3941.49	7346.99	17.0
062-07-02	131.76	179.08	32.31	LEFT	16	6/6/2002	615	3941.51	7347.00	18.0
062-08-02	109.71	133.47	28.91	LEFT	11	6/6/2002	615	3941.52	7347.01	19.0
062-09-02	135.41	184.22	35.23	LEFT	17	6/6/2002	615	3941.53	7347.02	17.0
062-10-02	81.61	115.84	20.75	LEFT	7	6/6/2002	615	3941.54	7347.04	18.0
062-11-	76.92	101.	20.01	LEFT	6	6/6/200	615	3941.	7347.	19.0

02		58				2		55	05	
077-01-02	140.83	153.19	34.72	LEFT	19	6/8/2002	614	3930.91	7407.28	17.0
077-01-02	132.68	175.63	44.57	LEFT	15	6/7/2002	614	3930.98	7407.13	16.5
077-02-02	113.38	151.42	31.61	LEFT	12	6/8/2002	614	3929.56	7405.93	18.0
077-03-02	120.41	163.09	33.52	LEFT	13	6/8/2002	614	3928.20	7404.57	19.0
077-05-02	88.31	122.94	29.18	LEFT	8	6/13/2002	614	3926.85	7403.21	20.0
078-01-02	125.71	170.56	34.52	LEFT	14	6/8/2002	614	3925.49	7401.86	21.0
078-01-02	132.16	174.95	44.40	LEFT	20	6/7/2002	614	3930.95	7407.20	17.0
078-02-02	130.36	177.11	33.31	LEFT	16	6/8/2002	614	3924.14	7400.50	22.0
078-02-02	149.31	197.66	50.16	LEFT	23	6/7/2002	614	3930.91	7407.28	17.5
078-03-02	122.11	153.23	32.72	LEFT	13	6/8/2002	614	3922.78	7399.15	23.0
078-04-02	101.24	131.01	26.25	LEFT	9	6/8/2002	614	3921.43	7397.79	24.0
078-05-02	126.55	171.74	30.92	LEFT	15	6/8/2002	614	3920.07	7396.44	25.0
078-06-02	88.76	122.91	21.06	RIGHT	8	6/8/2002	614	3918.72	7395.08	26.0
078-07-02	80.60	113.06	20.94	RIGHT	7	6/8/2002	614	3917.36	7393.73	27.0
078-08-02	106.52	140.62	28.44	LEFT	10	6/8/2002	614	3916.01	7392.37	29.0
200-01-02	104.72	137.60	25.61	LEFT	10	6/12/2002	621	3841.22	7424.33	40.0
200-01-02	112.67	149.16	37.85	LEFT	13	6/12/2002	621	3841.22	7424.33	31.0
200-02-02	132.27	179.80	31.77	LEFT	16	6/12/2002	621	3842.32	7425.42	40.0
200-03-02	114.45	154.70	27.34	LEFT	12	6/12/2002	621	3843.41	7426.52	39.0
200-04-02	75.28	99.45	16.86	RIGHT	6	6/12/2002	621	3844.51	7427.61	38.0
UID	**Length (mm)**	**Width (mm)**	**Height (mm)**	**Valve**	**Age**	**Harvested**	**Area**	**Lat.**	**Long.**	**Depth (m)**

200-06-02	45.08	60.10	12.02	LEFT	3	6/12/2002	621	3846.69	7429.80	35.0
200-07-02	124.27	168.53	22.68	LEFT	14	6/12/2002	621	3847.79	7430.90	33.0
200-08-02	78.29	103.77	13.65	LEFT	6	6/12/2002	621	3848.88	7431.99	31.0
202-01-02	121.49	137.28	23.88	LEFT	13	6/12/2002	621	3849.00	7426.68	22.0
202-02-02	140.19	190.95	30.57	LEFT	19	6/12/2002	621	3849.00	7426.68	22.0
202-03-02	126.21	171.26	26.25	LEFT	14	6/12/2002	621	3849.00	7426.68	22.0
202-03-02	103.55	137.08	34.79	LEFT	14	6/12/2002	621	3849.00	7426.67	22.0
202-04-02	130.04	176.65	31.68	LEFT	16	6/12/2002	621	3849.00	7426.67	22.0
202-06-02	80.56	110.72	16.82	LEFT	7	6/12/2002	621	3849.00	7426.67	22.0
202-07-02	68.09	94.41	12.66	LEFT	5	6/12/2002	621	3849.00	7426.67	22.0
227-01-02	100.75	128.09	24.13	LEFT	9	6/13/2002	615	3933.73	7333.04	36.0
227-02-02	105.44	136.23	28.40	LEFT	10	6/13/2002	615	3933.72	7333.03	36.5
227-03-02	119.34	150.73	29.81	LEFT	13	6/13/2002	615	3933.71	7333.02	35.0
227-03-02	130.28	172.46	43.77	LEFT	17	6/13/2002	615	3933.73	7333.04	36.0
227-04-02	69.98	89.19	18.66	RIGHT	5	6/13/2002	615	3933.70	7333.01	36.0
227-05-02	94.35	126.63	27.60	RIGHT	8	6/13/2002	615	3933.69	7332.99	36.0
227-05-02	103.17	136.57	34.66	LEFT	12	6/13/2002	615	3933.69	7333.19	36.0
228-01-02	98.81	131.75	26.35	LEFT	9	6/13/2002	615	3933.11	7323.84	33.0
228-02-02	128.57	174.58	29.45	LEFT	15	6/13/2002	615	3933.10	7323.83	33.5
228-02-02	112.22	148.56	37.70	LEFT	15	6/13/2002	615	3933.11	7323.84	33.0
228-06-02	50.06	66.75	13.35	LEFT	4	6/13/2002	615	3933.10	7323.82	32.5
228-07-02	95.44	127.25	25.45	LEFT	9	6/13/2002	615	3933.09	7323.82	33.0
228-08-02	134.08	182.35	32.25	RIGHT	17	6/13/2002	615	3933.08	7323.81	32.5

228-09-02	110.81	138.59	27.28	LEFT	11	6/13/2002	615	3933.08	7323.81	33.5
228-10-02	87.28	116.87	19.85	LEFT	7	6/13/2002	615	3933.07	7323.80	33.0
228-11-02	48.98	65.30	13.06	LEFT	3	6/13/2002	615	3933.06	7323.79	33.0
229-01-02	86.65	117.49	22.46	LEFT	7	6/13/2002	615	3934.95	7325.68	41.0
229-02-02	76.81	100.96	18.96	LEFT	6	6/13/2002	615	3936.83	7327.56	41.5
229-03-02	79.14	107.21	21.11	RIGHT	6	6/13/2002	615	3938.71	7329.44	40.5
229-04-02	74.85	99.80	19.96	RIGHT	6	6/13/2002	615	3940.59	7331.32	41.0
229-05-02	115.13	143.65	26.88	LEFT	12	6/13/2002	615	3942.48	7333.21	41.5
229-06-02	56.68	77.63	15.61	LEFT	4	6/13/2002	615	3944.36	7335.09	40.5
229-07-02	113.71	140.60	28.06	RIGHT	12	6/13/2002	615	3946.24	7336.97	41.0
229-08-02	54.71	69.41	15.72	LEFT	4	6/13/2002	615	3948.13	7338.85	41.5
229-09-02	115.66	151.50	27.84	RIGHT	12	6/13/2002	615	3950.01	7340.74	40.5
229-10-02	127.71	173.37	29.51	LEFT	15	6/13/2002	615	3951.89	7342.62	41.0
229-10-02	121.21	160.46	40.72	LEFT	19	6/13/2002	615	3933.06	7323.99	34.0
229-11-02	48.08	65.02	12.92	LEFT	3	6/13/2002	615	3953.77	7344.50	41.0
260-02-02	109.17	174.62	28.76	LEFT	11	6/20/2002	621	3816.02	7438.48	32.0
260-03-02	123.49	167.43	27.92	LEFT	14	6/20/2002	621	3816.02	7438.48	32.0
260-03-02	114.55	151.65	38.49	LEFT	14	6/20/2002	621	3816.13	7438.52	32.0
260-04-02	102.99	138.56	24.77	LEFT	10	6/20/2002	621	3816.02	7438.48	32.0
260-05-02	111.36	152.87	23.35	LEFT	11	6/20/2002	621	3816.02	7438.48	32.0
260-06-02	91.08	121.78	21.64	LEFT	8	6/20/2002	621	3816.02	7438.48	32.0
262-01-02	113.90	153.71	24.24	LEFT	12	6/20/2002	621	3806.13	7434.74	35.0
262-02-02	106.24	139.60	21.25	LEFT	10	6/20/2002	621	3806.13	7434.74	35.0

262-04-02	81.80	106.33	16.77	LEFT	7	6/20/2002	621	3806.13	7434.74	35.0
262-05-02	97.60	127.83	21.33	LEFT	9	6/20/2002	621	3806.13	7434.74	35.0
283-01-02	119.08	150.02	27.59	RIGHT	13	6/21/2002	625	3746.20	7500.68	28.0

UID	**Length (mm)**	**Width (mm)**	**Height (mm)**	**Valve**	**Age**	**Harvested**	**Area**	**Lat.**	**Long.**	**Depth (m)**
283-03-02	104.12	131.23	25.42	LEFT	10	6/21/2002	625	3746.18	7500.66	28.5
283-04-02	106.56	137.95	26.41	LEFT	10	6/21/2002	625	3746.16	7500.64	29.0
283-04-02	104.62	138.49	35.15	LEFT	17	6/21/2002	625	3746.20	7500.68	27.5
283-05-02	117.57	152.82	27.58	LEFT	12	6/21/2002	625	3746.15	7500.63	28.0
283-05-02	113.15	149.79	38.02	LEFT	14	6/21/2002	625	3746.18	7500.62	28.0
283-06-02	101.25	134.04	34.02	LEFT	11	6/21/2002	625	3746.15	7500.59	28.5
290-01-02	99.78	135.37	25.23	LEFT	9	6/21/2002	625	3736.19	7500.59	16.0
290-02-02	52.50	71.84	11.19	RIGHT	4	6/21/2002	625	3736.19	7500.59	16.0
290-03-02	57.31	81.00	14.51	RIGHT	4	6/21/2002	631	3736.19	7500.59	16.0
319-01-02	102.69	139.87	24.74	LEFT	10	6/23/2002	631	3653.93	7522.35	28.0
319-02-02	113.28	144.17	23.88	LEFT	12	6/23/2002	631	3653.93	7522.35	28.0
319-02-02	127.91	169.33	42.97	LEFT	18	6/23/2002	631	3653.91	7522.21	28.0
331-01-02	79.53	110.33	21.78	LEFT	6	6/24/2002	632	3633.65	7450.63	45.0
331-01-02	117.64	155.73	39.52	LEFT	11	6/24/2002	632	3633.65	7450.63	45.0
331-02-02	74.00	101.15	18.95	LEFT	6	6/24/2002	632	3633.62	7450.60	45.5
331-03-02	64.53	85.73	14.42	LEFT	5	6/24/2002	632	3633.59	7450.57	46.0
331-04-02	39.21	51.96	9.75	LEFT	3	6/24/2002	632	3633.56	7450.54	45.0
334-01-	89.48	119.	18.98	LEFT	8	6/24/20	632	3643.	7450.	46.0

02		64				02		90	70	
334-01-02	71.70	94.92	24.09	LEFT	10	6/24/2002	632	3643.94	7450.74	46.0
334-02-02	83.33	110.85	19.10	LEFT	7	6/24/2002	632	3643.91	7450.71	46.0
334-02-02	98.01	129.75	32.93	LEFT	8	6/24/2002	632	3643.93	7450.73	46.0
334-03-02	78.31	101.43	17.69	LEFT	6	6/24/2002	632	3643.92	7450.72	46.0
340-01-02	52.77	72.27	9.62	LEFT	4	6/25/2002	631	3643.66	7504.88	27.0
340-02-02	58.26	82.84	11.43	LEFT	4	6/25/2002	631	3643.66	7504.88	27.0
340-03-02	63.83	87.15	11.81	LEFT	5	6/25/2002	631	3643.66	7504.88	27.0
340-04-02	59.59	81.41	11.34	LEFT	4	6/25/2002	631	3643.66	7504.88	27.0
340-05-02	70.77	98.15	13.99	LEFT	6	6/25/2002	631	3643.66	7504.88	27.0
340-06-02	84.51	112.32	17.14	LEFT	7	6/25/2002	631	3643.66	7504.88	27.0
340-07-02	92.62	121.32	19.37	LEFT	9	6/25/2002	631	3643.66	7504.88	27.0
340-07-02	92.62	121.32	19.37	LEFT	9	6/25/2002	631	3643.66	7504.88	27.0
340-08-02	96.12	121.91	21.77	LEFT	9	6/25/2002	631	3643.66	7504.88	27.0
340-09-02	102.95	138.50	21.70	LEFT	10	6/25/2002	631	3643.66	7504.88	27.0
340-10-02	108.87	144.12	23.54	LEFT	10	6/25/2002	631	3643.66	7504.88	27.0
340-10-02	108.87	144.12	23.54	LEFT	10	6/25/2002	631	3643.66	7504.88	27.0
346-01-02	112.44	150.02	22.66	LEFT	11	6/25/2002	631	3651.15	7502.66	31.0
346-02-02	100.00	129.59	20.85	LEFT	9	6/25/2002	631	3651.15	7502.66	31.0
346-02-02	100.55	133.11	33.78	LEFT	11	6/25/2002	631	3651.28	7502.66	31.0
356-04-02	99.76	132.06	33.52	LEFT	12	6/25/2002	626	3703.77	7452.70	49.0
356-26-02	98.29	130.11	33.02	LEFT	14	6/25/2002	626	3703.79	7452.57	48.0
356-01-02	71.42	97.35	18.73	LEFT	6	6/25/2002	631	3707.57	7456.35	47.0
356-02-	86.38	110.	21.43	LEFT	7	6/25/20	631	3706.	7455.	47.0

02		01				02		31	09	
356-03-02	96.07	130.02	25.58	LEFT	9	6/25/2002	631	3705.05	7453.83	48.0
356-04-02	93.40	128.35	25.52	LEFT	8	6/25/2002	631	3703.79	7452.57	49.0
357-01-02	54.47	72.10	18.30	LEFT	6	6/25/2002	626	3713.78	7454.79	42.0
357-01-02	73.60	98.15	23.68	RIGHT	6	6/25/2002	631	3708.83	7457.61	48.0
357-02-02	78.58	105.01	21.62	LEFT	6	6/25/2002	631	3710.09	7458.88	49.0
357-03-02	77.25	91.56	20.60	LEFT	6	6/25/2002	631	3711.36	7460.14	43.0
357-04-02	67.20	87.82	17.36	LEFT	5	6/25/2002	631	3712.62	7461.40	42.0
357-05-02	54.98	73.09	16.55	LEFT	4	6/25/2002	631	3713.88	7462.66	42.0

UID	Length (mm)	Width (mm)	Height (mm)	Valve	Age	Harvested	Area	Lat.	Long.	Depth (m)
493-02-02	111.28	145.04	28.29	LEFT	11	7/7/2002	613	4038.66	7158.72	73.0
493-03-02	91.24	114.07	24.01	LEFT	8	7/7/2002	613	4038.68	7158.74	72.0
493-06-02	121.15	153.80	33.13	LEFT	13	7/7/2002	613	4038.69	7158.76	58.0
493-07-02	74.93	101.86	22.63	LEFT	6	7/7/2002	613	4038.71	7158.77	58.0
493-08-02	90.49	120.65	24.13	LEFT	8	7/7/2002	613	4038.73	7158.79	73.0
493-09-02	84.68	112.90	22.58	LEFT	7	7/7/2002	613	4038.74	7158.80	58.0
493-10-02	120.46	163.16	33.90	LEFT	13	7/7/2002	613	4038.76	7158.82	58.0

Table 2. Raw increment ring width data from live-collected *Hemimactra (Spisula) solidissima* valves collected from the continental shelf of the Mid-Atlantic Bight. These data are formatted in standard tree-ring raw width data file format for upload to NOAA-NCDC. Measurements are in units of .001mm of the thickness of increment ring width for each year. The end of series and missing value code is 999. The 10 values following the decade are the 10 annual measurements for the 10

years of that decade. First and last decade rows for each core may contain less than 10 values.

612 1 Continental Shelf WIDTH_RING HSSV CONDRO-
612 2 United States of America Hemimactra Spisula solidissima-
612 3 HUDLEY JOEL-

200405	1983	236	419	265	69	131	291	155			
200405	1990	97	51	26	30	29	59	999			
200504	1989	579									
200504	1990	271	172	153	146	103	71	999			
200501	1986	144	282	316	236						
200501	1990	553	418	299	129	52	37	999			
200502	1987	320	519	465							
200502	1990	147	999								
200503	1984	885	271	284	151	119	93				
200503	1990	77	68	58	54	39	50	999			
200505	1982	772	318	190	164	131	133	110	40		
200505	1990	46	999								
200512	1981	472	453	70	180	258	196	124	74	57	
200512	1990	40	32	37	36	40	41	999			
200902	1993	298	279	300	327	222	999				
200901	1989	99									
200901	1990	102	181	172	52	107	260	233	197	999	
201801	1980	697	262	292	235	209	131	118	76	85	48
201801	1990	56	999								
201803	1985	342	550	202	231	227					
201803	1990	112	999								
201804	1987	159	310	311							
201804	1990	426	999								
201805	1983	603	288	492	323	211	173	149			
201805	1990	75	999								
201903	1992	500	807	156	196	181	89	999			
201907	1990	207	207	187	738	151	188	165	77	999	
203323	1977	136	421	233							
203323	1980	362	325	228	187	96	79	41	46	29	29
203323	1990	28	34	51	999						
200406	1984	493	316	220	203	220	102				
200406	1990	78	45	19	54	29	34	999			
200507	1992	357	581	405	114	999					
201101	1985	550	524	240	360	150					
201101	1990	134	70	82	51	37	29	35	71	999	
201112	1984	258	339	560	302	307	195				
201112	1990	134	80	80	60	48	47	41	72	999	
203307	1978	203	98								
203307	1980	50	261	279	351	167	145	111	72	60	49
203307	1990	57	39	48	999						

203308 1980 541 306 360 139 171 153 62 71 55 66
203308 1990 35 44 18 999
203309 1979 548
203309 1980 348 389 345 199 104 93 66 71 59 52
203309 1990 42 21 23 999
203310 1980 117 442 653 303 182 105 67 62 56 54
203310 1990 31 54 71 999

613 1 Continental Shelf WIDTH_RING HSSV CONDRO-
613 2 United States of America Hemimactra Spisula solidissima-
613 3 HUDLEY JOEL-

300103 1975 340 73 170 109 174
300103 1980 282 303 254 160 94 62 70 54 29 47
300103 1990 27 23 35 999
300104 1968 244 214
300104 1970 344 285 137 203 177 66 90 59 108 62
300104 1980 59 40 77 72 41 21 23 17 24 24
300104 1990 22 27 24 999
300301 1979 57
300301 1980 226 300 128 342 157 220 258 179 77 54
300301 1990 46 999
301501 1984 476 313 377 321 267 190
301501 1990 105 73 56 48 25 34 32 44 28 22
301501 2000 17 999
301901 1983 76 93 459 247 508 232 185
301901 1990 119 147 58 47 36 53 57 45 41 21
301901 2000 17 999
301902 1989 223
301902 1990 136 129 227 153 272 311 355 191 189 60
301902 2000 55 999
301906 1984 92 120 144 125 366 245
301906 1990 375 168 136 81 91 45 46 35 41 39
301906 2000 44 999
301907 1983 250 450 249 70 212 109 236
301907 1990 145 82 75 66 66 108 77 71 49 50
301907 2000 148 999
301910 1992 202 159 171 618 338 177 158 50
301910 2000 53 999
307201 1979 111
307201 1980 259 203 493 373 232 182 164 83 64 69
307201 1990 47 43 30 38 13 36 999
346903 1976 367 362 422 249
346903 1980 241 113 105 52 115 46 101 36 37 33
346903 1990 28 29 19 999

346905 1984   469   586   357   202   172   128
346905 1990   94   87   253   999
346906 1979   233
346906 1980   396   521   325   230   146   113   73   65   71   33
346906 1990   28   27   33   999
346911 1973   245   170   220   262   417   211   77
346911 1980   171   126   50   51   30   42   48   29   14   36
346911 1990   46   32   47   999
349302 1991   183   188   252   239   329   228 236 114   75
349302 2000   71   999
349310 1991   254   270   349   274   255   163 170   65   73
349310 2000   97   999

614   1 Continental Shelf WIDTH_RING HSSV CONDRO-
614   2 United States of America Hemimactra Spisula solidissima-
614   3 HUDLEY JOEL-

402101 1985   72   78   259   100   213
402101 1990   152   137   139   99   91   37   47   15 999
402203 1989   126
402203 1990   192   145   407   157   372   182 193 118 999
403404 1988   117   154
403404 1990   194   280   222   275   132   146   75   55   999
404101 1985   368   412   330   190   106
404101 1990   52   21   38   51   24   25 999
404801 1978   203   291
404801 1980   364   196   187   92   78   66   66   44   38   42
404801 1990   53   27   36   27   24   18 999
404803 1983   401   390   300   118   157   111   45
404803 1990   37   35   45   33   37   30 999
405001 1982   263   494   384   147   186   139   65   41
405001 1990   50   17   29   37   30   37 999
407701 1993   221   133   192   259   186   154 173
407701 2000   179   999
407801 1985   244   208   235   456   198
407801 1990   159   147   110   61   82   52   51   37   31   36
407801 2000   29   999
407802 1980   142   115   121   161   252   250 149 103   84   112
407802 1990   59   52   54   38   30   49   29   37   41   32
407802 2000   16   999
421001 1985   157   147   251   382   261
421001 1990   340   227   143   109   118   62   74   91 999
412506 1979   55
412506 1980   238   161   227   134   337   209 104   85   62   67
412506 1990   182   123   62   44   62   39 119   99   999

412507 1985 488 271 360 234 197
412507 1990 60 72 26 33 31 31 23 22 999

615 1 Continental Shelf WIDTH_RING HSSV CONDRO-
615 2 United States of America Hemimactra Spisula solidissima-
615 3 HUDLEY JOEL-

506001 1985 117 394 211 340 232
506001 1990 105 75 71 44 63 42 55 54 41 39
506001 2000 54 999
506002 1983 147 87 87 404 281 127 80
506002 1990 133 47 45 58 132 87 52 38 48 57
506002 2000 58 999
510803 1979 243
510803 1980 97 209 426 319 205 142 55 52 82 44
510803 1990 61 59 68 80 68 70 999
510804 1985 46 125 281 220 262
510804 1990 241 208 185 105 55 46 999
519001 1979 124
519001 1980 180 89 74 61 41 55 64 55 70 48
519001 1990 43 36 34 999
519002 1974 251 302 342 133 411 300
519002 1980 97 76 169 374 351 134 71 34 33 34
519002 1990 29 48 57 999
522703 1989 202
522703 1990 123 61 65 43 41 55 45 31 34 41
522703 2000 38 999
522704 1984 198 164 112 91 140 119
522704 1990 150 286 371 265 211 121 71 62 51 82
522704 2000 60 999
522705 1989 159
522705 1990 380 261 131 71 30 62 63 107 111 60
522705 2000 45 999
522706 1987 280 177 242
522706 1990 190 189 300 198 124 96 94 121 87 43
522706 2000 69 999
522802 1986 81 134 311 242
522802 1990 93 68 64 68 48 47 51 41 45 35
522802 2000 48 999
522803 1982 111 246 156 505 474 271 115 174
522803 1990 210 151 96 119 82 34 52 47 43 50
522803 2000 31 999
522910 1982 79 213 277 218 282 224 169 126
522910 1990 84 78 56 44 48 39 40 38 28 30
522910 2000 26 999

522911 1991 57 217 357 412 279 191 132 108 115
522911 2000 89 999

621 1 Continental Shelf WIDTH_RING HSSV CONDRO-
621 2 United States of America Hemimactra Spisula solidissima-
621 3 HUDLEY JOEL-

120203 1987 58 386 444
120203 1990 334 220 193 74 61 67 59 37 45 44
120203 2000 63 999
126003 1987 286 288 245
126003 1990 155 367 261 250 126 96 57 64 51 35
126003 2000 51 999
130501 1978 16 124
130501 1980 239 364 328 260 236 135 78 41 34 57
130501 1990 29 62 49 999
130502 1980 56 284 251 271 197 84 175 155 152 110
130502 1990 55 35 59 999
130503 1980 66 206 114 265 291 244 171 109 80 58
130503 1990 51 27 43 999
130504 1978 191 248
130504 1980 265 279 298 266 242 117 95 57 39 30
130504 1990 32 37 42 999
131102 1978 83 125
131102 1980 644 356 311 181 105 86 48 32 40 31
131102 1990 42 38 35 999
131105 1980 143 759 252 226 148 98 78 38 39 39
131105 1990 32 38 59 999
131106 1981 68 133 61 278 340 248 251 136 78
131106 1990 68 33 42 999
111901 1986 48 245 232 74
111901 1990 110 64 48 65 49 51 999
111904 1981 303 255 299 327 267 211 222 181 92
111904 1990 262 264 258 226 131 71 999
112902 1978 72 43
112902 1980 93 100 78 125 90 62 60 36 70 62
112902 1990 72 63 67 49 52 81 999
112903 1976 357 105 133 202
112903 1980 114 306 308 97 104 294 163 260 98 59
112903 1990 32 34 36 45 38 37 999
120001 1978 70 329
120001 1980 417 275 103 97 64 73 71 77 66 72
120001 1990 30 73 53 50 50 35 22 42 39 39
120001 2000 76 999
120002 1988 40 323

120002 1990 246 275 296 158 140 130 70 74 68 44
120002 2000 59 999
212301 1984 134 373 353 272 219 153
212301 1990 70 70 40 48 30 46 37 47 999
232301 1977 354 58 457
232301 1980 294 204 156 108 85 93 56 30 37 38
232301 1990 43 51 49 999
232304 1984 182 191 196 206 109 106
232304 1990 80 89 53 999

625 1 Continental Shelf WIDTH_RING HSSV CONDRO-
625 2 United States of America Hemimactra Spisula solidissima-
625 3 HUDLEY JOEL-

512011 1985 70 183 168 152 140
512011 1990 204 55 31 999
515402 1977 479 380 282
515402 1980 174 137 65 67 33 46 38 50 27 49
515402 1990 47 45 53 41 30 54 999
516404 1977 77 243 247
516404 1980 239 192 89 61 45 33 50 45 27 49
516404 1990 62 51 60 26 81 32 999
516505 1976 227 672 349 263
516505 1980 153 126 107 85 59 51 90 85 61 127
516505 1990 94 96 105 77 109 79 999
516505 1984 64 302 182 175 257 118
516506 1990 289 230 197 67 61 39 999
518101 1976 163 246 384 355
518101 1980 283 191 109 95 43 45 52 55 51 39
518101 1990 32 32 66 999
518114 1980 224 395 320 298 108 92 113 50 35 51
518114 1990 52 54 71 999
518116 1980 160 278 382 946 172 81 89 86 55 35
518116 1990 54 45 80 999
528304 1984 394 279 252 228 207 65
528304 1990 32 36 66 51 56 53 36 23 66 46
528304 2000 37 999
528305 1987 147 107 72
528305 1990 193 121 298 248 145 74 96 68 60 46
528305 2000 49 999
528306 1990 199 232 396 316 113 166 133 38 31 37
528306 2000 51 999
528401 1988 210 292
528401 1990 402 393 212 196 122 83 142 52 999
529505 1986 201 133 244 380

```
529505  1990   304   276   171   107    97   108   77   24  999
541326  1979   204
541326  1980   285   188   151   117    79    58   68   61   49   38
541326  1990    31    30    47    38    43    56   48   67  999
541338  1980   119   279   259   216   104   106   61   44   58   52
541338  1990    32    91    42    32    39    63   53   59  999
541357  1978   107   189
541357  1980   246   196   106    61    55    37   47   34   31   29
541357  1990    29    45    42    52    46    54   71   77  999
```

```
626    1  Continental Shelf WIDTH_RING HSSV CONDRO-
626    2  United States of America  Hemimactra Spisula solidissima-
626    3  HUDLEY JOEL-
```

```
615503  1985   225   253   571   442   272
615503  1990   161   142    88    91    95    53  999
618701  1983   158   448   151   122   126   177  103
618701  1990    85    58    54   999
618703  1982    69   216   259   168   223    53   58   62
618703  1990    92    46    67   999
618902  1981   115   357   319   224   427   207  250  113   75
618902  1990    67    42    48   999
618905  1981   135   274   349   403   332   159   44   46   48
618905  1990    74    38    50   999
627502  1980    60   407   320   526   348   248  186  122  153   88
627502  1990    50    48    61    50    53    37  999
627504  1979   165
627504  1980   344   585   386   405   244   143  153  133  131   76
627504  1990    60    51    67    74    52    62  999
627605  1984   253   442   337   408   280   198
627605  1990   172    96    53    73    40    50  999
627606  1983   232   203   201   282   328   308  190
627606  1990   135    74    67    52    34    53  999
635604  1989   129
635604  1990   254   258   223   103    52   116   53   39   41   49
635604  2000    64   999
635626  1987   120   250   145
635626  1990   182   188   225   176    94    53  103   59   52   44
635626  2000    43   999
635701  1995    82   133   271   317   170
635701  2000    76   999
642114  1992    92   204   346   208   121    90  999
643208  1987    43    73   112
643208  1990   119   140   111    70    56    42   51   38  999
618902  1980    82   310   372   322   185   185  161   68   52   29
```

618902 1990 37 40 33 999

631 1 Continental Shelf WIDTH_RING HSSV CONDRO-
631 2 United States of America Hemimactra Spisula solidissima-
631 3 HUDLEY JOEL-

111401 1986 429 170 252 245
111401 1990 108 999
111404 1987 519 338 284
111404 1990 120 999
113601 1988 787 485
113601 1990 314 999
113602 1988 555 456
113602 1990 282 999
111402 1987 588 332 350
111402 1990 125 999
111403 1987 591 299 223
111403 1990 103 999
116105 1981 412 196 102 264 201 121 88 99 101
116105 1990 33 25 33 999
116202 1981 619 403 188 160 181 126 63 52 57
116202 1990 48 62 24 999
116203 1980 504 268 293 138 208 186 89 75 46 68
116203 1990 59 46 40 999
116204 1981 21 22 82 31 54 69 50 80 105
116204 1990 260 242 855 999
116701 1977 549 319 169
116701 1980 175 158 91 65 46 60 56 38 21 36
116701 1990 33 36 40 999
116702 1978 631 407
116702 1980 255 174 72 125 97 70 57 50 43 26
116702 1990 70 33 20 999
116704 1976 422 255 199 354
116704 1980 217 100 124 72 63 49 55 32 58 39
116704 1990 18 19 18 999
116706 1984 293 243 234 295 187 126
116706 1990 118 121 155 999
116707 1981 322 196 204 299 170 153 183 154 115
116707 1990 80 54 89 999
116708 1981 226 263 278 245 228 115 89 69 52
116708 1990 37 51 25 999
122004 1978 164 359
122004 1980 406 267 116 93 76 57 56 54 46 21
122004 1990 40 27 22 27 20 27 999
122005 1980 164 576 323 159 136 51 49 65 45 53

122005	1990	41	46	46	33	46	29	999			
122006	1980	127	340	344	336	177	184	143	71	63	41
122006	1990	35	45	40	44	41	23	999			
122008	1985	320	313	363	157	176					
122008	1990	161	94	96	59	55	61	999			
122009	1984	87	179	371	230	186	76				
122009	1990	92	76	78	59	24	65	999			
122301	1981	579	423	376	233	120	103	81	92	38	
122301	1990	51	42	63	40	25	37	999			
122302	1985	270	387	348	302	210					
122302	1990	137	71	86	70	65	68	999			
122302	1982	93	263	365	342	329	216	102	65		
122302	1990	77	44	58	46	26	54	999			
122303	1989	315									
122303	1990	443	375	177	118	117	73	999			
122304	1990	482	472	376	220	154	101	999			
122306	1991	400	369	330	313	225	999				
130703	1989	63									
130703	1990	171	149	341	218	335	134	136	82	999	
134007	1992	148	258	350	262	123	104	87	82		
134007	2000	133	999								
134602	1991	58	88	142	353	308	282	151	73	62	
134602	2000	88	999								
116205	1986	269	252	248	231						
116205	1990	250	191	91	999						
130502	1986	40	232	174	178						
130502	1990	194	120	109	108	74	53	43	28	999	
130503	1986	316	256	259	249						
130503	1990	176	160	143	113	75	49	41	48	999	
130603	1984	193	373	271	263	185	168				
130603	1990	86	48	49	55	48	43	37	41	999	
130605	1982	58	227	317	252	252	183	149	161		
130605	1990	161	90	128	82	37	85	31	87	999	
130604	1989	79									
130604	1990	150	140	300	253	300	160	88	59	999	
130606	1991	262	321	275	351	143	94	74	999		
130702	1983	48	177	216	295	102	144	96			
130702	1990	36	54	52	48	38	30	45	72	999	
130703	1982	323	276	336	185	176	172	91	69		
130703	1990	72	39	64	56	30	68	66	69	999	
131902	1975	267	360	223	422	153					
131902	1980	106	531	525	300	248	139	222	163	91	114
131902	1990	75	33	54	26	29	54	44	32	40	27
131902	2000	47	999								
131903	1983	142	466	295	276	212	198	176			
131903	1990	103	125	72	55	45	32	35	49	38	29

131903 2000 48 999
134010 1992 448 424 299 173 115 111 135 162
134010 2000 125 999
134011 1991 27 313 226 316 279 173 120 92 118
134011 2000 44 999

632 1 Continental Shelf WIDTH_RING HSSV CONDRO-
632 2 United States of America Hemimactra Spisula solidissima-
632 3 HUDLEY JOEL-

201602 1980 292 393 382 177 79 81 131 40 22 28
201602 1990 18 25 48 999
214101 1978 249 410
214101 1980 502 312 223 127 92 108 84 56 36 41
214101 1990 31 999
214102 1982 107 260 511 400 231 110 79 57
214102 1990 38 999
214104 1980 294 465 320 344 185 132 122 82 85 33
214104 1990 58 999
214501 1977 337 650 358
214501 1980 212 72 124 50 37 54 31 32 37 33
214501 1990 43 999
214502 1977 159 314 536
214502 1980 291 277 105 56 69 79 66 23 15 33
214502 1990 30 999
214503 1978 313 305
214503 1980 496 267 227 125 82 69 61 26 48 68
214503 1990 48 999
214504 1979 351
214504 1980 409 244 242 146 101 107 48 58 38 45
214504 1990 39 999
214505 1978 86 243
214505 1980 687 361 271 93 62 65 63 46 34 49
214505 1990 44 999
214507 1980 235 474 289 248 148 84 108 56 76 54
214507 1990 62 999
214508 1979 257
214508 1980 178 458 256 130 118 76 81 57 42 32
214508 1990 18 999
214509 1980 160 285 343 197 144 149 81 52 49 35
214509 1990 33 999
216101 1980 351 302 394 381 237 158 69 93 66 46
216101 1990 54 54 48 999
216105 1976 148 243 593 359
216105 1980 293 119 76 47 47 54 20 23 30 20

216105	1990	24	32	54	999						
216108	1978	130	389								
216108	1980	435	265	199	119	149	143	61	55	22	34
216108	1990	15	39	33	999						
216109	1980	172	148	350	352	282	137	122	68	47	50
216109	1990	58	44	48	999						
216201	1980	220	833	390	235	159	98	114	82	53	45
216201	1990	43	54	41	999						
216202	1979	115									
216202	1980	190	350	356	200	170	157	104	69	50	58
216202	1990	35	47	27	999						
216203	1979	34									
216203	1980	193	323	281	262	173	166	173	76	67	54
216203	1990	58	53	67	999						
216204	1985	104	240	294	226	237					
216204	1990	182	156	92	999						
216306	1982	22	167	228	281	201	99	99	80		
216306	1990	84	41	40	999						
216706	1980	137	86	164	204	213	268	190	120	114	89
216706	1990	47	50	34	999						
216707	1979	109									
216707	1980	209	200	172	297	191	165	158	145	65	60
216707	1990	42	72	62	999						
216708	1980	100	193	286	178	105	230	197	105	80	75
216708	1990	44	54	57	999						
225501	1978	174	159								
225501	1980	114	60	87	74	66	53	42	38	57	33
225501	1990	45	999								
225501	1981	168	162	389	290	171	111	104	53	80	
225501	1990	64	37	68	39	34	41	999			
233101	1990	27	224	102	149	212	78	89	78	169	168
233101	2000	48	999								
233402	1993	305	179	285	165	273	220	141			
233402	2000	39	999								
233404	1991	58	172	189	276	105	131	85	188	154	
233404	2000	60	999								
214103	1980	266	373	312	326	200	122	97	75	53	67
214103	1990	59	999								
214506	1980	171	349	632	252	172	101	78	92	54	100
214506	1990	58	999								
216207	1982	234	325	401	290	216	117	75	63	41	41
216207	1990	93	999								
216302	1979	78									
216302	1980	96	496	381	246	164	90	60	45	46	40
216302	1990	50	43	34	999						
216303	1980	238	231	266	431	248	138	64	89	85	79

216303	1990	51	60	44	999						
225502	1987	174	326	330							
225502	1990	45	96	40	43	51	52	999			
225503	1982	53	223	205	312	236	115	62	73	233	117
225503	1990	76	97	65	94	999					
225504	1985	279	244	235	157	144					
225504	1990	63	123	83	42	49	58	999			
225505	1983	38	160	127	110	226	256	173			
225505	1990	158	85	145	98	109	120	999			
231001	1983	35	379	435	323	222	121	70			
231001	1990	124	43	48	29	25	30	44	34	999	
231002	1982	518	439	315	169	179	70	87	69		
231002	1990	88	76	62	44	39	37	40	49	999	
231003	1985	65	447	406	243	177					
231003	1990	121	62	55	53	64	55	61	43	999	
231004	1985	187	235	154	92	230					
231004	1990	122	158	155	153	151	95	76	94	999	
232301	1986	357	466	257	210						
232301	1990	78	104	97	68	59	59	47	45	999	
232302	1984	51	431	237	190	142	70				
232302	1990	164	214	136	204	349	190	319	290	999	

Table 3. Individual shell Increment ring width index (RWI) data from live-collected Hemimactra (Spisula) *solidissima* valves after the removal of ontogenetic growth using a spline function. Measurements are in units of .001mm of the thickness of increment ring width for each year. The end of series and missing value code is 9.999. The 10 values following the decade are the 10 annual measurements for the 10 years of that decade. First and last decade rows for each core may contain less than 10 values.

UID	Year	0	1	2	3	4	5	6	7	8	9
001-04-94	1969	0.668									
001-04-94	1970	0.790	1.014	1.094	1.036	1.054	1.066	1.020	1.006	0.985	0.998
001-04-94	1980	0.992	0.990	0.983	0.995	1.008	1.008	1.003	1.000	0.996	0.996
001-04-	199	0.99	0.99	0.99	1.00	0.00	0.00	0.00	0.00	0.00	1.00

94	0	6	6	8	0	0	0	0	0	0	8
001-04-94	2000	0.993	0.982	9.999							
015-02-02	1990	0.990	0.946	1.081	0.917	1.041	0.976	0.981	1.021	1.030	1.004
015-02-02	2000	0.994	0.993	9.999							
019-01-02	1992	1.110	0.957	0.989	0.964	1.019	1.000	1.021	1.003		
019-01-02	2000	1.000	0.995	9.999							
019-02-02	1984	2.749	0.495	0.957	0.907	1.101	1.067				
019-02-02	1990	1.042	1.011	1.019	1.000	0.989	0.982	0.986	0.994	1.000	0.995
019-02-02	2000	0.991	1.001	9.999							
019-06-02	1992	1.019	0.944	1.014	1.004	1.013	0.996	1.014	0.993		
019-06-02	2000	0.992	1.000	9.999							
019-07-02	1989	1.583									
019-07-02	1990	0.856	0.884	1.016	0.985	1.033	1.027	1.007	0.995	1.002	0.992
019-07-02	2000	0.995	1.000	9.999							
019-07-02	1985	7.528	1.012	0.857	0.755	0.967					
019-07-02	1990	0.975	1.085	1.052	1.032	1.006	1.005	0.994	0.992	0.989	0.998
019-07-02	2000	1.001	0.987	9.999							
019-10-02	1989	1.595									
019-10-02	1990	0.724	1.097	0.938	1.017	1.006	0.998	1.008	1.005	1.014	0.921
019-10-02	2000	0.868	1.177	9.999							
060-01-02	1984	1.005	0.528	0.477	2.094	1.498	0.758				
060-01-02	1990	0.566	0.909	0.807	0.948	0.711	1.179	0.867	1.197	1.204	1.214
060-01-02	2000	1.038	1.208	9.999							
077-01-	198	1.00	0.86	1.02							

UID	Year	0	1	2	3	4	5	6	7	8	9
02	7	8	2	9							
077-01-02	1990	1.168	1.027	0.907	1.107	1.093	0.702	1.080	0.810	0.759	0.788
077-01-02	2000	0.812	1.218	9.999							
078-01-02	1982	1.445	0.503	0.758	1.365	0.741	0.926	0.821	1.470		
078-01-02	1990	1.175	0.894	0.938	0.593	1.176	1.041	1.199	1.040	1.095	0.869
078-01-02	2000	0.800	1.427	9.999							
078-02-02	1979	0.279									
078-02-02	1980	1.369	1.858	1.367	0.595	0.671	0.538	0.744	0.864	1.093	1.065
078-02-02	1990	1.289	0.583	1.511	1.158	1.149	1.199	0.862	0.542	0.998	1.132
UID	**Year**	**0**	**1**	**2**	**3**	**4**	**5**	**6**	**7**	**8**	**9**
078-02-02	2000	0.831	1.202	9.999							
200-01-02	1989	0.289									
200-01-02	2000	0.949	1.182	9.999							
202-03-02	1988	0.266	1.356								
202-03-02	1990	1.398	1.100	0.862	1.000	0.555	0.687	1.090	1.256	0.901	0.929
202-03-02	2000	1.132	1.052	9.999							
227-03-02	1985	1.105	1.033	0.797	0.721	1.212					
227-03-02	1990	1.134	1.324	0.767	0.972	0.762	0.838	1.252	1.116	0.819	1.097
227-03-02	2000	0.644	1.207	9.999							
227-05-02	1990	0.917	0.971	0.892	1.404	1.034	0.791	0.763	0.890	1.310	1.072
227-05-02	2000	1.343	0.908	9.999							
228-02-02	1987	0.594	0.771	1.544							
228-02-02	1990	1.161	1.076	0.896	0.698	1.099	0.988	0.535	1.017	1.065	0.964
228-02-	200	1.10	1.02	9.99							

02	0	5	5	9							
229-10-02	1983	0.470	1.096	1.294	0.979	1.290	1.109	0.961			
229-10-02	1990	0.867	0.727	0.869	0.809	0.810	1.082	1.027	1.177	1.217	1.073
229-10-02	2000	0.871	1.411	9.999							
260-03-02	1988	1.014	1.058								
260-03-02	1990	0.928	0.595	1.421	1.081	1.209	0.781	0.817	0.685	1.052	1.525
260-03-02	2000	1.052	0.850	9.999							
283-04-02	1985	1.077	0.901	0.985	1.115	1.328					
283-04-02	1990	0.580	0.408	0.624	1.397	1.187	1.344	1.281	0.870	0.546	1.011
283-04-02	2000	0.964	1.271	9.999							
283-05-02	1988	1.271	0.865								
283-05-02	1990	0.520	1.194	0.655	1.497	1.298	0.892	0.579	0.979	0.901	0.733
283-05-02	2000	1.038	1.351	9.999							
283-06-02	1991	0.880	0.855	1.343	1.177	0.540	1.077	1.251	0.578	1.092	
283-06-02	2000	0.715	1.195	9.999							
319-02-02	1983	1.238	0.860	0.883	0.621	1.240	1.144	0.808			
319-02-02	1990	1.286	1.082	0.606	1.216	0.678	0.813	1.534	1.242	0.892	1.088
319-02-02	2000	0.806	1.273	9.999							
319-02-02	1984	0.483	1.594	1.049	1.060	0.912	0.985				
319-02-02	1990	1.045	0.753	1.152	0.856	0.851	0.892	0.773	0.955	1.402	1.345
319-02-02	2000	1.415	0.534	9.999							
331-01-02	1991	0.328	1.747	0.686	0.965	1.450	0.629	0.802	0.678	1.335	
331-01-02	2000	1.209	0.690	9.999							
334-01-	199	0.69	1.12	0.96	1.38	0.64	0.96	0.64	1.04		

02	2	6	3	3	1	2	6	9	3		
334-01-02	2000	0.996	0.805	9.999							
334-02-02	1994	1.087	0.759	1.246	0.733	1.158	0.973				
334-02-02	2000	0.881	1.152	9.999							
340-07-02	1993	0.806	1.015	1.238	1.074	0.721	0.911	1.094			
340-07-02	2000	1.439	0.588	9.999							

UID	**Year**	**0**	**1**	**2**	**3**	**4**	**5**	**6**	**7**	**8**	**9**
340-10-02	1993	0.960	1.101	1.034	0.875	0.823	0.911	0.842			
340-10-02	2000	1.095	1.064	9.999							
340-10-02	1992	0.291	1.473	0.826	1.096	1.090	0.893	0.872	0.738		
340-10-02	2000	1.130	1.210	9.999							
346-02-02	1991	1.249	0.724	0.708	1.325	1.090	1.144	0.842	0.622	0.920	
346-02-02	2000	1.016	1.158	9.999							
356-04-02	1990	0.680	1.204	1.218	1.198	0.716	0.495	1.475	0.895	0.819	0.984
356-04-02	2000	0.991	1.153	9.999							
356-26-02	1988	0.741	1.408								
356-26-02	1990	0.780	0.958	0.997	1.268	1.142	0.758	0.544	1.314	0.924	1.120
356-26-02	2000	0.880	0.992	9.999							
357-02-02	1996	1.091	0.826	1.043	0.997						
357-02-02	2000	1.000	0.998	9.999							
493-02-02	1986	1.023	0.881	0.875	1.091						
493-02-02	1990	1.048	1.017	1.012	1.006	0.990	0.996	0.995	0.998	0.998	1.001
493-02-02	2000	1.002	0.995	9.999							
493-10-	198	1.29	0.91	0.83	0.85	0.98	1.07	1.06	1.03	1.01	

02	1	3	5	0	8	6	7	5	5	0	
493-10-02	1990	1.020	1.006	0.997	0.997	0.993	0.988	0.996	0.993	0.996	9.999
003-01-92	1972	1.031	0.857	0.870	0.922	1.093	1.082	1.009	1.023		
003-01-92	1980	1.027	1.005	0.997	0.987	0.989	0.996	0.995	0.989	0.992	1.000
003-01-92	1990	1.000	1.005	9.999							
005-02-92	1989	0.982									
005-02-92	1990	1.011	1.014	0.959	9.999						
005-05-92	1984	1.133	0.773	0.818	1.093	1.070	1.196				
005-05-92	1990	1.193	0.624	1.172	9.999						
018-01-92	1982	1.191	0.637	0.996	1.053	1.179	0.935	1.065	0.863		
018-01-92	1990	1.183	0.816	1.139	9.999						
018-03-92	1987	0.876	1.287	0.681							
018-03-92	1990	1.011	1.151	0.903	9.999						
018-04-92	1989	0.974									
018-04-92	1990	1.041	0.965	1.008	9.999						
018-05-92	1985	1.102	0.674	1.268	1.002	0.883					
018-05-92	1990	0.972	1.129	0.936	9.999						
114-01-92	1987	1.047	0.799	1.083							
114-01-92	1990	1.055	0.927	9.999							
114-02-92	1988	1.014	0.935								
114-02-92	1990	1.069	0.945	9.999							
114-03-92	1988	1.010	0.957								
114-03-92	1990	1.044	0.983	9.999							
114-04-	198	1.00	0.96								

92	8	7	9	
114-04-92	1990	1.037	0.973	9.999
136-01-92	1989	1.004		

UID	**Year**	**0**	**1**	**2**	**3**	**4**	**5**	**6**	**7**	**8**	**9**
136-01-92	1990	0.986	1.011	9.999							
136-02-92	1989	0.996									
136-02-92	1990	1.009	0.993	9.999							
141-01-92	1979	0.731									
141-01-92	1980	1.106	1.362	0.975	0.903	0.723	0.745	1.182	1.191	1.018	0.827
141-01-92	1990	1.156	1.082	9.999							
141-02-92	1983	0.728	0.877	1.307	1.082	0.866	0.695	0.906			
141-02-92	1990	1.145	1.409	9.999							
141-02-92	1980	0.830	1.155	1.014	1.204	0.931	0.779	0.877	0.939	0.851	1.271
141-02-92	1990	1.333	0.793	9.999							
141-04-92	1981	0.814	1.257	0.927	1.174	0.830	0.825	1.053	0.947	1.266	
141-04-92	1990	0.621	1.283	9.999							
145-01-92	1978	0.704	1.539								
145-01-92	1980	1.047	0.852	0.436	1.185	0.769	0.863	1.634	1.045	1.067	1.142
145-01-92	1990	0.922	1.079	9.999							
145-02-92	1978	0.589	1.000								
145-02-92	1980	1.614	0.954	1.123	0.592	0.471	0.859	1.373	1.544	0.713	0.567
145-02-92	1990	1.334	1.219	9.999							
145-03-92	1979	0.898									
145-03-	198	0.86	1.45	0.90	1.00	0.78	0.78	0.99	1.21	0.61	1.09

92	0	4	4	9	1	7	2	0	5	3	6
145-03-92	1990	1.392	0.903	9.999							
145-04-92	1980	0.910	1.215	0.875	1.099	0.884	0.839	1.219	0.743	1.148	0.890
145-04-92	1990	1.157	1.071	9.999							
145-04-92	1981	0.651	0.983	1.633	0.781	0.771	0.721	0.849	1.270	0.798	
145-04-92	1990	1.448	0.858	9.999							
145-05-92	1979	0.440									
145-05-92	1980	0.779	1.794	0.993	0.959	0.501	0.562	0.977	1.368	1.201	0.912
145-05-92	1990	1.226	1.013	9.999							
145-07-92	1981	0.722	1.408	0.950	1.025	0.856	0.707	1.242	0.808	1.228	
145-07-92	1990	0.921	1.075	9.999							
145-08-92	1980	0.959	0.637	1.637	1.046	0.690	0.869	0.787	1.142	1.067	1.047
145-08-92	1990	1.120	1.030	9.999							
145-09-92	1981	0.746	1.124	1.314	0.868	0.810	1.129	0.881	0.830	1.086	
145-09-92	1990	1.006	1.185	9.999							
255-01-92	1979	1.000									
255-01-92	1980	1.104	0.991	0.654	1.123	1.087	1.096	1.001	0.887	0.857	1.320
255-01-92	1990	0.785	1.081	9.999							
255-02-92	1988	0.774	1.160								
255-02-92	1990	1.158	1.015	0.761	0.756	1.228	0.863	1.134	9.999		
255-03-92	1986	0.997	0.990	1.106	0.880						
255-03-92	1990	0.948	1.184	0.709	1.266	0.883	0.979	1.045	9.999		
001-01-94	1976	0.662	0.893	0.972	1.077						
UID	**Yea**	**0**	**1**	**2**	**3**	**4**	**5**	**6**	**7**	**8**	**9**

	r										
001-01-94	1980	1.053	1.058	1.020	1.003	0.978	0.993	0.984	1.003	1.000	0.998
001-01-94	1990	0.998	0.998	1.000	0.996	9.999					
001-01-94	1976	0.618	1.113	1.125	0.978						
001-01-94	1980	1.005	0.964	1.024	1.030	1.012	1.000	0.990	0.984	1.000	1.003
001-01-94	1990	1.003	0.993	0.983	1.013	9.999					
001-02-94	1985	0.855	1.059	1.038	1.000	1.000					
001-02-94	1990	1.002	0.994	0.975	1.016	9.999					
001-02-94	1977	1.163	0.895	0.782							
001-02-94	1980	1.018	1.072	1.045	1.024	1.022	1.002	0.991	0.993	0.993	0.996
001-02-94	1990	0.995	1.000	0.994	1.000	9.999					
001-03-94	1979	0.689									
001-03-94	1980	0.884	1.078	1.069	1.044	1.014	1.001	0.988	0.985	0.993	1.001
001-03-94	1990	1.000	0.998	0.997	1.000	9.999					
001-03-94	1976	1.322	0.970	0.971	0.880						
001-03-94	1980	0.878	0.958	1.030	1.063	1.052	1.026	1.003	1.000	0.997	0.990
001-03-94	1990	0.995	0.994	0.992	0.997	9.999					
016-02-94	1981	0.813	1.180	1.338	0.821	0.529	0.783	1.770	0.801	0.673	
016-02-94	1990	1.158	0.776	0.877	1.278	9.999					
033-08-94	1982	1.106	0.799	1.236	0.649	1.076	1.284	0.699	1.026		
033-08-94	1990	0.951	1.317	0.828	1.308	0.764	9.999				
033-08-94	1980	1.424	0.623	0.278	1.252	1.222	1.546	0.824	0.869	0.859	0.746
033-08-94	1990	0.833	0.874	1.227	0.962	1.320	9.999				
033-09-	198	1.08	0.81	1.09	1.21	0.93	0.67	0.85	0.83	1.14	1.13

94	0	4	4	7	9	1	8	6	4	8	0
033-09-94	1990	1.123	1.308	1.182	0.726	1.034	9.999				
033-09-94	1982	0.413	1.196	1.642	0.883	0.732	0.662	0.706	1.043		
033-09-94	1990	1.273	1.351	0.724	1.047	1.120	9.999				
033-23-94	1978	1.073	0.799								
033-23-94	1980	1.101	1.100	1.116	1.020	0.765	0.754	0.837	1.025	0.715	1.162
033-23-94	1990	1.180	1.684	1.134	0.974	0.844	9.999				
033-23-94	1979	0.537									
033-23-94	1980	1.484	0.778	1.213	1.175	0.965	1.003	0.705	0.846	0.665	1.115
033-23-94	1990	0.958	1.089	0.991	1.019	1.270	9.999				
120-11-94	1986	0.768	1.224	0.993	0.915						
120-11-94	1990	0.860	1.382	0.614	1.146	9.999					
161-01-94	1979	0.976									
161-01-94	1980	0.851	1.147	1.235	0.957	0.883	0.570	1.115	1.069	0.901	1.131
161-01-94	1990	1.137	1.006	9.999							
161-05-94	1982	1.227	0.755	0.490	1.436	1.237	0.885	0.783	1.071		
161-05-94	1990	1.380	0.625	0.702	1.506	9.999					
161-05-94	1977	0.525	0.785	1.845							
161-05-94	1980	1.186	1.141	0.604	0.547	0.513	0.807	1.467	0.820	1.215	1.629
161-05-94	1990	0.940	0.895	0.931	1.254	9.999					

UID	**Year**	**0**	**1**	**2**	**3**	**4**	**5**	**6**	**7**	**8**	**9**
161-08-94	1979	0.476									
161-08-94	1980	1.322	1.472	0.980	0.867	0.641	1.020	1.285	0.758	0.981	0.564
161-08-	199	1.15	0.59	1.53	1.24	9.99					

94	0	9	0	9	0	9					
161-09-94	1981	0.950	0.637	1.272	1.241	1.125	0.713	0.911	0.770	0.781	
161-09-94	1990	1.050	1.315	1.002	1.070	9.999					
162-01-94	1979	0.483									
162-01-94	1980	1.802	0.969	0.774	0.763	0.709	1.197	1.178	0.977	0.969	0.982
162-01-94	1990	1.241	0.951	9.999							
162-02-94	1982	1.113	0.996	0.679	0.840	1.310	1.228	0.823	0.861		
162-02-94	1990	1.091	1.009	1.463	0.696	9.999					
162-02-94	1978	0.670	0.851								
162-02-94	1980	1.345	1.339	0.833	0.852	1.005	0.895	0.820	0.808	1.205	0.886
162-02-94	1990	1.402	0.969	9.999							
162-03-94	1981	1.143	0.780	1.103	0.663	1.214	1.327	0.820	0.912	0.706	
162-03-94	1990	1.203	1.154	1.002	0.988	9.999					
162-03-94	1978	0.301	1.054								
162-03-94	1980	1.375	1.103	1.070	0.802	0.925	1.217	0.712	0.843	0.861	1.054
162-03-94	1990	0.994	1.228	9.999							
162-04-94	1982	0.815	0.605	1.855	0.683	1.237	1.633	1.045	1.073		
162-04-94	1990	0.754	1.008	0.552	1.266	9.999					
162-04-94	1984	0.819	1.087	1.109	0.887	1.039	0.954				
162-04-94	1990	1.057	0.952	9.999							
162-04-94	1987	1.005	0.992	1.007							
162-04-94	1990	0.951	1.057	1.025	0.928	9.999					
162-04-94	1981	0.836	1.025	1.232	1.010	0.986	0.800	0.829	1.084	0.878	
162-04-	199	0.76	1.28	9.99							

94	0	7	6	9							
163-02-94	1981	0.967	0.854	0.919	1.510	1.023	0.768	0.512	0.974	1.146	
163-02-94	1990	1.223	0.886	1.158	0.959	9.999					
163-02-94	1978	0.563	0.436								
163-02-94	1980	1.755	1.290	0.946	0.821	0.653	0.674	0.777	1.088	1.091	1.389
163-02-94	1990	1.183	0.935	9.999							
163-06-94	1981	0.338	1.110	1.088	1.246	1.021	0.664	0.902	0.954	1.272	
163-06-94	1990	0.821	1.121	9.999							
167-01-94	1978	1.201	0.911								
167-01-94	1980	0.659	0.947	1.193	0.960	0.936	0.852	1.324	1.403	1.062	0.633
167-01-94	1990	1.105	0.987	1.022	1.069	9.999					
167-02-94	1979	1.152									
167-02-94	1980	0.974	0.849	0.844	0.517	1.269	1.301	1.161	1.102	1.075	0.993
167-02-94	1990	0.631	1.796	0.955	0.696	9.999					
167-04-94	1977	1.152	0.802	0.724							
167-04-94	1980	1.504	1.117	0.650	1.045	0.797	0.907	0.885	1.186	0.790	1.607
167-04-94	1990	1.243	0.689	0.906	1.126	9.999					

UID	**Year**	**0**	**1**	**2**	**3**	**4**	**5**	**6**	**7**	**8**	**9**
167-06-94	1985	1.035	0.921	0.927	1.251	0.965					
167-06-94	1990	0.845	0.939	0.958	1.094	9.999					
167-06-94	1979	1.215									
167-06-94	1980	0.630	0.987	1.046	1.001	1.265	1.009	0.785	0.968	1.018	0.749
167-06-94	1990	1.138	1.219	9.999							
167-07-	198	1.13	0.77	0.87	1.36	0.85	0.85	1.13	1.10		

94	2	5	5	6	9	6	6	9	2		
167-07-94	1990	0.996	0.860	0.701	1.314	9.999					
167-07-94	1978	0.753	1.192								
167-07-94	1980	1.006	0.807	1.369	0.934	0.909	1.029	1.178	0.691	0.828	0.698
167-07-94	1990	1.301	1.165	9.999							
167-08-94	1982	0.895	1.019	1.096	1.053	1.168	0.776	0.841	0.927		
167-08-94	1990	0.962	0.882	1.484	0.925	9.999					
167-08-94	1979	0.697									
167-08-94	1980	1.072	1.424	0.894	0.556	1.286	1.242	0.823	0.825	1.020	0.755
167-08-94	1990	1.063	1.207	9.999							
181-01-94	1980	0.653	0.907	1.355	1.286	1.143	0.932	0.691	0.826	0.527	0.758
181-01-94	1990	1.115	1.363	1.351	1.041	0.813	0.736	1.342	9.999		
181-14-94	1981	0.733	1.268	1.097	1.224	0.601	0.736	1.309	0.833	0.755	
181-14-94	1990	1.164	1.084	0.967	1.082	9.999					
181-16-94	1981	0.714	0.813	0.886	2.130	0.494	0.362	0.686	1.164	1.192	
181-16-94	1990	0.935	1.303	0.856	1.179	9.999					
187-01-94	1984	0.643	1.680	0.690	0.740	0.896	1.346				
187-01-94	1990	0.921	0.971	0.882	1.107	9.999					
187-03-94	1983	0.569	1.200	1.241	0.846	1.369	0.467	0.735			
187-03-94	1990	0.954	1.478	0.758	1.094	9.999					
189-02-94	1982	0.580	1.363	1.064	0.719	1.412	0.785	1.192	0.749		
189-02-94	1990	0.738	0.990	0.918	1.583	9.999					
189-02-94	1981	0.458	1.230	1.274	1.128	0.756	0.956	1.136	0.718	0.864	
189-02-	199	0.72	1.15	1.32	1.09	9.99					

94	0	1	2	3	6	9					
189-05-94	1982	0.684	1.016	1.097	1.248	1.201	0.805	0.363	0.644		
189-05-94	1990	0.980	1.731	0.905	1.151	9.999					
190-01-94	1980	1.329	0.768	0.460	0.811	1.580	1.546	0.740	0.572	0.447	0.721
190-01-94	1990	1.055	0.937	1.290	1.229	9.999					
305-01-94	1979	0.208									
305-01-94	1980	0.799	1.071	1.360	1.176	1.004	1.086	0.817	0.675	0.533	0.644
305-01-94	1990	1.376	0.756	1.543	1.128	9.999					
305-02-94	1981	0.395	1.421	1.089	1.183	0.966	0.480	1.110	1.074	1.199	
305-02-94	1990	1.072	0.719	0.631	1.465	9.999					
305-03-94	1981	0.672	1.366	0.586	1.153	1.203	1.093	0.939	0.809	0.851	
305-03-94	1990	0.895	1.101	0.763	1.473	9.999					
305-04-94	1979	0.854									
305-04-94	1980	1.009	1.007	1.031	1.128	1.103	1.189	0.742	0.837	0.738	0.753

UID	**Year**	**0**	**1**	**2**	**3**	**4**	**5**	**6**	**7**	**8**	**9**
305-04-94	1990	0.813	1.054	1.278	1.416	9.999					
311-02-94	1979	0.436									
311-02-94	1980	0.474	2.033	1.102	1.080	0.791	0.636	0.779	0.684	0.711	1.230
311-02-94	1990	1.089	1.446	1.213	1.031	9.999					
311-05-94	1981	0.391	1.993	0.753	0.878	0.824	0.838	1.061	0.809	1.132	
311-05-94	1990	1.244	0.937	0.919	1.150	9.999					
311-06-94	1982	1.051	1.132	0.354	1.215	1.301	0.970	1.144	0.820		
311-06-94	1990	0.689	0.938	0.763	1.971	9.999					
323-01-	197	1.19	0.20								

94	8	5	5								
323-01-94	1980	1.673	1.172	0.948	0.897	0.803	0.836	1.220	0.981	0.677	0.968
323-01-94	1990	1.019	1.083	1.169	1.022	9.999					
323-04-94	1985	0.968	0.986	1.022	1.190	0.790					
323-04-94	1990	0.982	0.908	1.204	0.922	9.999					
469-03-94	1983	0.841	1.016	1.053	1.028	1.008	0.995	0.983			
469-03-94	1990	0.989	1.003	1.001	1.000	9.999					
469-05-94	1976	0.627	0.885	1.096	1.070						
469-05-94	1980	1.072	1.028	1.004	0.993	0.994	0.989	0.987	0.989	1.001	0.998
469-05-94	1990	1.002	1.001	1.000	0.995	9.999					
469-06-94	1981	0.823	1.032	1.076	0.998	1.006	1.012	0.997	0.991	0.991	
469-06-94	1990	0.998	1.000	1.001	1.000	9.999					
469-10-94	1980	0.657	1.037	1.110	1.013	1.011	1.014	1.000	0.990	0.997	0.990
469-10-94	1990	0.992	0.998	1.000	1.002	9.999					
469-11-94	1986	1.071	0.953	0.964	1.030						
469-11-94	1990	1.011	0.993	0.997	1.001	9.999					
004-05-97	1986	1.108	0.908	0.823	0.976						
004-05-97	1990	1.363	0.868	0.971	0.842	0.495	1.642	0.939	1.125	9.999	
004-05-97	1985	0.769	1.475	1.091	0.344	0.727					
004-05-97	1990	1.714	1.075	0.909	0.728	0.584	0.898	0.855	1.441	9.999	
005-01-97	1991	0.980	1.037	0.985	1.046	0.887	0.865	1.372	9.999		
005-01-97	1988	0.798	1.129								
005-01-97	1990	1.123	0.870	1.124	0.866	0.943	1.095	0.995	0.983	9.999	
005-03-	198	1.25	0.57	0.97	0.85						

UID	Year	0	1	2	3	4	5	6	7	8	9
97	6	7	7	3	9						
005-03-97	1990	1.080	1.191	1.201	1.175	1.075	1.071	0.824	1.099	9.999	
005-04-97	1994	0.972	1.033	0.984	0.983	9.999					
005-12-97	1983	1.087	1.297	0.257	0.822	1.412	1.298	1.039			
005-12-97	1990	0.824	0.869	0.826	0.836	1.090	1.076	1.144	1.102	9.999	
041-01-97	1978	0.849	1.034								
041-01-97	1980	1.198	0.486	1.608	1.325	0.958	0.606	0.667	0.730	0.627	0.994
041-01-97	1990	1.260	1.125	1.472	1.055	1.009	0.917	0.952	9.999		
048-01-97	1985	1.049	0.652	1.076	1.326	1.032					
048-01-97	1990	1.017	0.807	0.697	0.857	0.852	1.422	1.037	9.999		
048-03-97	1983	1.075	0.681	0.928	1.518	1.212	0.801	0.622			
048-03-97	1990	0.371	0.913	0.916	1.438	1.472	0.869	0.763	9.999		
050-01-97	1978	0.561	1.020								
050-01-97	1980	0.561	1.680	1.592	1.007	0.510	0.969	0.679	0.665	0.832	1.136
050-01-97	1990	0.975	1.085	1.259	1.038	1.136	0.868	1.157	9.999		
072-01-97	1988	1.180	1.022								
072-01-97	1990	0.857	1.075	0.949	1.038	1.004	1.008	0.987	9.999		
072-01-97	1988	1.396	0.932								
072-01-97	1990	0.766	1.072	1.050	1.003	1.008	0.991	0.990	9.999		
072-02-97	1987	1.222	0.950	0.933							
072-02-97	1990	1.011	0.986	1.032	0.997	1.009	1.000	0.990	9.999		
072-02-97	1985	1.148	1.031	0.948	1.011	0.934					
072-02-	199	0.96	0.99	1.04	1.02	1.02	0.99	0.97	9.99		

97	0	2	2	3	0	6	5	5	9		
108-03-97	1986	0.699	0.851	1.321	0.894						
108-03-97	1990	1.030	1.000	0.985	1.094	0.876	0.749	1.381	9.999		
119-01-97	1987	0.487	1.461	1.212							
119-01-97	1990	0.381	1.163	1.050	1.038	1.070	0.889	0.945	9.999		
129-02-97	1979	0.938									
129-02-97	1980	0.375	0.755	1.690	1.556	0.479	0.517	1.508	0.902	1.646	0.763
129-02-97	1990	0.601	0.443	0.636	0.874	1.332	1.312	1.471	9.999		
154-02-97	1978	1.085	1.057								
154-02-97	1980	1.003	0.830	0.917	0.635	0.969	0.686	1.249	1.170	1.546	0.785
154-02-97	1990	1.307	1.163	1.057	1.208	0.921	0.665	1.170	9.999		
155-03-97	1986	0.887	0.734	1.402	1.132						
155-03-97	1990	0.877	0.739	0.959	0.835	1.079	1.320	0.906	9.999		
164-04-97	1978	0.420	1.277								
164-04-97	1980	1.300	1.341	1.234	0.704	0.627	0.617	0.593	1.102	1.108	0.676
164-04-97	1990	1.165	1.375	1.070	1.218	0.521	1.618	0.650	9.999		
165-05-97	1977	0.537	1.774	1.068							
165-05-97	1980	0.975	0.715	0.764	0.850	0.873	0.742	0.718	1.289	1.162	0.774
165-05-97	1990	1.495	1.046	1.033	1.113	0.816	1.164	0.855	9.999		
165-06-97	1985	0.461	1.667	0.899	0.828	1.186					
165-06-97	1990	0.539	1.310	1.122	1.171	0.563	0.855	1.423	9.999		
220-04-97	1979	0.551									
220-04-97	1980	1.267	1.562	1.193	0.642	0.670	0.735	0.747	0.978	1.216	1.282
220-04-	199	0.69	1.47	1.07	0.91	1.15	0.86	1.16	9.99		

UID	Year	0	1	2	3	4	5	6	7	8	9
97	0	0	2	3	7	3	2	1	9		
220-05-97	1981	0.475	1.789	1.166	0.735	0.872	0.482	0.682	1.233	1.034	
220-05-97	1990	1.315	1.031	1.149	1.152	0.847	1.233	0.829	9.999		
220-06-97	1981	0.522	1.265	1.237	1.272	0.769	0.982	0.998	0.686	0.865	
220-06-97	1990	0.783	0.851	1.233	1.141	1.282	1.249	0.757	9.999		
220-08-97	1986	0.944	0.992	1.300	0.695						
220-08-97	1990	0.983	1.137	0.857	1.122	0.865	0.946	1.151	9.999		
220-09-97	1985	0.603	0.889	1.576	1.018	1.000					
220-09-97	1990	0.549	0.906	0.977	1.235	1.107	0.501	1.365	9.999		
233-01-97	1982	1.063	0.961	1.106	0.935	0.689	0.859	0.958	1.456		
233-01-97	1990	0.748	1.138	0.990	1.535	1.033	0.696	1.110	9.999		
233-02-97	1986	0.840	1.144	1.063	1.065						
233-02-97	1990	0.962	0.899	0.689	1.115	1.057	1.030	1.075	9.999		
233-02-97	1983	0.513	1.063	1.246	1.128	1.190	0.971	0.635			
233-02-97	1990	0.598	1.046	0.830	1.352	1.186	0.678	1.329	9.999		
233-03-97	1990	0.923	1.086	1.067	0.831	0.921	1.160	0.968	9.999		
233-04-97	1991	0.976	1.036	1.033	0.912	0.998	1.051	9.999			
233-06-97	1992	1.000	1.004	0.982	1.029	0.983	9.999				
255-01-97	1980	0.781	0.696	1.615	1.276	0.879	0.719	0.883	0.595	1.145	1.113
255-01-97	1990	0.742	1.500	0.936	0.879	1.129	9.999				
255-02-97	1981	0.413	1.252	0.968	1.418	1.191	0.734	0.540	0.870	0.687	
255-02-97	1990	1.712	0.798	0.908	1.081	1.081	9.999				
255-03-	198	0.55	1.46	0.89	0.65	1.19	1.34	1.03	0.47		

97	2	3	2	7	2	0	2	7	6		
255-03-97	1990	1.192	1.048	0.686	0.962	1.280	9.999				
275-02-97	1981	0.271	1.395	0.941	1.478	1.043	0.869	0.816	0.699	1.174	
275-02-97	1990	0.921	0.706	0.858	1.259	1.122	1.266	0.945	9.999		
275-04-97	1980	0.526	0.978	1.565	1.051	1.212	0.860	0.625	0.849	0.945	1.192
275-04-97	1990	0.878	0.849	0.826	1.156	1.303	0.919	1.091	9.999		
276-05-97	1985	0.769	1.237	0.931	1.201	0.967					
276-05-97	1990	0.873	1.037	0.840	0.679	1.280	0.891	1.342	9.999		
276-06-97	1984	1.088	0.890	0.808	1.041	1.180	1.202				
276-06-97	1990	0.911	0.884	0.711	0.951	1.027	0.834	1.446	9.999		
009-01-99	1995	1.009	0.982	0.984	1.048	0.967					
009-01-99	2000	9.999									
009-01-99	1991	0.981	0.820	1.283	1.281	0.426	0.728	1.334	1.063	0.898	
009-01-99	2000	9.999									
011-01-99	1987	0.990	1.155	0.678							
011-01-99	1990	1.337	0.773	0.992	0.849	1.154	1.094	1.005	1.003	0.799	1.205
011-01-99	2000	9.999									
011-01-99	1986	0.765	0.932	1.512	0.886						
011-01-99	1990	1.071	0.883	0.851	0.658	1.154	1.044	0.984	0.812	0.847	1.382
011-01-99	2000	9.999									
019-02-99	1994	0.859	1.362	0.483	1.061	1.210	0.917				
019-02-99	2000	9.999									
019-07-99	1992	1.133	0.881	0.557	1.733	0.477	0.915	1.182	0.973		
019-07-	200	9.99									

99	0	9									
021-01-99	1989	0.655									
021-01-99	1990	0.964	1.097	1.176	0.938	0.880	0.869	0.935	1.157	1.014	9.999
022-03-99	1983	0.489	1.539	0.821	1.416	1.134	0.835	0.399			
022-03-99	1990	0.501	0.760	1.861	1.321	0.871	0.695	0.916	1.091	1.094	9.999

UID	Year	0	1	2	3	4	5	6	7	8	9
034-04-99	1982	1.128	0.420	0.846	1.678	1.328	0.990	0.864	0.447		
034-04-99	1990	0.571	1.169	0.748	1.108	1.048	1.129	1.235	0.986	0.962	9.999
123-01-99	1984	0.538	1.334	1.233	1.034	1.003	0.930				
123-01-99	1990	0.613	0.920	0.773	1.228	0.869	1.309	0.969	1.112	9.999	
125-06-99	1986	1.114	0.743	1.181	0.935						
125-06-99	1990	0.977	1.159	1.068	0.770	0.732	1.106	0.598	1.425	0.965	9.999
210-01-99	1980	0.399	1.455	0.876	1.154	0.667	1.728	1.184	0.696	0.703	0.647
210-01-99	1990	0.883	0.988	1.463	0.646	0.978	1.066	1.216	1.027	1.128	9.999
284-01-99	1989	0.905									
284-01-99	1990	0.945	1.130	1.162	0.794	1.012	0.881	0.765	1.525	0.763	9.999
295-05-99	1987	1.143	0.618	0.942							
295-05-99	1990	1.312	1.061	1.095	0.854	0.711	0.854	1.247	1.269	0.738	9.999
305-02-99	1987	1.029	0.918	1.026							
305-02-99	1990	1.109	0.909	0.978	1.060	1.057	0.927	0.814	0.891	1.332	9.999
305-02-99	1987	0.375	1.529	0.986							
305-02-99	1990	0.985	1.148	0.821	0.898	1.094	0.957	0.912	1.043	1.102	9.999
305-03-99	1985	0.711	1.347	1.012	1.076	0.871					
305-03-	199	0.93	1.08	0.74	1.29	1.01	0.54	1.38	0.51	1.36	9.99

99	0	8	6	3	1	6	8	4	4	6	9
305-03-	198	0.38	1.14	1.37	1.04	1.09	0.89	0.86			
99	3	3	9	8	9	7	6	8			
305-03-	199	1.17	0.82	0.62	0.83	1.14	1.13	1.09	0.98	1.12	9.99
99	0	4	6	2	2	2	4	7	7	4	9
305-04-	199	0.97	1.05	0.88	1.21	0.79	0.93	1.13	9.99		
99	2	2	4	7	4	0	6	2	9		
305-04-	199	0.97	1.08	0.71	1.20	0.93	1.20	0.86	0.77	1.22	9.99
99	0	3	7	9	2	7	7	2	9	2	9
307-02-	198	0.97	0.92	1.28	0.83	0.96	1.19	0.83			
99	3	4	7	4	4	8	7	9			
307-02-	199	0.86	0.60	1.13	1.25	1.23	0.96	0.70	0.91	1.23	9.99
99	0	6	6	6	4	2	9	4	2	9	9
307-02-	198	0.39	1.13	1.20	1.62	0.61	1.03				
99	4	1	2	9	2	8	5				
307-02-	199	0.86	0.84	0.59	1.16	1.12	0.60	1.25	1.09	1.02	9.99
99	0	8	8	2	9	3	0	1	1	8	9
307-03-	199	0.95	1.14	0.72	1.31	0.73	1.09	9.99			
99	3	0	4	2	6	2	6	9			
307-03-	199	0.84	1.16	0.70	1.29	0.79	1.32	0.69	1.01	1.04	9.99
99	0	6	5	8	6	4	2	0	6	5	9
310-01-	198	1.03	1.08	1.01	0.73	1.08	0.59	0.97			
99	3	3	4	0	6	7	3	6			
310-01-	199	0.94	1.97	0.81	1.08	0.77	0.74	0.92	1.33	1.00	9.99
99	0	6	4	0	4	5	7	6	3	3	9
310-01-	198	0.15	1.41	1.50	1.17	0.95	0.67	0.53	0.92		
99	2	9	5	0	2	2	2	1	3		
310-01-	199	1.07	1.14	0.99	0.99	0.97	1.02	1.18	9.99		
99	0	8	3	5	6	8	6	4	9		
310-02-	198	0.92	1.25	0.90	0.57						
99	6	8	6	5	7						
310-02-	199	1.45	0.78	1.02	1.02	1.05	1.15	0.84	0.80	1.15	9.99
99	0	5	2	2	0	8	5	9	2	8	9
310-02-	198	0.29	1.53	1.31	0.89	0.85	0.85				
99	4	1	7	8	8	7	1				
310-02-	199	0.67	0.86	1.01	1.26	1.07	1.19	0.87	9.99		
99	0	0	3	5	9	4	2	2	9		
323-01-	198	0.25	1.88	1.05	0.97	0.90	0.57	0.00			
99	3	0	9	8	1	2	1	7			

Table 7. Chronology data statistics for live-collected *Hemimactra (Spisula) solidissima*. Columns include unique specimen identification, first and last years,

number of years (age), mean index value, median index value, index standard deviation, and index skew, mean sensitivity, and first order autocorrelation.

UID	first	last	Age	mean	median	stdev	skew	sens	ar1
001-01-94	1976	1993	18	1.918	2.175	0.713	-1.11	0.142	0.771
001-01-94	1976	1993	18	1.679	1.841	0.638	-0.639	0.131	0.768
001-02-94	1985	1993	9	1.633	1.786	0.582	-0.702	0.196	0.537
001-02-94	1977	1993	17	1.752	2.099	0.768	-0.96	0.183	0.799
001-03-94	1979	1993	15	1.787	2.037	0.65	-1.167	0.159	0.714
001-03-94	1976	1993	18	1.583	1.911	0.712	-0.577	0.112	0.859
001-04-94	1969	1993	25	1.835	2.049	0.635	-1.082	0.095	0.829
003-01-92	1972	1991	20	1.692	1.974	0.65	-1.03	0.117	0.818
004-05-97	1985	1996	12	0.151	0.09	0.145	1.012	0.457	0.589
004-05-97	1984	1996	13	0.143	0.097	0.124	0.829	0.563	0.549
005-01-97	1990	1996	7	0.295	0.299	0.229	0.066	0.44	0.659
005-01-97	1987	1996	10	0.189	0.162	0.082	0.17	0.279	0.529
005-02-92	1988	1991	4	0.363	0.392	0.167	-0.283	0.541	-0.153
005-03-97	1985	1996	12	0.179	0.085	0.237	2.134	0.301	0.263
005-04-97	1993	1996	4	0.364	0.381	0.193	-0.19	0.652	-0.026
005-05-92	1983	1991	9	0.212	0.133	0.226	1.597	0.373	0.3
005-12-97	1982	1996	15	0.141	0.07	0.148	1.255	0.365	0.515
009-01-99	1994	1998	5	0.285	0.298	0.039	-0.576	0.152	-0.356
009-01-99	1990	1998	9	0.156	0.172	0.07	0.032	0.439	0.301
011-01-99	1986	1998	13	0.184	0.08	0.181	1.042	0.321	0.631
011-01-99	1985	1998	14	0.176	0.108	0.158	0.937	0.375	0.748
015-02-02	1990	2001	12	1.239	1.32	0.701	-0.316	0.297	0.769
016-02-94	1981	1993	13	0.132	0.079	0.137	0.913	0.466	0.765
018-01-92	1981	1991	11	0.201	0.131	0.186	1.595	0.317	0.317
018-03-92	1986	1991	6	0.277	0.229	0.152	0.723	0.444	0.097
018-04-92	1988	1991	4	0.302	0.31	0.109	-0.183	0.32	0.001
018-05-92	1984	1991	8	0.289	0.25	0.18	0.531	0.439	0.261
019-01-02	1992	2001	10	1.184	1.306	0.639	-0.286	0.256	0.737
019-02-02	1984	2001	18	1.736	2.095	0.784	-0.992	0.192	0.812
019-02-99	1993	1998	6	0.322	0.188	0.277	0.768	0.562	0.201
019-06-02	1992	2001	10	1.315	1.485	0.596	-0.527	0.223	0.693
019-07-02	1989	2001	13	1.487	1.764	0.778	-0.49	0.221	0.789
019-07-02	1985	2001	17	1.429	1.771	0.751	-0.619	0.193	0.843
019-07-99	1991	1998	8	0.24	0.188	0.206	1.693	0.527	-0.159
019-10-02	1989	2001	13	0.901	1.01	0.488	-0.421	0.24	0.792
021-01-99	1989	1998	10	0.196	0.162	0.12	0.557	0.382	0.578
022-03-99	1983	1998	16	0.128	0.072	0.111	1.203	0.45	0.538
UID	**first**	**last**	**Age**	**mean**	**median**	**stdev**	**skew**	**sens**	**ar1**
033-08-94	1979	1993	15	0.133	0.098	0.099	0.843	0.404	0.59

033-09-94	1979	1993	15	0.161	0.071	0.166	1.029	0.266	0.681
033-09-94	1981	1993	13	0.169	0.071	0.188	1.455	0.444	0.636
033-23-94	1977	1993	17	0.143	0.056	0.15	0.877	0.305	0.75
033-23-94	1978	1993	16	0.145	0.088	0.132	0.781	0.357	0.684
034-04-99	1982	1998	17	0.134	0.08	0.11	1.299	0.388	0.65
041-01-97	1978	1996	19	0.136	0.07	0.122	0.958	0.334	0.653
048-01-97	1985	1996	12	0.161	0.136	0.106	0.559	0.355	0.729
048-03-97	1983	1996	14	0.144	0.109	0.107	0.781	0.446	0.652
050-01-97	1978	1996	19	0.14	0.068	0.141	1.54	0.358	0.671
060-01-02	1984	2001	18	0.103	0.073	0.094	2.083	0.364	0.495
072-01-97	1988	1996	9	1.049	1.026	0.652	-0.088	0.328	0.701
072-01-97	1988	1996	9	1.224	1.488	0.69	-0.375	0.275	0.718
072-02-97	1987	1996	10	0.994	1.105	0.569	-0.275	0.286	0.74
072-02-97	1985	1996	12	1.315	1.296	0.78	-0.033	0.21	0.802
077-01-02	1987	2001	15	0.17	0.181	0.105	0.113	0.241	0.818
078-01-02	1982	2001	20	0.098	0.075	0.071	2.461	0.337	0.192
078-02-02	1979	2001	23	0.097	0.07	0.101	2.079	0.363	0.703
108-03-97	1986	1996	11	0.161	0.185	0.089	-0.119	0.381	0.536
114-01-92	1987	1991	5	0.241	0.245	0.121	0.452	0.514	-0.251
114-02-92	1988	1991	4	0.349	0.341	0.189	0.092	0.519	-0.04
114-03-92	1988	1991	4	0.304	0.261	0.208	0.418	0.561	0.118
114-04-92	1988	1991	4	0.315	0.311	0.164	0.056	0.469	0.124
119-01-97	1987	1996	10	0.181	0.229	0.089	-0.422	0.538	0.006
120-11-94	1986	1993	8	0.125	0.146	0.065	-0.27	0.463	0.104
123-01-99	1984	1997	14	0.135	0.07	0.121	0.853	0.357	0.771
125-06-99	1986	1998	13	0.175	0.123	0.135	0.923	0.409	0.562
129-02-97	1979	1996	18	0.119	0.084	0.102	0.919	0.468	0.468
136-01-92	1989	1991	3	0.529	0.485	0.24	0.176	0.451	-0.017
136-02-92	1989	1991	3	0.431	0.456	0.138	-0.175	0.334	-0.016
141-01-92	1979	1991	13	0.175	0.108	0.154	0.846	0.334	0.793
141-02-92	1983	1991	9	0.199	0.11	0.166	0.694	0.503	0.594
141-02-92	1980	1991	12	0.165	0.11	0.124	0.448	0.314	0.795
141-04-92	1981	1991	11	0.193	0.132	0.141	0.549	0.377	0.719
145-01-92	1978	1991	14	0.148	0.052	0.183	1.533	0.451	0.679
145-02-92	1978	1991	14	0.147	0.074	0.153	1.192	0.468	0.701
145-03-92	1979	1991	13	0.164	0.082	0.144	0.887	0.387	0.717
145-04-92	1980	1991	12	0.152	0.104	0.129	0.766	0.296	0.733
145-04-92	1981	1991	11	0.187	0.101	0.173	1.485	0.509	0.514
145-05-92	1979	1991	13	0.162	0.065	0.189	1.636	0.446	0.547
145-07-92	1981	1991	11	0.167	0.108	0.132	1.026	0.403	0.638
145-08-92	1980	1991	12	0.142	0.1	0.128	1.157	0.412	0.522
UID	**first**	**last**	**Age**	**mean**	**median**	**stdev**	**skew**	**sens**	**ar1**
145-09-92	1981	1991	11	0.139	0.144	0.104	0.643	0.311	0.72

154-02-97	1978	1996	19	0.11	0.05	0.13	1.714	0.334	0.702
155-03-97	1986	1996	11	0.218	0.161	0.162	0.948	0.337	0.636
161-01-94	1979	1991	13	0.173	0.093	0.139	0.493	0.281	0.797
161-05-94	1982	1993	12	0.14	0.102	0.113	1.062	0.456	0.344
161-05-94	1977	1993	17	0.128	0.054	0.158	1.627	0.413	0.712
161-08-94	1979	1993	15	0.139	0.119	0.132	1.03	0.477	0.734
161-09-94	1981	1993	13	0.144	0.122	0.114	0.797	0.292	0.741
162-01-94	1979	1991	13	0.182	0.098	0.221	1.937	0.405	0.462
162-02-94	1982	1993	12	0.165	0.094	0.177	1.468	0.368	0.522
162-02-94	1978	1991	14	0.138	0.11	0.108	0.882	0.347	0.754
162-03-94	1981	1993	13	0.155	0.089	0.136	1.222	0.351	0.478
162-03-94	1978	1991	14	0.141	0.121	0.097	0.505	0.317	0.674
162-04-94	1982	1993	12	0.156	0.075	0.234	2.167	0.543	0.239
162-04-94	1987	1993	7	0.219	0.248	0.062	-1.162	0.201	0.267
162-04-94	1984	1991	8	0.191	0.204	0.071	-0.128	0.319	0.265
162-04-94	1981	1991	11	0.172	0.117	0.127	0.448	0.355	0.823
163-02-94	1981	1993	13	0.156	0.089	0.117	0.887	0.319	0.696
163-02-94	1978	1991	14	0.134	0.069	0.143	1.431	0.361	0.592
163-06-94	1981	1991	11	0.122	0.099	0.085	0.526	0.404	0.562
164-04-97	1978	1996	19	0.09	0.06	0.077	1.206	0.438	0.751
165-05-97	1977	1996	20	0.151	0.1	0.144	2.474	0.345	0.559
165-06-97	1985	1996	12	0.165	0.178	0.094	0.035	0.518	0.1
167-01-94	1978	1993	16	0.118	0.058	0.14	1.926	0.306	0.531
167-02-94	1979	1993	15	0.142	0.07	0.17	1.736	0.451	0.566
167-04-94	1977	1993	17	0.123	0.063	0.124	1.135	0.382	0.604
167-06-94	1985	1993	9	0.197	0.187	0.072	0.187	0.204	0.589
167-06-94	1979	1991	13	0.132	0.12	0.072	0.277	0.31	0.707
167-07-94	1982	1993	12	0.168	0.162	0.082	0.475	0.312	0.467
167-07-94	1978	1991	14	0.139	0.152	0.074	0.373	0.303	0.625
167-08-94	1982	1993	12	0.14	0.102	0.099	0.215	0.29	0.82
167-08-94	1979	1991	13	0.131	0.105	0.077	0.574	0.386	0.525
181-01-94	1980	1996	17	0.132	0.066	0.118	0.944	0.278	0.873
181-14-94	1981	1993	13	0.143	0.092	0.123	0.867	0.33	0.754
181-16-94	1981	1993	13	0.189	0.086	0.249	2.115	0.499	0.351
187-01-94	1984	1993	10	0.148	0.124	0.113	1.732	0.411	0.169
187-03-94	1983	1993	11	0.119	0.069	0.081	0.602	0.474	0.441
189-02-94	1982	1993	12	0.187	0.161	0.131	0.438	0.442	0.451
189-02-94	1981	1993	13	0.144	0.082	0.123	0.639	0.361	0.714
189-05-94	1982	1993	12	0.163	0.105	0.139	0.555	0.411	0.783
190-01-94	1980	1993	14	0.116	0.074	0.113	1.351	0.397	0.67
200-01-02	1989	2001	13	0.148	0.13	0.103	0.503	0.356	0.486
UID	**first**	**last**	**Age**	**mean**	**median**	**stdev**	**skew**	**sens**	**ar1**
202-03-02	1988	2001	14	0.149	0.065	0.142	0.954	0.368	0.681

210-01-99	1980	1998	19	0.104	0.067	0.09	1.09	0.386	0.544
220-04-97	1979	1996	18	0.104	0.055	0.119	1.471	0.338	0.804
220-05-97	1981	1996	16	0.116	0.05	0.145	2.105	0.383	0.555
220-06-97	1981	1996	16	0.128	0.067	0.117	0.906	0.288	0.781
220-08-97	1986	1996	11	0.169	0.157	0.114	0.557	0.236	0.667
220-09-97	1985	1996	12	0.127	0.082	0.098	1.224	0.487	0.582
227-03-02	1985	2001	17	0.082	0.061	0.051	0.781	0.237	0.675
227-05-02	1990	2001	12	0.139	0.122	0.071	0.701	0.318	0.646
228-02-02	1987	2001	15	0.112	0.082	0.084	0.993	0.364	0.703
229-10-02	1983	2001	19	0.11	0.078	0.09	0.73	0.245	0.833
233-01-97	1982	1996	15	0.154	0.081	0.171	1.297	0.362	0.683
233-02-97	1986	1996	11	0.183	0.137	0.125	0.389	0.253	0.817
233-02-97	1983	1996	14	0.149	0.085	0.126	0.654	0.418	0.801
233-03-97	1990	1996	7	0.231	0.177	0.145	0.282	0.349	0.614
233-04-97	1991	1996	6	0.301	0.298	0.165	-0.011	0.308	0.582
233-06-97	1992	1996	5	0.327	0.33	0.067	-0.423	0.143	0.258
255-01-92	1979	1991	13	0.077	0.06	0.045	1.039	0.29	0.637
255-01-97	1980	1994	15	0.121	0.08	0.103	1.326	0.388	0.681
255-02-92	1988	1996	9	0.168	0.117	0.105	0.552	0.382	0.684
255-02-97	1981	1994	14	0.115	0.068	0.09	0.913	0.442	0.63
255-03-92	1986	1996	11	0.161	0.145	0.064	0.582	0.246	0.577
255-03-97	1982	1994	13	0.116	0.11	0.071	0.6	0.479	0.453
260-03-02	1988	2001	14	0.167	0.14	0.112	0.264	0.334	0.658
275-02-97	1981	1996	16	0.172	0.105	0.153	0.922	0.391	0.633
275-04-97	1980	1996	17	0.184	0.133	0.156	1.15	0.297	0.762
276-05-97	1985	1996	12	0.2	0.185	0.144	0.349	0.375	0.758
276-06-97	1984	1996	13	0.166	0.19	0.104	0.139	0.275	0.812
283-04-02	1985	2001	17	0.113	0.056	0.112	1.148	0.365	0.691
283-05-02	1988	2001	14	0.123	0.102	0.077	0.963	0.41	0.48
283-06-02	1991	2001	11	0.156	0.133	0.122	0.609	0.426	0.657
284-01-99	1989	1998	10	0.21	0.203	0.121	0.378	0.405	0.634
295-05-99	1987	1998	12	0.177	0.152	0.106	0.413	0.388	0.656
305-01-94	1979	1993	15	0.137	0.078	0.117	0.653	0.502	0.775
305-02-94	1981	1993	13	0.145	0.152	0.087	0.281	0.454	0.44
305-02-99	1987	1998	12	0.157	0.152	0.095	0.197	0.2	0.751
305-02-99	1987	1998	12	0.113	0.108	0.068	0.297	0.338	0.411
305-03-94	1981	1993	13	0.133	0.109	0.092	0.474	0.441	0.617
305-03-99	1985	1998	14	0.154	0.145	0.098	0.673	0.48	0.701
305-03-99	1983	1998	16	0.125	0.072	0.095	0.62	0.277	0.756
305-04-94	1979	1993	15	0.149	0.117	0.108	0.117	0.216	0.887
305-04-99	1992	1998	7	0.217	0.262	0.112	-0.143	0.349	0.469
UID	**first**	**last**	**Age**	**mean**	**median**	**stdev**	**skew**	**sens**	**ar1**
305-04-99	1990	1998	9	0.17	0.15	0.093	0.313	0.418	0.414

307-02-99	1983	1998	16	0.125	0.07	0.106	0.869	0.291	0.763
307-02-99	1984	1998	15	0.103	0.069	0.075	1.273	0.452	0.522
307-03-99	1993	1998	6	0.255	0.245	0.121	0.131	0.536	-0.128
307-03-99	1990	1998	9	0.181	0.149	0.1	0.553	0.509	0.092
310-01-99	1983	1998	16	0.139	0.07	0.154	1.351	0.372	0.689
310-01-99	1982	1996	15	0.135	0.07	0.137	1.125	0.354	0.665
310-02-99	1986	1998	13	0.146	0.153	0.051	0.329	0.318	0.138
310-02-99	1984	1996	13	0.142	0.064	0.139	1.214	0.364	0.566
311-02-94	1979	1993	15	0.144	0.083	0.172	1.724	0.404	0.519
311-05-94	1981	1993	13	0.15	0.078	0.197	2.195	0.42	0.297
311-06-94	1982	1993	12	0.145	0.106	0.106	0.546	0.491	0.585
319-02-02	1983	2001	19	0.119	0.054	0.128	1.764	0.423	0.565
319-02-02	1984	2001	18	0.133	0.088	0.119	1.249	0.325	0.677
323-01-94	1978	1993	16	0.132	0.072	0.13	1.27	0.427	0.316
323-01-99	1983	1996	14	0.12	0.074	0.106	1.796	0.352	0.305
323-04-94	1985	1993	9	0.135	0.109	0.059	0.019	0.208	0.626
331-01-02	1991	2001	11	0.122	0.102	0.066	0.162	0.608	-0.328
334-01-02	1992	2001	10	0.142	0.143	0.068	0.404	0.537	-0.042
334-02-02	1994	2001	8	0.201	0.2	0.089	-0.431	0.541	0.004
340-07-02	1993	2001	9	0.172	0.133	0.095	0.679	0.342	0.63
340-10-02	1993	2001	9	0.212	0.162	0.144	0.589	0.362	0.595
340-10-02	1992	2001	10	0.179	0.149	0.1	0.135	0.429	0.218
346-02-02	1991	2001	11	0.155	0.102	0.107	0.755	0.392	0.621
356-04-02	1990	2001	12	0.115	0.083	0.084	0.714	0.41	0.709
356-26-02	1988	2001	14	0.124	0.111	0.071	0.316	0.352	0.598
357-02-02	1996	2001	6	0.175	0.152	0.1	0.324	0.536	0.269
413-26-99	1980	1998	19	0.087	0.058	0.07	1.461	0.245	0.799
413-38-99	1981	1998	18	0.095	0.06	0.077	1.352	0.377	0.743
413-57-99	1979	1998	20	0.078	0.053	0.062	1.5	0.249	0.83
421-01-99	1991	1998	8	0.168	0.148	0.097	0.775	0.431	0.358
421-14-99	1993	1998	6	0.177	0.162	0.098	0.608	0.519	0.221
432-08-99	1988	1998	11	0.078	0.07	0.036	0.396	0.284	0.664
432-12-99	1989	1998	10	0.121	0.097	0.086	1.651	0.494	0.041
469-03-94	1983	1993	11	1.29	1.457	0.393	-1.218	0.144	0.583
469-05-94	1976	1993	18	1.402	1.564	0.473	-1.19	0.126	0.742
469-06-94	1981	1993	13	1.368	1.524	0.4	-1.153	0.12	0.641
469-10-94	1980	1993	14	1.498	1.7	0.484	-1.301	0.146	0.642
469-11-94	1986	1993	8	0.859	0.898	0.459	-0.051	0.27	0.643
493-02-02	1986	2001	16	1.548	1.785	0.613	-0.923	0.142	0.781
493-10-02	1981	2001	21	1.327	1.55	0.579	-0.811	0.129	0.85

Table 8. Raw increment ring width data from Pliocene *S. confraga* valves collected from the coastal plain in Virginia. Measurements are in units of .001mm of the

thickness of increment ring width for each year. Unique identification displays valve. Numbers refer to increment age.

UID	1	2	3	4	5	6	7	8	9	10
SC001R	0.40	0.38	0.19	0.19	0.24	0.17	0.08	0.04	0.06	0.08
SC003L	0.22	0.16	0.31	0.47						
SC004R	0.20	0.19	0.29	0.18						
SC005R	0.24	0.36	0.16	0.20						
SC006R	0.39	0.20	0.17	0.10	0.12					
SC007R	0.32	0.22	0.07	0.21	0.12	0.16				
SC008R	0.38	0.04	0.12	0.15	0.12	0.02				
SC009L	0.27	0.28	0.22	0.12	0.13					
SC010L	0.34	0.15	0.17	0.13						
SC011R	0.49	0.22	0.29	0.14	0.11					
SC012L	0.32	0.17	0.20	0.11	0.16					
SC013L	0.19	0.20	0.25	0.15	0.02					
SC014L	0.15	0.21	0.17	0.18						
SC015R	0.16	0.34	0.20	0.21						
SC016R	0.21	0.29	0.16	0.12	0.16	0.08	0.09			
SC017L	0.21	0.15	0.23	0.12	0.09					
SC018L	0.20	0.19	0.13	0.08	0.05	0.07	0.08	0.17	0.12	

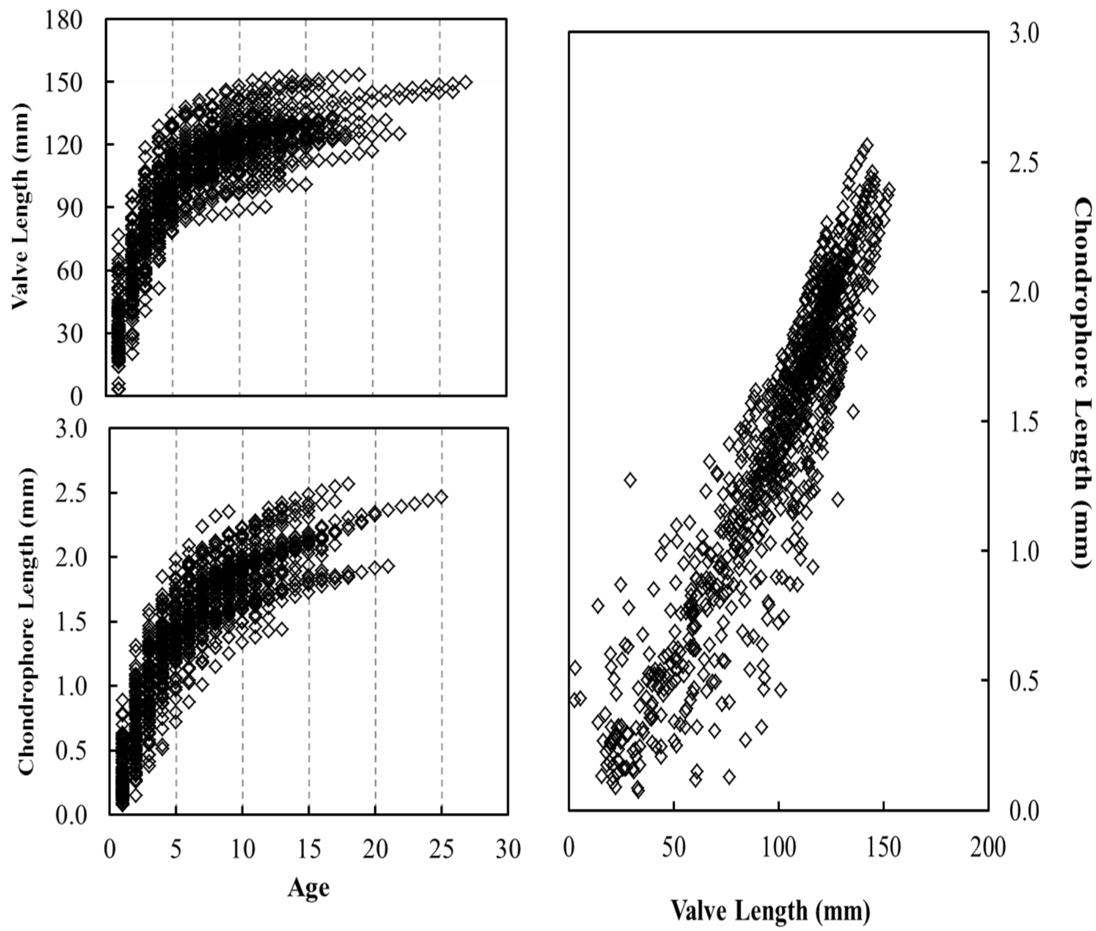

Figure 1. Comparison of valve and chronodrophore lengths (mm) against age for live-collected *Hemimactra (Spisula) solidissima* from along the mid-Atlantic Bight. Valve and chrondrophore length versus age display similar growth curves. Valve versus chondrophore length displays a linear relationship (R^2=0.84, p=1.64×10^{-20}).

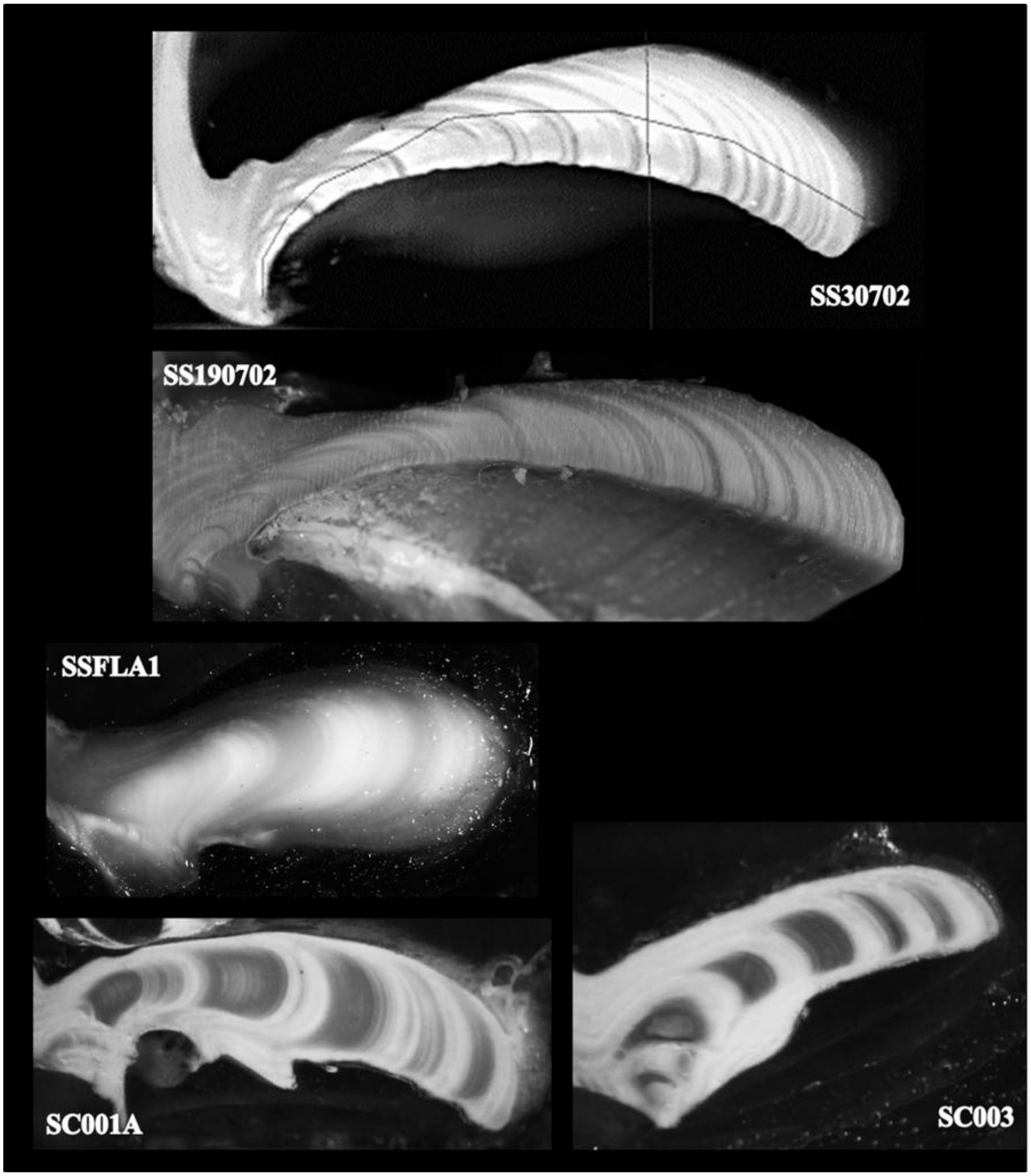

Figure 12. Black and white images of the Spisula chondrophore prior to sampling for isotopic analysis. SS30702 and SS190702 are *S. solidissima* (modern), SSFLA1 is *S.s.simlis*, (modern), and SC001A and SC003 are *S. confraga* (Pliocene).

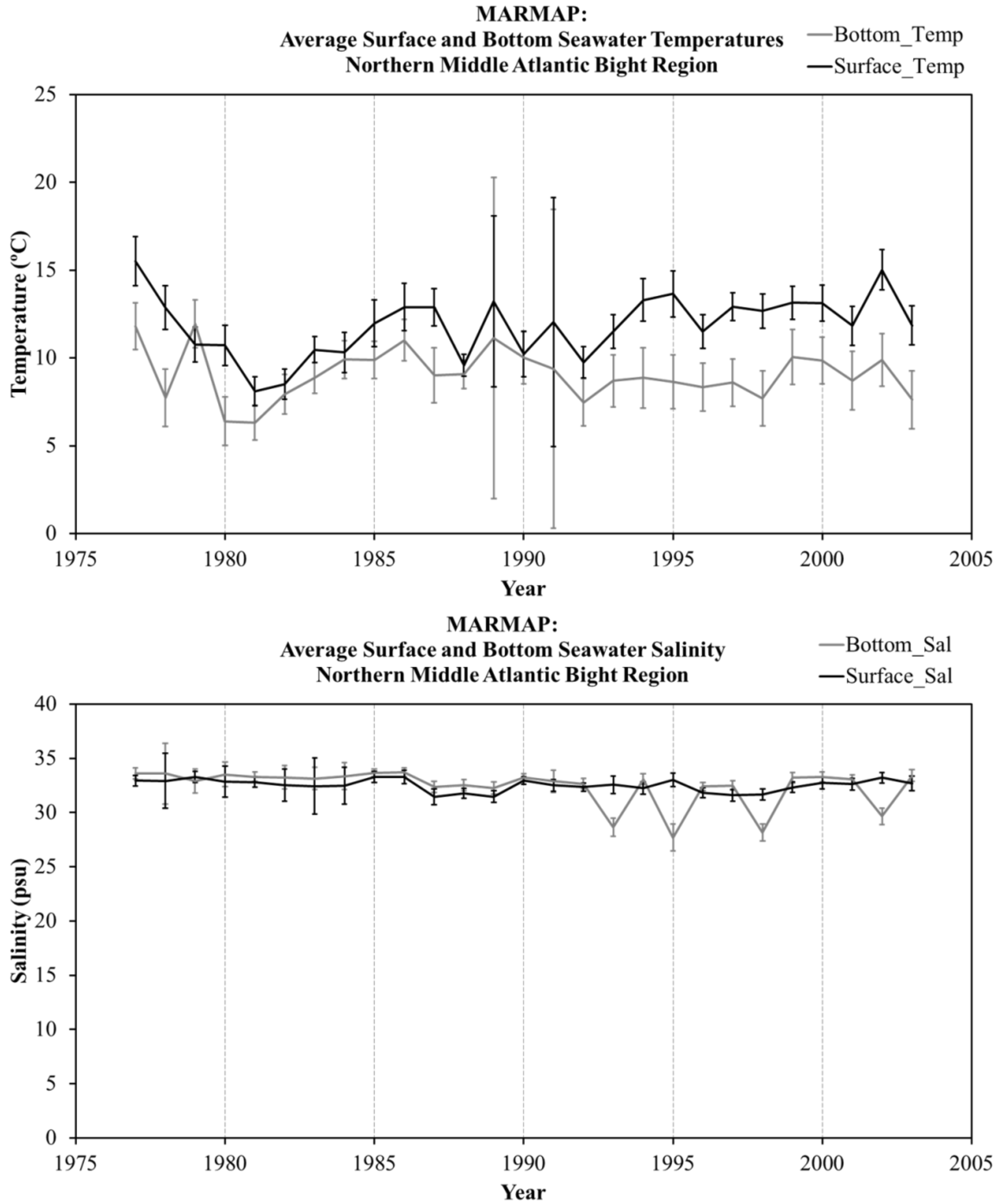

Figure 3. Mean average surface and bottom seawater temperature and salinity from the northern mid-Atlantic Bight. Data is from the Northeast Fisheries Science center (NEFSC) Marine Resources Monitoring, Assessment, and Prediction (MARMAP) program years 1977-2002.

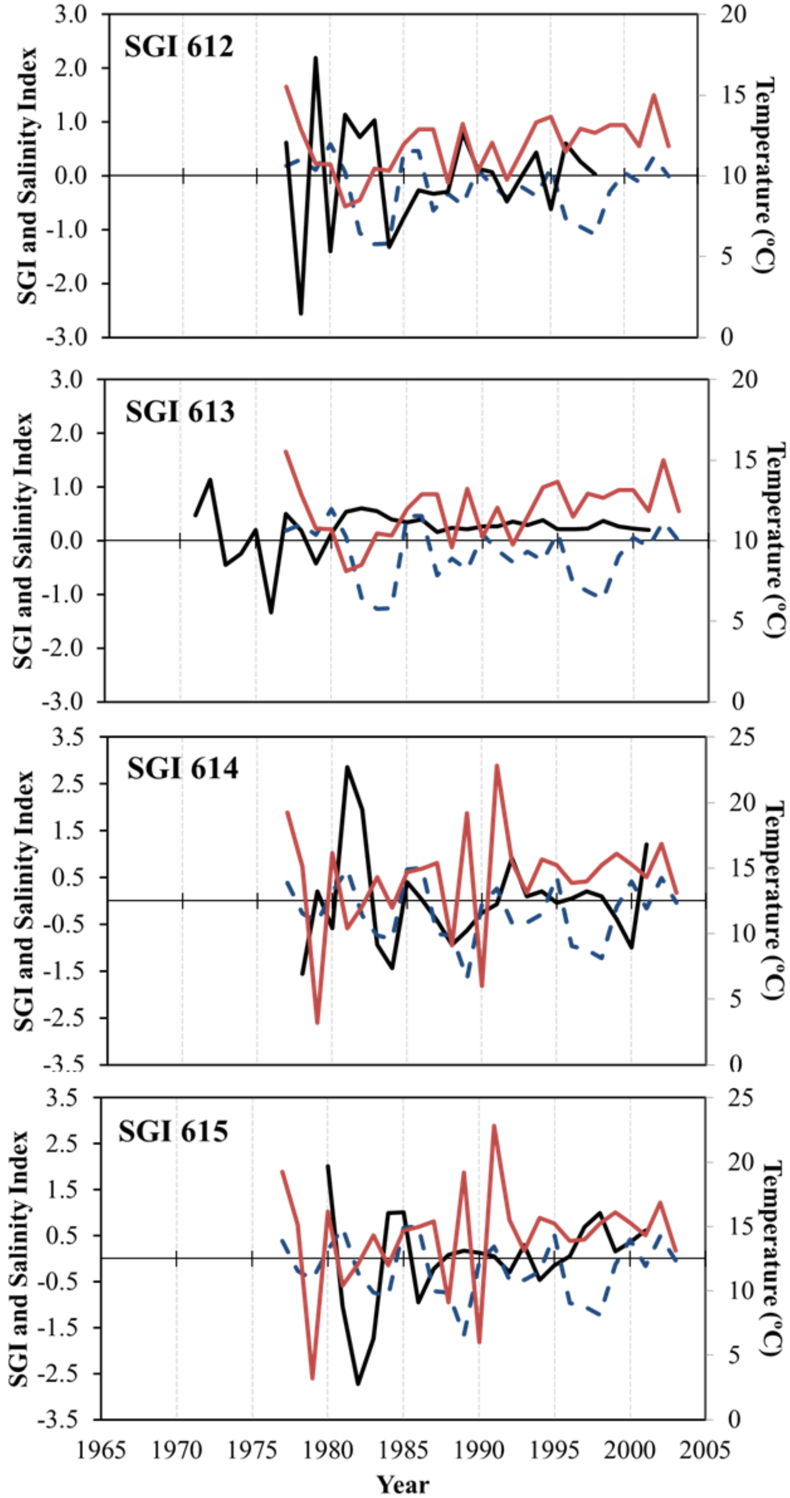

Figure 4. Standardized growth indices from the regional area chronologies in the New York Bight (612 & 613) and off the New Jersey shore (614 & 615) (black line) plotted with mean annual surface and bottom seawater temperatures (red line) and salinity (blue dashed line) from the northern mid-Atlantic Bight (NEFSC-MARMAP data).

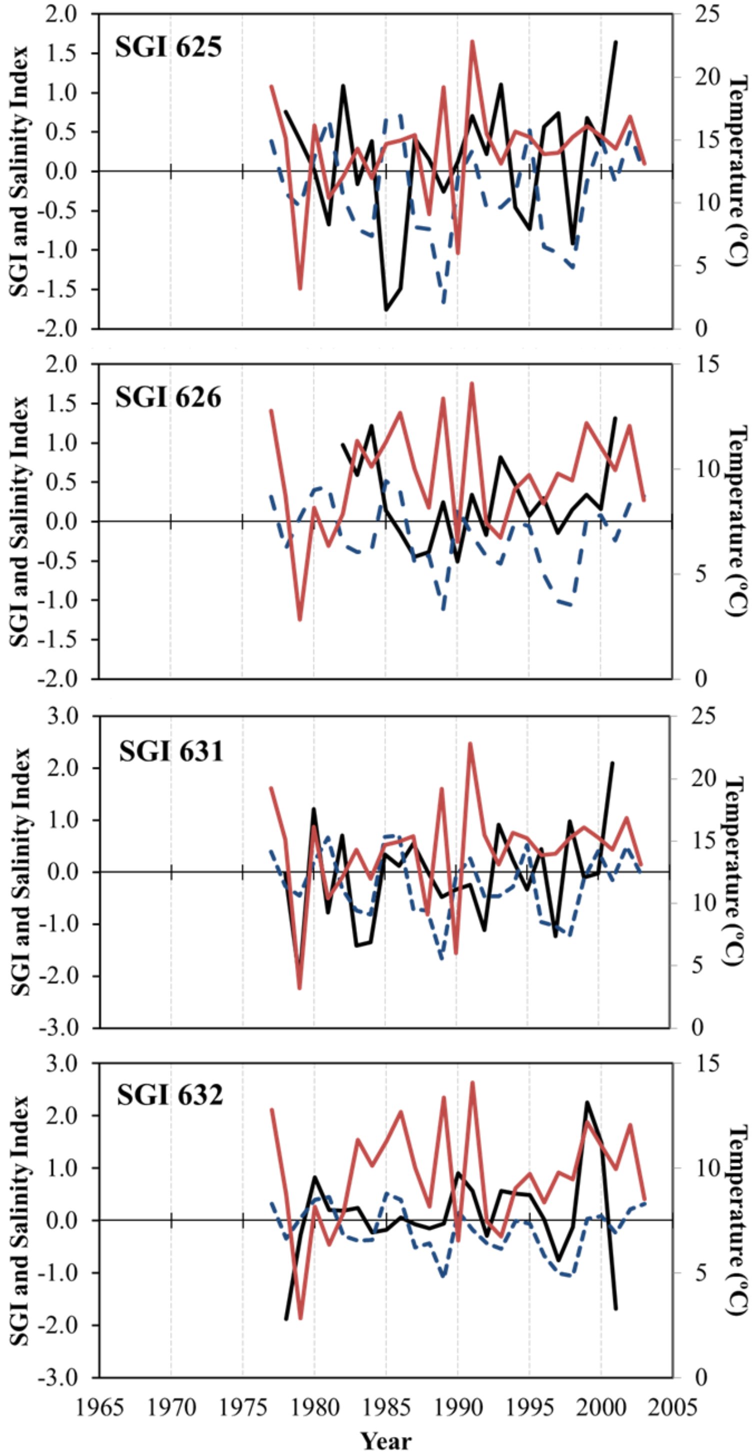

Figure 5. Standardized growth indices from the regional area chronologies off the Delmarva peninsula (625 & 626) and off the Hampton roadstead (631 & 632) (black line) plotted with mean annual surface and bottom seawater temperatures (red line) and salinity (blue dashed line) from the northern mid-Atlantic Bight (NEFSC-MARMAP data).

APPENDIX B: GLYCYMERIS AND PANOPEA

Table 1. Shell genus and species identification and measurements of preservation, weight, length, width and valve for unpaired Glycymerididae

Identification	Genus	Species[1]	Broken[2]	Weight (g)	Length (mm)	Width (mm)	Valve
CHR-A01	*Costaglycymeris*	*subovata*		10.18	54.35	57.76	Right
CHR-A02	*Glycymeris*	*americana*		27.63	67.06	65.65	Left
CHR-A03	*Glycymeris*	*americana*		22.15	61.53	71.19	Left
CHR-A04	*Glycymeris*	*americana*		25.21	67.58	69.27	Left
CHR-A05	*Glycymeris*	*americana*		40.64	74.63	76.08	Left
CHR-A06	*Glycymeris*	*americana*	YES	20.12	66.35	71.24	Left
CHR-A07	*Costaglycymeris*	*subovata*		26.61	60.48	62.13	Right
CHR-A08	*Glycymeris*	*americana*		8.40	51.27	53.31	Left
CHR-A09	*Costaglycymeris*	*subovata*		16.97	58.14	61.06	Left
CHR-A10	*Glycymeris*	*americana*		23.72	65.04	65.65	Left
CHR-B01	*Costaglycymeris*	*subovata*		13.95	54.4	58.11	Right
CHR-B02	*Costaglycymeris*	*subovata*		13.40	54.65	54.42	Right
CHR-B03	*Glycymeris*	*?*	YES	10.29	51.42	55.53	Left
CHR-B04	*Costaglycymeris*	*subovata*		11.03	47.85	51.85	Left
CHR-B05	*Costaglycymeris*	*subovata*		16.39	59.66	62.25	Left
CHR-B06	*Costaglycymeris*	*subovata*		21.20	60.85	62.14	Left
CHR-B07	*Costaglycymeris*	*subovata*		16.46	54.97	57.5	Left
CHR-B08	*Glycymeris*	*americana*	YES	15.26	62.27	65.08	Left

CHR-B09	*Costaglycymeris*	*subovata*		28.18	60.23	68.57	Right
CHR-B10	*Glycymeris*	*americana*		14.26	60.85	64.39	Right
CHR-C01	*Glycymeris*	*americana*		10.11	58.35	64.13	Left
CHR-C02	*Glycymeris*	*americana*		15.88	55.29	58.94	Left
CHR-C03	*Costaglycymeris*	*subovata*		8.18	50.18	54.48	Left
CHR-C04	*Glycymeris*	*americana*		12.41	55.73	61.16	Left
CHR-C05	*Costaglycymeris*	*subovata*		25.03	63.37	64.61	Left
CHR-C06	*Costaglycymeris*	*subovata*	YES	15.59	53.85	53.8	Right
CHR-C07	*Glycymeris*	*americana*		16.81	58.28	61.47	Right
CHR-C08	*Glycymeris*	*americana*		21.25	61.37	64.79	Right
CHR-C09	*Glycymeris*	*americana*	YES	14.35	60.81	67.03	Left
CHR-C10	*Glycymeris*	*americana*		23.18	60.01	61.75	Left
CHR-D01	*Glycymeris*	*americana*	YES	22.07	72.08	50.55	Left
CHR-D02	*Costaglycymeris*	*subovata*		16.46	56.85	59.59	Right
CHR-D03	*Glycymeris*	*americana*		22.62	65.9	67.01	Right
CHR-D04	*Costaglycymeris*	*subovata*		13.84	53.59	53.13	Left
CHR-D05	*Glycymeris*	*americana*		19.51	63.77	62.21	Right
CHR-D06	*Glycymeris*	*americana*		14.48	52.28	55.32	Left
CHR-D07	*Glycymeris*	*americana*		13.30	54.04	59.55	Right
CHR-D08	*Glycymeris*	*americana*	YES	--	--	--	--
CHR-D09	*Glycymeris*	*americana*	YES	17.14	65.39	61.05	Right
CHR-D10	*Glycymeris*	*americana*		15.13	57.82	64.31	Left
CHR-E01	*Glycymeris*	*americana*	YES	13.62	62.01	63.16	Right

Identification	Genus	Species[1]	Broken[2]	Weight (g)	Length (mm)	Width (mm)	Valve
CHR-E02	*Costaglycymeris*	*subovata*		11.16	49.77	56.98	Left
CHR-E03	*Costaglycymeris*	*subovata*	YES	18.12	58.66	61.31	Right
CHR-E04	*Costaglycymeris*	*subovata*		29.51	59.79	57.87	Right
CHR-E05	*Glycymeris*	*americana*	YES	16.67	52.27	59.13	Right
CHR-E08	*Costaglycymeris*	*subovata*		17.16	54.85	58.99	Left
CHR-E09	*Costaglycymeris*	*subovata*		14.30	51.07	55.95	Right
CHR-E10	*Glycymeris*	*americana*	YES	10.91	52.27	56.44	Left
CHR-F01	*Costaglycymeris*	*subovata*		19.03	56.93	55.17	Right
CHR-F02	*Costaglycymeris*	*subovata*		18.67	57.97	59.39	Right
CHR-F03	*Glycymeris*	*americana*	YES	21.42	65.02	61.72	Left
CHR-F04	*Glycymeris*	*americana*	YES	16.92	64.8	--	Left
CHR-F05	*Costaglycymeris*	*subovata*		17.54	54.44	59.2	Left
CHR-F06	*Costaglycymeris*	*subovata*		12.74	50.35	52.3	Left
CHR-F07	*Costaglycymeris*	*subovata*		12.93	47.81	50.09	Left
CHR-F08	*Glycymeris*	*americana*		22.96	66.21	69.71	Right
CHR-F09	*Glycymeris*	*americana*	YES	25.98	76.88	74.4	Right
CHR-F10	*Costaglycymeris*	*subovata*	YES	16.32	53.43	56.6	Right
CHR-G01	*Costaglycymeris*	*subovata*		17.23	57.25	55.19	Left
CHR-G02	*Glycymeris*	*americana*		19.83	64.21	67.41	Left
CHR-G03	*Glycymeris*	*americana*		17.84	64.56	68.28	Left
CHR-G04	*Glycymeris*	*americana*		25.51	68.47	70.2	Left
CHR-G05	*Glycymeris*	*americana*	YES	11.08	59.07	--	Left

CHR-G06	*Glycymeris*	*americana*		31.48	71.35	72.66	Left
CHR-G07	*Costaglycymeris*	*subovata*		19.53	55.19	58.01	Left
CHR-G08	*Glycymeris*	*americana*	YES	--	--	--	Right
CHR-G09	*Glycymeris*	*americana*		25.65	65.59	70.28	Right
CHR-G10	*Glycymeris*	*americana*	YES	14.59	59.28	63.16	Right
CHR-H01	*Glycymeris*	*americana*		20.33	63.65	58.92	Left
CHR-H02	*Costaglycymeris*	*subovata*		18.41	55.59	55.79	Left
CHR-H03	*Glycymeris*	*americana*		10.11	51.79	56.54	Left
CHR-H04	*Costaglycymeris*	*subovata*		24.84	60.68	60.32	Right
CHR-H05	*Glycymeris*	*americana*	YES	12.31	50.47	59.17	Left
CHR-H06	*Glycymeris*	*americana*		6.94	44.6	49.37	Right
CHR-H07	*Costaglycymeris*	*subovata*		20.27	53.33	58.25	Left
CHR-H08	*Costaglycymeris*	*subovata*		21.21	55.15	60.91	Left
CHR-H09	*Glycymeris*	*americana*	YES	15.65	58.87	61.59	Left
CHR-H10	*Glycymeris*	*americana*	YES	23.95	72.47	75.27	Right
CHR-I01	*Glycymeris*	*americana*	YES	11.75	--	--	Left
CHR-I02	*Glycymeris*	*americana*		8.87	52.72	50.73	Right
CHR-I03	*Glycymeris*	*americana*		9.55	54.11	56.44	Left
CHR-I04	*Glycymeris*	*americana*	YES	26.68	59.22	67.05	Left
CHR-I05	*Glycymeris*	*americana*		43.05	79.52	82.69	Left
CHR-I06	*Glycymeris*	*americana*		26.03	70.23	71.07	Right
CHR-I07	*Costaglycymeris*	*subovata*		12.63	52.47	54.68	Right
CHR-I08	*Glycymeris*	*americana*	YES	--	--	--	Right

Identification	Genus	Species[1]	Broken[2]	Weight (g)	Length (mm)	Width (mm)	Valve
CHR-I09	*Glycymeris*	*americana*	YES	18.76	59.87	63.09	Left
CHR-I10	*Glycymeris*	*americana*		29.16	71.95	68.79	Right
CHR-J01	*Glycymeris*	*americana*		31.39	65.35	67.98	Right
CHR-J02	*Glycymeris*	*americana*		12.45	57.1	59.9	Left
CHR-J03	*Costaglycymeris*	*subovata*		20.71	58.71	58.77	Left
CHR-J04	*Glycymeris*	*americana*		23.17	64.72	71.29	Left
CHR-J05	*Glycymeris*	*americana*		40.68	73.52	77.72	Left
CHR-J06	*Glycymeris*	*americana*		30.82	76.02	74.13	Left
CHR-J07	*Glycymeris*	*americana*		25.40	65.01	67.27	Right
CHR-J08	*Glycymeris*	*americana*		25.18	66.43	68.62	Left
CHR-J09	*Glycymeris*	*americana*		17.38	59.04	63.18	Right
CHR-K02	*Glycymeris*	*americana*		18.03	67.61	69.01	Right
CHR-K03	*Glycymeris*	*americana*		29.88	64.87	69.69	Left
CHR-K04	*Glycymeris*	*americana*		33.60	69.5	68.95	Left
CHR-K05	*Glycymeris*	*americana*		21.83	65.27	67.35	Right
CHR-K06	*Glycymeris*	*americana*	YES	20.02	63.76	69.02	Right
CHR-K07	*Glycymeris*	*americana*		22.88	63.69	64.19	Left
CHR-K08	*Glycymeris*	*americana*		22.48	64.55	69.38	Right
CHR-K09	*Glycymeris*	*americana*		24.94	61.19	63.82	Left
CHR-K10	*Glycymeris*	*americana*	YES	16.83	--	--	--
CHR-L01	*Glycymeris*	*americana*		25.11	71.77	69.76	Right
CHR-L02	*Glycymeris*	*americana*		25.17	70.76	74.37	Right

CHR-L03	*Glycymeris*	*americana*	YES	12.21	--	--	Right
CHR-L04	*Costaglycymeris*	*subovata*		29.59	63.19	64.88	Left
CHR-L05	*Costaglycymeris*	*subovata*		27.71	63.51	65.52	Right
CHR-L06	*Costaglycymeris*	*subovata*		24.67	610.01	61.24	Right
CHR-L07	*Costaglycymeris*	*subovata*		16.55	57.62	58.65	Right
CHR-L08	*Costaglycymeris*	*subovata*		21.02	57.1	57.94	Right
CHR-L09	*Costaglycymeris*	*subovata*	YES	24.54	58.39	58.95	Left
CHR-L10	*Costaglycymeris*	*subovata*		16.03	56.86	58.99	Left
CHR-M01	*Costaglycymeris*	*subovata*		18.81	--	61.39	Left
CHR-M02	*Costaglycymeris*	*subovata*		21.21	59.16	59.35	Right
CHR-M03	*Glycymeris*	*americana*	YES	22.17	--	--	Left
CHR-M04	*Costaglycymeris*	*subovata*		12.12	55.45	59.59	Right
CHR-M05	*Costaglycymeris*	*subovata*		18.22	58.68	59.51	Left
CHR-M06	*Costaglycymeris*	*subovata*		19.79	58.12	59.86	Right
CHR-M07	*Costaglycymeris*	*subovata*		18.46	53.8	57.01	Right
CHR-M08	*Costaglycymeris*	*subovata*		8.05	44.43	46.56	Left
CHR-M09	*Costaglycymeris*	*subovata*		9.25	44.19	45.44	Right
CHR-M10	*Costaglycymeris*	*subovata*		4.12	40.06	40.76	Right
LTR-A02	*Glycymeris*	*americana*		56.50	74.75	75.54	Right
LTR-A03	*Glycymeris*	*americana*		53.31	70.67	72.29	Right
LTR-A04	*Glycymeris*	*americana*		56.67	76.21	78.75	Left

[1] Identification based on R.D.K. Thomas 1970 and L. W. Ward. 1992
[2] 'Broken' refers to a state of preservation where more than fifty-percent of the valve is unmeasureable (either missing or too fragmented) using calipers.

Table 29. Shell genus and species identification and measurements of preservation, articulated shell weight, right valve weight, best preserved length and width for paired Glycymeris

UID	Genus	Species[1]	Broken[2]	Weight (g)	Right Valve Weight (g)	Length (mm)	Width (mm)
CHR-N01	*Glycymeris*	*americana*	YES	32.71	16.18	66.48	60.95
CHR-N02	*Glycymeris*	*americana*		50.36	26.11	67.95	75.25
CHR-N03	*Glycymeris*	*americana*		63.57	31.91	68.43	71.13
CHR-N04	*Glycymeris*	*americana*		27.52	13.58	60.26	62.06
CHR-N05	*Glycymeris*	*americana*		37.83	20.10	68.27	69.15
CHR-N06	*Glycymeris*	*americana*		38.69	19.65	63.17	63.16
CHR-N07	*Costaglycymeris*	*subovata*		45.62	22.54	58.52	60.93
CHR-N08	*Glycymeris*	*americana*		40.18	20.24	61.67	64.27
CHR-N09	*Glycymeris*	*americana*		36.31	18.90	61.34	63.66
CHR-N10	*Glycymeris*	*americana*	YES	40.19	21.55	65.63	71.23
CHR-P01	*Glycymeris*	*americana*	YES	38.80	19.21	66.31	65.53
CHR-P02	*Glycymeris*	*americana*		53.54	22.64	76.83	74.36
CHR-P03	*Glycymeris*	*americana*		45.63	23.87	68.75	67.88
CHR-P04	*Glycymeris*	*americana*	YES	29.29	15.45	68.30	68.02
CHR-P05	*Glycymeris*	*americana*		47.82	24.72	67.15	67.82
CHR-P06	*Glycymeris*	*americana*		27.42	14.03	60.48	62.41
CHR-P07	*Glycymeris*	*americana*		29.35	15.05	61.18	62.84
CHR-P08	*Glycymeris*	*american*	YES	30.97	16.60	59.44	65.57

		a					
CHR-P09	*Glycymeris*	*americana*	YES	33.45	16.14	65.89	65.94
CHR-P10	*Glycymeris*	*americana*		26.85	14.42	60.28	61.85
CHR-Q01	*Glycymeris*	*americana*		34.90	18.71	64.30	65.29
CHR-Q02	*Glycymeris*	*americana*		24.86	12.36	55.55	58.34
CHR-Q03	*Costaglycymeris*	*subovata*		36.23	19.37	60.04	60.89
CHR-Q04	*Glycymeris*	*americana*	YES	20.38	--	--	--
CHR-Q05	*Glycymeris*	*americana*		18.98	9.77	51.77	55.57
CHR-Q06	*Glycymeris*	*americana*		17.96	8.55	47.67	51.29
CHR-Q07	*Glycymeris*	*americana*		12.58	6.64	49.47	51.33
CHR-Q08	*Costaglycymeris*	*subovata*		29.40	14.66	53.64	56.63
CHR-Q09	*Costaglycymeris*	*subovata*		36.61	17.17	53.45	56.81
CHR-Q10	*Costaglycymeris*	*subovata*		26.78	13.88	50.69	55.95
LTR-A01	*Glycymeris*	*americana*		94.90	46.45	68.92	73.18

[1] Identification based on R.D.K. Thomas 1970 and L. W. Ward. 1992
[2] 'Broken' refers to a state of preservation where more than fifty-percent of the valve is unmeasureable (either missing or too fragmented) using calipers.

Table 3. Shell genus and species identification and measurements of preservation, weight, length, width and valve for unpaired *Panopea reflexa*

Identification	Genus	Species[1]	Broken[2]	Weight (g)	Length (mm)	Width (mm)	Valve
LTR-W01	*Panopea*	*reflexa*		33.72	64.45	106.85	Left
LTR-W02	*Panopea*	*reflexa*		37.96	68.77	100.96	Right

LTR-W03	*Panopea*	*reflexa*		48.77	71.17	107.5	Right
LTR-W04	*Panopea*	*reflexa*	YES	45.49	74.31	--	Left
LTR-W05	*Panopea*	*reflexa*	YES	25.48	69.53	--	Right
LTR-W06	*Panopea*	*reflexa*		48.91	65.13	110.24	
LTR-W07	*Panopea*	*reflexa*		51.34	63.9	103.8	
LTR-W08	*Panopea*	*reflexa*		36.06	67.94	101.08	Left
LTR-W09	*Panopea*	*reflexa*		21.67	60.05	100.05	Right
LTR-W10	*Panopea*	*reflexa*		42.68	74.59	113.43	Left
LTR-X01	*Panopea*	*reflexa*	YES	43.83	--	--	Right
LTR-X02	*Panopea*	*reflexa*	YES	26.79	--	--	Right
LTR-X03	*Panopea*	*reflexa*		71.74	71.15	111.96	Right
LTR-X04	*Panopea*	*reflexa*		73.58	65.96	94.72	Right

[1] Identification based on L. W. Ward. 1992
[2] 'Broken' refers to a state of preservation where more than fifty-percent of the valve is unmeasureable (either missing or too fragmented) using calipers.

Table 4. Shell genus and species identification and measurements of preservation, articulated shell weight, right valve weight, best preserved length and width for paired *Panopea reflexa*

UID	Genus	Species[1]	Broken[2]	Weight (g)	Right Valve Weight (g)	Length (mm)	Width (mm)
LTR-X05	*Panopea*	*reflexa*		49.27	24.62	63.18	97.29
LTR-X06	*Panopea*	*reflexa*		78.45	38.36	65.53	107.37
LTR-X07	*Panopea*	*reflexa*		139.68	70.26	68.79	109.04

[1] Identification based on L. W. Ward. 1992
[2] 'Broken' refers to a state of preservation where more than fifty-percent of the valve is unmeasureable (either missing or too fragmented) using calipers.

Table 10. These are measurements in the units of .001 mm for the thickness of external (EX) increment widths for specimens of *Glycymeris americana* from the Yorktown and Chowan River Formations. Missing values and end of record code is -999. The unique identification (UID) of each shell is listed next to age arranged in decades (floating chronology). The 10 values following the decade are the 10 annual measurements for the 10 years of the decade.

UID	D	1	2	3	4	5	6	7	8	9	0
A02-EX	0	11.046	16.036	4.964	6.371	4.619	4.129	3.913	3.225	3.081	2.004
A02-EX	10	1.317	1.407	2.052	1.453	1.069	1.008	1.378	0.835	1.036	0.797
A02-EX	20	0.505	0.466	0.515	0.596	0.487	0.396	0.691	0.499	0.555	0.433
A02-EX	30	0.546	0.523	0.259	0.688	0.343	0.475	0.468	0.366	0.362	0.520
A02-EX	40	0.616	0.461	0.621	0.501	0.596	0.372	0.248	0.482	0.538	0.549
A02-EX	50	0.787	0.304	-999							
A03-EX	0	3.531	7.442	6.876	6.012	6.828	3.723	2.220	2.933	3.414	2.552
A03-EX	10	1.549	1.596	2.240	1.667	1.821	0.778	1.013	1.226	0.897	0.783
A03-EX	20	1.549	1.596	2.240	1.667	1.821	0.778	1.013	1.226	0.897	0.783
A03-EX	30	0.337	0.200	0.222	0.265	0.248	0.233	0.159	0.260	-999	
A04-EX	0	3.312	5.537	3.957	4.886	7.139	5.580	4.839	4.580	2.888	4.264
A04-EX	10	3.312	5.537	3.957	4.886	7.139	5.580	4.839	4.580	2.888	4.264
A04-EX	20	0.589	0.567	1.073	0.536	0.603	0.469	0.524	0.605	0.113	0.106
A04-EX	30	0.893	0.402	0.332	0.348	0.470	0.259	0.182	0.426	0.445	0.276

A04-EX	40	0.151	0.083	0.154	-999						
A06-EX	0	1.679	3.064	4.175	4.192	2.640	3.182	3.329	2.927	5.702	4.601
A06-EX	10	4.584	2.213	1.985	2.450	2.613	2.664	1.877	0.946	1.572	1.541
A06-EX	20	1.705	1.506	0.588	0.223	0.174	0.472	0.551	0.396	0.516	0.642
A06-EX	30	1.067	-999								
A08-EX	0	4.127	7.649	8.216	6.260	5.233	3.156	3.159	1.656	2.109	0.039
A08-EX	10	0.950	0.950	0.475	0.674	0.580	1.058	1.221	-999		
A10-EX	0	0.873	1.142	3.779	5.061	5.034	5.611	5.575	3.022	3.336	5.234
A10-EX	10	2.916	2.717	2.773	1.351	1.244	1.825	1.214	1.129	1.320	1.407
A10-EX	20	1.187	0.685	0.614	0.843	0.626	0.070	0.388	0.430	0.283	0.514
A10-EX	30	0.348	0.443	0.217	0.458	0.240	0.159	0.108	0.140	0.205	0.319
A10-EX	40	-999									
B03-EX	0	4.236	12.174	8.283	9.961	5.138	5.588	1.430	0.871	1.111	1.073
B03-EX	10	0.567	-999								
B10-EX	0	3.658	4.688	7.948	5.198	6.960	5.559	2.641	4.142	2.797	2.421
B10-EX	10	2.024	1.524	0.623	0.673	1.843	0.715	0.743	1.100	0.581	0.359
B10-EX	20	0.292	0.171	0.261	0.330	1.144	0.398	0.507	0.457	-999	
C01-EX	0	4.944	5.255	5.793	4.208	3.669	5.410	5.973	3.916	3.425	3.784
C01-EX	10	0.896	1.168	1.637	0.669	0.828	0.844	0.990	-999		
C02-EX	0	4.713	3.879	4.347	6.694	3.274	3.637	5.098	6.075	3.423	2.743
C02-EX	10	2.531	2.376	0.438	0.515	0.915	0.387	0.476	0.398	0.683	0.579
C02-EX	20	-999									
C04-EX	0	1.414	2.431	3.567	2.928	3.093	4.197	2.933	3.422	3.025	2.349

C04-EX	10	2.466	1.603	2.816	2.085	1.905	1.804	1.986	1.079	2.063	0.837
C04-EX	20	0.622	1.524	1.039	0.706	0.893	0.708	0.776	0.744	0.638	-999
C07-EX	0	3.505	5.795	6.175	6.819	4.482	2.675	2.382	1.843	1.587	3.281
C07-EX	10	2.645	2.648	1.744	1.198	1.248	1.273	1.204	0.641	0.742	0.732
C07-EX	20	0.797	0.589	0.513	0.286	0.439	0.403	0.395	0.453	0.435	0.[18]7
C07-EX	30	-999									
C08-EX	0	3.991	7.773	7.701	6.021	7.354	2.673	2.352	2.250	2.118	2.656
C08-EX	10	1.892	1.295	0.724	0.724	0.376	0.496	0.800	0.678	0.670	0.566
C08-EX	20	1.089	0.734	0.609	0.716	-999					
C09-EX	0	5.173	6.141	3.631	3.474	1.428	4.099	3.685	4.594	4.987	4.015
C09-EX	10	3.823	2.439	1.931	1.631	1.513	1.420	1.295	1.210	-999	
D01-EX	0	2.090	4.147	5.353	5.551	3.844	6.672	5.651	4.030	2.733	1.966
D01-EX	10	1.268	1.183	0.911	1.295	1.491	0.941	1.137	0.964	1.461	1.151
D01-EX	20	0.748	0.618	0.558	0.380	0.561	0.745	0.556	0.573	0.427	0.581
D01-EX	30	0.306	0.418	0.400	0.831	0.492	0.221	0.330	0.275	0.254	0.440
D01-EX	40	0.222	0.410	0.332	0.339	0.280	0.506	0.327	0.396	0.412	0.288
D01-EX	50	0.360	0.602	0.588	0.555	0.461	0.402	0.294	-999		
D03-EX	0	4.503	5.873	5.713	6.724	4.401	5.790	3.788	2.856	2.234	2.005
D03-EX	10	2.571	2.052	1.762	1.603	0.789	1.406	1.598	1.119	0.730	0.575
D03-EX	20	2.925	0.583	0.853	0.611	0.674	0.600	0.553	0.462	0.534	0.553
D03-EX	30	0.480	-999								
D05-EX	0	4.197	7.453	7.661	5.840	4.327	2.698	1.160	0.887	1.018	2.871
D05-EX	10	1.531	1.902	1.324	0.618	0.987	0.525	0.963	0.660	0.631	0.755

D05-EX	20	0.457	0.479	0.541	0.280	0.450	1.183	0.969	0.753	0.480	0.767
D05-EX	30	0.540	0.656	0.561	0.432	0.350	0.573	0.627	0.379	0.561	0.496
D05-EX	40	-999									
E01-EX	0	6.917	4.861	5.575	2.966	4.458	5.646	5.205	6.429	7.485	5.599
E01-EX	10	0.649	0.538	0.359	0.715	0.828	0.798	1.161	0.237	-999	
E05-EX	0	3.285	4.322	5.111	4.218	3.585	2.773	2.641	2.561	1.655	1.389
E05-EX	10	1.360	1.531	2.003	1.401	0.556	0.947	1.452	3.956	0.610	0.611
E05-EX	20	1.087	0.723	0.796	0.719	0.363	0.753	0.932	0.658	0.747	1.373
E05-EX	30	-999									
E10-EX	0	3.908	4.296	6.248	1.887	2.143	5.204	5.171	3.631	2.734	2.281
E10-EX	10	1.907	1.974	1.728	0.943	0.970	1.026	0.787	0.704	1.300	0.902
E10-EX	20	0.557	0.391	0.438	0.551	-999					
F03-EX	0	3.574	4.214	5.474	9.352	6.199	6.052	5.486	3.832	3.014	2.639
F03-EX	10	3.779	2.357	1.106	0.752	0.785	0.739	0.811	-999		
F04-EX	0	4.243	6.876	6.966	4.166	4.368	4.204	2.638	2.365	2.553	1.377
F04-EX	10	1.139	1.142	1.227	1.260	0.673	0.632	0.941	1.117	0.891	0.788
F04-EX	20	0.770	0.986	0.959	1.040	0.844	0.926	0.991	0.513	1.227	1.333
F04-EX	30	0.497	0.590	0.316	0.297	0.253	0.352	1.307	-999		
F08-EX	0	5.718	7.200	6.570	5.754	4.574	6.087	3.300	2.694	2.696	2.386
F08-EX	10	2.228	1.571	1.562	0.959	0.697	0.630	1.024	0.606	0.847	1.023
F08-EX	20	1.003	0.528	0.451	0.572	0.550	0.847	0.688	0.298	0.473	0.492
F08-EX	30	0.314	-999								
F09-EX	0	3.699	5.738	6.894	6.799	5.559	4.524	2.639	3.525	3.016	2.155

F09-EX	10	1.177	0.016	0.952	2.199	2.954	0.963	1.539	1.554	1.073	2.052
F09-EX	20	1.387	0.777	1.614	0.782	0.529	0.453	0.827	1.221	0.924	0.778
F09-EX	30	0.739	0.540	0.336	0.369	0.938	0.944	0.233	0.314	0.422	0.436
F09-EX	40	0.462	0.355	-999							
G02-EX	0	3.494	4.082	8.279	6.627	6.505	5.919	4.338	2.239	2.951	2.712
G02-EX	10	2.299	0.734	0.855	1.088	0.958	1.650	0.402	0.621	0.583	0.951
G02-EX	20	0.828	0.491	0.469	0.622	0.466	0.360	0.246	0.265	0.168	0.536
G02-EX	30	0.611	0.353	0.138	0.286	0.284	0.209	-999			
G03-EX	0	2.739	3.670	3.851	4.393	5.558	5.234	4.857	5.312	3.615	2.501
G03-EX	10	2.751	2.409	2.037	0.984	0.942	0.979	0.821	0.703	0.602	0.458
G03-EX	20	0.591	0.922	0.703	0.451	0.362	0.666	0.691	0.992	0.574	0.353
G03-EX	30	0.348	0.594	0.495	0.330	0.402	-999				
G04-EX	0	3.499	3.603	4.518	6.877	5.831	5.696	2.092	2.752	2.752	2.888
G04-EX	10	3.603	2.629	2.313	2.121	5.905	1.444	2.650	2.283	1.144	1.240
G04-EX	20	0.500	0.622	0.523	0.547	0.804	0.445	0.396	0.460	0.340	0.561
G04-EX	30	0.370	0.636	0.303	0.258	0.392	0.726	0.337	0.277	-999	
G05-EX	0	5.398	3.582	5.936	2.846	4.451	3.145	3.313	2.925	2.646	2.686
G05-EX	10	3.383	2.520	1.499	1.914	1.551	1.065	1.573	1.335	0.686	0.759
G05-EX	20	0.800	1.010	1.066	0.627	-999					
G06-EX	0	4.177	6.708	5.709	6.881	4.451	5.629	5.020	2.899	2.496	1.568
G06-EX	10	1.255	1.849	2.256	2.007	1.859	1.424	0.589	6.602	0.908	1.371
G06-EX	20	0.329	0.575	0.744	0.557	0.391	0.591	0.178	0.527	0.483	0.591
G06-EX	30	0.548	0.401	0.443	0.705	0.454	0.540	0.462	0.685	0.386	0.473

G06-EX	40	-999									
G08-EX	0	3.502	4.912	6.035	6.214	10.608	4.814	3.615	3.735	3.043	1.354
G08-EX	10	1.197	1.525	1.498	0.942	1.020	0.532	0.628	0.671	0.496	0.831
G08-EX	20	-999									
G09-EX	0	2.733	3.387	4.753	2.744	3.997	4.735	5.250	5.173	5.034	3.477
G09-EX	10	2.520	14.108	2.028	1.805	0.995	1.107	1.267	5.062	1.078	0.695
G09-EX	20	0.438	0.288	0.470	1.213	5.210	0.395	0.201	0.631	0.186	0.263
G09-EX	30	0.310	0.746	0.382	0.403	0.429	0.561	0.542	-999		
G10-EX	0	2.226	4.703	4.011	3.265	5.358	4.942	4.518	2.780	2.301	1.688
G10-EX	10	1.791	1.969	2.132	1.171	1.238	4.064	1.509	1.793	1.238	1.[13]5
G10-EX	20	1.035	0.439	0.928	0.779	0.381	1.046	0.407	0.291	1.576	1.525
G10-EX	30	1.440	0.568	0.551	0.560	0.644	0.441	-999			
GLYA-EX	0	7.600	3.984	4.870	7.541	2.368	4.092	4.743	4.367	2.695	2.223
GLYA-EX	10	1.078	0.994	1.570	1.088	0.982	1.426	0.743	0.710	0.495	0.656
GLYA-EX	20	0.589	0.600	0.551	0.966	0.560	1.112	1.012	-999		
GLYC-EX	0	6.415	6.293	10.659	7.433	5.116	4.697	2.298	1.569	3.771	2.751
GLYC-EX	10	0.913	0.781	1.091	0.978	0.573	0.577	0.035	0.522	0.601	0.581
GLYC-EX	20	0.531	0.455	0.542	0.468	0.296	0.412	0.444	0.242	0.232	0.285
GLYC-EX	30	0.338	0.188	0.176	0.442	0.226	0.314	0.210	0.229	0.144	0.165
GLYC-EX	40	0.128	0.118	0.292	0.236	0.183	0.358	0.457	-999		
H03-EX	0	2.786	2.625	5.243	5.325	4.848	3.940	3.160	3.780	2.791	1.962
H03-EX	10	3.531	2.636	2.075	1.492	1.262	0.554	0.352	0.497	0.786	0.343
H03-EX	20	-999									

H05-EX	01	5.485	4.415	4.409	3.666	4.432	1.740	2.692	1.119	4.781	3.087
H05-EX	02	4.058	1.565	1.961	1.523	1.948	1.153	0.908	1.101	0.681	1.011
H05-EX	03	0.457	0.358	1.177	1.049	0.344	0.877	0.307	0.465	0.204	0.172
H05-EX	0	-999									
H06-EX	01	3.559	4.656	4.275	5.385	3.850	2.588	2.454	4.032	2.250	1.986
H06-EX	0	2.839	2.369	1.025	0.974	-999					
H09-EX	01	1.575	1.942	8.548	3.938	3.521	3.439	4.702	3.047	1.889	1.674
H09-EX	02	2.566	1.533	1.912	1.170	2.224	1.155	1.397	1.475	1.541	0.958
H09-EX	0	0.275	0.353	0.341	0.572	0.485	0.586	0.490	0.232	-999	
H10-EX	01	3.492	4.032	3.774	5.506	7.096	5.281	3.460	4.451	3.509	2.996
H10-EX	02	3.013	4.389	0.799	0.534	0.794	1.771	1.627	1.268	1.229	1.295
H10-EX	03	1.503	1.202	1.046	0.972	0.581	0.385	0.594	0.661	2.035	0.743
H10-EX	0	0.369	0.497	0.633	0.709	-999					
I02-EX	01	3.107	4.199	8.768	4.451	5.294	4.470	4.304	5.003	4.114	2.426
I02-EX	0	1.458	1.821	0.797	0.325	0.475	0.304	0.446	0.303	-999	
I03-EX	01	3.303	4.066	8.251	4.951	5.631	4.378	4.358	3.304	2.248	1.867
I03-EX	02	1.746	2.498	0.775	0.759	0.813	1.245	0.900	0.934	0.607	0.532
I03-EX	0	-999									
I04-EX	01	3.772	4.563	5.301	5.825	6.023	5.873	3.406	4.018	2.206	1.249
I04-EX	02	2.891	1.727	1.397	0.706	0.804	0.913	1.527	1.422	0.979	0.548
I04-EX	0	0.491	0.853	0.835	0.780	0.761	-999				
I06-EX	01	3.345	4.393	2.620	3.220	1.668	3.700	4.028	2.586	2.335	2.072
I06-EX	0	1.838	3.763	3.766	4.103	4.772	3.567	2.612	1.863	0.912	1.049

I06-EX	20	0.745	0.552	0.959	0.649	0.720	0.632	0.722	0.767	0.609	0.748
I06-EX	30	0.433	0.369	0.454	0.467	0.452	0.512	0.492	0.388	0.356	0.402
I06-EX	40	0.375	0.310	0.550	0.449	0.289	-999				
J01-EX	0	3.062	4.760	7.481	4.986	4.195	5.208	4.361	3.369	2.563	2.577
J01-EX	10	2.368	1.515	1.254	1.294	1.016	1.036	1.027	1.321	1.015	0.774
J01-EX	20	0.595	0.384	0.554	0.358	0.422	0.507	0.397	0.673	0.408	0.319
J01-EX	30	0.275	0.330	0.521	0.353	0.465	0.311	0.852	0.234	0.111	0.341
J01-EX	40	0.217	0.201	0.473	0.237	0.223	-999				
J02-EX	0	4.206	8.202	7.802	6.041	4.522	4.096	1.994	2.746	2.839	1.663
J02-EX	10	2.265	0.872	0.948	1.287	0.891	0.553	0.708	1.367	0.738	0.419
J02-EX	20	0.247	-999								
J04-EX	0	4.277	4.079	5.037	5.206	4.347	5.567	4.677	4.082	2.112	2.631
J04-EX	10	2.488	2.773	1.992	1.677	2.005	1.251	1.320	1.133	0.532	0.583
J04-EX	20	0.726	0.651	0.665	0.341	0.374	0.433	0.561	0.317	-999	
J05-EX	0	2.486	3.510	3.899	4.622	3.007	4.402	4.057	5.182	4.053	3.312
J05-EX	10	2.871	2.894	2.114	2.051	1.773	1.658	1.814	1.301	1.145	1.270
J05-EX	20	1.048	0.859	0.720	2.782	0.427	2.474	0.696	0.286	0.308	0.299
J05-EX	30	0.631	0.315	0.305	0.246	0.526	0.375	0.621	0.352	0.378	0.382
J05-EX	40	0.547	0.352	0.335	0.503	0.473	0.372	0.378	0.451	-999	
J06-EX	0	5.832	7.664	5.771	7.377	5.362	5.766	4.193	2.663	2.398	1.887
J06-EX	10	1.385	2.006	1.476	0.937	1.058	1.440	0.887	0.990	0.666	0.550
J06-EX	20	0.705	0.602	0.525	0.905	0.386	0.657	0.745	0.861	0.505	0.330
J06-EX	30	1.137	0.375	0.458	2.216	0.383	0.251	0.310	0.342	0.276	0.407

J06-EX	40	0.345	0.272	0.411	0.220	0.286	0.165	4.176	0.240	0.441	0.310
J06-EX	50	0.289	0.344	0.275	-999						
J07-EX	0	1.575	4.037	2.934	3.219	4.998	5.102	4.083	3.515	3.859	3.316
J07-EX	10	2.178	1.485	2.091	1.758	1.840	1.672	1.180	0.947	0.814	0.971
J07-EX	20	1.012	0.671	0.320	0.343	0.025	0.583	0.682	0.605	0.793	0.858
J07-EX	30	0.342	0.913	0.594	0.310	0.243	0.310	0.605	0.297	0.605	0.341
J07-EX	40	0.253	0.386	0.080	0.429	0.221	0.266	0.156	0.287	0.311	0.278
J07-EX	50	0.396	-999								
J08-EX	0	2.920	6.761	6.712	5.709	5.985	5.611	4.290	3.323	2.486	0.921
J08-EX	10	1.456	1.925	1.131	0.770	0.836	0.639	1.243	0.861	0.825	0.887
J08-EX	20	0.803	0.492	0.727	0.858	0.617	0.957	0.537	0.160	0.644	0.397
J08-EX	30	0.496	0.408	0.176	0.598	0.508	0.506	-999			
J09-EX	0	3.841	4.284	5.542	7.101	2.442	2.723	4.076	2.695	4.269	1.797
J09-EX	10	2.420	1.493	2.087	0.940	0.473	1.057	1.251	2.211	2.036	1.364
J09-EX	20	1.211	0.924	0.991	-999						
J10-EX	0	3.082	4.658	4.181	6.744	5.061	5.986	4.269	4.092	3.492	3.247
J10-EX	10	2.361	1.905	2.875	2.479	1.993	0.762	2.086	0.502	0.350	0.447
J10-EX	20	0.339	0.280	0.363	0.464	0.271	0.237	0.375	0.414	-999	
K02-EX	0	2.844	7.363	6.670	7.881	6.678	6.506	4.542	4.526	2.517	2.582
K02-EX	10	2.266	1.890	1.421	1.360	0.693	1.167	0.959	0.868	0.430	0.872
K02-EX	20	0.221	0.662	0.554	0.355	0.176	0.174	0.760	0.286	-999	
K04-EX	0	2.387	2.559	6.772	4.704	3.872	5.209	6.726	3.934	3.621	2.015
K04-EX	10	1.761	1.548	1.623	1.395	1.145	1.222	1.331	1.123	1.335	0.905

K04-EX	20	0.671	0.518	0.675	1.149	1.210	0.906	0.770	0.670	0.875	0.297
K04-EX	30	0.286	0.275	0.341	0.756	0.390	1.135	0.452	0.439	0.837	0.[18]1
K04-EX	40	0.527	0.266	0.303	0.619	0.289	-999				
K05-EX	0	4.734	6.333	6.170	4.160	4.231	4.857	4.459	3.981	3.077	2.429
K05-EX	10	1.938	2.024	1.553	0.574	1.694	1.194	0.792	0.638	0.704	0.716
K05-EX	20	0.774	1.222	0.745	0.716	0.694	0.675	0.365	0.255	0.297	0.190
K05-EX	30	0.166	0.275	0.118	0.221	0.104	0.332	0.150	0.272	0.241	0.258
K05-EX	40	0.230	-999								
K06-EX	0	3.263	3.647	4.963	9.035	6.418	3.763	2.963	2.911	2.322	2.519
K06-EX	10	2.510	1.688	1.335	1.486	0.800	1.802	0.682	0.898	1.443	0.484
K06-EX	20	0.529	0.049	0.187	0.319	0.594	0.353	0.553	0.386	0.396	0.287
K06-EX	30	0.550	0.354	0.363	0.366	0.440	0.220	0.221	0.342	0.297	0.397
K06-EX	40	0.484	0.341	0.209	-999						
K08-EX	0	4.325	3.939	4.736	4.721	5.992	4.081	4.493	4.348	2.746	3.072
K08-EX	10	2.622	1.103	1.269	1.793	1.109	1.530	1.954	0.718	0.717	0.758
K08-EX	20	0.473	0.682	0.540	0.345	0.334	0.227	0.286	0.236	0.242	0.363
K08-EX	30	0.512	0.407	0.427	0.528	0.297	0.121	0.310	0.168	0.298	0.320
K08-EX	40	0.341	-999								
K09-EX	0	2.509	4.962	6.666	7.088	6.478	6.095	4.672	5.435	3.364	2.454
K09-EX	10	1.955	1.994	1.406	0.937	0.609	0.749	0.739	0.341	0.291	0.235
K09-EX	20	0.259	0.265	0.298	0.458	0.371	0.220	0.220	-999		
K10-EX	0	2.541	3.620	7.772	2.465	5.699	6.657	5.885	4.908	4.324	2.585
K10-EX	10	2.464	3.047	0.755	0.566	0.861	0.944	0.123	1.293	0.474	0.939

K10-EX	20	0.772	0.926	0.980	0.610	0.501	-999				
L02-EX	0	8.855	3.440	3.673	3.949	3.651	5.167	3.410	3.366	4.584	3.170
L02-EX	10	4.385	4.177	3.054	2.598	3.147	2.515	2.413	1.773	1.811	1.483
L02-EX	20	1.340	1.874	0.948	0.581	0.692	0.913	0.414	0.485	0.650	0.695
L02-EX	30	0.464	0.938	0.238	0.502	0.407	0.516	0.366	0.232	0.386	-999
LA01-EX	0	2.733	3.013	10.411	8.662	6.536	5.849	4.137	2.949	2.369	1.983
LA01-EX	10	1.981	1.881	1.916	1.127	0.984	0.611	0.953	0.452	0.684	0.722
LA01-EX	20	0.352	0.490	0.364	0.594	0.420	3.341	0.445	0.347	3.116	0.452
LA01-EX	30	0.466	0.347	0.599	0.942	0.308	0.184	0.447	0.409	0.324	-999
LA02-EX	0	4.819	5.186	6.057	5.862	7.571	5.622	4.862	4.454	4.905	2.510
LA02-EX	10	2.263	1.463	1.159	1.485	1.014	1.066	1.574	1.172	0.880	0.639
LA02-EX	20	0.332	0.572	0.594	1.017	0.561	0.451	0.331	0.388	0.474	0.473
LA02-EX	30	0.353	0.640	0.517	0.441	0.682	0.463	0.266	0.408	0.440	0.143
LA02-EX	40	0.209	0.176	-999							
LA04-EX	0	3.875	5.447	6.269	8.428	7.017	3.236	1.712	1.863	1.497	2.642
LA04-EX	10	1.672	1.635	1.646	1.304	1.034	1.633	1.248	0.939	1.765	2.016
LA04-EX	20	2.040	1.319	1.105	1.423	0.616	1.636	1.157	1.428	0.754	0.405
LA04-EX	30	0.838	0.329	0.577	0.297	0.891	0.600	0.672	0.624	-999	
N02-EX	0	4.996	2.973	9.223	5.171	7.592	5.281	4.237	1.153	2.196	1.354
N02-EX	10	1.486	1.661	1.080	1.327	1.815	1.316	1.453	1.055	1.078	0.926
N02-EX	20	0.524	1.028	0.805	0.264	0.738	0.641	0.369	0.446	0.518	1.360
N02-EX	30	0.926	1.073	-999							
N03-EX	0	6.084	7.008	5.203	5.507	6.446	4.680	5.202	4.278	2.120	2.340

N03-EX	10	2.289	2.289	1.318	0.660	1.091	0.858	0.616	0.935	1.178	0.771
N03-EX	20	0.999	0.524	0.605	0.572	0.604	0.839	0.716	0.676	0.204	-999
N04-EX	0	3.020	4.110	6.210	6.068	4.070	2.390	2.699	4.525	1.049	2.322
N04-EX	10	2.763	2.322	1.848	0.821	0.717	1.215	1.244	1.141	0.767	1.475
N04-EX	20	1.382	1.475	0.745	1.138	0.785	0.973	0.813	0.397	0.393	-999
N05-EX	0	5.919	6.300	6.976	7.158	4.987	6.316	3.410	2.877	1.871	1.461
N05-EX	10	1.678	2.037	2.607	1.606	1.144	1.024	0.897	0.669	0.897	0.776
N05-EX	20	0.743	1.144	0.578	0.479	0.622	0.314	0.358	0.297	0.297	0.386
N05-EX	30	0.358	0.627	0.254	-999						
P01-EX	0	2.799	5.479	4.153	3.534	3.472	4.824	6.741	6.333	2.955	3.426
P01-EX	10	3.273	3.198	3.163	2.002	1.221	1.415	1.322	1.238	0.939	0.711
P01-EX	20	0.956	0.785	0.807	0.730	0.769	0.273	0.211	0.306	-999	

Table 11. These are measurements in the units of .001 mm for the thickness of internal (INT) increment widths for specimens of *Glycymeris americana* from the Yorktown and Chowan River Formations. Missing values and end of record code is -999. The unique identification (UID) of each shell is listed next to age arranged in decades (floating chronology). The 10 values following the decade are the 10 annual measurements for the 10 years of the decade.

UID	D	1	2	3	4	5	6	7	8	9	0
A03-INT	0	10.908	8.249	3.460	3.321	5.923	4.173	3.602	4.409	2.985	3.672
A03-INT	10	3.006	2.829	2.525	1.507	1.808	0.916	0.868	0.764	0.795	1.040
A03-INT	20	1.039	0.950	0.761	0.544	0.903	0.621	0.715	0.614	0.617	0.639
A03-INT	30	0.623	0.651	0.668	0.654	0.463	-999				
A04-INT	0	4.282	8.191	4.337	5.472	3.046	3.032	3.547	1.879	1.633	3.403

A04-INT	10	4.576	3.671	4.285	1.897	2.386	1.573	0.691	0.581	1.039	1.750
A04-INT	20	0.954	0.817	0.556	1.060	0.633	1.014	0.588	0.398	0.848	0.588
A04-INT	30	0.647	0.603	0.484	0.436	0.532	0.471	0.436	0.350	0.600	0.442
A04-INT	40	0.220	0.220	0.272	0.253	-999					
A05-INT	0	6.976	6.729	3.541	5.733	7.333	7.060	3.767	3.743	3.352	3.327
A05-INT	10	1.826	2.160	2.126	1.742	2.149	1.173	0.671	0.796	1.640	1.266
A05-INT	20	0.929	0.810	0.933	0.681	1.021	1.943	0.337	0.675	0.455	0.604
A05-INT	30	0.814	0.542	0.786	0.823	0.431	0.691	0.662	0.393	0.736	0.588
A05-INT	40	0.447	0.246	0.591	0.618	0.249	0.132	0.966	0.468	0.253	0.373
A05-INT	50	0.399	0.490	0.711	0.608	0.415	0.420	0.305	0.328	-999	
A06-INT	0	6.840	5.442	5.841	2.814	3.605	1.746	6.081	6.083	4.228	4.090
A06-INT	10	2.174	2.042	2.669	2.340	3.064	3.358	1.547	1.857	2.015	1.160
A06-INT	20	0.752	0.376	0.378	0.432	0.787	0.782	0.598	0.772	0.357	0.331
A06-INT	30	0.463	0.428	-999							
A08-INT	0	4.203	4.845	4.541	3.763	3.722	4.997	2.993	2.965	3.286	2.753
A08-INT	10	2.190	3.378	3.434	2.005	2.206	0.779	0.767	0.568	0.697	0.683
A08-INT	20	-999									
A10-INT	0	4.334	3.676	4.500	5.669	5.195	5.957	5.697	6.190	2.640	1.938
A10-INT	10	3.101	2.400	3.357	1.265	0.892	2.505	1.427	0.665	0.923	0.912
A10-INT	20	0.615	1.125	0.908	0.456	0.531	0.815	0.433	0.361	0.560	0.463
A10-INT	30	0.358	0.509	0.410	0.498	0.393	0.387	0.209	0.310	0.388	0.217
A10-INT	40	0.551	0.228	0.468	0.155	0.302	0.287	0.225	0.343	0.277	-999
B03-INT	0	6.177	3.810	4.709	7.356	8.356	4.314	2.452	3.457	1.520	4.263

B03-INT	10	3.587	1.832	0.342	0.490	0.665	0.369	0.788	0.633	0.734	0.967
B03-INT	20	0.526	0.467	0.406	0.504	0.385	0.333	-999			
B10-INT	0	4.956	3.388	5.653	5.292	4.833	5.087	5.336	4.926	3.557	1.461
B10-INT	10	1.866	3.362	1.923	3.338	2.635	2.002	1.338	0.978	1.049	1.702
B10-INT	20	0.845	0.696	0.548	0.709	0.547	0.826	0.890	0.730	0.317	0.314
B10-INT	30	0.120	0.234	-999							
C01-INT	0	4.327	4.394	11.145	5.843	4.485	3.990	4.676	6.171	3.418	3.880
C01-INT	10	4.024	2.507	2.325	0.730	1.022	0.962	0.564	0.931	0.479	-999
C02-INT	0	5.016	5.641	5.079	6.385	6.225	6.546	5.069	3.266	3.200	3.947
C02-INT	10	2.637	2.649	3.384	1.951	0.808	1.212	0.391	0.749	0.615	-999
C04-INT	0	6.563	5.495	6.227	4.016	4.544	4.724	4.033	2.176	3.101	2.286
C04-INT	10	2.147	1.973	2.076	3.211	1.302	2.142	0.756	0.855	0.530	0.616
C04-INT	20	1.095	0.263	0.725	0.523	1.060	0.199	-999			
C07-INT	0	5.163	5.339	7.073	6.180	7.465	5.585	3.599	3.420	3.384	2.974
C07-INT	10	2.797	1.797	1.360	1.894	1.260	1.224	0.657	0.797	1.043	0.865
C07-INT	20	0.878	0.631	0.471	0.476	0.606	0.733	0.763	0.315	-999	
C08-INT	0	5.619	4.254	4.755	5.094	7.006	6.422	5.701	4.613	3.553	2.767
C08-INT	10	2.154	2.803	2.153	1.720	1.316	1.308	0.734	1.316	1.045	0.682
C08-INT	20	0.343	0.648	1.109	0.690	0.549	0.505	0.847	0.412	1.785	0.303
C08-INT	30	0.645	0.446	0.360	0.467	0.437	0.264	-999			
C09-INT	0	6.789	4.684	4.165	6.940	3.663	1.775	3.207	2.486	2.221	3.408
C09-INT	10	3.385	1.820	4.639	3.307	1.437	1.266	1.872	1.416	1.380	0.956
C09-INT	20	0.546	0.299	0.565	0.445	-999					

D03-INT	0	6.205	9.454	6.691	6.273	3.365	3.400	4.589	2.544	3.275	2.817
D03-INT	10	3.223	1.885	0.830	1.965	3.384	2.129	2.474	1.530	1.004	0.798
D03-INT	20	1.400	0.817	0.738	1.221	0.815	0.613	0.812	0.796	0.418	0.336
D03-INT	30	0.371	0.408	0.458	0.224	0.530	0.366	0.403	0.317	0.298	0.282
D03-INT	40	0.482	0.747	0.369	1.243	0.126	0.779	0.395	-999		
D05-INT	0	6.175	3.011	5.415	4.499	3.280	9.023	3.544	3.156	1.957	2.610
D05-INT	10	2.034	1.349	2.436	2.338	0.831	1.731	1.249	2.226	1.418	0.807
D05-INT	20	0.615	0.292	0.705	0.762	1.343	0.624	0.958	0.389	0.582	0.707
D05-INT	30	0.857	0.580	0.965	0.551	0.357	0.350	0.454	0.732	0.851	0.720
D05-INT	40	0.564	0.554	-999							
D07-INT	0	4.227	3.073	3.028	5.441	4.515	3.751	4.918	2.766	3.314	3.518
D07-INT	10	2.540	2.517	5.019	2.419	1.766	2.564	1.883	1.438	0.972	1.329
D07-INT	20	0.796	0.580	0.295	0.612	-999					
D10-INT	0	6.091	3.671	5.730	5.781	5.786	2.874	2.398	2.205	1.074	1.005
D10-INT	10	2.280	1.571	2.321	2.604	1.716	2.168	1.079	0.882	0.814	0.852
D10-INT	20	1.023	0.313	0.671	1.483	0.917	0.745	0.420	0.721	0.584	0.243
D10-INT	30	0.382	0.446	0.692	0.384	0.382	0.185	0.435	0.380	0.440	0.603
D10-INT	40	0.308	0.400	0.400	0.301	0.360	0.713	0.650	0.418	0.625	0.559
D10-INT	50	0.310	-999								
E05-INT	0	5.625	5.404	5.362	5.485	3.464	1.588	2.031	2.702	2.825	2.652
E05-INT	10	1.542	2.925	1.592	2.000	1.928	1.303	1.303	1.125	1.164	0.782
E05-INT	20	0.867	0.907	0.651	0.537	0.572	1.105	1.366	1.153	-999	
E10-INT	0	4.886	4.929	3.922	2.207	2.751	3.861	3.951	2.777	2.470	5.191

E10-INT	10	3.783	3.028	2.614	2.204	2.271	1.501	1.261	1.223	1.128	0.793
E10-INT	20	1.176	1.351	0.681	0.403	0.434	0.571	0.278	-999		
G03-INT	0	6.494	4.452	4.438	4.413	4.526	5.561	5.069	4.784	5.684	3.479
G03-INT	10	2.451	3.010	2.480	2.354	3.218	1.068	1.003	0.991	0.977	0.687
G03-INT	20	0.521	0.952	0.189	0.591	0.295	0.407	0.279	0.424	0.479	0.467
G03-INT	30	0.471	0.340	0.372	0.402	0.176	0.320	0.265	0.256	0.268	0.244
G03-INT	40	0.350	0.260	0.288	0.288	0.284	0.414	-999			
G04-INT	0	7.691	5.117	3.708	5.231	6.076	6.337	5.538	1.854	2.670	2.842
G04-INT	10	3.188	3.725	2.721	2.417	2.552	1.326	1.518	1.734	1.346	1.313
G04-INT	20	0.991	0.982	0.366	1.083	0.748	0.343	0.496	0.317	0.661	0.489
G04-INT	30	0.495	0.424	0.433	0.258	0.098	0.097	0.265	0.355	0.243	0.229
G04-INT	40	0.189	0.128	0.221	0.710	0.297	0.477	0.333	0.186	-999	
G05-INT	0	7.969	6.415	4.307	5.021	3.676	4.100	3.230	3.449	2.815	2.459
G05-INT	10	1.585	0.780	0.769	1.269	1.703	0.980	0.839	1.111	1.691	0.997
G05-INT	20	0.750	0.600	1.116	0.744	0.465	1.340	0.492	2.089	1.265	0.683
G05-INT	30	0.434	0.342	0.580	0.173	0.324	0.145	0.147	0.317	0.627	0.672
G05-INT	40	-999									
G06-INT	0	6.041	2.484	6.005	7.324	5.645	6.965	4.054	5.403	4.700	3.716
G06-INT	10	2.754	2.338	1.867	2.397	1.560	1.331	1.564	1.062	1.166	0.865
G06-INT	20	0.651	0.872	1.107	1.008	0.445	0.543	0.505	0.673	0.528	0.561
G06-INT	30	0.437	0.287	0.583	0.554	0.339	0.240	0.367	0.282	0.550	0.447
G06-INT	40	0.311	0.296	0.743	0.384	0.329	0.973	0.543	0.812	0.544	0.694
G06-INT	50	0.215	0.254	-999							

G09-INT	01	7.826	5.650	5.587	7.158	5.432	4.844	5.158	4.379	3.704	3.820
G09-INT	02	2.813	2.513	1.690	1.416	1.375	0.665	1.325	0.768	0.618	0.389
G09-INT	03	0.507	1.091	0.991	0.657	0.764	0.290	0.717	0.370	0.286	0.359
G09-INT	04	0.455	0.384	0.650	0.473	0.297	0.234	0.442	0.296	0.322	0.240
G09-INT	0	0.680	0.301	0.291	-999						
G10-INT	01	8.676	5.493	4.292	3.817	4.750	4.941	4.412	4.884	4.887	4.625
G10-INT	02	2.598	1.873	1.744	1.069	0.938	0.476	1.106	0.745	1.027	0.402
G10-INT	03	0.713	0.395	0.168	0.354	0.422	0.351	0.570	0.688	0.578	0.215
G10-INT	0	0.210	0.254	0.354	0.103	0.170	0.173	0.457	0.159	-999	
H01-INT	01	12.647	4.756	8.460	6.007	6.097	5.007	5.036	3.171	3.327	2.603
H01-INT	02	1.312	1.830	1.611	1.035	0.515	0.557	0.366	0.448	0.215	0.262
H01-INT	03	0.277	0.299	0.395	0.354	0.414	0.191	0.472	0.668	0.396	0.428
H01-INT	04	0.673	0.408	0.608	0.452	0.630	0.773	0.657	0.311	0.373	0.626
H01-INT	0	0.408	0.387	0.537	0.244	0.185	0.540	0.609	0.310	-999	
H03-INT	01	6.623	5.094	4.818	4.694	5.858	4.519	3.807	2.246	3.709	2.060
H03-INT	02	0.551	3.051	2.862	1.707	1.743	0.465	0.556	0.660	0.778	0.744
H03-INT	0	0.783	1.386	0.431	-999						
H05-INT	01	6.964	4.196	4.621	6.106	2.795	7.303	5.435	5.061	4.269	4.603
H05-INT	02	4.846	1.637	2.141	2.033	0.703	0.638	0.379	0.366	0.473	0.324
H05-INT	03	0.448	0.509	0.473	0.365	0.445	0.395	0.452	0.395	0.315	0.398
H05-INT	0	0.366	0.359	0.513	-999						
H06-INT	01	5.645	4.197	5.190	4.249	4.799	3.889	5.156	5.979	3.245	1.164
H06-INT	0	0.925	1.252	1.120	0.751	0.584	1.438	1.487	0.225	-999	

H09-INT	01	6.090	4.391	4.214	6.210	3.929	3.746	3.359	2.313	3.017	3.967
H09-INT	02	2.408	2.949	3.055	3.226	2.448	2.500	1.277	1.381	2.108	0.751
H09-INT	03	0.865	0.836	0.634	0.651	0.314	0.300	0.940	0.642	0.616	0.455
H09-INT	0	1.143	-999								
H10-INT	01	7.542	5.411	4.628	3.978	5.798	6.679	5.877	2.651	4.211	3.711
H10-INT	02	2.747	3.580	3.664	0.803	1.123	0.837	1.621	1.430	1.724	1.184
H10-INT	03	1.533	1.652	1.350	1.183	1.255	0.656	0.566	0.691	0.896	0.262
H10-INT	04	0.731	0.844	0.934	0.676	0.381	0.364	0.505	0.272	0.323	0.453
H10-INT	0	0.209	-999								
I02-INT	01	5.771	4.894	4.773	7.397	5.660	5.758	4.242	4.268	2.620	2.853
I02-INT	02	4.278	2.926	1.444	1.053	0.827	0.675	0.710	0.564	0.223	0.235
I02-INT	0	0.848	0.514	0.202	0.428	0.334	0.294	0.238	-999		
I03-INT	01	6.084	3.294	4.682	8.250	10.703	4.595	3.961	4.437	4.210	2.181
I03-INT	02	1.621	0.691	0.895	0.629	0.592	0.684	0.514	0.629	0.495	0.450
I03-INT	0	0.587	1.003	1.465	0.995	-999					
I05-INT	01	6.689	5.884	7.813	7.083	5.815	3.696	5.704	5.779	3.440	2.607
I05-INT	02	1.859	1.443	1.381	0.839	2.124	1.241	1.218	1.204	0.860	0.539
I05-INT	03	0.657	0.433	0.424	0.379	0.415	0.396	0.962	0.479	0.302	0.328
I05-INT	04	0.483	0.396	0.337	0.408	0.433	0.443	0.412	0.291	0.314	0.209
I05-INT	05	0.355	0.330	0.618	0.553	0.400	0.703	0.385	0.328	0.185	0.234
I05-INT	06	0.216	0.256	0.250	0.347	0.743	0.355	0.301	0.301	0.381	0.370
I05-INT	0	0.355	0.400	0.530	0.564	1.396	0.471	-999			
I10-INT	0	9.353	4.550	5.796	7.693	6.535	5.371	2.212	3.491	2.523	1.999

I10-INT	10	2.349	2.289	2.169	1.482	2.341	1.859	0.774	1.161	1.352	0.985
I10-INT	20	1.056	1.391	0.408	0.381	0.645	0.375	0.480	0.313	0.333	0.307
I10-INT	30	0.259	0.221	0.275	0.476	0.245	0.316	0.245	0.265	0.259	0.354
I10-INT	40	0.240	0.275	0.273	0.369	0.390	0.379	0.370	0.224	0.302	0.419
I10-INT	50	0.229	0.176	0.379	0.374	0.243	0.404	0.326	0.440	0.476	0.340
I10-INT	60	0.332	0.203	0.374	0.544	-999					
J01-INT	0	10.340	8.324	7.134	5.617	3.542	5.044	4.618	3.368	2.852	2.364
J01-INT	10	2.629	1.808	1.086	1.352	1.205	1.057	1.086	1.383	1.051	0.980
J01-INT	20	0.535	0.515	0.641	0.495	0.496	0.544	0.537	0.245	0.370	0.256
J01-INT	30	0.341	0.152	0.130	0.390	0.352	0.400	0.152	0.395	0.380	0.534
J01-INT	40	0.215	0.286	0.224	0.157	0.601	0.224	0.192	0.661	0.366	0.280
J01-INT	50	0.191	0.412	0.289	0.157	0.330	0.621	0.399	0.811	0.563	0.714
J01-INT	60	0.399	0.565	0.549	0.286	0.564	0.302	0.282	0.181	0.140	0.230
J01-INT	70	-999									
J02-INT	0	7.584	4.816	8.674	7.698	5.950	4.834	4.251	6.009	2.232	1.693
J02-INT	10	2.572	2.094	1.708	1.351	1.187	0.882	1.990	0.399	1.349	0.554
J02-INT	20	-999									
J04-INT	0	7.839	5.636	4.455	5.510	3.615	6.027	5.289	4.719	4.372	2.071
J04-INT	10	2.661	2.814	2.486	2.545	1.385	2.852	1.937	1.031	1.600	0.676
J04-INT	20	0.749	1.520	0.786	0.459	0.457	0.418	0.408	0.401	0.666	0.181
J04-INT	30	-999									
J05-INT	0	6.683	4.203	4.613	5.409	7.240	4.512	4.131	5.087	4.130	3.952
J05-INT	10	2.753	2.918	2.006	2.017	1.630	1.912	1.616	1.408	1.426	0.995

J05-INT	20	1.495	0.768	0.674	0.776	0.602	0.760	0.539	0.419	0.352	0.203
J05-INT	30	0.283	0.580	0.389	0.363	0.354	0.556	0.492	0.791	0.596	0.262
J05-INT	40	0.419	0.351	0.314	0.442	0.295	0.488	0.340	0.292	0.420	0.124
J05-INT	50	0.477	0.554	0.227	0.331	0.339	0.194	0.431	0.207	0.302	0.207
J05-INT	60	0.179	0.340	0.220	0.107	0.206	0.217	0.206	0.130	0.092	0.074
J05-INT	70	0.118	0.192	0.194	0.374	-999					
J06-INT	0	8.081	7.862	8.018	6.604	6.312	6.532	4.615	3.722	3.034	2.157
J06-INT	10	1.916	1.327	1.300	3.169	0.987	2.130	0.962	1.345	0.716	0.965
J06-INT	20	0.805	0.831	0.479	0.276	0.307	0.305	0.234	0.503	0.283	0.656
J06-INT	30	0.389	0.568	0.398	0.195	0.248	0.176	0.429	0.379	0.437	0.420
J06-INT	40	0.484	0.262	0.476	0.221	0.380	0.256	0.617	0.437	0.303	0.352
J06-INT	50	0.642	0.517	0.437	0.568	0.331	0.423	0.412	0.583	-999	
J07-INT	0	5.446	3.598	5.584	3.632	3.185	5.702	4.716	4.268	3.642	3.920
J07-INT	10	2.906	2.605	1.362	1.479	1.611	1.367	1.430	1.566	1.485	1.013
J07-INT	20	0.748	0.851	0.822	0.955	0.626	0.412	0.495	0.715	0.429	0.399
J07-INT	30	0.475	0.280	0.379	0.438	0.475	0.621	0.364	0.272	0.674	0.406
J07-INT	40	0.638	0.523	0.335	0.325	0.623	0.445	0.238	0.648	0.408	0.561
J07-INT	50	0.295	0.526	0.348	0.423	0.381	0.280	0.297	0.313	0.366	0.257
J07-INT	60	0.379	0.240	0.235	0.164	0.198	-999				
J08-INT	0	6.430	5.626	7.040	7.172	6.093	5.703	2.388	3.396	4.422	3.563
J08-INT	10	2.603	0.987	1.664	1.825	2.016	1.800	1.250	1.098	1.257	0.957
J08-INT	20	0.935	0.618	0.766	0.772	0.811	0.846	0.681	0.618	0.626	0.540
J08-INT	30	0.572	0.423	0.518	1.196	0.660	0.531	0.775	0.495	0.233	0.253

J08-INT	40	-999									
J09-INT	0	8.725	4.621	5.651	5.361	6.291	5.746	5.714	1.729	2.689	2.083
J09-INT	10	1.788	1.122	1.767	1.934	1.291	0.623	0.564	1.732	1.764	1.163
J09-INT	20	1.496	0.667	1.058	0.476	0.507	0.397	0.570	1.974	0.321	0.384
J09-INT	30	1.308	2.151	1.742	2.125	0.696	2.287	-999			
K01-INT	0	5.667	3.160	3.311	4.940	4.124	3.990	3.609	4.102	5.047	3.782
K01-INT	10	1.426	3.489	3.189	1.712	1.883	2.197	1.991	1.469	1.292	1.617
K01-INT	20	1.050	0.452	0.299	0.568	0.296	0.586	0.428	0.588	0.578	0.654
K01-INT	30	0.699	0.646	0.269	0.704	0.278	0.867	0.188	0.921	0.350	0.842
K01-INT	40	0.425	0.872	0.246	0.350	0.798	0.592	0.447	0.516	0.296	0.217
K01-INT	50	0.306	0.342	0.334	0.212	-999					
K02-INT	0	5.513	3.913	3.679	5.704	7.717	7.344	6.525	6.260	4.585	3.969
K02-INT	10	3.011	2.576	2.968	2.252	1.545	1.123	1.294	1.318	1.011	1.138
K02-INT	20	0.498	0.856	0.647	0.615	0.492	0.409	0.557	0.312	0.360	0.648
K02-INT	30	0.330	0.335	0.326	-999						
K04-INT	0	3.495	3.125	3.687	3.672	4.392	3.897	3.855	4.420	6.710	4.472
K04-INT	10	4.016	3.986	2.101	1.788	1.570	1.747	1.176	1.430	2.335	1.025
K04-INT	20	3.157	1.073	0.558	0.646	0.489	0.383	0.359	0.423	0.331	0.542
K04-INT	30	0.810	0.976	0.756	0.645	0.531	0.345	0.308	0.335	0.630	0.320
K04-INT	40	0.381	0.497	0.300	0.218	0.391	0.360	0.315	0.289	0.580	0.522
K04-INT	50	0.354	0.345	0.182	0.205	0.430	0.359	0.360	0.340	0.327	0.129
K04-INT	60	0.172	0.296	0.171	0.198	0.417	0.297	0.474	0.217	0.384	0.187
K04-INT	70	-999									

K05-INT	0	4.539	3.617	6.384	3.590	3.346	6.216	4.567	3.962	4.969	4.529
K05-INT	10	4.755	5.465	2.604	1.687	0.749	1.551	2.332	1.699	0.669	0.749
K05-INT	20	0.787	0.308	0.409	0.694	0.793	0.830	0.552	0.452	0.443	0.303
K05-INT	30	0.342	0.226	0.205	0.104	0.205	0.089	0.198	0.192	0.256	0.209
K05-INT	40	0.296	0.397	0.218	0.211	0.265	0.260	0.264	0.235	0.253	0.251
K05-INT	50	0.168	0.100	0.566	0.363	0.139	-999				
K06-INT	0	5.227	3.386	4.743	4.128	3.885	4.896	5.974	2.968	3.653	2.829
K06-INT	10	2.644	2.910	2.632	2.423	2.397	1.870	1.836	0.830	0.739	0.758
K06-INT	20	0.568	0.975	1.067	0.421	0.415	0.380	0.428	0.532	0.321	0.330
K06-INT	30	0.400	0.385	0.392	0.268	0.232	0.187	0.440	0.636	0.522	0.475
K06-INT	40	0.198	0.351	0.189	0.125	0.196	0.374	0.290	0.374	0.434	0.404
K06-INT	50	0.262	0.244	0.247	0.148	0.231	0.143	-999			
K07-INT	0	6.429	3.366	2.785	6.346	5.955	5.290	6.280	3.186	2.080	2.644
K07-INT	10	2.123	1.612	1.985	1.979	1.594	1.493	1.476	1.599	1.100	0.505
K07-INT	20	0.627	0.586	0.663	0.785	0.311	0.522	0.606	0.508	0.511	0.791
K07-INT	30	0.618	0.393	0.473	0.317	0.695	0.633	0.410	0.476	0.389	0.446
K07-INT	40	0.593	0.301	0.272	0.271	0.321	0.674	0.459	0.246	0.344	0.443
K07-INT	50	0.408	0.224	0.327	0.590	0.261	-999				
K09-INT	0	9.061	6.593	7.502	6.393	4.014	2.581	2.639	3.464	5.125	5.421
K09-INT	10	3.948	2.426	2.053	0.812	0.550	0.845	0.699	0.381	0.354	0.302
K09-INT	20	0.265	0.571	0.916	0.570	0.461	0.366	0.328	0.156	0.475	0.583
K09-INT	30	0.237	0.408	0.154	0.299	0.299	0.202	0.150	0.261	0.171	0.143
K09-INT	40	0.187	0.223	0.112	0.483	0.782	0.651	0.772	0.198	0.154	0.147

K09-INT	50	0.132	1.045	0.405	-999						
K10-INT	0	5.214	4.145	4.798	7.196	9.065	5.781	6.143	5.201	2.569	1.741
K10-INT	10	3.269	2.734	1.594	1.239	1.056	1.426	1.199	1.375	1.187	0.856
K10-INT	20	0.505	0.630	0.463	0.551	0.372	0.226	0.514	0.991	0.320	-999
L01-INT	0	7.210	1.798	5.241	3.013	2.837	4.702	2.777	4.753	2.961	3.038
L01-INT	10	1.872	2.247	2.446	2.489	1.842	1.613	1.075	1.295	0.982	0.688
L01-INT	20	1.303	1.089	0.830	1.067	1.045	0.652	0.635	0.765	1.151	0.663
L01-INT	30	1.136	0.691	0.622	1.026	0.915	0.756	0.728	0.726	0.676	0.777
L01-INT	40	0.283	0.146	0.354	0.369	0.320	0.443	0.330	0.371	0.610	0.401
L01-INT	50	0.333	0.253	0.370	0.564	0.161	0.227	0.176	0.313	0.389	0.305
L01-INT	60	0.215	0.292	0.166	0.262	0.124	0.146	0.663	0.296	-999	
L03-INT	0	4.546	3.149	2.524	3.873	6.254	4.071	5.601	4.932	2.544	5.551
L03-INT	10	6.155	2.786	3.622	2.713	3.233	1.954	0.830	0.227	-999	
LA01-INT	0	5.937	6.085	6.508	8.108	8.048	6.790	5.433	3.946	3.397	1.718
LA01-INT	10	2.458	2.544	2.319	1.822	0.953	1.171	0.642	0.854	0.591	0.736
LA01-INT	20	0.662	0.638	0.937	0.734	0.877	0.589	0.747	0.546	0.498	0.604
LA01-INT	30	0.711	0.608	0.604	0.561	0.591	0.385	0.286	1.781	1.420	1.271
LA01-INT	40	0.378	0.264	0.267	-999						
LA02-INT	0	6.062	5.859	6.060	6.457	5.945	7.888	7.423	5.863	4.949	2.844
LA02-INT	10	1.997	1.303	1.936	1.238	1.139	1.069	1.480	1.311	1.040	1.696
LA02-INT	20	0.638	0.678	0.868	0.338	0.491	0.983	0.595	0.626	0.444	0.366
LA02-INT	30	0.218	0.329	0.382	0.272	0.308	0.465	0.572	0.297	0.321	0.284
LA02-INT	40	0.332	0.391	0.402	0.332	0.471	0.243	0.388	0.525	0.473	0.719

LA02-INT	50	0.475	-999								
LA03-INT	0	8.949	6.844	8.286	7.782	3.709	6.052	4.664	2.891	2.005	2.573
LA03-INT	10	1.571	1.320	1.003	0.926	0.702	0.503	0.737	0.819	0.577	1.869
LA03-INT	20	0.770	0.518	0.593	0.426	0.386	0.444	0.423	0.581	0.286	0.491
LA03-INT	30	0.344	0.792	0.434	0.534	0.370	0.321	0.351	0.465	0.390	0.950
LA03-INT	40	0.695	1.247	0.508	0.338	0.247	0.241	0.204	0.367	0.358	0.437
LA03-INT	50	0.615	0.645	0.544	1.487	0.757	-999				
LA04-INT	0	7.132	4.220	5.217	5.408	6.793	8.684	6.495	3.325	3.635	4.440
LA04-INT	10	4.037	5.077	3.883	2.845	1.673	1.064	0.780	0.772	1.086	0.808
LA04-INT	20	0.661	0.555	0.640	0.748	0.785	0.748	0.440	0.496	0.871	0.319
LA04-INT	30	0.290	0.206	0.251	0.505	0.314	0.693	0.550	0.376	0.551	0.254
LA04-INT	40	0.344	0.515	0.211	0.682	0.706	0.762	0.193	0.582	0.431	-999
N01-INT	0	7.432	12.190	5.983	7.195	6.896	6.807	6.671	4.448	2.656	2.843
N01-INT	10	1.730	2.265	2.184	1.883	1.204	1.408	1.386	1.158	1.034	0.495
N01-INT	20	1.597	0.894	0.579	0.796	0.588	0.606	0.468	-999		
N02-INT	0	8.761	6.609	6.234	6.588	6.184	6.584	5.445	4.081	3.453	2.159
N02-INT	10	2.097	2.436	1.730	1.691	1.386	1.481	0.945	1.400	0.779	1.006
N02-INT	20	0.936	1.132	0.664	0.478	0.605	0.779	0.747	0.440	0.523	0.530
N02-INT	30	0.769	0.418	0.571	0.332	0.249	-999				
N04-INT	0	7.350	3.701	2.569	4.010	3.683	2.241	4.481	1.639	4.537	3.079
N04-INT	10	4.853	3.250	2.941	2.359	2.850	2.057	2.699	2.548	1.581	2.448
N04-INT	20	2.898	1.214	1.245	0.430	-999					
N06-INT	0	5.547	4.131	3.399	4.324	4.411	4.142	3.582	5.443	4.836	5.152

N06-INT	10	2.956	3.748	2.849	2.498	1.572	1.497	2.726	1.583	0.688	0.638
N06-INT	20	1.215	0.934	0.899	0.608	0.510	0.355	0.573	0.406	0.194	0.315
N06-INT	30	0.581	0.268	-999							
N08-INT	0	8.072	4.544	7.152	6.607	6.343	5.347	3.497	3.357	4.361	2.759
N08-INT	10	2.454	2.434	2.311	2.416	2.625	1.822	2.671	0.619	1.374	0.764
N08-INT	20	-999									
N09-INT	0	5.219	3.526	5.603	4.248	3.663	3.781	4.620	4.367	4.136	5.619
N09-INT	10	3.616	3.456	3.437	2.577	1.841	1.770	1.591	0.768	0.981	0.941
N09-INT	20	1.204	1.212	0.492	0.648	0.681	0.861	0.612	0.474	1.784	0.914
N09-INT	30	0.618	0.955	0.756	-999						
N10-INT	0	6.724	11.674	6.170	6.987	6.133	5.106	5.961	4.739	4.238	2.300
N10-INT	10	1.946	1.487	1.904	1.879	0.716	0.300	-999			
P01-INT	0	5.964	3.321	2.889	3.488	2.847	5.364	3.474	4.674	6.965	4.726
P01-INT	10	4.316	3.520	4.107	2.706	3.158	1.738	1.559	1.886	1.060	1.478
P01-INT	20	0.894	0.808	1.376	0.663	0.756	0.481	0.382	0.543	0.315	0.288
P01-INT	30	0.461	0.459	0.345	0.280	0.658	0.320	0.177	-999		
P02-INT	0	5.778	2.978	4.169	7.218	2.285	4.399	2.140	4.944	4.350	2.991
P02-INT	10	3.901	2.782	1.955	2.480	2.753	2.042	3.901	2.915	2.147	2.025
P02-INT	20	1.917	1.573	0.972	0.769	0.831	0.971	0.814	0.747	0.538	0.544
P02-INT	30	0.716	0.676	0.611	0.508	0.628	0.701	0.628	0.724	0.538	0.789
P02-INT	40	0.404	0.425	0.422	0.444	0.374	0.627	0.549	0.364	0.478	0.646
P02-INT	50	0.389	0.640	0.590	0.379	0.554	0.311	0.142	0.214	0.209	-999
P03-INT	0	5.513	3.809	5.736	7.020	7.419	6.919	6.361	5.210	4.375	2.759

P03-INT	10	3.159	0.918	1.126	0.587	0.836	0.680	1.105	0.657	1.011	0.366
P03-INT	20	0.574	0.676	0.564	0.800	0.679	0.303	0.580	0.854	0.729	0.705
P03-INT	30	0.264	0.350	0.505	0.328	0.393	0.328	0.215	0.181	0.253	0.235
P03-INT	40	0.217	0.370	0.303	0.191	0.331	0.418	0.404	0.337	0.127	0.276
P03-INT	50	0.838	0.608	0.240	-999						
P05-INT	0	4.685	0.602	2.455	2.866	5.017	5.004	3.822	3.496	3.430	2.963
P05-INT	10	1.953	2.892	2.104	3.164	2.376	3.145	2.001	1.170	0.983	0.922
P05-INT	20	1.533	0.757	1.300	0.836	0.613	1.001	0.751	0.983	0.730	0.486
P05-INT	30	0.636	0.653	0.700	0.688	0.575	0.783	1.138	0.625	0.572	0.603
P05-INT	40	0.408	0.185	0.130	0.271	0.603	0.803	1.583	2.584	1.856	3.312
P05-INT	50	2.879	-999								
P07-INT	0	5.678	4.802	5.634	4.623	4.440	6.808	4.151	4.679	4.546	4.919
P07-INT	10	2.540	1.720	2.717	4.220	1.208	0.811	0.420	0.297	-999	
P08-INT	0	3.067	7.859	13.875	7.200	6.219	5.385	5.880	6.602	2.678	2.513
P08-INT	10	2.613	1.088	2.179	1.681	1.545	1.126	0.678	1.500	1.087	0.775
P08-INT	20	0.628	0.465	0.831	0.907	1.134	0.581	0.338	0.572	0.511	0.389
P08-INT	30	0.685	0.330	0.944	0.388	0.282	0.460	0.327	0.372	0.469	0.343
P08-INT	40	0.211	0.501	0.158	0.337	-999					
P09-INT	0	6.141	8.941	2.101	2.600	4.518	4.680	5.100	1.952	3.798	3.462
P09-INT	10	4.334	2.608	3.193	2.032	1.659	2.219	1.731	2.029	1.604	0.493
P09-INT	20	0.836	1.222	1.524	1.983	0.528	0.766	0.371	0.421	0.274	0.609
P09-INT	30	1.105	0.901	1.643	0.821	0.549	0.743	0.446	0.560	0.459	0.366
P09-INT	40	0.299	0.246	0.192	0.593	0.566	0.458	0.405	0.332	0.380	0.710

P09-INT	50	0.345	0.263	0.294	0.634	0.694	0.615	0.640	0.520	0.250	0.431
P09-INT	60	0.911	0.304	1.263	0.516	0.231	-999				
P10-INT	0	5.038	3.680	4.471	6.245	4.922	4.318	5.881	4.905	3.699	3.252
P10-INT	10	3.298	1.911	3.583	2.554	2.107	1.008	1.169	0.967	1.881	0.873
P10-INT	20	0.639	0.642	0.728	0.455	0.805	0.861	0.614	0.361	0.278	0.253
P10-INT	30	-999									
Q01-INT	0	6.593	3.058	7.139	4.339	3.859	5.975	6.388	2.771	2.728	1.890
Q01-INT	10	1.210	0.755	0.974	0.870	1.370	1.485	1.792	1.657	2.559	0.458
Q01-INT	20	0.781	0.562	0.527	0.288	0.272	0.251	0.109	0.227	0.286	0.282
Q01-INT	30	0.351	0.168	0.509	0.408	0.242	0.514	0.227	0.680	0.594	0.227
Q01-INT	40	0.251	0.540	0.708	0.461	0.556	0.366	0.302	0.514	0.405	2.178
Q01-INT	50	0.119	0.110	0.067	0.150	0.098	0.729	1.079	0.255	0.407	0.775
Q01-INT	60	0.660	0.153	0.231	-999						
Q02-INT	0	5.526	3.820	5.110	6.962	5.919	4.235	3.879	0.999	2.665	3.956
Q02-INT	10	3.543	2.846	1.962	0.872	1.827	1.228	0.731	1.815	1.478	1.741
Q02-INT	20	1.223	1.098	0.534	0.645	-999					
Q03-INT	0	5.097	2.487	4.147	4.449	5.571	4.101	4.180	5.963	4.855	4.458
Q03-INT	10	4.358	4.526	3.903	1.408	1.172	1.339	2.849	2.314	1.981	0.412
Q03-INT	20	0.313	0.867	0.418	-999						
Q06-INT	0	5.800	2.932	6.085	4.394	3.145	7.345	6.711	3.393	3.387	3.201
Q06-INT	10	1.332	1.983	1.289	0.925	0.291	1.145	0.725	0.463	0.464	0.444
Q06-INT	20	0.268	0.078	-999							
Q08-INT	0	6.116	3.288	3.938	5.553	5.394	6.031	4.720	4.581	3.594	3.374

Q08-INT	10	2.283	1.565	1.100	1.983	0.717	1.481	0.379	-999		
QO5-INT	0	6.863	6.104	3.334	3.376	3.481	3.457	6.862	6.738	4.785	4.219
QO5-INT	10	2.664	0.470	1.019	1.202	0.439	0.782	0.950	0.927	0.940	0.851
QO5-INT	20	1.178	0.958	0.289	0.240	-999					
QO8-INT	0	6.116	3.288	3.938	5.553	5.394	6.031	4.720	4.581	3.594	3.374
QO8-INT	10	2.283	1.565	1.100	1.983	0.717	1.481	0.379	-999		

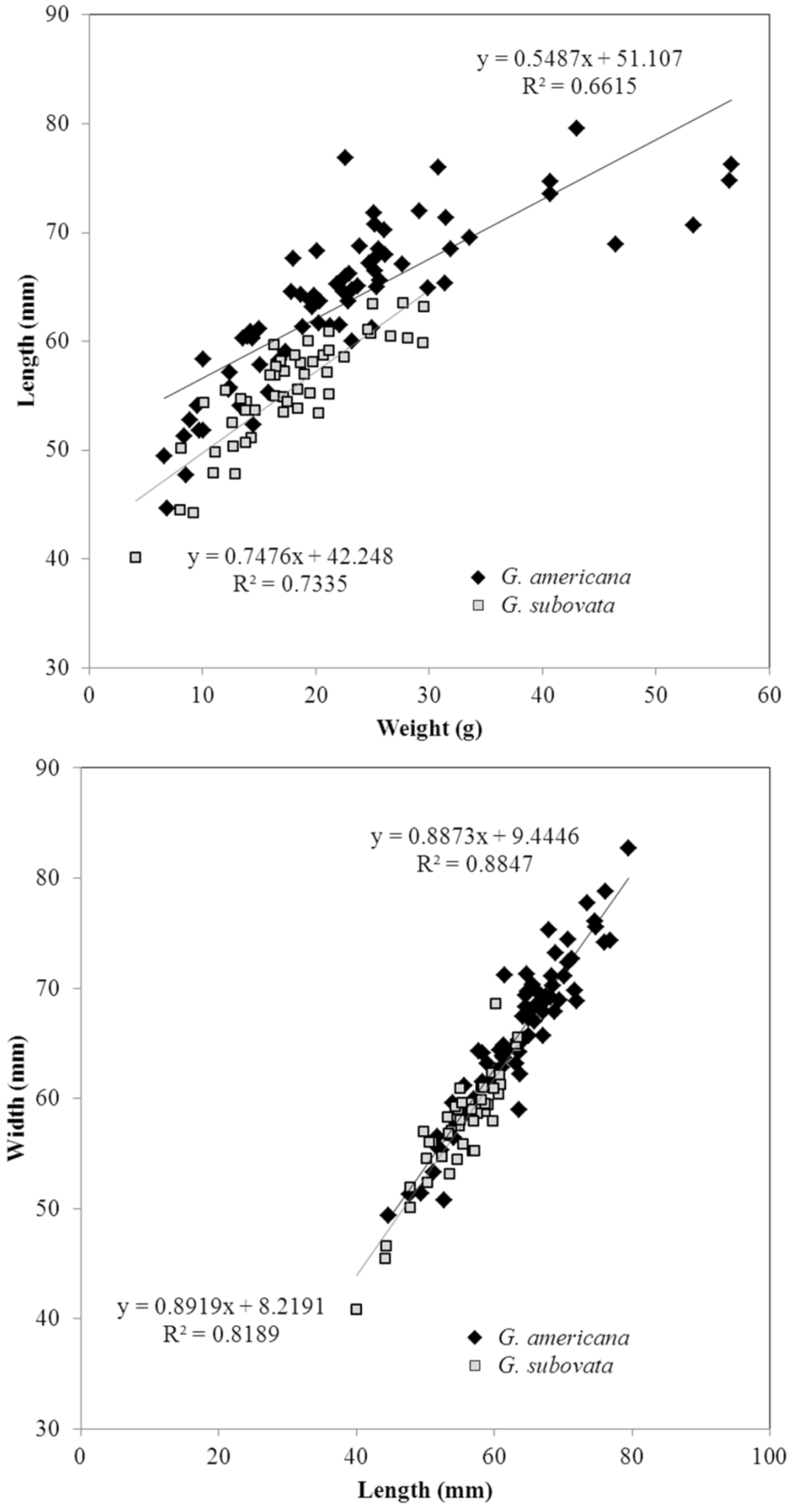

Figure 13. Graphs showing the relationships between length (mm) and weight (g) and width (mm) and length for *G. americna* and *[Costa]glycymeris subovata* specimens from the Yorktown and Chowan River Formations.

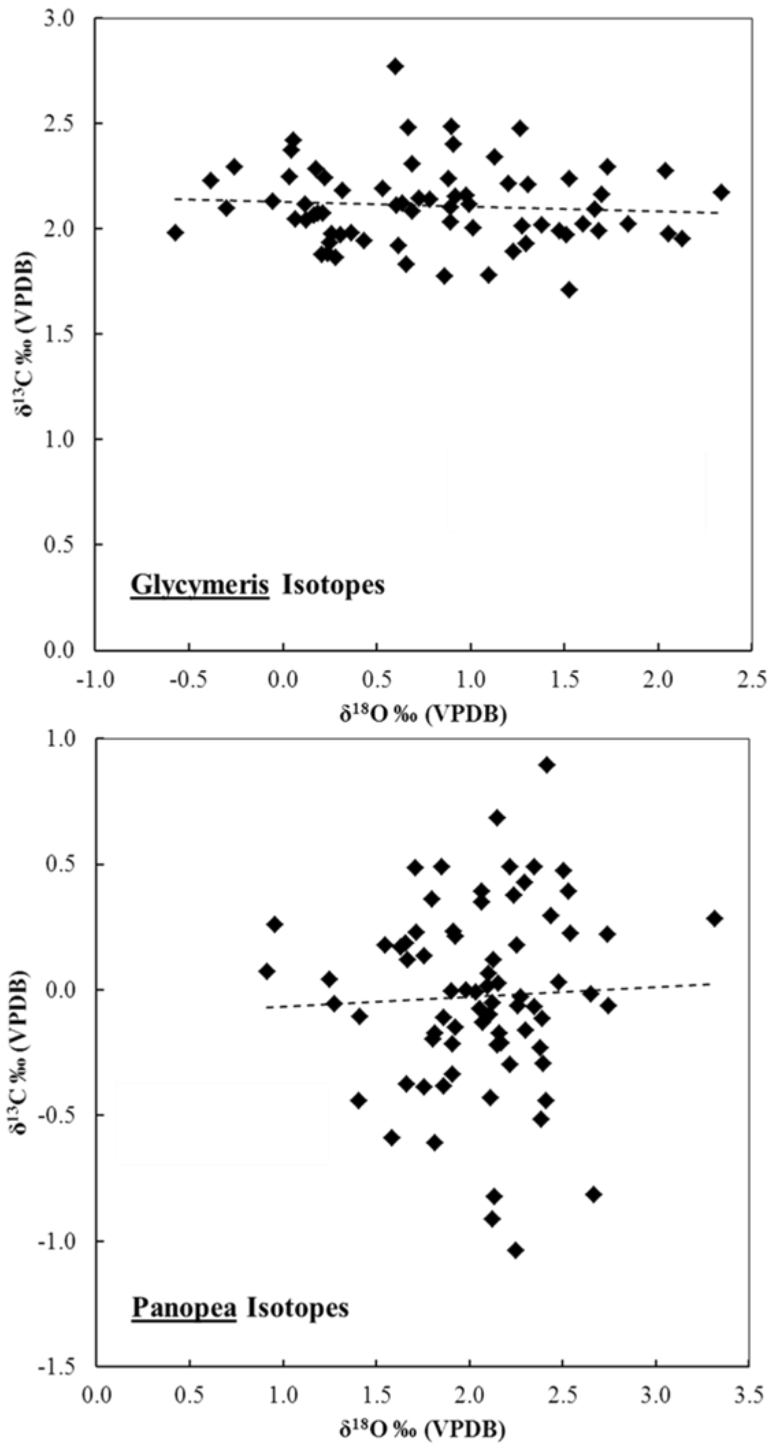

Figure 2. Graphs showing the relationship between δ^{18}O‰ (VPDB) and δ^{13}C‰ (VPDB) for samples of aragonite micro-milled from specimens of G. americana and P. reflexa taken from the Yorktown and Chowan River Formations.

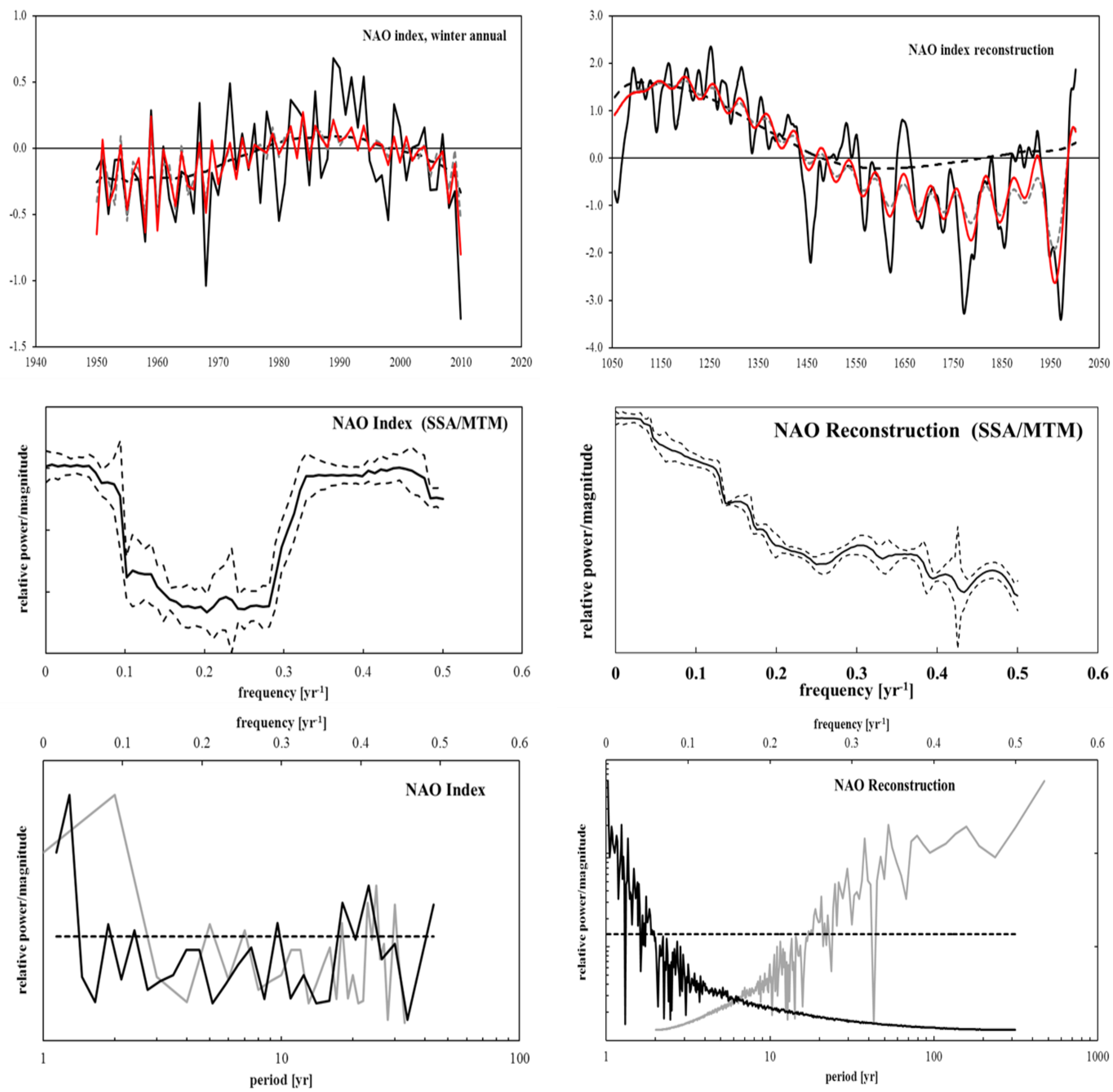

Figure 3. NAO Index (instrumental: 1950-2011) and NAO index (Reconstruction 1050-2011). Top Panels: Plot of the mean annual time series (black solid) with a trend (thick-dashed line), cyclic (thin-dashed), and slow (red) component series. Center Panels: A plot of SSA-MTM spectrum with 95% confidence interval. Bottom Panels: A smoothed periodogram (gray line) and a FFT plot (black line).

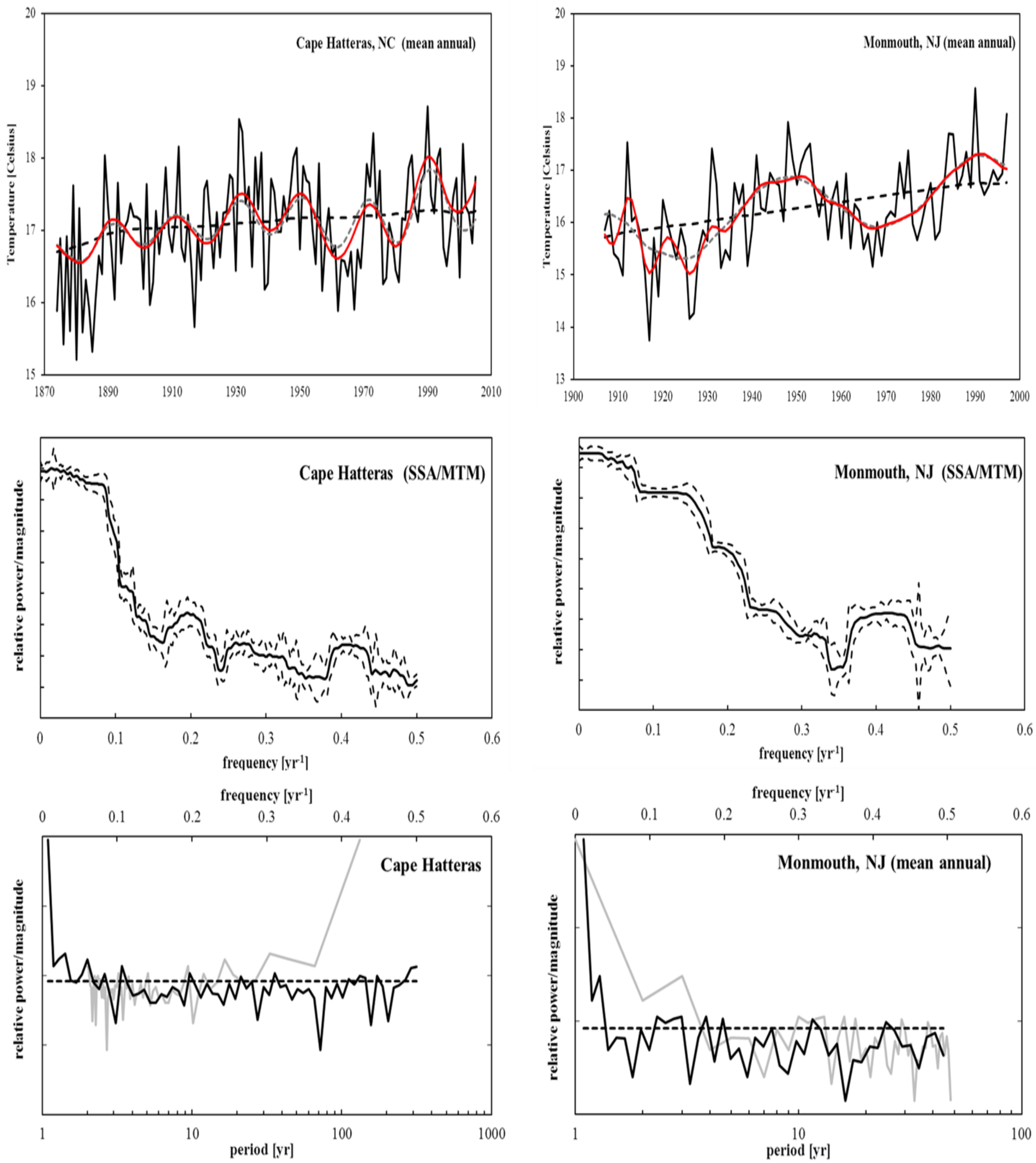

Figure 4. Cape Hatteras, NC and Long Branch Oakhurst, NJ sea surface temperatures. Top Panels: Plot of the mean annual time series (black solid) with a trend (thick-dashed line), cyclic (thin-dashed), and slow (red) component series. Center Panels: A plot of SSA-MTM spectrum with 95% confidence interval. Bottom Panels: A smoothed periodogram (gray line) and a FFT plot (black line).

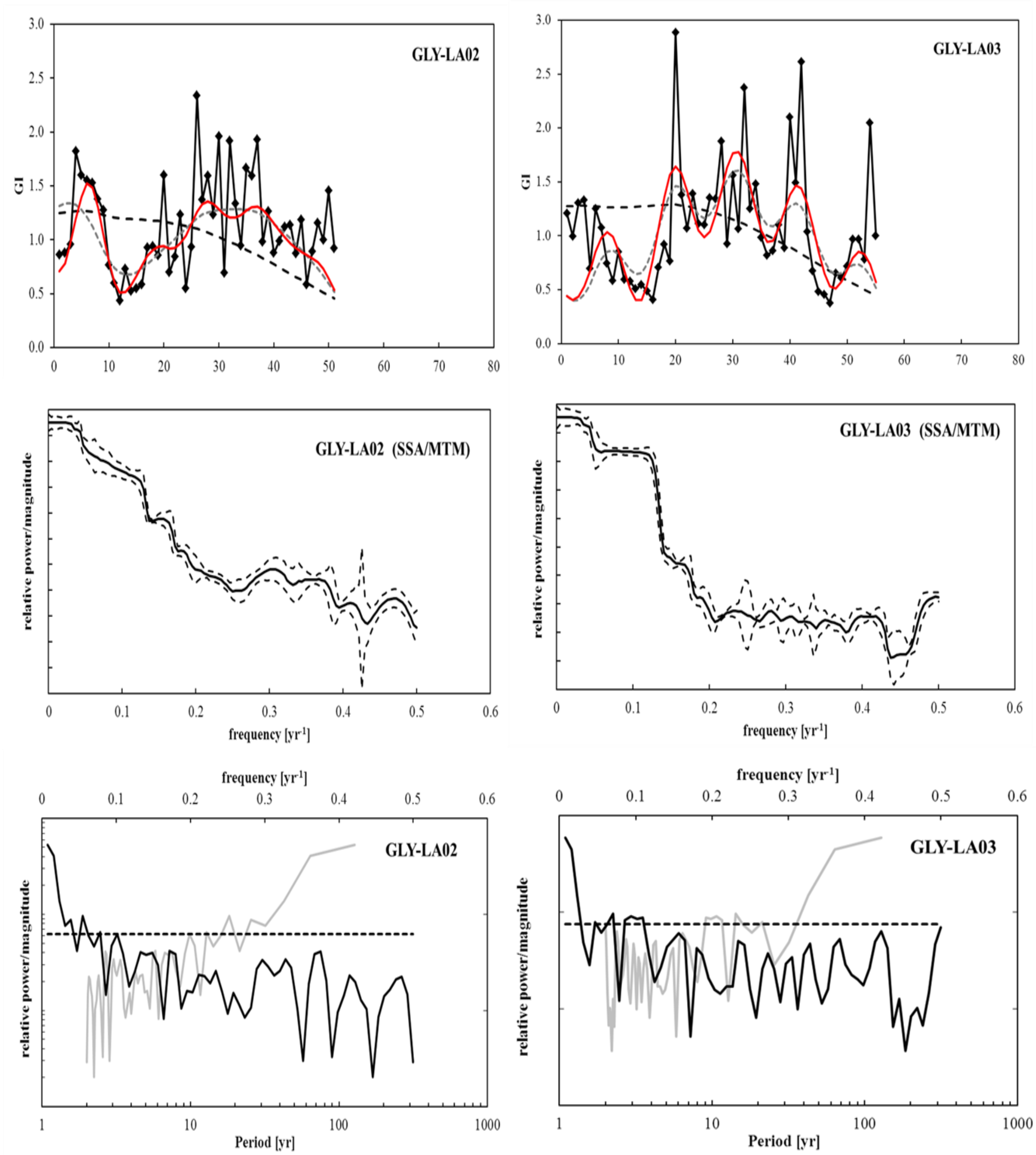

Figure 5. GLY-LA02 and GLY-LA03 standardized growth indices. Top Panels: Plot of the mean annual time series (black solid) with a trend (thick-dashed line), cyclic (thin-dashed), and slow (red) component series. Center Panels: A plot of SSA-MTM spectrum with 95% confidence interval. Bottom Panels: A smoothed periodogram (gray line) and a FFT plot (black line).

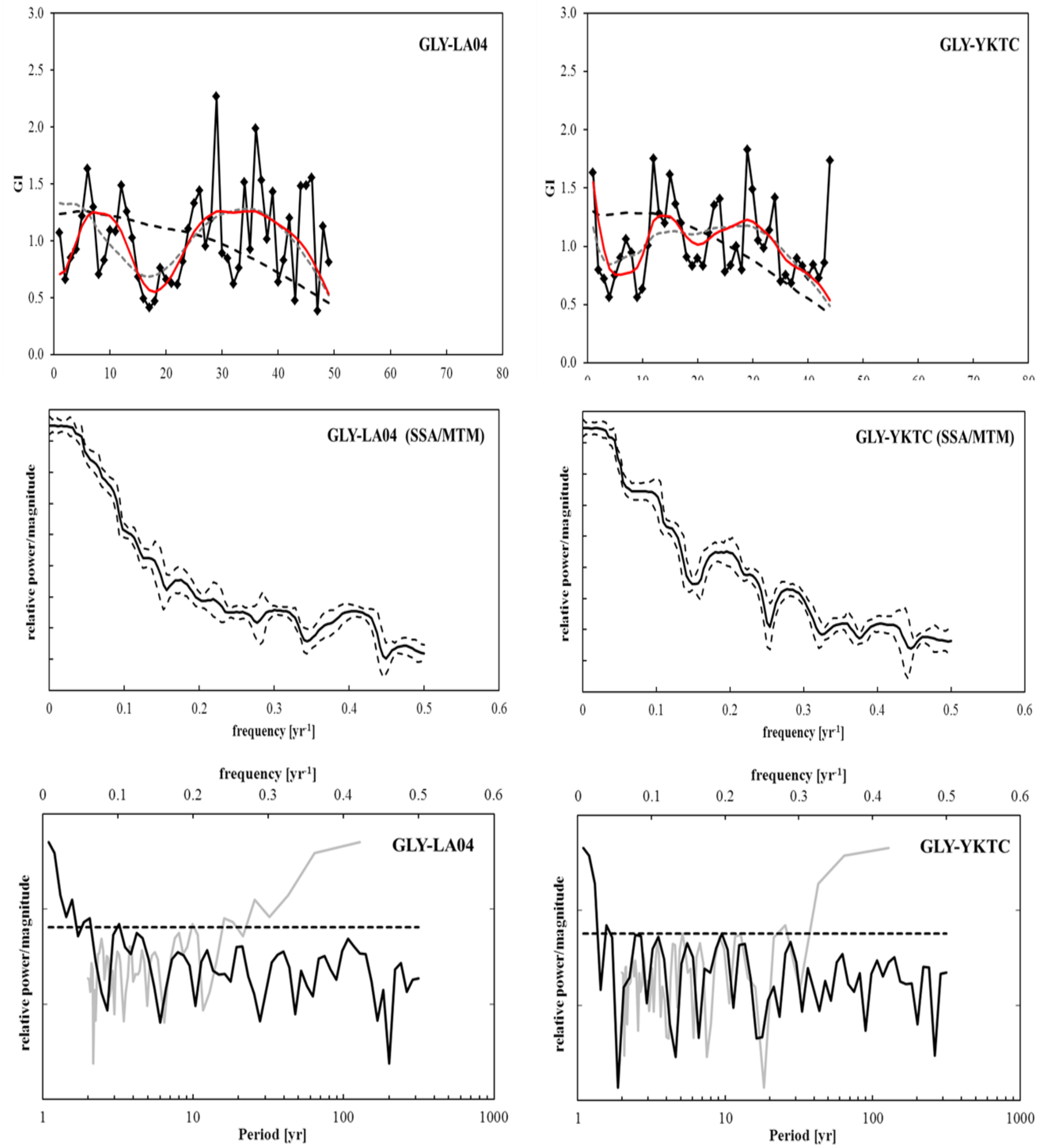

Figure 6. GLY-LA04 and GLY-YKTC standardized growth indices. Top Panels: Plot of the mean annual time series (black solid) with a trend (thick-dashed line), cyclic (thin-dashed), and slow (red) component series. Center Panels: A plot of SSA-MTM spectrum with 95% confidence interval. Bottom Panels: A smoothed periodogram (gray line) and a FFT plot (black line).

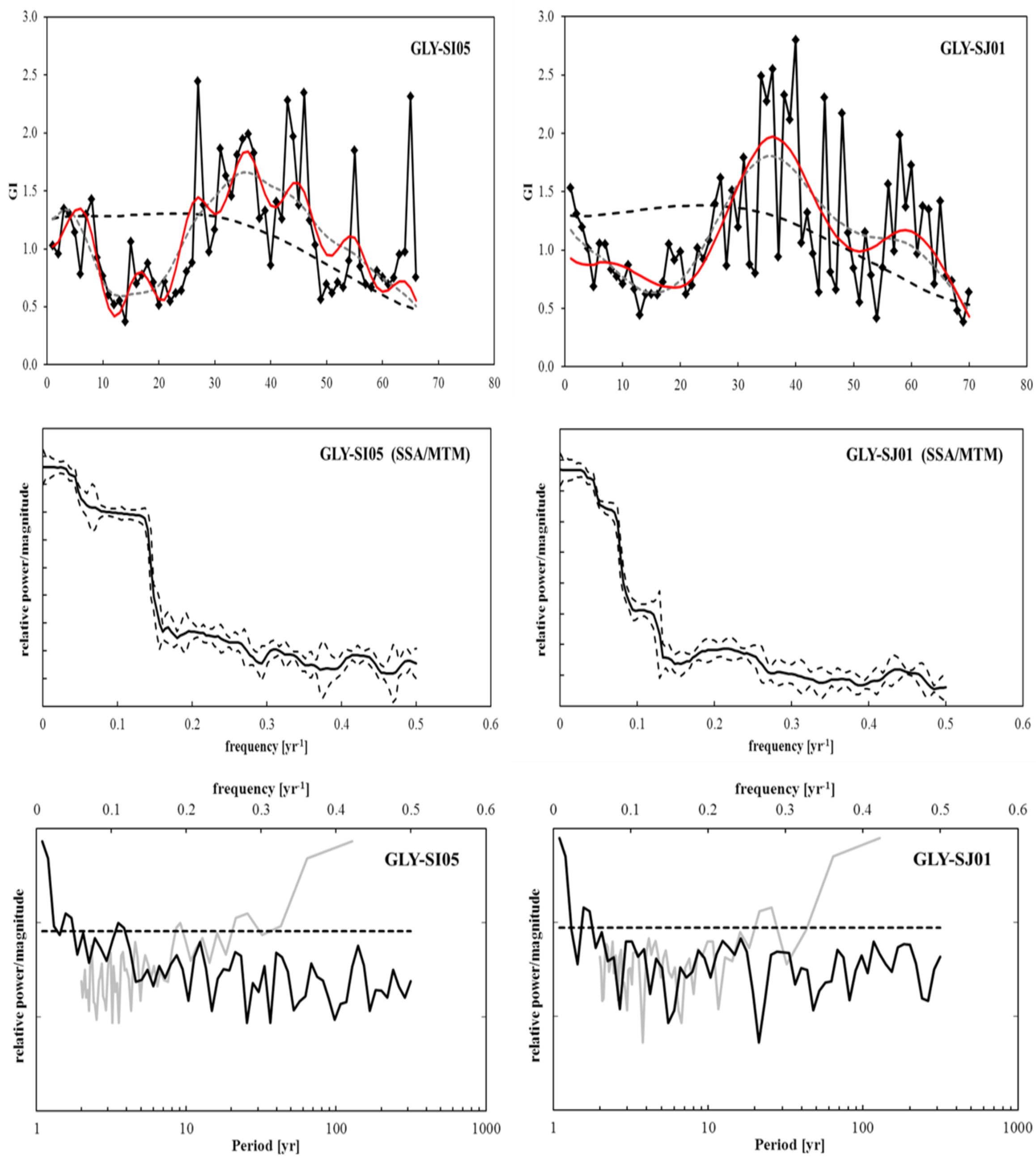

Figure 7. GLY-SI05 AND GLY-SJ01 standardized growth indices. Top Panels: Plot of the mean annual time series (black solid) with a trend (thick-dashed line), cyclic (thin-dashed), and slow (red) component series. Center Panels: A plot of SSA-MTM spectrum with 95% confidence interval. Bottom Panels: A smoothed periodogram (gray line) and a FFT plot (black line).

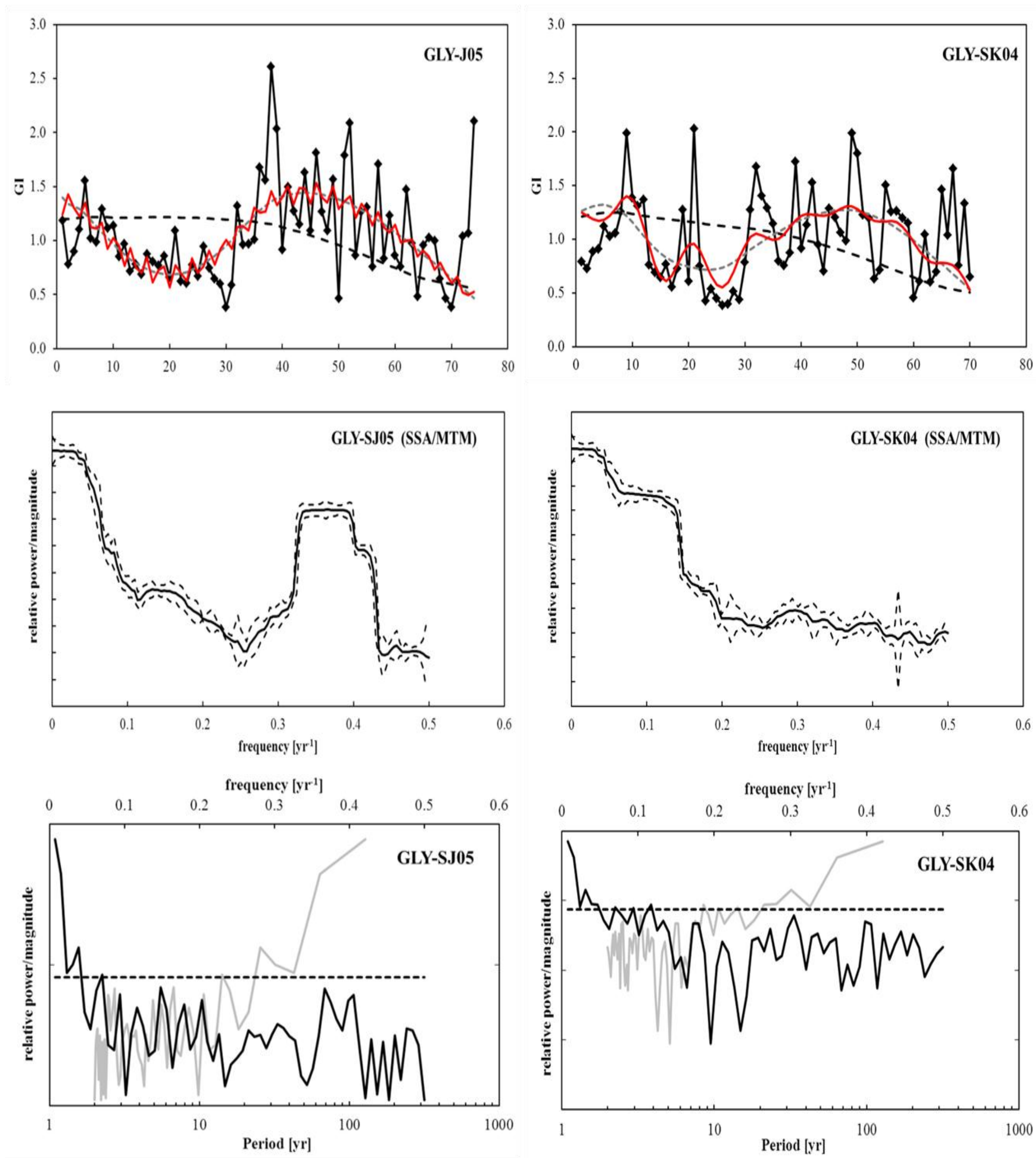

Figure 8. GLY-SJ05 AND GLY-SK04 standardized growth indices. Top Panels: Plot of the mean annual time series (black solid) with a trend (thick-dashed line), cyclic (thin-dashed), and slow (red) component series. Center Panels: A plot of SSA-MTM spectrum with 95% confidence interval. Bottom Panels: A smoothed periodogram (gray line) and a FFT plot (black line).

‘R’ Environment Code

Clear console & load Libraries

```
rm(list=ls())

library(Rssa)
library (dplR)
library(multitaper)
library(RODBC)
library(TSA)
library(RSEIS)
library(dplR)
```

###Read in raw increment files and detrend in dplR

```
glchwn <- read.rwl('gly_chwn.rwl')
glyktn <- read.rwl('gly_yktn.rwl')
glchwn.rwi <- detrend(glchwn, method='Spline')
glyktn.rwi <- detrend(glyktn, method='Spline')
```

####Read in annual times series

```
GlyRwi <- read.table(file = "GlyRwi.txt",sep="\t", header = TRUE)
NAO <- read.table(file = "NAO.txt",header = TRUE)
cape <- read.table(file = "cape_annual.txt",header = TRUE)
monj <- read.table(file = "longoak_annual.txt", sep="\t", header = TRUE)
```

(x) variables

```
glyla02 <- GlyRwi(,2)
glyla03 <- GlyRwi(,3)
glyla04 <- GlyRwi(,4)
glyyktC <- GlyRwi(,5)
glysi05 <- GlyRwi(,6)
glysj01 <- GlyRwi(,7)
glysj05 <- GlyRwi(,8)
glysk04 <- GlyRwi(,9)
glysl01 <- GlyRwi(,10)
cap <- cape(,2)
monj <- longoak(,2)
nao <- NAO(,2)
```

make a FFT and simple Periodogram

```
fourier<-fft(x)  # calculate fft of data
magnitude<-Mod(fourier) # extract the power spectrum
phase<-Arg(fourier)# extract the phase which is atan(Im(fourier)/Re(fourier))
### select only first half of vectors
magnitude_firsthalf <- magnitude(1:(length(magnitude)/2))
phase_firsthalf<-phase(1:(length(magnitude)/2))
```

```
### generate x-axis
x.axis <- 1:length(magnitude_firsthalf)/length(magnitude)
# plot the power spectrum
plot(x=x.axis,y=magnitude_firsthalf,type="l")
###export to clipboard
write.table(x.axis,"clipboard",sep="\t",col.names=NA)
write.table(magnitude_firsthalf,"clipboard",sep="\t",col.names=NA)
```

###Singular Spectrum Analysis

```
s <- new.ssa(x, L, svd_method = c("svd")) # Perform the decomposition using the L window length and full svd
summary(s) # Show various information about the decomposition
plot(s) # Show the plot of the eigenvalues

f <- reconstruct(s, groups = list(1, c(2, 3), 4)) # Reconstruct into 3 series
plot(pste, type='l') # Plot the original series
lines(f$F1, col = "blue") # Extract the trend
lines(f$F1+f$F2, col = "red") # Add the periodicity
lines(f$F1+f$F2+f$F3, col = "green") # Add slow-varying component
trend <- f$F1
period <- f$F1+f$F2
slow <- f$F1+f$F2+f$F3
write.table(pste,"clipboard",sep="\t",col.names=NA)
write.table(trend,"clipboard",sep="\t",col.names=NA)
write.table(period,"clipboard",sep="\t",col.names=NA)
write.table(slow,"clipboard",sep="\t",col.names=NA)
plot(slow, type='l')
```

###Take SSA = slow from above and use Multitaper Method

```
resSpec1 <- spec.mtm(slow, k=10, nw=5, nFFT = "default",
centreWithSlepians = TRUE, dpssIN = NULL,
returnZeroFreq = TRUE, Ftest = FALSE,
jackknife = TRUE, jkCIProb = 0.95, plot = TRUE)
```

###Retrieve MTM frequency and spectrum magnitude and 95% confidence interval

```
spe <- resSpec1(("spec"))
fre <- resSpec1(("freq"))
jkmax <- resSpec1$mtm$jk$upperCI
jkmin <- resSpec1$mtm$jk$lowerCI
write.table(fre,"clipboard",sep="\t",col.names=NA)
write.table(spe,"clipboard",sep="\t",col.names=NA)
write.table(jkmax,"clipboard",sep="\t",col.names=NA)
write.table(jkmin,"clipboard",sep="\t",col.names=NA)
```

REFERENCES

Atkinson, L.P., Lee, T.N., Blanton, J.O. and Chandler, W.S. (1983). Climatology of the southeastern United States continental shelf waters. *Journal of Geophysical Research*, 88, C8, 4705-4718.

Berggren, W.A., Hollister, C.D. (1977). Plate tectonics and paleocirculation—commotion in the ocean. *Tectonophysics* 38:11–48

Berthou P., Blanchard, M., Noel, P., Vergnaud-Grazzini, C. (1986). The analysis of stable isotopes of the shell applied to the determination of the age of four bivalves of the Normano-Breton Gulf, Western Channel. *ICES* 1986/K:16.

R. H. Bailey and S. A. Tedesco (1986). Paleoecology of a Pliocene coral thicket from North Carolina: an example of temporal change in community structure and function. *Journal of Paleontology* 60(6):1159-1176

Black, B. A., C. Copenheaver, D. C. Frank, M. J. Stuckey, and R. E. Kormanyos (2009). Multi-proxy reconstructions of northeastern Pacific sea surface temperature data from trees and Pacific geoduck, *Palaeogeography, Palaeoclimatoloy, Palaeoecology*, 278, 40–47.

Blackwelder, B.W. (1981a). Late Cenozoic stages and molluscan zones of the middle U.S.Atlantic Coastal Plain. *Journal of Paleontology*, Memoir, 12: Part II.

Blackwelder, B.W. (1981b). Stratigraphy of upper Pliocene and lower Pleistocene marine andestuarine deposits of northeastern North Carolina and southeastern Virginia. *U.S. Geological Survey Bulletin*, 1502-B: B1-B16.

Buick, D. P., and L. C. Ivany (2004). 100 years in the dark: Extreme longevity of Eocene bivalves from Antarctica, *Geology*, 32, 921–924.

Bunn, A.G. (2008). A dendrochronology program library in R (dplR). *Dendrochronologia*,26:115-124

Chandler, M., D. Rind, and R. Thompson. (1994). Joint investigations of the middle Pliocene climate: II. GISS GCM Northern Hemisphere. Global Planetary Change, 9: 197-219.

CLIMAP (1981). Seasonal reconstructions of the Earth's surface at the last glacial maximum in Map Series, Technical Report MC-36. Boulder, Colorado: Geological Society of America.

Cronin, T.M. (1991). Pliocene shallow water paleoceanography of the North Atlantic Ocean based on marine ostracodes. *Quaternary Science Review*, 10: 175-188.

Cronin, T.M. and J.E. Hazel. (1980). Ostracode biostratigraphy of Pliocene and Pleistocene deposits of the Cape Fear Arch region, North and South Carolina. *U.S. Geological Survey Professional Paper*, 1125-B: B1-B25.

Cronin, T.M., H.J. Dowsett, G.S. Dwyer, P.A. Baker, and M.A. Chandler. (2005). Mid-Pliocene deep-sea bottom-water temperatures based on ostracode Mg/Ca ratios. *Marine Micropaleontology*, 54: 249-261.

Dowsett, H. J., Robinson, M. M., and Foley, K. M. (2009). Pliocene three-dimensional global ocean temperature reconstruction, *Climate of the Past*, 5, 769-783.

Dowsett, H., Robinson, M., Dwyer, G., Chandler, M. and Cronin, T., (2006). PRISM3 DOT1 Atlantic basin reconstruction. U.S. Geological Survey Data Series, 189: 4p.

Dowsett, H.J. (2007). Faunal re-evaluation of Mid-Pliocene conditions in the western equatorial Pacific. *Micropaleontology,* 53(6): 447-456.

Dowsett, H.J., Chandler, M.A., Cronin, T.M. and Dwyer, G.S., (2005). Middle Pliocene sea surface temperature variability. *Paleoceanography*, 20(2):PA2014.

Dowsett, H.J., Robinson, M.M., Stoll, D.K. and Foley, K.M., (2010). Mid-Piacenzian mean annual sea surface temperature analysis for data-model comparisons. *Stratigraphy* 7: 189-198.

Dowsett, H.J., T.M. Cronin, R.Z. Poore, R.S. Thompson, R.C. Whatley, and A.M. Wood. (1992). Micropaleontological evidence for increased meridional heat transport in the North Atlantic Ocean during the Pliocene. *Science*, 258: 1133-1135.

Goewert, A.E. and D. Surge. (2008). Seasonal growth patterns in shells of the Pliocene scallop, Chesapecten madisonius. *Geo-Marine Letters Special Issue: Advances in Mollusc Sclerochronology*,

Goman, M., Ingram, B.L., Strom, A., (2007). Composition of stable isotopes in geoduck (*Panopea abrupta*) shells: a preliminary assessment of annual and seasonal paleoceanographic changes in the northeast Pacific. *Quaternary International*, 188, 117–125.

Hallmann, N., B.R. Schöne, A. Strom, and J.Fiebig (2008), An intractable climate archive — Sclerochronological and shell oxygen isotope analyses of the Pacific geoduck, *Panopea abrupta* (bivalve mollusk) from Protection Island (Washington State, USA), *Palaeogeography, Palaeoclimatology, Palaeoecology*, Volume 269, Issues 1–2, 4 November 2008, Pages 115-126.

Hansen, J., M. Sato, R. Ruedy, K. Lo, D.W. Lea, and M. Medina-Elizade, (2006). Global temperature change. *Proc. Natl. Acad. Sci.,* 103, 14288-14293

Haywood, A.M. and P.J. Valdes (2004). Modeling Pliocene warmth: contribution of atmosphere, oceans and cryosphere. *Earth and Planetary Science Letters*, 218: 363-377.

Haywood, A.M., P. Dekens, A.C. Ravelo, and M. Williams. (2005). Warmer tropics during the mid-Pliocene? Evidence from alkenone paleothermometry and a fully coupled ocean-atmosphere GCM. *Geochemistry, Geophysics, and Geosystems*, 6: 1-20.

Hill, D.J.; Csank, A.Z.; Dolan, A.M.; Lunt, D.J. (2011). Pliocene climate variability: Northern Annular Mode in models and tree-ring data. *Palaeogeography, Palaeoclimatology, Palaeoecology*, 309 (1-2). 118-127

Ivany, L.C., T. Brey, M. Huber, D.P. Buick and B.R. Schöne (2011). El Niño in the Eocene greenhouse recorded by fossil bivalves and wood from Antarctica. *Geophysical Research Letters*, 38, L16709, doi:10.1029/2011GL048635.

Jansen, E., J. Overpeck, K.R. Briffa, J.-C. Duplessy, F. Joos, V. Masson-Delmotte, D. Olago, B. Otto-Bliesner, W.R. Peltier, S. Rahmstorf, R. Ramesh, D. Raynaud, D. Rind, O. Solomina, R. Villalba, and D. Zhang, 2007: Palaeoclimate. In Climate Change (2007) The Physical Science Basis. Contribution of Working Group I to the Fourth Assessment Report of the Intergovernmental Panel on Climate Change. S. Solomon, D. Qin, M. Manning, Z. Chen, M. Marquis, K.B. Averyt, M. Tignor, and H.L. Miller, Eds. Cambridge University Press, pp. 433-497

Jones, D.S. (1980). Annual cycle of shell growth increment formation in two continental shelf bivalves and its paleoecologic significance. *Paleobiology*, 6(3): 331-340.

Jones, D.S. (1983). Sclerochronology: reading the record of the molluscan shell. *American Scientist*, 71: 384-391.

Jones, D.S. and I.R. Quitmyer. (1996). Marking time with bivalve shells: oxygen isotopes and season of annual increment formation. *Palaios*, 11: 340-346

Korobeynikov, A. (2010). Computation- and space-efficient implementation of SSA. *Statistics and Its Interface*, Vol. 3, No. 3, p. 257-268

Krantz, D.E. (1990) Mollusk-Isotope Records of Plio-Pleistocene Marine Paleoclimate, U.S. Middle Atlantic Coastal Plain. *Palaios*, 5: 317-335.

Krantz, D.E. (1991). A chronology of Pliocene sea-level fluctuations: The U.S. Middle Atlantic Coastal Plain record. *Quaternary Science Reviews*, 10: 163-174.

Ramsay K., Kaiser M.J.., Richardson C.A., Veale L.O. and Brand A.R. (2000). Can shell scars on dog cockles (*Glycymeris glycymeris L*.) be used as an indicator of fishing disturbance? *Journal of Sea Research*, 43, 167–176.

Raymo, M.E., B. Grant, M. Horowitz, and G.H. Rau. (1996). Mid-Pliocene warmth: stronger greenhouse and stronger conveyor. *Marine Micropaleontology*, 27: 313-326.

Reynolds, D.J., (2011a). Stable isotope analysis of biogenic carbonate within the internal growth increments of marine bivalve *Glycymeris glycymeris*. *Quaternary Newsletter*, 123, 67-69.

Reynolds, D.J, (2011b). Establishing multi-bivalve species sclerochronology. PhD Thesis, Bangor University.

Robinson, M. M., H. J. Dowsett, G. S. Dwyer, and K. T. Lawrence, 2008. Reevaluation of mid-Pliocene North Atlantic sea surface temperatures, *Paleoceanography,* 23, PA3213

Schöne, B. R., J. Fiebig, M. Pfeiffer, R. Gleß, J. Hickson, A. L. A. Johnson, W. Dreyer, and W. Oschmann (2005), Climate records from a bivalve Methuselah (Arctica islandica, Mollusca; Iceland), *Palaeogeography, Palaeoclimatoloy, Palaeoecology*, 228, 130–148.

Schöne, B. R., W. Oschmann, J. Rössler, A. Freyre Castro, S. D. Houk, I. Kröncke, W. Dreyer, R. Janssen, H. Rumohr, and E. Dunca (2003),North Atlantic oscillation dynamics recorded in shells of a long-lived bivalve, *Geology*, 31, 1037–1040.

Schöne, B.R., Castro, A.D.F, Fiebig, J., Houk, S.D., Oschmann, W., and W. Kröncke, (2004), Sea surface water temperatures over the period 1884-1983 reconstructed from oxygen isotope ratios of a bivalve mollusk shell (*Arctica islandica*, southern North Sea). *Palaeogeography, Palaeoclimatology, Palaeoecology* 212, p. 215-232.

Schöne, B.R., Dunca, E., Fiebig, J. and M. Pfeiffer (2005). Mutvei's solution: An ideal agent for resolving microgrowth structures of biogenic carbonates. *Palaeogeography, Palaeoclimatology*, *Palaeoecology*, 228, 149– 166.

Steíngrímsson, S.A., (1989). A comparative ecological study of two *Glycymeris glycymeris* (L.) populations off the Isle of Man. PhD Thesis, University of Liverpool.

Strom, A., (2003). Climate and fisheries in the Pacific Northwest: historical perspectives from geoducks and early explorers. Thesis (M.S.). University of Washington. 55pp.

Strom, A., R. C. Francis, N. J. Mantua, E. L. Miles, and D. L. Peterson (2004). North Pacific climate recorded in growth rings of geoduck clams: A new tool for paleoenvironmental reconstruction, *Geophysical Research Letters,* 31, L06206.

Thompson, R.D.K. (1970). Functional morphology, ecology and evolution in the genus *Glycyemeris* (Bivalvia). Dissertation, Harvard University, Cambridge, MA.

Thompson, R.D.K. (1975). Functional morphology, ecology, and evolutionary conservatism in the *Glycymerididae* (Bivalvia). *Palaeontology*, 18, Part 2, 217-254.

Trouet V., Esper, J., Graham, N.E., Baker, A., Scourse, J.D. and Frank, D.C. (2009). Persistent Positive North Atlantic Oscillation Mode Dominated the Medieval Climate Anomaly, *Science*, Vol. 324, No. 5923, pp. 78-80.

Von Bertalanffy, L., (1957), Quantitative Laws in Metabolism and Growth: The Quarterly Review of Biology, v. 32, p. 217-231.

Wara, M. W., A. C. Ravelo, and M. L. Delaney (2005), Permanent El Niño–like conditions during the Pliocene warm period, *Science*, 309, 758–761.

Ward, L.W. (1992). Molluscan biostratigraphy of the Miocene, Middle Atlantic Coastal Plain of North America, *Virginia Museum of Natural History Memoir* 2: pp. 159.

Ward, L.W. and Blackwelder, B.W. (1987). Late Pliocene and Early Pleistocene Mollusca From the James City and Chowan River Formations at the Lee Creek Mine, In: Ray, C.E., ed. Geology and Paleontology of the Lee Creek Mine, North Carolina, II, *Smithsonian Contributions to Paleobiology*, 61: 1-283.

Ward, L. W., and Gilinsky, N. L.,(1993). Molluscan assemblage of the Chowan River Formation, Part A. Biostratigraphic analysis of the Chowan River Formation (upper Pliocene) and adjoining units, the Moore House Member of the Yorktown Formation (upper Pliocene) and the James City Formation (lower Pleistocene): Virginia Museum of Natural History Memoir 3, part A., 33 p.

Ward, L.W. and G.L. Strickland. (1985). Outline of Tertiary stratigraphy and depositional history of the U.S. Atlantic Coastal Plain. In: C.W. Poag (Eds.), *Geologic evolution of the United States Atlantic margin*. New York, Van Nostrand Reinhold Company. 87-123.

Williams, M. and Haywood, A. M. and Harper, E. M. and Johnson, A. L. A. and Knowles, T. and Leng, M. J. and Lunt, D. J. and Okamura, B. and Taylor, P. D. and Zalasiewicz, J. (2009). Pliocene climate and seasonality in North Atlantic shelf seas. Philosophical Transactions of the Royal Society A, 367 (1886). pp. 85-108.

Witbaard, R., M.I. Jenness, K. van der Borg, and G. Ganssen (1994). Verification of annual growth increments in *Arctica islandica* L. from the North Sea by means of oxygen and carbon isotopes. *Netherlands Journal of Sea Research*, 33(1). 91-101.

Wolfe, D.A. (2008). Mollusks taken by Beam Trawl in the vicinity of Gray's Reef National Marine Sanctuary on the Continental Shelf off Georgia, Southeastern U.S. *NOAA Technical Memorandum* NOS NCCOS 88. 40 pp.

Zachos, J., Pagani, M., Sloan, L., Thomas, E. & Billups, K. (2001). Trends, rhythms, and aberrations in global climate 65 Ma to present. *Science,* 292, 686–693.

Zirkel, J. and Schöne B.R. (2010). Fossile Funde aus dem Kasseler Meeressand. Hessen Archäologie 2009, *Jahrbuch für Archäologie und Paläontologie in Hessen*. Konrad Theiss Verlag GmbH, Stuttgart, 2010, 18-19.